LUT
Lappeenranta
University of Technology

Mahmoud S. M. Abdel Wahed

GEOCHEMISTRY AND WATER QUALITY OF LAKE QARUN, EGYPT

Thesis for the degree of Doctor of Science (Technology) to be presented with due permission for public examination and criticism in the Chamber Music Hall at the Mikaeli Concert and Congress Hall, Mikkeli, Finland on the 10th of June, 2015, at noon.

Acta Universitatis
Lappeenrantaensis 637

Supervisors Professor Mika Sillanpää
Department of Chemical Technology
LUT School of Engineering Science
Lappeenranta University of Technology
Finland

Professor Mohamed Ibrahim El-Sayed
Department of Geology
Faculty of Science
Beni-Suef University
Egypt

Reviewers Professor B. Charlotte Schreiber
Department of Earth and Space Sciences
University of Washington
Seattle, USA

Professor Shichang Kang
State Key Laboratory of Cryospheric Sciences
Cold and Arid Regions Environmental and Engineering Research Institute (CAREERI)
University of Chinese Academy of Sciences (UCAS)
Chinese Academy of Sciences
China

Opponent

Professor B. Charlotte Schreiber
Department of Earth and Space Sciences
University of Washington
Seattle, USA

ISBN 978-952-265-794-7
ISBN 978-952-265-795-4 (PDF)
ISSN-L 1456-4491
ISSN 1456-4491

Lappeenranta University of Technology
University Press 2015

ABSTRACT

Mahmoud S. M. Abdel Wahed

Geochemistry and water quality of Lake Qarun, Egypt

Lappeenranta 2015
73 pages
Acta Universitatis Lappeenrantaensis 637
Diss. Lappeenranta University of Technology
ISBN 978-952-265-794-7, ISBN 978-952-265-795-4 (PDF), ISSN-L 1456-4491, ISSN 1456-4491

Water geochemistry is a very important tool for studying the water quality in a given area. Geology and climate are the major natural factors controlling the chemistry of most natural waters. Anthropogenic impacts are the secondary sources of contamination in natural waters. This study presents the first integrative approach to the geochemistry and water quality of surface waters and Lake Qarun in the Fayoum catchment, Egypt. Moreover, geochemical modeling of Lake Qarun was firstly presented. The Nile River is the main source of water to the Fayoum watershed. To investigate the quality and geochemistry of this water, water samples from irrigation canals, drains and Lake Qarun were collected during the period 2010–2013 from the whole Fayoum drainage basin to address the major processes and factors governing the evolution of water chemistry in the investigation area. About 34 physicochemical quality parameters, including major ions, oxygen isotopes, trace elements, nutrients and microbiological parameters were investigated in the water samples. Multivariable statistical analysis was used to interpret the interrelationship between the different studied parameters. Geochemical modeling of Lake Qarun was carried out using Hardie and Eugster's evolutionary model and a model simulated by PHREEQC software. The crystallization sequence during evaporation of Lake Qarun brine was also studied using a Jänecke phase diagram involving the system Na–K–Mg–Cl–SO_4–H_2O.

The results show that the chemistry of surface water in the Fayoum catchment evolves from Ca-Mg-HCO_3 at the head waters to Ca–Mg–Cl–SO_4 and eventually to Na–Cl downstream and at Lake Qarun. The main processes behind the high levels of Na, SO_4 and Cl in downstream waters and in Lake Qarun are dissolution of evaporites from Fayoum soils followed by evapoconcentration. This was confirmed by binary plots between the different ions, Piper plot, Gibb's plot and $\delta^{18}O$ results. The modeled data proved that Lake Qarun brine evolves from drainage waters via an evaporation–crystallization process. Through the precipitation of calcite and gypsum, the solution should reach the final composition "Na–Mg–SO_4–Cl". As simulated by PHREEQC, further evaporation of lake brine can drive halite to precipitate in the final stages of evaporation.

Significantly, the crystallization sequence during evaporation of the lake brine at the concentration ponds of the Egyptian Salts and Minerals Company (EMISAL) reflected the findings from both Hardie and Eugster's evolutionary model and the PHREEQC simulated model. After crystallization of halite at the EMISAL ponds, the crystallization sequence during evaporation of the residual brine (bittern) was investigated using a Jänecke phase diagram at 35 °C. This diagram was more useful than PHREEQC for predicting the evaporation path especially in the case of this highly concentrated brine (bittern). The predicted crystallization path using a Jänecke phase diagram at 35 °C showed that halite, hexahydrite, kainite and kieserite should

appear during bittern evaporation. Yet the actual crystallized mineral salts were only halite and hexahydrite. The absence of kainite was due to its metastability while the absence of kieserite was due to opposed relative humidity. The presence of a specific $MgSO_4.nH_2O$ phase in ancient evaporite deposits can be used as a paleoclimatic indicator.

Evaluation of surface water quality for agricultural purposes shows that some irrigation waters and all drainage waters have high salinities and therefore cannot be used for irrigation. Waters from irrigation canals used as a drinking water supply show higher concentrations of Al and suffer from high levels of total coliform (TC), fecal coliform (FC) and *fecal streptococcus* (FS). These waters cannot be used for drinking or agricultural purposes without treatment, because of their high health risk. Therefore it is crucial that environmental protection agencies and the media increase public awareness of this issue, especially in rural areas.

Keywords: Water quality; geochemistry; water chemistry; Fayoum; Lake Qarun; EMISAL; geochemical modeling; surface water; PHREEQC; microbiological contamination; evaporation–crystallization; evapoconcentration; drainage waters; agricultural purposes; drinking water

ACKNOWLEDGEMENTS

First of all, I would like to thank my supervisor, Prof. Mika Sillanpää, for his support and encouragement to finalize my thesis. I offer him my hearty appreciation for kindly providing all the facilities to complete this study. His ambitious attitude to research work has also motivated me greatly during my studies. I really want to thank him for giving me this opportunity in his well-equipped laboratory in Mikkeli city. "Thank you very much" does not seem sufficient for him, but it is said from the bottom of my heart!

I also want to thank my co-supervisor Prof. Mohamed Ibrahim El-Sayed for his encouragement during the whole course of this work and his efficient revisions of my manuscripts. Many thanks to my co-authors, Prof. Adel M'nif, Prof. Christian Wolkersdorfer, and Dr. Essam A. Mohamed for their detailed comments on and inspirational input into the manuscript. These experiences will be greatly beneficial to me for years to come.

I express my sincerely gratitude to Professor B. Charlotte Schreiber and Professor Shichang Kang, the reviewers of my thesis, for their valuable comments and important suggestions regarding the thesis.

The financial support during my stay in Finland of the Ministry of Higher Education in Egypt and also of the Lappeenranta University of Technology is highly appreciated.

I also wish to thank all my colleagues in our laboratory in Mikkeli. I want to name Chaker, Heikki, Philipp, Irina, Olga, Sara, Evgenia, Marina and Mikko in particular; you are very good friends.

Finally, my warmest thanks go to my wife and my daughter. They spent hard times with me during my stay and studies in Finland. It was very cold here in Finland, but they preferred to stay with me and always supported me. Also I would like to thank my father, my mother, my brothers and my sisters for their assistance throughout my life. Really, I can't live without my family.

Mahmoud S. M. Abdel Wahed
June 2015
Mikkeli, Finland

LIST OF PUBLICATIONS

1. Publications

The publications are listed in roman numerals in the text as follows:

I. **Mahmoud S.M. Abdel Wahed**, Essam A. Mohamed, Mohamed I. El-Sayed, Adel M'nif, Mika Sillanpää, Hydrogeochemical processes controlling the water chemistry of a closed saline lake located in Sahara Desert: Lake Qarun, Egypt. Aquatic Geochemistry 21(2015)31-57.

II. **Mahmoud S.M. Abdel Wahed**, Essam A. Mohamed, Mohamed I. El-Sayed, Adel M'nif, Mika Sillanpää, Geochemical modeling of evaporation process in Lake Qarun, Egypt. Journal of African Earth Sciences 97(2014)322-330.

III. **Mahmoud S.M. Abdel Wahed**, Essam A. Mohamed, Christian Wolkersdorfer, Mohamed I. El-Sayed, Adel M'nif, Mika Sillanpää, Assessment of water quality in surface waters of the Fayoum watershed, Egypt. Environmental Earth Sciences (2015), In Press. DOI: 10.1007/s12665-015-4186-0

IV. **Mahmoud S.M. Abdel Wahed**, Essam A. Mohamed, Mohamed I. El-Sayed, Adel M'nif, Mika Sillanpää, Crystallization sequence during evaporation of a high concentrated brine involving the system Na–K–Mg–Cl–SO_4–H_2O. Desalination 355(2015)11-21.

2. Conferences

Mahmoud S.M. Abdel Wahed, Essam A. Mohamed, Christian Wolkersdorfer, Mohamed I. El-Sayed, Adel M'nif, Mika Sillanpää, Water quality of Fayoum surface water, Fayoum Province, Egypt. Published Presentation in "Deltas in Times of Climate Change II, Rotterdam, Netherlands, 24-26 September 2014".

http://library.wur.nl/WebQuery/kvk?achternaam==Abdel%20Wahed

Author's contribution to publications I-IV

The author planned, designed and carried out all sampling trips, analyzed the data, interpreted the results and had the main responsibility for writing the manuscripts.

Author's contribution to the conference presentation

The author designed and prepared the presentation and also presented it at the conference "Deltas in Times of Climate Change II, Rotterdam, Netherlands, 24-26 September 2014″

Table of Contents

Abbreviations

APHA	American Public Health Association
CA	Cluster Analysis
COD	Chemical Oxygen Demand
DO	Dissolved Oxygen
EC	Electrical Conductivity
EDTA	Ethylenediaminetetraacetic Acid
EMISAL	The Egyptian Salts and Minerals Company
FC	Fecal Coliform
FIMS	Flow Injection Mercury Systems
FINAS	Finnish Accreditation Service
FS	*Fecal Streptococcus*
GAAS	Graphite Furnace Atomic Absorption Spectrometry
GPS	Global Positioning System
ICP-OES	Inductively Coupled Plasma-Optical Emission Spectrometry
MRSI	McMaster Research Group for Stable Isotopologues
PCA	Principal Component Analysis
PE	Polyethylene
RH	Relative Humidity
SAR	Sodium Adsorption Ratio
TC	Total Coliform
TDS	Total Dissolved Solids
TOC	Total Organic Carbon
USEPA	U.S. Environmental Protection Agency
WHO	World Health Organization
V-SMOW	Vienna Standard Mean Ocean Water

1. INTRODUCTION

Closed (endorheic) lakes are lakes that have no outlet except via evaporation. When water escapes by evaporation, salts, nutrients and pollutants are continuously concentrated in the remaining water. Most endorheic lakes are saline with variable levels of salinity [1]. The largest endorheic lakes in the world are the Caspian Sea, Aral Sea, Lake Balkhash, Lake Chad, Lake Titicaca, Qinghai Lake and the Great Salt Lake. These lakes basically depend on the balance of inflows and evaporation and are very susceptible to changes driven by both natural causes including climatic variability and climate change, and/or anthropogenic impacts. This also means that these lakes can be used as significant indicators of climate change and also can point to records of the paleo-hydroclimatic variability over a large area [2]. Furthermore, variations in their inflows can have very significant effects on their water level. For example, the Aral Sea receives now ten times less water than it used to from its recharge sources [3]; thus it has reduced in size to approximately 10% of its previous surface area and holds less than 10% of its former volume [4]. The water level of Great Salt Lake in the USA has recently raised because of increased rainfall in its catchment, and Qinghai Lake in China has varied in size following the variation in its catchment precipitation [2].

The geochemical evolution of closed lakes primarily depends on the chemistry of the inflowing waters and the rate of evaporation. In a closed hydrological regime, the composition of lake water basically depends on soil and rock mineralogy, which are chemically altered by inflow waters in the drainage basin adjoining the lake [5, 6]. Closed salt lakes, with variable degrees of salinity, are characteristic marks of the arid and semiarid regions [7]. The common cause of salinity increase in closed lakes is that the salt content is continuously built up by evaporation [8]. The evolution history of endorheic basin waters can be divided into two stages. In the first stage, the inflow waters in the watershed area obtain solutes during chemical weathering of soil and bedrock. In the second stage, subsequent evaporation leading to up-concentration of ions which causes selective precipitation of specific dissolved minerals, further affecting the final composition of the brine [6]. The evolution of brine in an endorheic basin waters has been the topic of substantial scientific attention [9, 10]. Natural waters in the Sierra Nevada in the western United States were studied by Garrels and McKenzie [11] and they concluded that mineral crystallization fractionation during evaporative concentration is the major control of brine

advancement. Hardie and Eugster [6] subsequently suggested an evolutionary model that deals with the evolution of natural waters chemistry during evaporation in terms of a sequence of chemical divides. A chemical divide is a point along the evolution sequence of brine at which removal of a specific solid phase exhausts the water in certain ions and further progressive evaporation proceeds the solution to a distinctive pathway [12]. Accordingly, if there is binary salt is crystallized throughout evaporation and the concentration ratio (in equivalences) of the two ions forming the salt is dissimilar from the ratio of these ions in the initial solution, any progressive evaporation will cause building up in the ion present in higher relative concentration in the solution, and a depletion in the ion present in lower relative concentration [12]. There are many modifications of the basic Hardie-Eugster evolutionary model, but the most simple and clear one was proposed by Drever [12]. In this modified model, the final resulted brines are distinguished by the fractional removal of constituents from solutions (chemical divide). The most significant limitation of Hardie and Eugster's model [6], however, is the lack of capability to add elements to the solution during brine evolution pathway. Yet this model is still widely used to interpret the geochemical evolution of many natural brines and saline lakes [13-17].

The study of saline lakes helps in understanding processes under extreme conditions. Insight these processes will significantly expand our understanding of normal lakes as well [7]. Saline lakes not only have economic implications but also can be important in the geologic record as sensitive indicators of past tectonic and climatic changes [7].

Lake Qarun, the object of the present study, is one of the endorheic saline lakes located in the North African Sahara Desert. It is the merely significant natural lake in Middle Egypt [18]. It is situated in an arid region occupying the lowest part of the Fayoum Depression in the Western Desert of Egypt (Figs. 1 and 2).

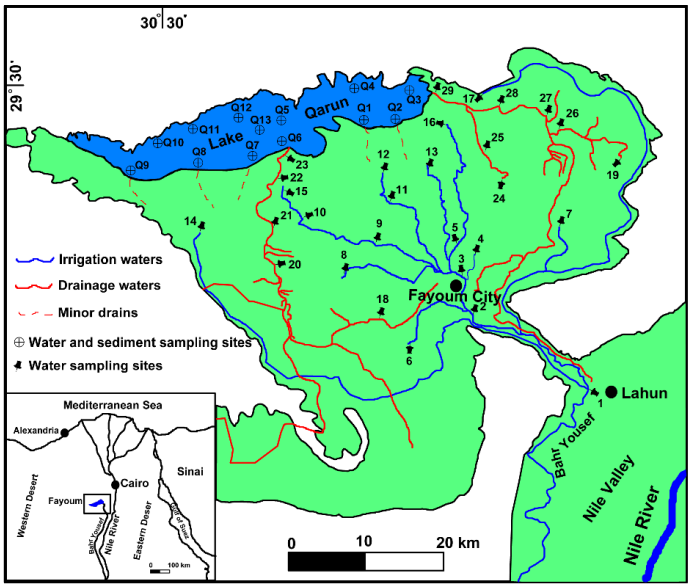

Figure 1. Location map showing the study area and sampling sites (Paper **III**).

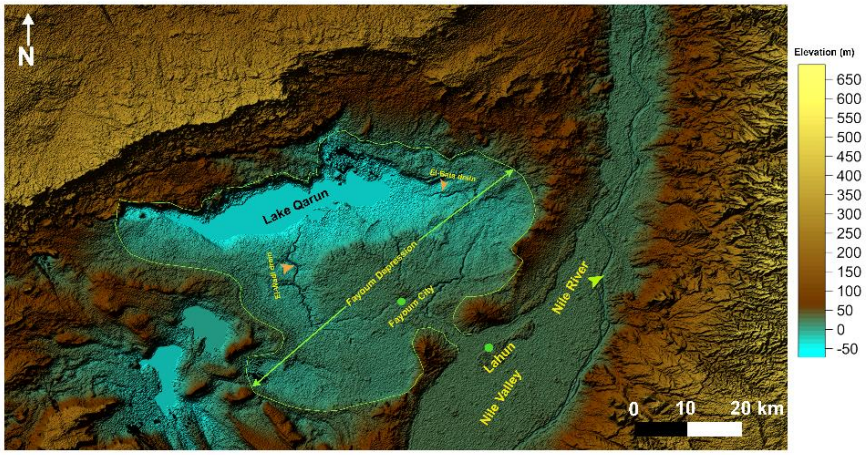

Figure 2. Digital elevation map showing the land slopes from Lahun to Lake Qarun. The lake occupies the deepest part of the Fayoum Depression (Paper **III**).

Historically, Lake Qarun is the remaining part from a huge natural paleo-freshwater lake, previously known as “Lake Moeris”, which persisted until the mid-Holocene period [19]. Lake Moeris has been used as reservoir of Nile water during flooding periods to provide the Nile Valley with water during dry seasons [20].

In the recent past, the intensive development through building dams and bridges across the Nile course obstructed excess flooding waters from connecting with the Fayoum Depression, resulting in the isolation of Lake Qarun from the Nile, and thus it became an inland closed lake. As the climatic conditions are warm and dry almost all year round, the lake might have vanished under intensive continuous evaporation. To balance this water loss by evaporation, all agricultural drainage waters from the cultivated lands surrounding the lake were diverted to Lake Qarun [20]. In view of the fact that the lake has no natural outflow [21], the drainage water in Lake Qarun is subjecting to evaporative concentration. Annually, a volume of freshwater almost equal to that of the inflowing drainage water is evaporated from the lake while the dissolved solutes are concentrated in the lake [20, 22]. The lake brine gradually evaporates and its salinity increases. The salinity of the lake increased significantly with time, from about 10.5‰ in 1906 and 30‰ in 1985 to about 42‰ in 1992 [13, 23]. Variations in the water and salinity levels of Lake Qarun were measured irregularly throughout the 20th century [25-28]. The salinity increases of the past century have been mainly attributed to evaporative concentration of drainage water within the lake [24, 28]. Lake Qarun was used to support a major fishery in the Fayoum Governorate, but its increasing salinity has become unfavorable for most of the freshwater fish species that were originally living in the lake. All the fish species that were originally living in freshwater ecosystem are extinct except *Tilapia zillii* [18]. Accordingly, new marine-type fish species from the Mediterranean Sea were added to adapt the increase in lake salinity since the 1920s [29]. The continuous increase in the salinity of Lake Qarun can eventually lead to a biologically “dead” water body [20]. A salt extraction project was proposed as an economic and environmental solution to stop the continuous increase in Lake Qarun salinity. It was planned to keep the total dissolved solids (TDS) level of the lake at 35 g/L (i.e. at marine system levels) by extracting an amount of salts equal to those carried annually by drainage water to the lake at sequential stages. Since the implementation of the approved feasibility study, the Egyptian Salts and Minerals Company (EMISAL) initiated this step as an industrial complex site. EMISAL was established as an environmental, ecological and economic project on Lake Qarun. A zone has

been separated from the lake and partitioned into a series of four successive concentration ponds for economic salt extraction. The salt-extraction process is based on brine-concentration technology via evaporation–precipitation cycles using solar radiation energy. The salinity of Lake Qarun reflects the drastic change in the lake chemistry. It has turned from an ancient freshwater system into a normal marine system in the late 20th century as evidenced by the study of microfossils [30-32] and water chemistry measurements [25].

During the 20th century, Lake Qarun has increasingly become the object of several ecological studies. Physical and chemical variables are documented by Ball [24], Naguib [26], Meshal [20], Ishak and Abdel-Malek [22], Rasmy and Estefan [28], Soliman [27], El Sayed and Guindy [25], Gupta and Abd El-Hamid [33], Mansour and Sidky [34, 35], Hussein et al. [36], Abd Ellah [37] and Abdel-Satar et al. [38]. Studies on the paleoenvironmental changes recorded in Lake Qarun were conducted by Flower et al. [31], Keatings et al. [39, 40], and Baioumy et al. [41, 42]. The plankton communities in Lake Qarun were investigated by Sabae [43, 44], Sabae and Rabeh [45], Abdel-Malek and Ishak [46], Abdel-Moniem [47] and recently Mansour and Sidky [34,35], Fathy and Flower [18], Mageed [48], Ali et al. [49] and Saif et al. [50].

Ball [24] documented the evolution history of Lake Qarun and made the first attempt to estimate the evaporation from Lake Qarun using tank observation. It was concluded that there is a net annual water loss from the lake and reported that the salinity of the lake increased from 17.7‰ in 1918 to 30.8‰ in 1932.

Naguib [26] studied the salinity of Lake Qarun in the period 1953–1955 by collecting water samples from different locations in the lake and reported that the average salinity of the lake was 31.49‰.

Meshal [20] discussed the salt budget and the problem of salinity increase in Lake Qarun, demonstrating that the salinity of the lake increased from 13.25‰ to 31.73‰ in the period from 1901 to 1970. This increase in salinity was attributed to evaporative concentration of dissolved salts carried by drainage waters. This study concluded that over time the continuous increase in salinity can turn the lake into a “dead” water body if nothing is done to control this. The proposed solution to this problem is to extract an amount of salts equal to the amount conveyed to the lake by drainage water; this can be achieved by removing the required volume of lake brine.

Ishak and Abdel-Malek [22] reviewed some physicochemical changes in the lake such as the lake level, salinity, dissolved oxygen (DO) and nutrients during the period from 1892 to 1973. They concluded that building up of salts with time is the main significant factor affecting the ecology of the lake and that there is a reverse relationship between the salinity and lake level.

Rasmy and Estefan [28] studied the experimental separation of saline mineral from Lake Qarun brine by mechanical evaporation at 70^0 C and outlined the general chemical constituents of the lake water. They suggested that there is great potential for the extraction of economic mineral salts from the lake. Also, they compared the lake composition with both seawater and other common saline lakes such as Great Salt Lake, the Salton Sea and the Dead Sea. They noted, for example, that one unique characteristic of the lake is that it is higher in sulfate and lower in chloride than seawater.

Soliman [27] reviewed the annual and seasonal mean variations of salinity in Lake Qarun at different water levels during the period 1906–1982. Generally, salinity showed a negative relationship with the water level. This depended on the ratio between the inflow drainage water and outflow by evaporation, as well as on the salt content of the inflow water. The conclusion was that a progressive increase in the salinity of the lake will may occur over time. This impacts negatively on the fish productivity of the lake.

El Sayed and Guindy [25] investigated the sulfate enrichment in Lake Qarun and stated that groundwater seepage is the main source of sulfate in Lake Qarun. Dissolved Na_2SO_4 salt was recognized as the main source of sulfate in the groundwater.

Gupta and Abd El-Hamid [33] studied the water quality evaluation of Lake Qarun. They mentioned that the lake water is more contaminated than the Nile water. The lake found to have lower DO and higher salinity and nutrients than the Nile River. The main source of contaminates was attributed to the large input from agricultural and domestic wastewaters.

Mansour and Sidky [34, 35] studied the heavy metals pollution in Lake Qarun and Wadi El-Rayan lakes in the Fayoum Province. Heavy metals were measured in water, sediments and fish samples. This investigation revealed that Lake Qarun was more polluted than Wadi El-Rayan lakes. Anthropogenic sources such as industrial and domestic wastes and pesticides in agricultural returns were thought to be the main source of pollution to Lake Qarun.

Hussein et al. [36] monitored the water quality of Lake Qarun during 2003 and 2004. They measured some chemical and biological parameters such as DO, COD, TOC, chlorophyll, nutrients, and some trace elements. The main findings showed that the lake suffers from high levels of nutrients that can produce algal blooms under appropriate conditions (i.e. temperature, sunlight, and calm water). Also, some trace metals were accumulated and detected in the gills of fish samples.

Abd Ellah [37] investigated the temporal and spatial variations in Lake Qarun's salinity. The lake salinity was low in winter and high in summer. The results also showed that the water salinity is low in the eastern side of the lake and gradually increases north-westward. These variations depend on the ratio between the drainage water inflow and the outflow by evaporation.

Abdel-Satar et al. [38] studied the concentrations of some nutrients, trace metals and major ions in Lake Qarun water and sediments. The results revealed that the discharge of drainage sewage causes an enrichment of lake sediments with metals and also increases the concentration level of nutrients in the lake water. They stated that the salinity of lake water fluctuates based on the input drainage water and the rate of evaporation.

Flower et al. [31] studied some environmental changes in Lake Qarun by assessing recent paleolimnological records in core samples from bottom sediments of the lake. They concluded that the lake has been affected by a combination of anthropogenic activities and climatic changes during the past 5000 years. More recently, during most of the 20th century, the lake salinity increased, reaching seawater-like levels by the late 1980s.

Keatings et al. [39, 40] used ostracod-based paleoenvironmental reconstruction to investigate the changes in salinity and water level in Lake Qarun during the 20th century. The oxygen isotope ($\delta^{18}O$) values of the ostracod calcite provided information about the effect of evaporation in controlling the change in lake level. Other tools such as Sr/Ca ratio or Mg/Ca ratio did not yield enough information. Yet some ostracod species could be used as indicators of the evolution of the lake's water chemistry during the Holocene period [40].

Baioumy et al. [41, 42] reconstructed the Lake Qarun level due to climate changes during the last 7000 years. They studied the long-term variations in the lake level using sedimentological, mineralogical, and geochemical analyses of sediment cores taken from the lake along with

carbon and oxygen isotopes. They summarized that interactions between global and local climatic changes and human activities could produce variations in the lake level.

The studies of plankton communities in Lake Qarun made by Sabae [43, 44], Sabae and Rabeh [45], Abdel-Malek and Ishak [46], Abdel-Moniem [47] and Mansour and Sidky [34,35] have been reviewed in Fathy and Flower [18].

Mageed [48] studied the diversity of holozooplankton in Lake Qarun. He sought to clarify the relationship between these plankton communities and the state of pollution in the lake. Three groups of these organisms were recorded; Protozoa, Rotifera and Copepoda. The first two groups were found to represent 78.81% of the total stock. The diversity index showed a lower value, however, which indicated that the lake ecosystem is unstable or polluted.

Ali et al. [49] studied the water quality of Lake Qarun and its impact on the expression of immune response genes in the fish species *Solea aegyptiaca*. They concluded that lake water pollution enhances the up-regulation of some immune genes of the studied species. They stated that such applications might be useful to assess the water quality promptly and at low cost.

Saif et al. [50] studied seagrass (*Ruppia cirrohsa*) distribution in Lake Qarun and stated how it can be used as an indicator for water quality.

As yet no studies have been conducted on the geochemistry and/or the geochemical evolution of Lake Qarun. All previous investigations focused only on single aspect of the lake and did not conduct a holistic approach to the geochemical evolution of all the Fayoum watershed's water types and Lake Qarun. The Nile is the main source of water to the Fayoum watershed while Lake Qarun acts as a sink for all drainage waters. To track the geochemistry, water quality and geochemical evolution of Lake Qarun in the studied catchment, it is important to follow the course of the Nile water once it enters the catchment area at Lahun (Fig. 1). Within the catchment, water samples can be categorized into irrigation waters, drainage waters and Lake Qarun waters (Fig. 1). Agricultural returns and all excess waters are usually collected in drains. Most waters flow into one of the two major drains: El-Wadi or El-Bats, which, together with minor drains, finally drain into Lake Qarun (Fig. 1). Most previous studies did not present a full picture of the geochemical alterations of inflow waters in the Fayoum watershed which control the evolution of water chemistry in Lake Qarun. To the best of our knowledge, no geochemical

models have been executed for the lake. This study takes an integrative approach to the geochemical evolution of both Lake Qarun and all the water types of the Fayoum watershed.

2. OBJECTIVES OF THE STUDY

The overall objective of this study was to introduce a full geochemical history and water quality evolution of surface waters in a specific catchment, the Fayoum watershed. The main goal was to study Nile water evolution through its flow path from when it enters the Fayoum Depression to its final destination at Lake Qarun. The crystallization sequence during evaporation of Lake Qarun water and geochemical modeling of the lake were also investigated.

The specific aims of the study were:

1. Investigating the main geochemical processes controlling the surface water chemistry in the Fayoum watershed and the consequent evolution of Lake Qarun water based on the chemistry of the inflowing drainage waters (Papers **I** and **II**).
2. Conducting a simulated geochemical model using the PHREEQC program as a first attempt to determine the main sources of the solute budget to Lake Qarun (Paper **II**).
3. Comparing Hardie and Eugster's evolutionary model (1970) of closed-basin waters undergoing evaporation with the simulated model carried out by PHREEQC (Papers **I** and **II**).
4. Modeling Lake Qarun evolution due to a predicted intensive evaporation caused by decreasing inflow waters accompanied with high rates of evaporation as a result of predicted climate change in terms of global warming (Paper **I**).
5. Investigating the water quality in the Fayoum watershed and evaluation of all water types for their suitability for drinking or agricultural purposes against the WHO and FAO's guidelines (Paper **III**).
6. Studying the fate of contaminants through source–sink pathway (Paper **III**).
7. Evaluating the pollution level of metals content in Lake Qarun sediments (Paper **III**).
8. Studying the mineral crystallization sequence during evaporation of Lake Qarun water and its economic potential at EMISAL (Egyptian Salts and Minerals Company) concentration ponds using Jänecke phase diagrams as a tool for predicting the crystallization path (Paper **IV**).

3. MATERIALS AND METHODS

3.1. Site and Lake Qarun catchment description

The Fayoum Governorate, with a population of 2.48 million (January 2005 census) and Fayoum City as the principal town, occupies a natural closed depression in the Western Desert of Egypt between 29°02′ and 29°35′ N and 30°23′ and 31°05′ E. It extends over 6068 km^2 and is situated about 95 km southwest of Cairo (Fig. 1). The Nile River, on which the irrigation and agricultural system mainly depends, is the main source of water and the province has internal drainage with Lake Qarun as the general receiver for agricultural wastewater. The catchment lies in Egypt's arid belt with a hot long dry summer and a mild short winter and consequently, the climate is mostly hot and dry [41]. In addition, it is characterized by low seasonal rainfall and a high of evaporation. Fayoum City is a water distribution center for domestic demands in the province and a network of canals and small pumping stations also delivers water to the agricultural regions. While all other Egyptian Governorates are conveyed to the Nile River, the Fayoum Governorate is unique in that all its drainage water flows to Lake Qarun.

Lake Qarun is situated in the lowest part of the Fayoum Depression with an elevation of ≈ 43 m below sea level (Fig. 2). It is located between the longitudes of 30° 24′ & 30° 49′ E and latitudes of 29° 24′ & 29° 33′ N (Fig. 1). About 67% of the lake has a depth of between 2 and 5 m, while 18% of the lake is deeper than 5 m [41]. The deepest region (≈ 8 m) is located in the middle part of the lake while the shallowest region lies in the eastern portion of the lake [41]. To the north, the area is totally desert covered by rock and sand exposures without any marks of vegetation while in the south and southeast, cultivated land slopes steeply towards the lake which makes it a natural sink for agricultural drainage water.

3.2. Climate

The studied catchment lies in Egypt's arid belt with a hot long dry summer and a mild short winter and consequently, the climate is generally warm and dry [41]. In addition, it is characterized by low seasonal rainfall and a high evaporation rate. Rainfall is extremely low at <10 mm annually [31]. Annually, the mean minimum and maximum temperatures are 14.5 °C and 31 °C, respectively. The lowest evaporation rate (1.9 mm/day) is recorded in January while

the highest value (7.3 mm/day) is recorded in June and the annual mean relative humidity varies between 50 and 62% [51].

3.3. Hydrology

The irrigation and agricultural system in the Fayoum region depends mainly on Nile water. Fayoum City, the principal town in the area, is a water distribution center for the Fayoum (domestic demands) and a network of canals and small pumping stations deliver water to the agricultural regions. The lake is surrounded to the south and southeast by cultivated land which slopes steeply towards the lake, forming a sink for drainage water (Figs. 1 and 2). The lake is now used as a general reservoir for both agricultural drainage wastewater and sewage waters. It is known that agriculture returns and excess water are passed to Lake Qarun by two principal drains, El-Wadi and El-Bats [52]. The El-Bats drain collects agricultural drainage waters from the eastern and northeastern parts of the Fayoum watershed while the El-Wadi drain receives drainage water from the middle region (Fig. 1). The lake gains drainage water about 338×106 m^3/year from the El-Bats and El-Wadi drains and about 67.8×10^6 m^3/year from groundwater while it loses about 415×10^6 m^3/year by evaporation [20, 37, 39, 52]. The lake has no outflow except by evaporation [20, 21]. The net water budget in Lake Qarun is negative [52]. During some winter seasons, however, flooding can occur. This is possibly due to the low evaporation rate of the lake water in winter. During winter, the drainage water inflow to the lake thus exceeds the water loss by evaporation, possibly raising the lake water level [53]. In fact, the water budget in Lake Qarun can vary annually. So careful and accurate calculations are needed to estimate the exact change in annual water storage of Lake Qarun. At the same time Lake Qarun is becoming shallower due to siltation on the lake bottom, which can reduce its storing capacity [18]. A volume of freshwater nearly equal to that of the inflowing drainage water is lost annually from the lake through evaporation [20, 22]. In his 1973 doctoral study, Meshal [20] reported that drainage water annually carries an average $\approx 385\times10^6$ kg of dissolved salts to the lake. After 10 years, Rasmy and Estefan [28] stated that this quantity has increased to 470×10^6 kg. The solute budget conveyed annually to Lake Qarun mainly depends on the variation in inflow water.

3.4. Geology and geomorphology

The Fayoum Depression is a natural depression in the Western Desert of Egypt, extending over 6068 km^2. Tableland areas surround the Fayoum Depression from the east, west and south separating it from neighboring depressions, the Nile Valley and Wadi El Rayan. Approximately 1800 km^2 of cultivated land forms the second lowest area of the Fayoum Depression after Lake Qarun. Most of the cultivated soils in the Fayoum Depression are deep alluvial loam or clayey, derived mainly from the Nile flood alluvium [51]. The Fayoum Depression has a dense net of irrigation canals and drains. The area includes three main landscapes, lacustrine plain, alluvial-lacustrine plain, and alluvial plain [51, 54]. The southern shore of Lake Qarun is mostly surrounded by lacustrine deposits. These deposits cover an area of 198 km^2 and are classified as highly saline and poor productivity soils [54]. The evaluation of salinity, sodicity, and water table of soils revealed that most alluvial-lacustrine and lacustrine soils in the Fayoum Depression are damaged by salinization, waterlogging and sodification [51]. Geologically, the stratigraphic sequence in the area ranges in age from Quaternary to Tertiary (Fig. 3). The Fayoum Depression itself is excavated in Middle Eocene rocks, which are essentially composed of gyps-ferrous shale, white marls, limestone and sand [55, 56]. The Quaternary deposits are widely distributed over the Fayoum area in the form of Aeolian, Nilotic (alluvial sediments) and lacustrine deposits. The alluvial sediments are composed of sands and gravels of variable sizes intercalated with calcareous silt and clay contents [57]. The lacustrine deposits include claystone, gypsum, and calcareous materials intercalated with ferruginous sandy silt [58]. The lacustrine deposits have prevailed in the area and extend to the south of Lake Qarun. In the whole area, Quaternary sediments directly overlay the limestone deposits of the Eocene Age.

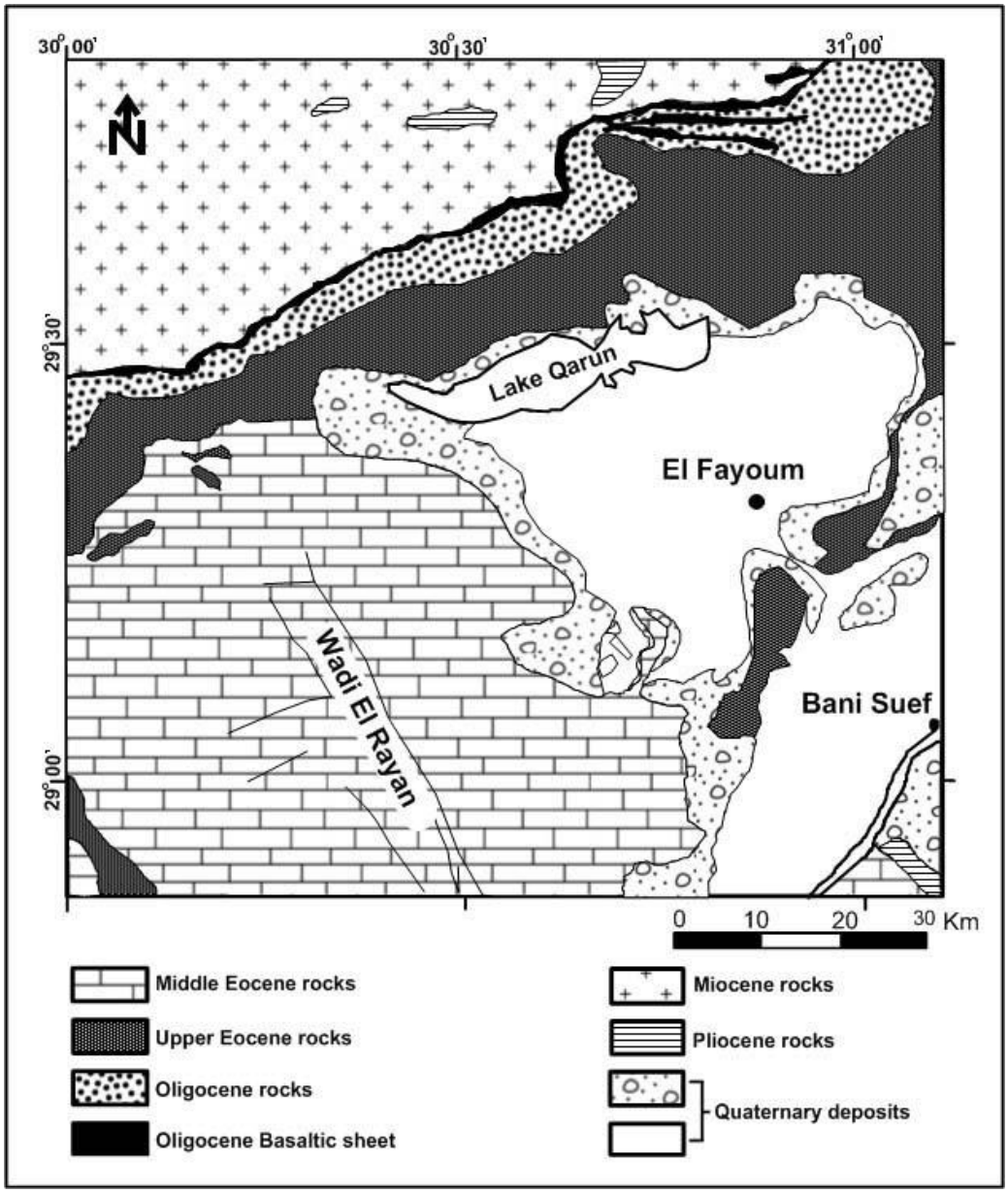

Figure 3. Geological map of Fayoum area (Paper **I**).

3.5. Sampling and analysis

3.5.1. Water

In June 2010, 2011 and 2012, surface water samples at Lake Qarun were collected regularly from 13 sites (Q1–Q13). In June 2012, additional surface water samples from irrigation canals and the drainage network were collected from 29 sites (samples 1–29, Fig. 1). All samples were analyzed for sodium (Na^+), calcium (Ca^{2+}), magnesium (Mg^{2+}), potassium (K^+), sulfate (SO_4^{2-}), chloride (Cl^-) bicarbonate (HCO_3^-) and silica (SiO_2). In June 2012, the water from these sites were also analyzed for nitrate (NO_3^-), phosphorus (PO_4^{3-}), Arsenic (As), copper (Cu), lead (Pb), cadmium (Cd), lithium (Li), cobalt (Co), molybdenum (Mo), chromium (Cr), nickel (Ni), aluminum (Al), manganese (Mn), iron (Fe), selenium (Se), Beryllium (Be), Barium (Ba) and oxygen isotopes ($\delta^{18}O$). In April 2013, water samples from all previous sites were collected for microbiological analysis of total coliform (TC), fecal (thermotolerant) coliform (FC) and *F. streptococcus* (FS).

At all sampling locations, GPS coordinates were recorded. Electrical conductivity (EC), pH and temperature were measured in the field using a SG78-SevenGo Duo pro (pH/Ion/Conductivity) portable meter with an accuracy ± 0.002 pH units, ± 0.5% of full scale EC and ±0.1 °C for temperature. After in situ measurements, the water samples for major ions and (semi-)metal analyses were filtered through a 0.45 µm filter membrane. The filtered samples were transferred into pre-acid-washed polyethylene (PE) containers which divided into three portions: (1) water samples acidified to pH < 2 for all (semi-)metal analysis (the term (semi-)metals is used as a substitute for the longer term "metals and semi-metals"); (2) water samples for main anion analysis and (3) water samples for oxygen isotopes analysis. All sampling containers were left to dry for 2 days after acid or deionized washing. Water samples for microbiological analysis were collected using sterilized dark glass bottles. The PE and glass bottles were filled without air bubbles and tightly capped immediately with PE screw caps. Then the water samples were kept at 4 °C and transported to the laboratory as soon as possible after sampling. Microbiological analysis, HCO_3^- and NO_3^- were conducted immediately after samples reached the lab and the remaining analyses were conducted within the next 24 h. Total dissolved solids (TDS) were calculated using the sum of the major ions (Na^+, K^+, Ca^{2+}, Mg^{2+}, HCO_3^-, SO_4^{2-}, Cl^-, SiO_2 and

NO_3^-), assuming that the fraction below 0.45 µm can be considered "dissolved", which is not exactly true, as constituents commonly attach to (nano-)particles.

Major ions, (semi-)metal and microbiological analyses were carried out at the Water Quality Central Laboratory, Fayoum Drinking Water and Sanitation Company, Fayoum, Egypt. The analyses were conducted in accordance with approved analytic methods APHA [59] as summarized in Table 1. All analytical procedures were accredited according to ISO/IEC 17025. These methods were applied in papers **I**, **II** and **III**.

Table 1

Analytical methods of the studied water samples, after APHA [59] (modified from papers **I–III**)

Analytical parameter	**Method**	**Uncertainty %**
SO_4^{2-}	4500-SO_4^{2-} E	12.9
Cl^-	4500-Cl^- B	4.1
HCO_3^-	2320-B Titration method	1.8
Na^+	3120 B, ICP method by ICP-OES	3.6
K^+	3120 B, ICP method by ICP-OES	5
Mg^{2+}	3120 B, ICP method by ICP-OES	11.6
Ca^{2+}	3120 B, ICP method by ICP-OES	9
SiO_2	4500- SiO_2 C	8.7
NO_3^-	4500-NO_3^- B	–
PO_4^{3-}	4500-P D	–
Al	3120 B, ICP method by ICP-OES	2.2
As	3120 B, ICP method by ICP-OES	3.1
Ba	3120 B, ICP method by ICP-OES	3.1
Be	3120 B, ICP method by ICP-OES	–
Cd	3120 B, ICP method by ICP-OES	5.2
Cr	3120 B, ICP method by ICP-OES	3.8
Co	3120 B, ICP method by ICP-OES	–
Cu	3120 B, ICP method by ICP-OES	3.1
Fe	3120 B, ICP method by ICP-OES	3.5
Pb	3120 B, ICP method by ICP-OES	5
Li	3120 B, ICP method by ICP-OES	–
Mn	3120 B, ICP method by ICP-OES	3.4
Ni	3120 B, ICP method by ICP-OES	3.1
Se	3120 B, ICP method by ICP-OES	3.5
Mo	3120 B, ICP method by ICP-OES	3.3
TC (Total Coliform)	9222 B	15.4
FC (Fecal Coliform)	9222 D	7
FS (*Fecal Streptococcus*)	9230 C	7

The water samples in paper **IV** were analyzed for Na^+, K^+, Mg^{2+}, $SO_4^{2-}$and Cl^-. Potassium and Na^+ were measured by flame atomic absorption spectrometry [59]. Mg^{2+} was analyzed by complexometric titration with EDTA. The SO_4^{2-} was analyzed by the gravimetric method while Cl^- was determined by the potentiometric method [59]. For each brine sample, the analysis for each ion was done in triplicate and the average value was used.

Water samples were analyzed for oxygen isotope composition ($\delta^{18}O$) in papers **I** and **III** using a Gas Bench II system (Thermo Finnigan, Bremen, Germany) coupled with a Thermo Finnigan Delta plus XP isotope ratio mass spectrometer in the stable isotopologues laboratory at McMaster University, Canada. The details of the analytical procedures are described in [60]. All oxygen isotope results were obtained by calculating the mean of the last 10 measurements and normalized using two inter-laboratory water standards (MRSI-1 and MRSI-2). The $\delta^{18}O$ values of the samples were reported normalized to V-SMOW and the precision for replicate sample analyses is $\leq 0.08‰$.

3.5.2. Sediments

As Lake Qarun is a sink for the drainage waters in the Fayoum Governorate, the (semi-)metal content of its sediments was also investigated (Paper **III**). For this purpose, surficial lake sediment samples were collected in June 2010 from the 13 sites Q1–Q13 (Fig. 1). The upper 15 cm of the sediments were taken with a grab sampler, collected in acid-rinsed polyethylene plastic bags and kept at 4 °C. These samples were dried at room temperature and then a nylon-2 mm sieve was used to remove shell fragments and coarse debris. Afterwards the samples were squashed and mildly ground to pass a 63 µm nylon mesh using an agate mortar and pestle. Subsequent analysis of (semi-)metal content was conducted for the < 63 µm grain size fraction. For analysis, the sediment samples were digested using aqua regia and the extractions were analyzed for Fe, Pb, Co, Mn, Cu, Zn, Ni, Cd, Mo, Cr, Al, As, Hg and Sb. The (semi-)metal analysis of sediment was conducted at Viljavuuspalvelu Oy (Soil Analysis Service Ltd), Mikkeli, Finland. Cu, Mn, Al, Fe, Co, V, Mo and Zn were detected with a Thermo Scientific ICAP 6000, while As, Ni, Pb, Sb, Cr and Cd were detected with a PerkinElmer SIMAA6100 GAAS. Hg was

measured with a PerkinElmer Analyst 100 and FIMS 100 instrument. All analytical procedures are accredited by FINAS according to ISO/IEC 17025.

In addition to chemical analyses, grain size analyses were also conducted. After the sediments were air dried at room temperature, 50 g of the sample were taken and treated with 35% H_2O_2 and 1N HCl to remove organic matter and carbonate respectively. After treatment, sediment samples were wet sieved through a 63 µm nylon mesh and the sand fraction (>63 µm) dried and weighed. The remaining fraction of silt and clay (<63 µm) was determined by the pipette method based on the method described in Kroetsch and Wang [61] at Viljavuuspalvelu Oy (Soil Analysis Service Ltd), Mikkeli, Finland.

3.6. Simulated geochemical modeling

A simulated geochemical model evaporation process was carried out using PHREEQC versions 2 and 3 [62, 63] at a constant partial CO_2 pressure of $10^{-3.5}$ and temperature of 25 °C. Whenever water becomes saturated with calcite, gypsum or halite, these solid phases will precipitate and the solution will remain in equilibrium with them. Simulated evaporation of natural waters by PHREEQC is widely used because of its capability of removing moles of water from a solution [63-65]. Merkel and Planer-Friedrich [66] offer a practical guide for modeling natural and contaminated aquatic systems, including useful instructions regarding PHREEQC software. In paper **II**, the modeling concept was that Lake Qarun evolved geochemically through the progressive evaporation of drainage water inflow joined with fractional precipitation of minerals when solution reaches supersaturation with respect to these minerals, assuming that the lake has no outflow except by evaporation. Water samples were selected from the two drains (El-Bats and El-Wadi) as initial solutions which represent the main inflow feeding Lake Qarun system. PHREEQC version 2 with a PHREEQC database [63] was used for modeling. The models were applied to simulate the evolution of 1 L from the El-Bats and El-Wadi drains during evapoconcentration by the removal 95% of water in sequential steps. This concentration factor is considered as reasonable for relatively closed basin systems (such as closed lakes) which have potential annual evapotranspiration exceeds inflow [63, 64]. Moreover, at the final step this concentration factor achieved an ionic strength close to that measured in Lake Qarun ($I \approx 0.63$).

The modeled results, including major ion evolution and mineral saturation indices, were compared with the real results measured in Lake Qarun.

In paper **I**, the simulation was carried out to answer the question; what is the expected evolution of Lake Qarun water under further evaporation? The model was performed using the PHREEQC-3 software program with a Pitzer database [62]. This software was compiled on March 13, 2014. It is a computer program designed to perform a wide variety of aqueous geochemical calculations [62]. One of the new features of the PHREEQC version 3 is the Pitzer aqueous model (Pitzer database), which can be used for concentrated brines of high ionic strengths beyond the range of application of the Debye-Hückel theory [62]. The model was designed to simulate the evaporative concentration of 1 L from Lake Qarun by the removal of 52.5 moles of water in 20 steps (i.e. 94.6% of water removed). Thus the maximum concentration factor allowed by PHREEQC-3 (94.6% of water evaporated), was applied. Other conditions were the same as stated in paper **II**. The output results of the simulated models were compared with Hardie and Eugster's evolutionary model [6] as described above in the introduction.

4. RESULTS AND DISCUSSIONS

4.1. Introductory remarks

All results of the water sample analyses are presented in Appendix I. Samples 1–17 represent water samples collected from irrigation canals whereas samples 18–29 were collected from drainage waters and samples Q1–Q13 from Lake Qarun (Fig. 1). This section discusses the different hydrochemical water types, the main mechanisms controlling the geochemical evolution of surface water in the Fayoum catchment, modeling and crystallization sequence during evaporation of Lake Qarun brine, and water quality evaluation for drinking and agricultural purposes.

4.2. Electrical Conductivity (EC) and Total Dissolved Solids (TDS)

Water salinity, expressed by electrical conductivity (EC) and total dissolved solids (TDS), is an important parameter for fast evaluation of water quality and water geochemistry in the Fayoum watershed. Drainage water in Fayoum Governorate is the secondary source of irrigation because of water scarcity. So water salinity is also used to evaluate the suitability of irrigation and drainage waters for agriculture in the investigation area. Figure 4 shows that the EC and TDS of water increase in the order: irrigation waters < drainage waters <<< lake waters (Paper **III**).

In general, electrical conductivities of drainage waters were higher than those of irrigation waters. One exception was sample 17 from an irrigation canal (3.76 mS/cm), which had the maximum of all irrigation and drainage waters (Appendix I). The plotting of the mean concentrations of Na^+, K^+, Ca^{2+}, Mg^{2+}, Cl- and SO_4^{2-} and of EC, TDS and $\delta^{18}O$ for the different water types (irrigation waters, drainage waters and Lake Qarun waters) showed similar trends where all these parameters increased on the way to Lake Qarun. This indicates that evaporative concentration and dissolution of evaporites were probably the main processes behind the concentration increase of major ions, EC and TDS (Papers **II** and **III**). The characteristic elevation of salinity of sample 17 was possibly due to the water depth, which was too shallow when this sample was taken, and to the fact that the water flows for long distance from sampling site 1 to sampling site 17 (Fig. 1).

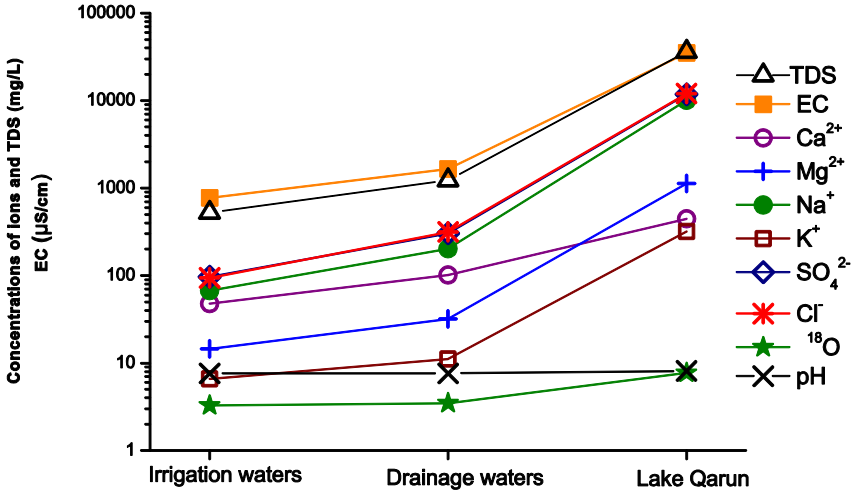

Figure 4. Means plot showing increasing concentrations of Na^+, K^+, Ca^{2+}, Mg^{2+}, Cl^- and SO_4^{2-}, EC, TDS, $\delta^{18}O$ and pH as waters flow towards Lake Qarun (Paper **III**).

Therefore water salinity increased by evaporation. Sample 17 had the highest value of $\delta^{18}O$ (+4.22) of all the irrigation and drainage waters (Appendix I). The $\delta^{18}O$ was concentrated by evaporative concentration [67].

4.3. Hydrochemical evolution of water types in the Fayoum catchment

Based on the Piper plot (Fig. 5), the studied waters can be classified into three types; Ca-Mg-HCO_3 (T1), Ca-Mg-Cl-SO_4 (T2) and Na-Cl (T3). More details about the distribution and characterization of these different water types can be found in Paper **I**. As shown in the Piper plot, the waters evolve from the T1 type at the head waters to the T2 type and eventually the T3 type downstream and at Lake Qarun. This relative increase of SO_4^{2-} and Cl^- compared to HCO_3^- as well as the relative increase of Na^+ compared to Ca^{2+} and Mg^{2+} towards Lake Qarun indicate the presence of evaporites in the investigation area (Paper **I**) [68]. Since the climate of the Fayoum catchment is always dry and hot, dissolved Na^+, Mg^{2+}, Cl^- and SO_4^{2-} concentrations continue to build up in the lake by evaporation with the dominance of Na^+ and Cl^-, while Ca^{2+} and HCO_3^- precipitate as carbonates (Paper **II**).

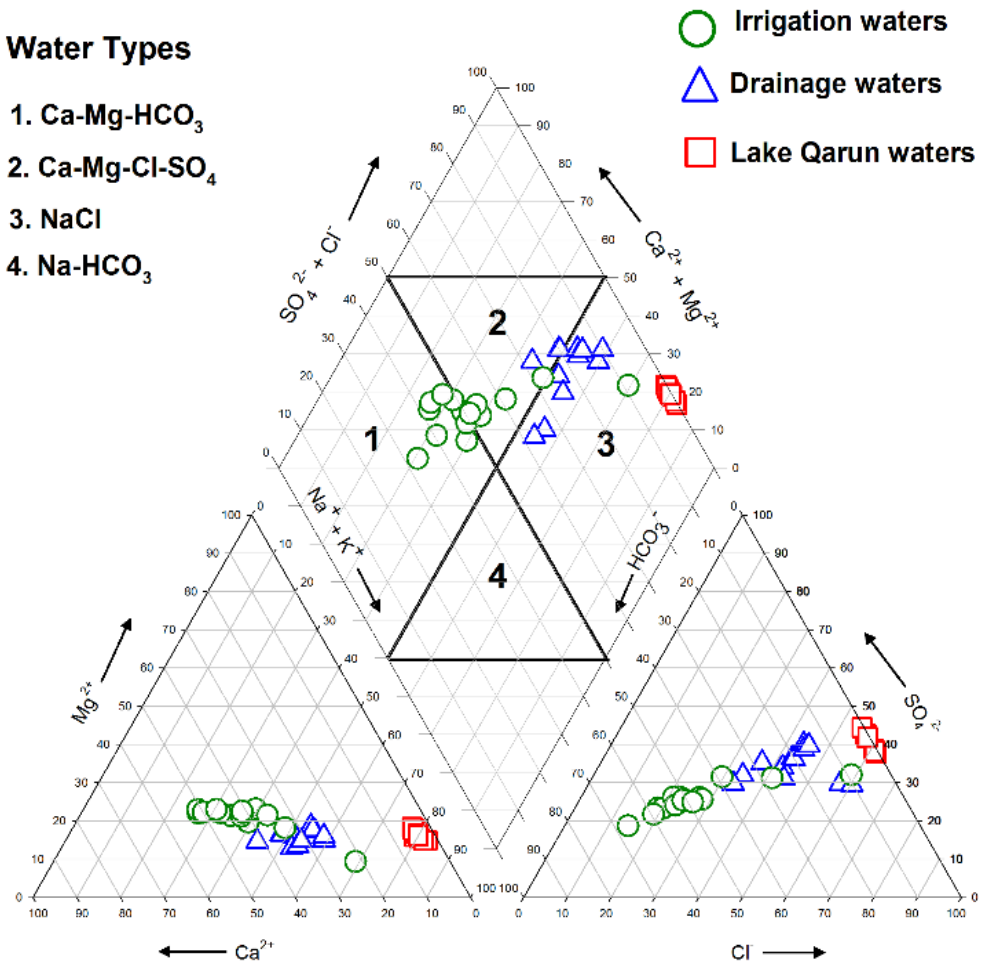

Figure 5. Piper plot of the different water types. The water evolves from a Ca-Mg-HCO3 type at the head waters to Na-Cl downstream and at Lake Qarun passing through the Ca-Mg-Cl-SO4 type (Paper **III**).

To verify the contribution of gypsum and halite dissolution to irrigation and drainage waters of types T2 and T3, binary plotting of [(Ca^{2+} + Mg^{2+}) – 0.5HCO_3^-] against SO_4^{2-} (Fig. 6) and of Na^+ against Cl^- (Fig. 7) was conducted. The contribution of gypsum to the concentration of Ca^{2+} can be estimated by studying the relationship between non-carbonate mineral-derived Ca and Mg using the formula [(Ca^{2+} + Mg^{2+}) - 0.5HCO_3^-] plotted against SO_4^{2-}[69]. The binary plotting of [(Ca^{2+} + Mg^{2+}) - 0.5HCO_3^-] against SO_4^{2-} for all irrigation and drainage waters showed strong positive correlations R^2 = 0.969 and R^2 = 0.785 for T2 and T3, respectively, but a weak correlation R^2 = 0.039 in the case of T1 (Fig. 6). This indicates that dissolution of gypsum probably influences T2 and T3 waters and has no effect on T1 waters. The binary plotting of Na^+ against Cl^- (Fig. 7) for all irrigation and drainage waters showed strong positive correlations in the case of T2 waters (R^2 = 0.957) and T3 waters (R^2 = 0.968) but a weak correlation (R^2 = 0.480) in the case of T1 (Fig. 7). This means that the dissolution of halite along with gypsum controls the chemical evolution of T2 and T3 waters, but does not influence T1 waters.

Mineral equilibrium and saturation indices calculations could predict the reactive mineralogy [70]. The SI of calcite, gypsum and halite for all water samples are given in Figure 8. The results showed that T1 waters are undersaturated with respect to calcite, gypsum and halite. Close to Lake Qarun, most irrigation and T2 and T3 type drainage waters became supersaturated with respect to calcite and still undersaturated with respect to gypsum and halite (Fig. 8). Therefore the dissolution of gypsum and halite is expected to contribute to the solute budget of T2 and T3 waters. Consequently, in the presence of HCO_3^-, the Ca^{2+} ion supplied by gypsum dissolution increases the ion activity product ($a_{Ca}{}^{2+}$ + $a_{CO3}{}^{2-}$) and then increases the saturation index of calcite [71]. This process may explain why the saturation state with respect to calcite changed from undersaturation in the case of T1 to supersaturation for T2 and T3 waters (Fig. 8). After that, all saturation indices for Lake Qarun waters increase due to the effect of evapoconcentration. As the saturation state indicates the direction of the process, precipitation of carbonate minerals accompanied by the dissolution of evaporites such as gypsum and halite may have influenced the chemical evolution of water from Ca–Mg–HCO_3 at locations of T1 type to Ca–Mg–SO_4–Cl at T2 and eventually to Na–Cl downstream and at Lake Qarun (Paper **I**).

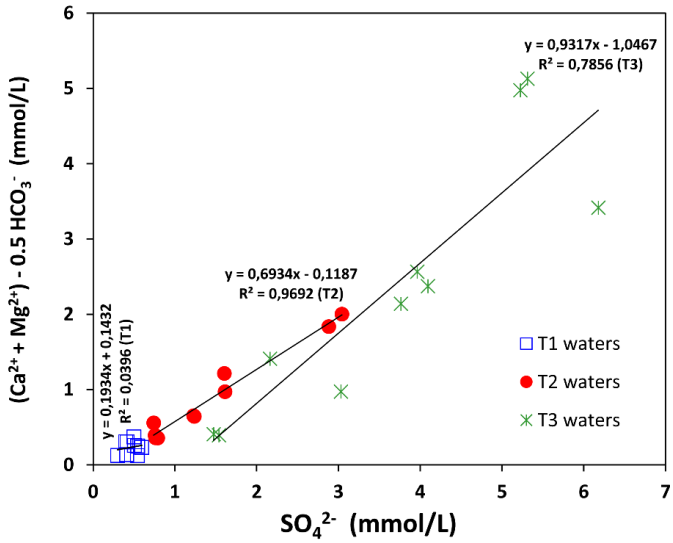

Figure 6. Binary plot of $(Ca^{2+} + Mg^{2+}) - 0.5HCO_3^-$ against SO_4^{2-} of irrigation and drainage waters in the Fayoum Depression showing the contribution of gypsum dissolution to T2 and T3 waters (Paper **I**).

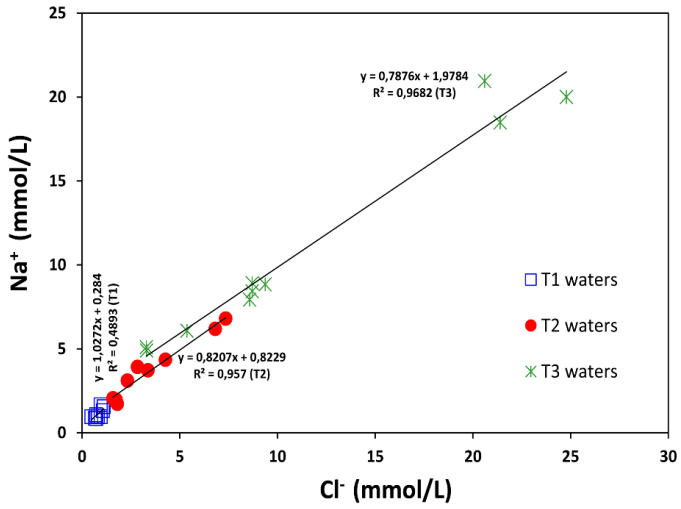

Figure 7. Binary plot of Na^+ versus Cl^- of irrigation and drainage waters showing the significant dissolution effect of NaCl salt on T2 and T3 waters (Paper **I**).

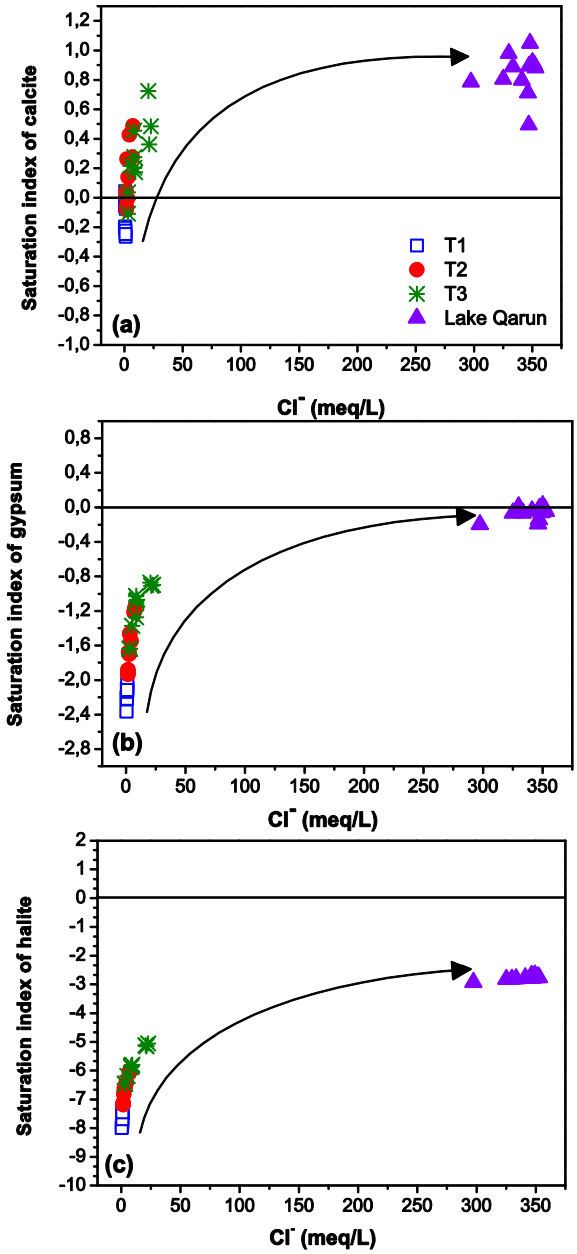

Figure 8. Calculated saturation indices of (a) calcite, (b) gypsum and (c) halite of the water samples. All saturation indices increase towards Lake Qarun due to the effect of evapoconcentration (Paper **I**).

4.4. Mechanisms controlling the water chemistry in the Fayoum catchment

A Gibbs's plot [72] suggested a simple plot of TDS versus the weight ratio of $Na^+/(Na^+ + Ca^{2+})$ could help in understanding the major natural mechanisms controlling surface water chemistry (Fig. 9). A Gibbs plot of data from the investigation area indicates that rock weathering and evaporation-crystallization are the main mechanisms controlling the surface water chemistry. This supports the earlier suggestions that weathering of evaporites has influenced the evolution of water types from carbonate dominance at the head waters to sulfate and chloride dominance downstream (Paper **I**).

Lake Qarun water is characterized by a high Na/(Na + Ca) ratio and a high TDS concentrations, suggesting that it is mainly controlled by an evaporation-crystallization process (Fig. 9). The hot and dry climatic conditions prevailed throughout the area strengthen the evaporation trend from head waters to Lake Qarun as is obvious on Gibbs's model (Fig. 9). Thus, under arid and dry conditions, the continuous evaporation has an obvious effect on the water chemistry of Lake Qarun resulting in both higher levels of Na^+ and Cl^- than those found in the upstream and transition areas and a great increase in the TDS of the lake water (Fig. 9).

Variation in the oxygen isotope composition of water is expected to be a function of evaporative enrichment [67]. Increasing evaporative concentration is reflected by increasing $\delta^{18}O$. Given that $\delta^{18}O$ and TDS are expected largely to increase by evaporation [67], there is a strong positive correlation ($R^2 = 0.99$) between $\delta^{18}O$ and EC (Fig. 10). The rise in the EC values of water along its path from the source at sampling site 1 to Lake Qarun (Fig.1 and Appendix I) and the increase in $\delta^{18}O$ from +3.09‰ at sampling site 1 to > +7‰ at the lake confirm that evaporative concentration is the main mechanism controlling the evolution of lake water. These findings are in good agreement with those of Gibbs's model (Fig. 9).

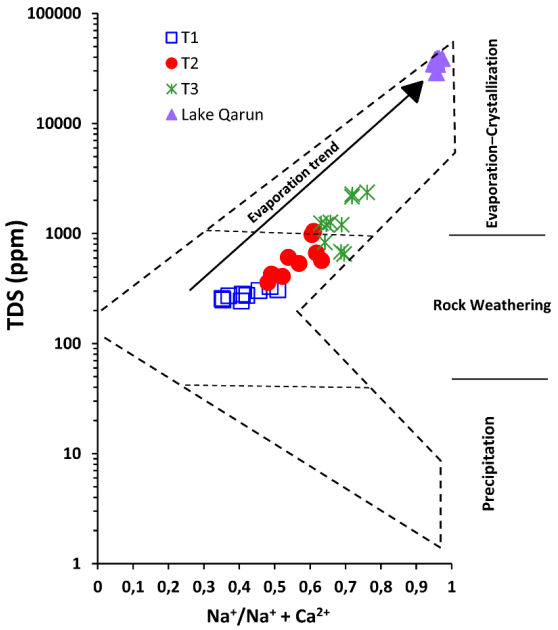

Figure 9. A Gibbs plot showing the mechanisms controlling the major ion composition of the surface water in the Fayoum Depression. Lake Qarun water is mainly controlled by an evaporation-crystallization process (Paper **I**).

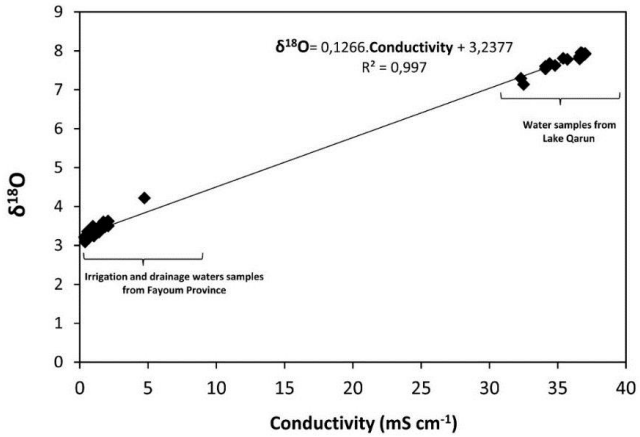

Figure 10. Relation between $\delta^{18}O$ and conductivity of surface water samples collected from the Fayoum Depression. The positive strong correlation reflects the evaporation effect on both TDS and $\delta^{18}O$ values of the surface water in the Fayoum catchment (Paper **I**).

4.5. Geochemical modeling

As evidenced by the Gibbs's plot and $\delta^{18}O$ results, evaporation-crystallization is the main mechanism influencing the geochemical evolution of Lake Qarun water. Two different geochemical models were used for modeling this evaporation process in Lake Qarun; (1) a simulated model using the PHREEQC program and (2) Hardie and Eugster's evolutionary model (Papers **I** and **II**).

4.5.1. Simulation modeling

The modeling hypothesis is that Lake Qarun evolved geochemically through the progressive evaporation of drainage water inflow through the El-Bats and El-Wadi drains accompanied with progressive fractional precipitation of solid mineral phases when solution reaches supersaturation with respect to these minerals (Paper **II**). Selected output modeled results demonstrating the behavior of major ions during the simulated evaporation are shown in Figure 11, while the experimental data of major ions evolution is given in Figure 12. It can be observed that the modeling data (Fig. 11) reproduced the same trends seen in real data (Fig. 12). Results indicate that calcite precipitation caused Na^+, Mg^{2+}, $SO_4^{2-}$and Cl^- to accumulate in the water preferentially over HCO_3^- and Ca^{2+}. Additionally, the calculated saturation indices of calcite, gypsum and halite evolved similarly in the modeled data (Fig. 13) and the real data (see Fig. 8). Indeed, both cases showed: (1) Calcite precipitation, but the saturation limit (SI = 0) was used in the model to control calcite precipitation; (2) Gypsum remains undersaturated at most salinities, but at the latest stages it just reaches saturation state in Lake Qarun, and (3) halite remains undersaturated in all waters. The modeling not only showed similar trends seen in real hydrochemical data, but also produced final concentrations of major ions which are consistent with those observed in Lake Qarun (Appendix **II**). Only minor differences were noted. For example, SO_4^{2-}concentration was higher in Lake Qarun than in the modeled results, which indicates that there is another source of SO_4^{2-} apart from surface drainage water. The excess of SO_4^{2-} ion in lake water is probably originated from groundwater seepage [18, 25].

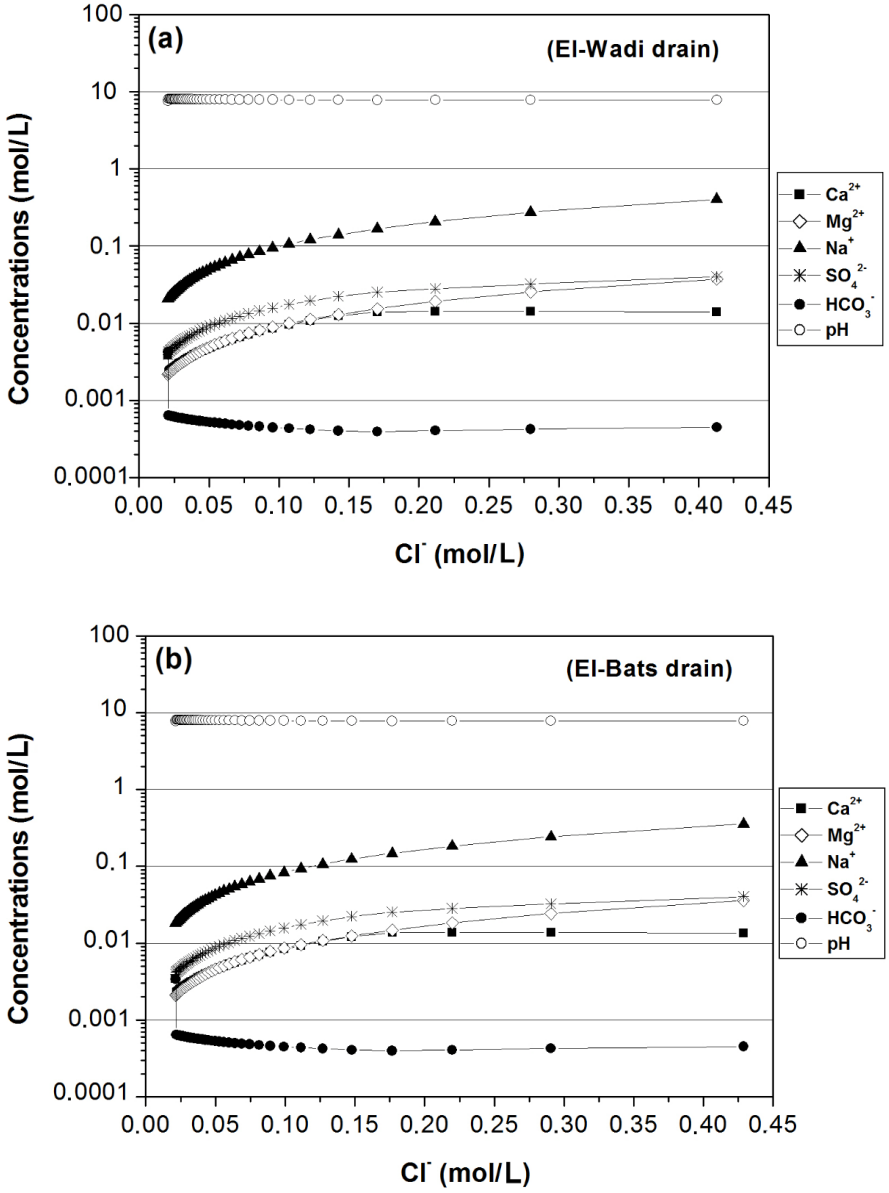

Figure 11. Modeled evaporative concentration of water samples taken from (a) El-Wadi drain and (b) El-Bats drain, in equilibrium with a partial CO_2 pressure of $10^{-3.5}$ atm., using PHREEQC-2 Interactive, in 40 steps. Calcite, gypsum and halite precipitation are allowed (Paper **II**).

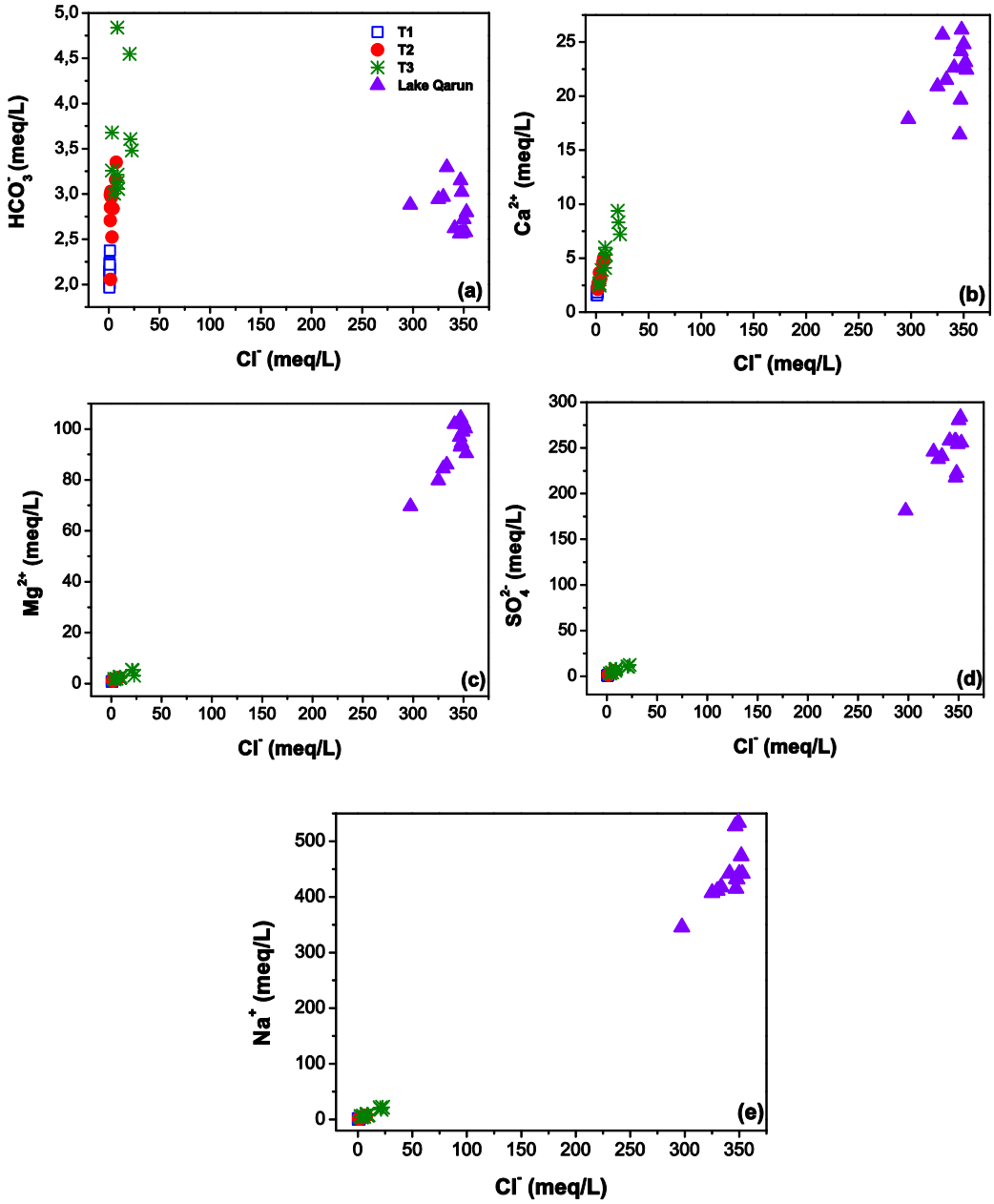

Figure 12. Concentrations of (a) HCO_3, (b) Ca, (c) Mg, (d) SO_4 and (e) Na plotted against Cl for the sampled waters. All ions in Lake Qarun increase with increasing Cl except HCO_3, which was removed as a result of $CaCO_3$ precipitation (Paper **I**).

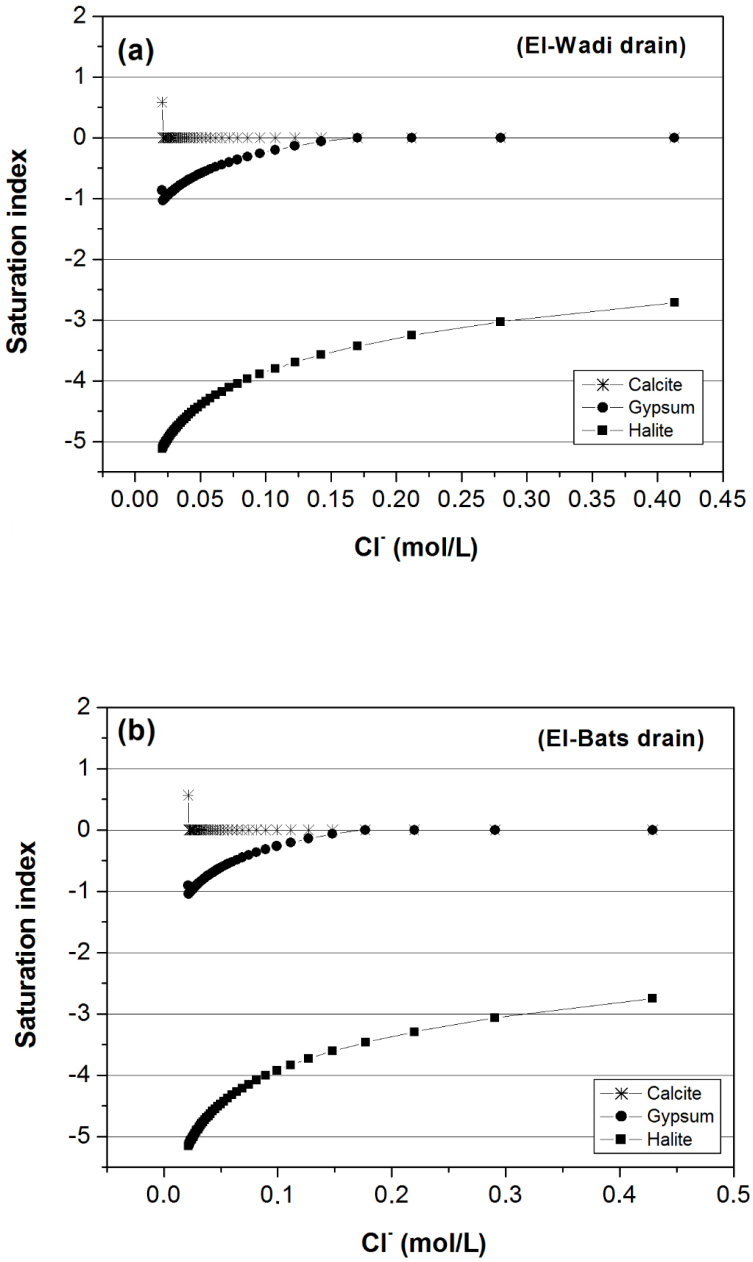

Figure 13. Evolution of mineral saturation indices during an evaporation model by PHREEQC-2 Interactive, in 40 steps. (a) El-Wadi drain and (b) El-Bats drain (Paper **II**).

Furthermore, the maximum alkalinities in Lake Qarun are higher than those predicted by the models. This latter observation reflects the impact of continuous drainage water inflow into the lake with higher HCO_3^- and/or because calcite precipitated more slowly in Lake Qarun than the increase in concentration of $Ca^{2+}$and HCO_3^- as evaporation proceeded [65].

The other simulated evaporation model was used to predict the evolution of Lake Qarun as a result of further progressive evaporation due to either decrease in the water inflow or increase in evaporation rates as a result of potential climate change (global warming). In this simulated model, the lake water was used as an initial solution (Paper **I**). Currently, the lake water is supersaturated with respect to calcite, saturated with respect to gypsum at some locations and undersaturated with respect to halite at all locations (Fig. 8). Also HCO_3^- was depleted during calcite precipitation (Fig. 12). Further evaporation of the lake water as simulated using PHREEQC–3 shows Ca^{2+} is removed due to gypsum precipitation and the final solution should have the composition "Na–Mg–SO_4–Cl" (Fig. 14a). The simulated saturation indices also showed that calcite and gypsum are precipitated and reach equilibrium with the solution during the further evaporation of lake water (Fig. 14b). Calcite precipitation is limited by HCO_3^- while gypsum precipitation is limited by Ca^{2+}. In contrast, the solution reached supersaturation with respect to halite only at the last step of evaporation (Fig. 14b).

4.5.2. Hardie and Eugster's model

Hardie and Eugster's model has been simply modified by Derver [12] (Fig. 15). This modified model is obviously very basic and it is generalized to cover a wide range of starting compositions of the water to be evaporated. In most of natural waters, the first mineral to precipitate, and hence to cause the first chemical divide, is calcite [5-7, 12]. Further evaporation moves the solution along path I or path II depending on whether the concentration level of Ca^{2+} (in equivalents) is higher or lower than the carbonate alkalinity (in equivalents) (Fig. 15). In the present case, close to the head of the Fayoum irrigation system, the waters of type T1 (samples 1–9) have $2mCa^{2+} < mHCO_3^-$ on average. The total average of $mHCO_3^-$ of T1 waters is 2.14 mmol/L while the total average of $2mCa^{2+}$ is 1.77 mmol/L (calculated from data in Appendix 1). This initial composition during evaporation should force the solution to follow path I (Fig. 15).

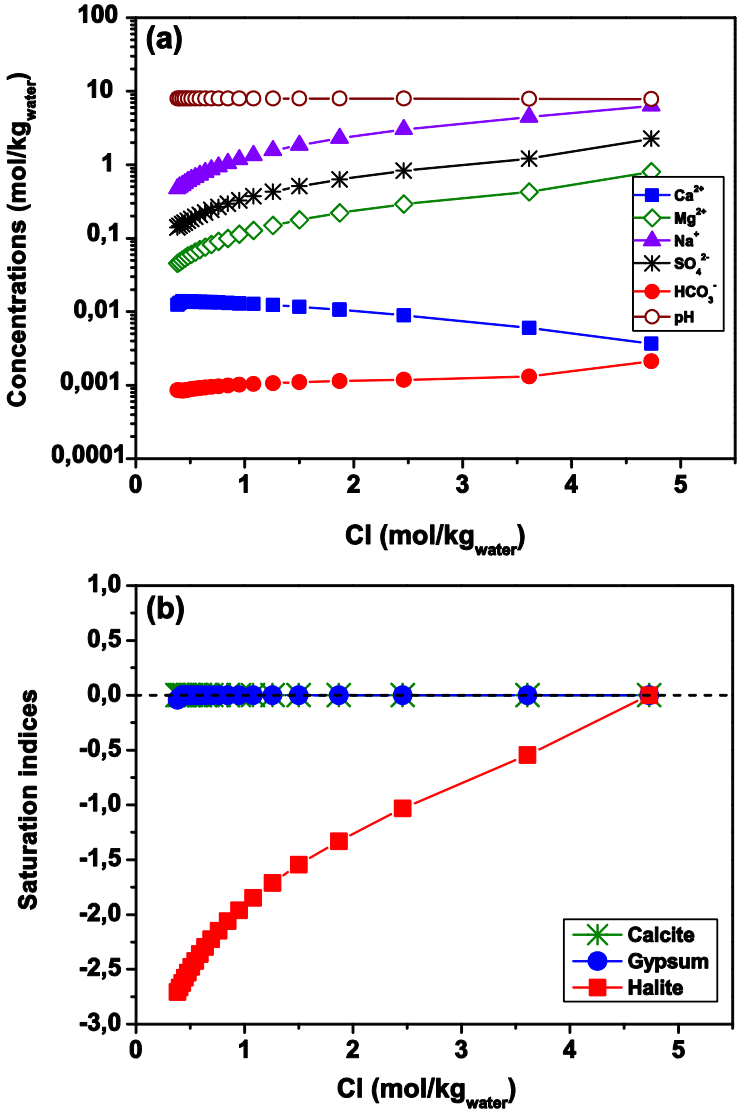

Figure 14. (a) Modelled evaporative concentration of Lake Qarun water in equilibrium with a partial CO_2 pressure of $10^{-3.5}$ atm., using PHREEQC-3. Calcite, gypsum and halite precipitation are permitted. (b) Evolution of mineral saturation indices of calcite, gypsum and halite during a simulated evaporation of Lake Qarun water modeled by PHREEQC-3 (Paper **I**).

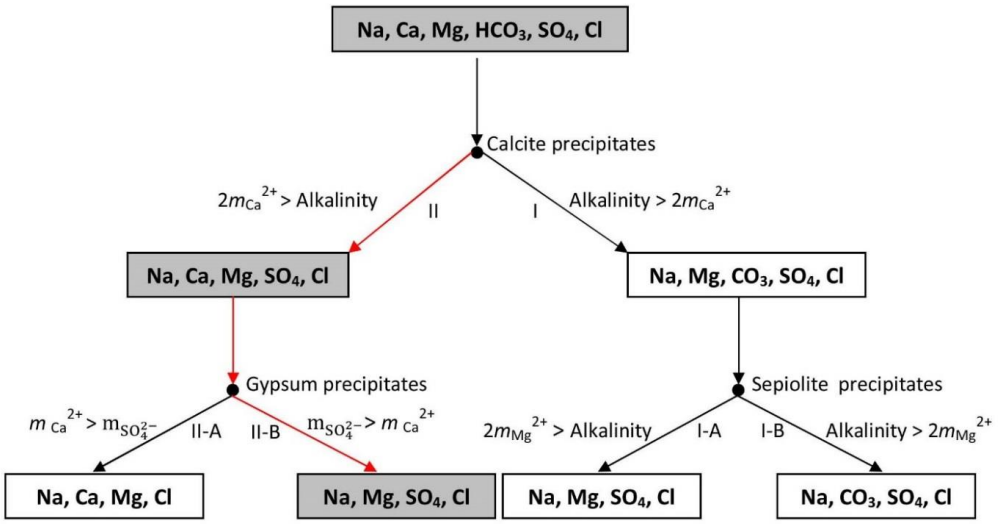

Figure 15. Possible paths during evaporation of natural water (a model modified from Hardie and Eugster [6] by Drever [12]. Lake Qarun water evolves along the path II–IIB (Papers **I** and **II**).

Yet along the flow path of surface water towards Lake Qarun, the Ca^{2+} supplied by gypsum dissolution produced a significant increase in the $2mCa^{2+}/mHCO_3^-$ ratio (Paper **I**). As a result, the average composition of water changed from $2mCa^{2+} < mHCO_3^-$ at the head of the Fayoum irrigation system (T1 waters) to $2mCa^{2+} > mHCO_3^-$ downstream, specifically in the drainage waters at the El-Wadi and El-Bats outlets, which represent the main inflow into the lake (samples 23 and 29, respectively). In both outlets $2mCa^{2+} > mHCO_3^-$ with an average $2mCa^{2+} \approx 5.6$ mmol/L and an average $mHCO_3^-$ of 3.3 mmol/L (calculated from Appendix I). Accordingly, during evaporation, these initial solutions should follow path II (Figs. 15). In Lake Qarun, calcite precipitation (the first chemical divide) causes Ca^{2+} to build up in solution whilst HCO_3^- diminishes and the lake water progressively evolves to $2mCa^{2+} >> mHCO_3^-$ (Papers **I** and **II**). Along path II, the next mineral to precipitate is gypsum, which causes the second chemical divide (Fig. 15). Further evaporation will force the solution to move along path IIA or path IIB depending on whether the Ca^{2+} concentration is greater or lesser than the concentration of SO_4^{2-} (Fig. 15). The current status of Lake Qarun water is $mSO_4^{2-} >> mCa^{2+}$ with an average

$m\mathrm{SO}_4^{2-}/m\mathrm{Ca}^{2+}$ ratio of lake water is ≈11 (calculated from data in Appendix I). This means that the solution will follow path IIB (Fig. 15). The precipitation of gypsum will produce $m\mathrm{SO}_4^{2-}$ >>> $m\mathrm{Ca}^{2+}$ because of the initial excess of SO_4^{2-}over Ca^{+2} in lake water. Continuous potential precipitation of gypsum will remove Ca^{2+} whilst SO_4^{2-} will build up in solution until lake water reaches the final composition "Na–Mg–SO_4–Cl" (Fig. 15). At some locations of Lake Qarun, the water reached saturation state with respect to gypsum (Fig. 8). This suggests that the gypsum divide is second to the calcite divide in Lake Qarun water which supports the assertion that the lake water will evolve along path II→IIB. Gypsum never appears along path I [5]. This also supports our hypothesis that the lake water should evolve following path II rather than path I. Gypsum precipitation is not expected to significantly affect the SO_4^{2-}concentration due to the huge initial excess of SO_4^{2-} over Ca^{2+} in Lake Qarun.

These findings are in significant agreement with the previous results of the simulated evaporation models (Figs. 11, 13 and 14), in which a gypsum divide succeeded a calcite divide during the predicted evolution of Lake Qarun, eventually reaching the final composition "Na–Mg–SO_4–Cl". Accordingly, the simulated model can be used to predict the evolution of Lake Qarun water through time. This can be done by monitoring changes in both climate and the ionic composition of the lake with time and inputting these data into the PHREEQC software to run the simulated model.

4.6. Crystallization sequence during evaporation of Lake Qarun brine

EMISAL was established as an economic project for the recovery of mineral salts from Lake Qarun. The process of salt-extraction in EMISAL is designed to use the solar radiation energy for up-concentration of the brines in the storage ponds via evaporation–crystallization cycles (Paper **IV**). Apart from the economic aspect, this project is also of scientific importance. As discussed above, both the simulation and the Hardie and Eugster's model showed that precipitation of calcite and gypsum contributes to the evolution of lake brine. In addition, halite precipitation was predicted at the latest stages of the PHREEQC simulated evaporation (Fig. 14b). These findings are practically achieved at EMISAL concentration ponds (Paper **IV**). In these ponds, calcite, gypsum and halite are sequentially precipitated during the evaporation of

lake brine (Paper **IV**). This supports the findings of both the PHREEQC and the Hardie and Eugster's evolutionary modeling.

At EMISAL ponds, after the precipitation of halite, the residual brine (bittern) is stored as raw brine for further processing. This bittern is highly concentrated and is rich in K-Mg salts. These salts have high economic value because of their use in various industrial applications. Accordingly, EMISAL planned to extract Epsom salt ($MgSO_4.7H_2O$) from this bittern. In recent studies of seawater evaporation progress, $MgSO_4$–salts are predicted to precipitate after halite [72, 73]. So determination of the crystallization limit between NaCl and the next magnesium sulfate salts will help avoid the co-precipitation of any magnesium sulfate salts as contaminants with halite in NaCl in the crystallization ponds. This will also assist in keeping the $MgSO_4$–salts as dissolved components at a desirable quantity in the residual bittern. It is therefore necessary to study the crystallization path of this residual bittern during evaporation to determine the boundaries between the expected crystallized salts. Modeling the evaporation path with the PHREEQC program has some limitations with this type of bittern because of its high ionic strength [63]. The alternative solution was to use a Jänecke phase diagram involving the system Na–K–Mg–Cl–SO_4–H_2O (Paper **IV**). Pond 2/2 (Fig. 16), one of the NaCl crystallization ponds, was selected to follow the brine evolution during evaporation.

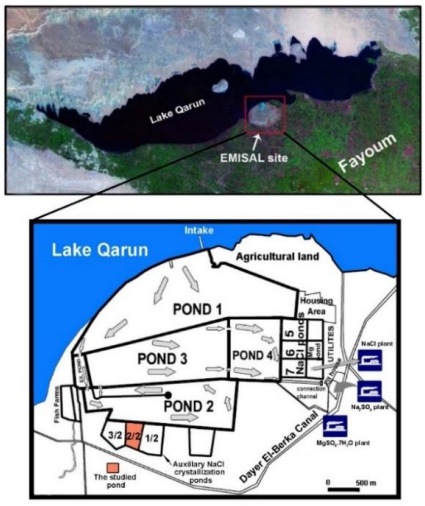

Figure 16. Concentration ponds at the EMISAL site (modified from paper **IV**)

For this purpose field work studies were conducted during solar evaporation together with experimental isothermal evaporation at 35 °C. The study performed on an initial brine had the density 1.246 and composed of Mg^{2+}, Na^{+}, K^{+}, Cl^{-}, and SO_4^{2-} (Paper **IV**). The Jänecke phase diagram at 35 °C involving the system Na–K–Mg–Cl–SO_4–H_2O was used to predict the crystallization path during evaporation of the studied brine (Fig. 17). The Jänecke diagram was set at a temperature of 35 °C rather than at 25 °C to adopt the field work which was done during the summer season under high temperatures and dry conditions (Paper **IV**). The solid phases included in the Jänecke diagram at 35 °C are summarized in Table 2.

Table 2

Solid phases appear in the Jänecke phase diagram at 35 °C during evaporation of brine involving the system Na–K–Mg–Cl–SO_4–H_2O with halite saturation throughout (Paper **IV**).

Name	Chemical composition
Halite	NaCl
Sylvite	KCl
Hexahydrite	$MgSO_4.6H_2O$
Kieserite	$MgSO_4.H_2O$
Glaserite	$K_3Na(SO_4)_2$
Thenardite	Na_2SO_4
Bloedite	$Na_2\,Mg(SO_4)_2.4H_2O$
Kainite	$KMgClSO_4.11/4H_2O$
Leonite	$K_2Mg(SO_4)_2.4H_2O$
Bischofite	$MgCl_2.6H_2O$
Carnallite	$KMgCl_3.6H_2O$

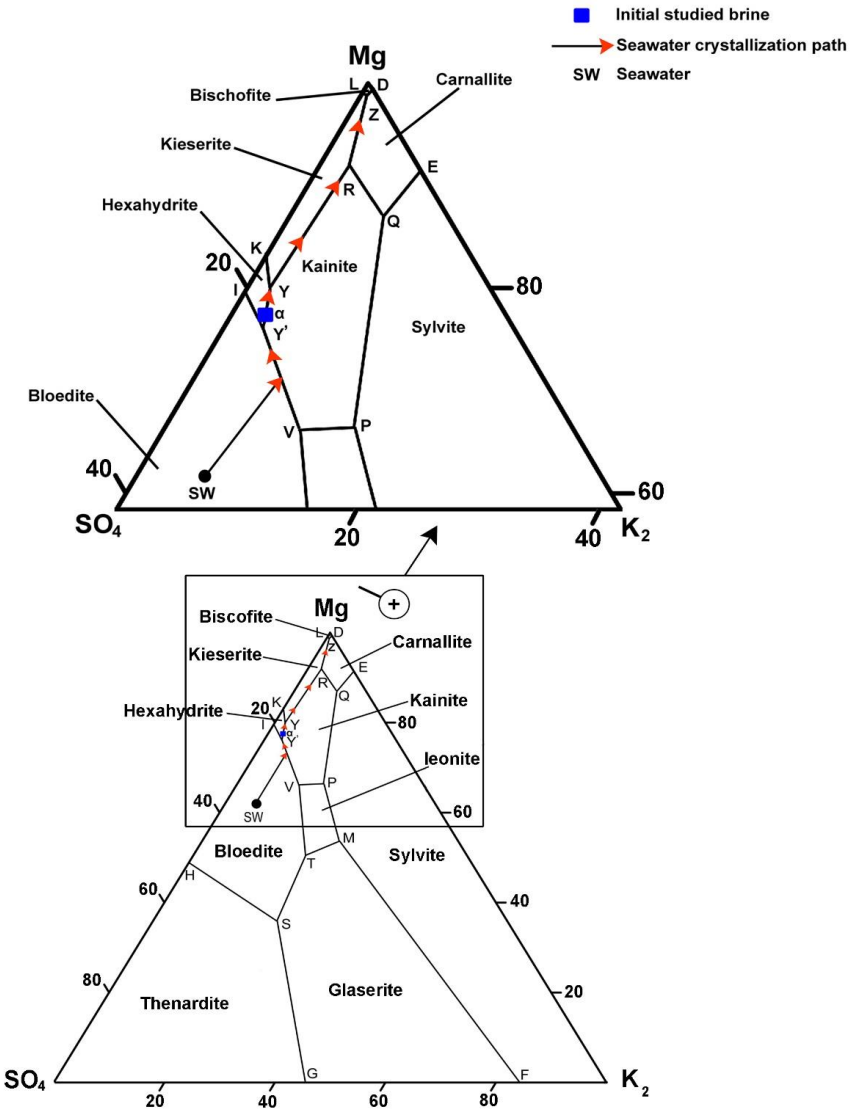

Figure 17. Location of the studied initial brine on the Jänecke phase diagram at 35 °C involving the system Na–K–Mg–Cl–SO_4–H_2O with halite saturation throughout. The diagram and the seawater crystallization path are redrawn from Usdowski and Dietzel [75] and Bąbel and Schreiber [73] (Paper **IV**).

The location of the Jänecke coordinates (mole ∑ K_2 + Mg + SO_4 = 100) of the initial brine on the Jänecke phase diagram at 35 °C is the primary step to predict the crystallization path during evaporation of the studied brine (Fig. 17). In the case when the solution reaches the drying-up point (Z), the crystallization path should follow the line ″α–Y–R–Z″ and minerals should appear in sequence as follows (Fig. 17):

″α″: halite

″α–Y″: halite + hexahydrite + kainite

″Y–R″: halite + kieserite + kainite

″R–Z″: halite + kieserite + carnallite

″Z″: halite + kieserite + carnallite + bischofite

The graphical representation of Jänecke coordinates K_2, Mg and SO_4 of the studied brine during its experimental evaporation in the lab and also during solar evaporation at the studied EMISAL is given in Figure 18. As shown in this figure, the experimental and solar crystallization paths both showed good agreement with the paths predicted. Both paths overlap the predicted crystallization path along the segment "α–Y–R–Z" which follows the path seawater crystallization (Fig. 18). In both cases, however, the evaporation process stopped at points "X" and "X*" for experimental evaporation and solar evaporation, respectively, and neither of them reached point "Z" (Fig. 18). This was perhaps because at some extreme high-salinity conditions and above a critical concentrations the brine becomes hygroscopic and adsorbs humidity from the air rather than drying [73]. In both cases, the real mineral crystallization sequences should be precipitated according to the obtained experimental path ″α–Y–X″ and/or the solar evaporation path ″α–Y–X*″ (Fig. 18). Along both paths, the solid phases precipitated from solution should appear as follows:

″α″: halite

″α–Y″: halite + hexahydrite + kainite

″Y–X″ or ″Y–X*″: halite + kieserite + kainite

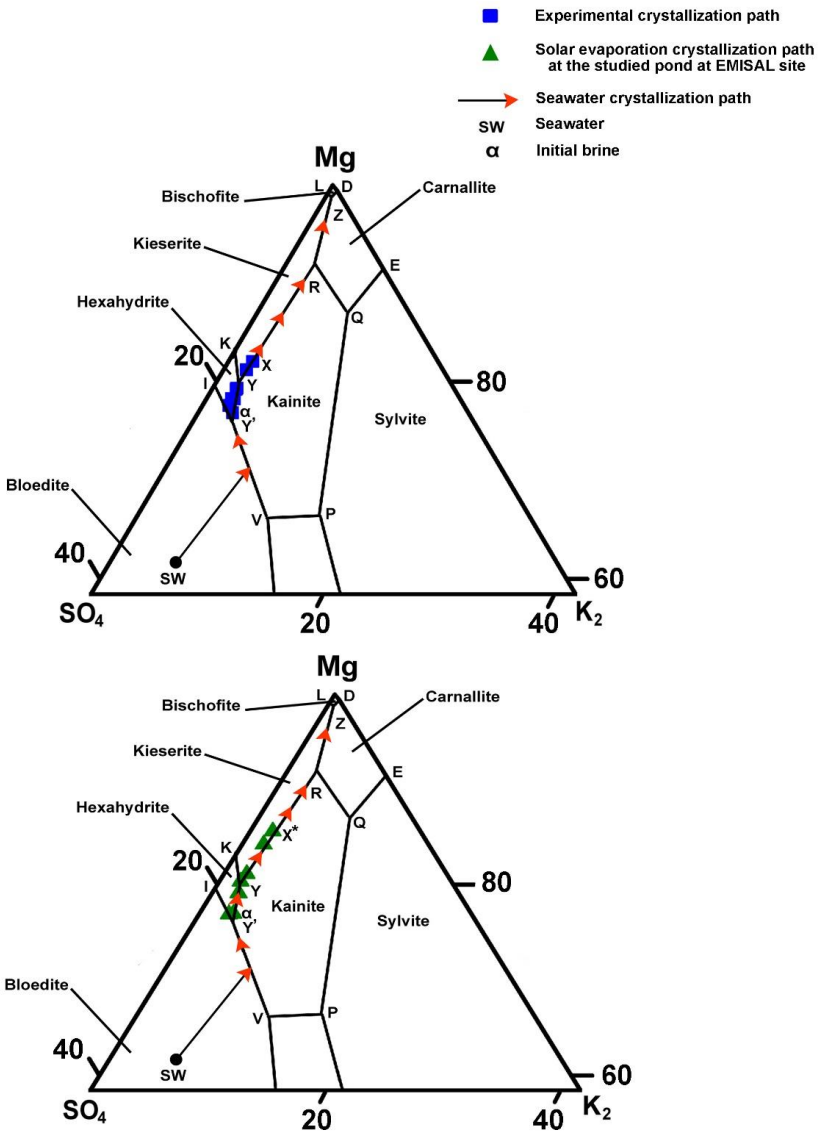

Figure 18. Graphical representations of the Jänecke coordinates (mole Σ K_2 + Mg + SO_4 =100) on the Jänecke phase diagram at 35 °C showing (i) experimental crystallization path and (ii) solar evaporation crystallization path (Paper **IV**).

In both cases the real collected salt phases during brine evaporation showed the presence of halite and hexahydrite only, while kainite and kieserite phases had disappeared (Fig. 19). The absence of kainite is probably due to its metastability [76, 77]. The absence of primary kainite has often been demonstrated by difficulties in nucleating kainite during evaporative concentration [76]. Alternatively, the absence of kieserite is attributed to the fact that relative humidity (RH) in the field and in the lab was higher than the RH required for the formation of kieserite. According to the phase diagram of the $MgSO_4 + nH_2O$ system (Fig. 20), at 35 °C, hexahydrite is the only stable phase at RH ≈ 50%–65% while kieserite is only stable at RH < 50% at the same temperature [78]. In the present study, the RH in the lab was adjusted to 55% throughout the experimental isothermal evaporation at 35 °C. In contrast, at the EMISAL site, during July and August 2011, the RH was recorded at 51% and 55% and the temperatures recorded were 37.1 and 36.8, respectively. At these periods, the crystallization of the second sequence by solar evaporation (at densities of 1.301–1.330) was achieved with precipitation of hexahydrite ($MgSO_4.6H_2O$) only rather than kieserite ($MgSO_4.H_2O$) or epsomite ($MgSO_4.7H_2O$). Kieserite is more stable at lower RH and/or higher temperature (Fig. 20). In addition, kieserite can be altered to hexahydrite easily as humidity increases by hydration while hexahydrite is not easily reverted to kieserite on dehydration [79]. This makes the study of the phases in the $MgSO_4.nH_2O$ system very important in the interpretation of the history of water on Mars [79]. This also means that the presence of these deposits in ancient evaporites can be used as sensitive indicator of past climatic changes. Another possible reason for the absence of kieserite is that the supersaturation required for precipitation of magnesium sulfate salts with water molecules lesser than six molecules for each Mg^{2+} ion (i.e. kieserite) decreases with increasing concentrations of the solution [80].

Technically, based on the crystallization sequence (Paper **IV**), the residual brine after halite crystallization should be pumped from the halite crystallization storage pond (pond 2/2) at a density of ≈ 1.300. This helps prevent $MgSO_4$–salts precipitating as contaminants with NaCl in the crystallization pond (pond 2/2). Furthermore, at this density, pumping out the residual brine keeps most of the magnesium sulfate salts dissolved in it, which enables production at its designated capacity without any loss of quantity in the NaCl pond.

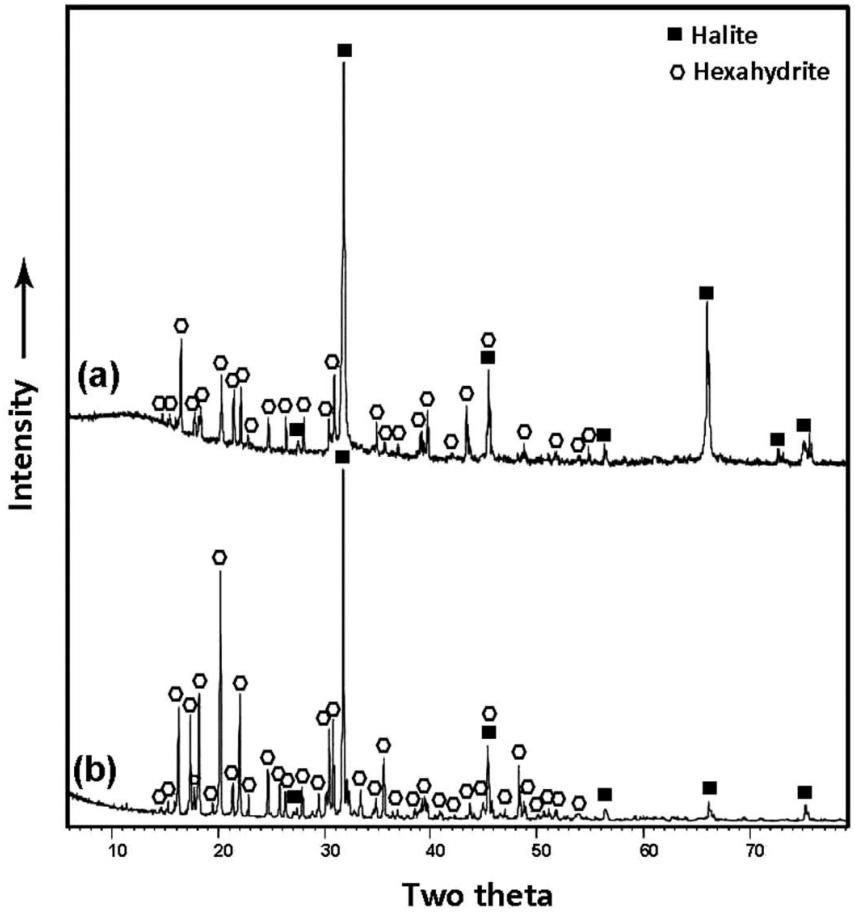

Figure 19. XRD pattern of hexahydrite and halite salts that were precipitated through (a) experimental isothermal evaporation at 35 °C and (b) solar evaporation at the studied pond at EMISAL (Paper **IV**)

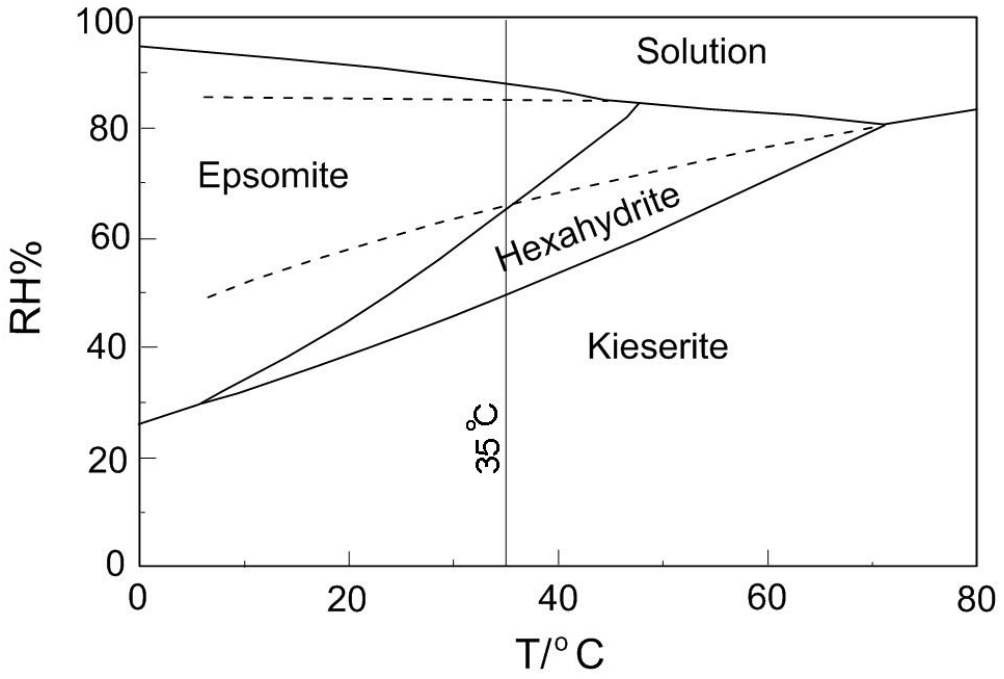

Figure 20. RH–T phase diagram of $MgSO_4$ + H_2O with the deliquescence-crystallization equilibria of epsomite, hexahydrite, and kieserite; dashed curves represent the metastable deliquescence humidities of kieserite and hexahydrite (modified after Steiger and Linnow [78]).

4.7. Water quality in the Fayoum catchment (Paper III)

Population growth, competition for water from upper Nile basin countries, potential climate change and pollution are threatening water security in Egypt. To assess the influence of these factors on the quantity and quality of drinking and irrigation water, monitoring the Egyptian Governorates is of crucial importance. The Fayoum Governorate was selected for this research. A total of 42 water samples from irrigation and drainage canals as well as Lake Qarun were collected (Fig. 1). Major ions, (semi-)metals, nutrients, salinity and microbiological parameters were examined.

4.7.1. Major ions and (semi-)metals in the studied waters

The mean concentrations of the major ions Na^+, K^+, Ca^{2+}, Mg^{2+}, SO_4^{2-} and Cl^- increased in the order irrigation waters < drainage waters <<< lake waters (see Fig. 4) and followed the trend of the EC. In contrast, the mean concentration of HCO_3^- decreased in in the order drainage waters > lake water > irrigation water while the mean concentration of SiO_2 decreased from drainage waters > lake water ≥ irrigation water (Fig. 21).

The metals Al, Ba, Cr, Co, Cu, Ni, Fe, Li and Mn were detected with different concentrations in all waters with the highest mean concentrations in drainage waters and lowest in Lake Qarun. One exception is Li, which had the highest mean concentration in Lake Qarun (Fig. 21). Mn was measured below the detection limit in the irrigation waters, detected in some drainage waters and detected in lower concentrations in the lake water. All the other (semi-)metals (As, Be, Cd, Pb and Se) were below their respective detection limits. In general, the mean concentrations of the metals Al, Ba, Cr, Co, Cu, Ni, Fe and Mn were in the order drainage waters > irrigation waters > lake water (Fig. 21). In the irrigation water samples, the highest concentrations of Al, Ba, Cr, Co, Fe and Ni were observed at sampling site 13 (Appendix I). Yet drainage water at sampling site 22 had the highest concentrations of Al, Cr, Co and Fe.

Mechanisms governing the chemical composition and behavior of the studied waters were assessed by finding interrelationships and identifying co-variations of parameters, using a Principal Component Analysis (PCA) with SPSS® 21 (Fig. 22).

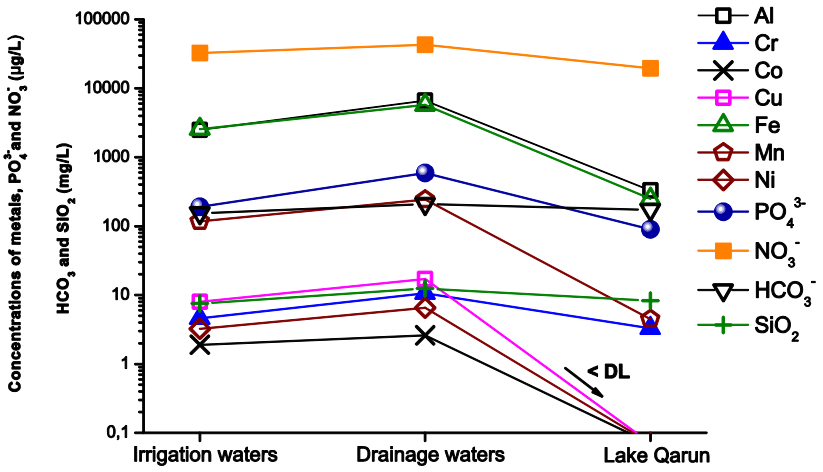

Figure 21. Means plot showing the behavior of Al, Fe, Co, Ni, Cu, Mn, NO_3^-, PO_4^{3-}, HCO_3^- and SiO_2 with the highest values in drainage waters and lowest values in Lake Qarun. ″< DL″ means that Cu, Ni and Co are below detection limits in Lake Qarun (Paper **III**).

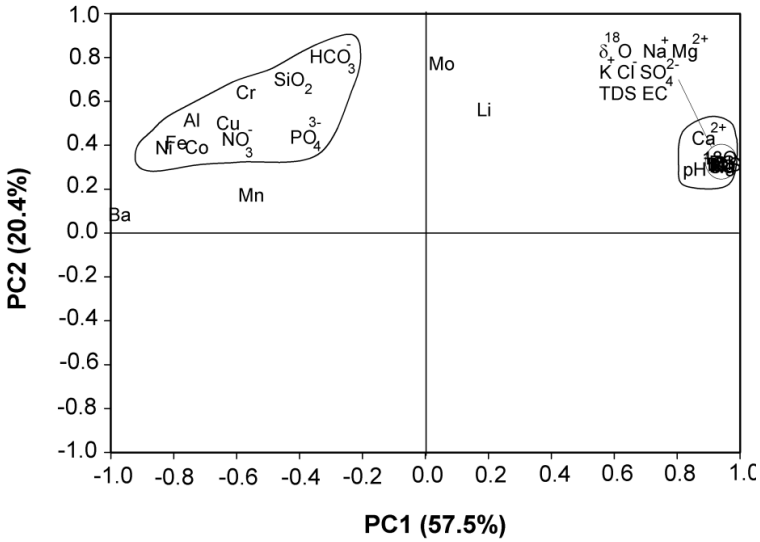

Figure 22. Principal component analysis (PC2 *vs* PC1) of the investigated parameters in all studied waters. The first component (PC1) represents 57.5% of total variations, the second component (PC2) another 20.4% of the total variation in all data. Two distinct parameter assemblages can be identified and are discussed in the text (Paper **III**).

PCA can provide a clarifying view of the parameter interrelationships. Therefore this analysis was carried out with the complete set of measured parameters of all samples (Appendix I).

Despite considerable parameter variations between individual samples, the first two principal components (PC1 & PC2) of the PCA represent 77.9% of the total variances in the irrigation, drainage and lake waters (Fig. 22). Two interrelated groups can be identified by the PCA. The first one consists of the major ions Na^+, K^+, Ca^{2+}, Mg^{2+}, Cl^- and SO_4^{2-} as well as EC, TDS, $\delta^{18}O$ and pH. The co-location of these major ions with EC, TDS and $\delta^{18}O$ indicates that they are similarly hydrogeochemically controlled, which can be seen by the evaporative concentration process. Yet dissolution of evaporites can also contribute to the concentrations of these ions in drainage waters.

The initial pH of the solution at equilibrium can be calculated by the following equations [81]:

$CO_{2(g)} + H_2O \rightleftharpoons HCO_3^- + H^+$ $\quad K_H K_1$

$$\{H^+\} = \frac{K_H K_1 p_{CO_2}}{\{HCO_3^-\}}$$

Where K_1 is the dissociation constant of H_2CO_3, K_H is the equilibrium constant of the CO_2 solubility in water.

Yet during evaporation evolution, the co-existence of pH with Na^+, K^+, Ca^{2+}, Mg^{2+}, Cl^-, SO_4^{2-}, EC, TDS and $\delta^{18}O$ while HCO_3^- is located on the opposite side of the PC-plot can be explained by the following equation [82]:

$$2HCO_3^- \rightarrow CO_3^{2-} + CO_{2(g)} \uparrow + H_2O$$

This mechanism, where CO_2 is degassing from the lake, explains the pH increase associated with the concentration of evaporites in alkaline lakes whereas the carbonate alkalinity (HCO_3^- + $2CO_3^{2-}$) remains unaltered [64,82]. Total carbonate (HCO_3^- + CO_3^{2-}) decreases in closed saline lakes due to degassing and carbonate mineral precipitation [83]. The presence of Ca^{2+} independently of HCO_3^- is possibly due to the initial excess of Ca^{2+} relative to HCO_3^- in the inflowing drainage waters to Lake Qarun. In addition, through $CaCO_3$ precipitation, the HCO_3^- is depleted while unreacted Ca^{2+} builds up in solution (Paper **II**). The plotting of the mean concentrations of Na^+, K^+, Ca^{2+}, Mg^{2+}, Cl^- and SO_4^{2-}as well as EC, TDS, $\delta^{18}O$ and pH for the

different water types (irrigation waters, drainage waters and Lake Qarun waters) showed similar trends where all these parameters increased on the way to Lake Qarun (Fig. 4). This explains why these parameters plot together on the PC plot (Fig. 22).

The second assemblage of parameters that plot in the same area of the PC plot are Al, Fe, Co, Ni, Cu, Mn, NO_3^-, PO_4^{3-}, HCO_3^- and SiO_2 (Fig. 22), which indicates a similar geochemical development, processes or sources. These increase from irrigation waters to drainage waters and decrease in Lake Qarun (Fig. 21). The presence of NO_3^- and PO_4^{3-} in this group indicates the contribution of fertilizers to the water chemistry whilst SiO_2 and HCO_3^- most likely indicate the weathering of clay and silicate minerals from the soils. Lake Qarun is the main sink of all constituents carried by the drainage water inlets. Adsorption of metals on the surface of lake sediments under alkaline conditions is possibly the main mechanism behind the depletion of these metals in the lake water. In addition, the presence of pH on the opposite side to metals on the PC plot reflects the negative relationship between the mobility of these metals and pH in Lake Qarun (Fig. 22).

Cluster analysis (CA) was applied to group similar water sampling sites (spatial variability) based on the measured physiochemical parameters. Hierarchical agglomerative CA was performed by SPSS® using Between-Groups Linkage with Euclidean distances as a measure of similarity. The dendrogram of the sampling sites (Fig. 23) shows that there are two distinct groups. Group 1 consists of the Lake Qarun sampling sites (Q1–Q13). These are sampling sites that have lower concentrations of Al, Fe, Cr, Co, Ni, Cu, Mn, SiO_2, HCO_3^-, $PO_4^{3-}$and NO_3^- and higher concentrations of Na^+, K^+, Ca^{2+}, Mg^{2+}, Cl^-, SO_4^{2-}, EC, TDS, $\delta^{18}O$ and pH. Group 2 consists of irrigation and drainage water sites which have higher concentrations of Al, Fe, Cr, Co, Ni, Cu, Mn, SiO_2, HCO_3^-, PO_4^{3-} and NO_3^- and lower concentrations of Na^+, K^+, Ca^{2+}, Mg^{2+}, Cl^-, SO_4^{2-}, EC, TDS, $\delta^{18}O$ and pH than sites in Group 1. Group 2 can be subdivided further into drainage (Group 2A, except irrigation water site 13) and irrigation water sites (Group 2B, except drainage water sites 18, 19, 24, 25 and 27). The cluster classifications varied with significance levels between Group 1, Sub-Group 2A and Sub-Group 2B.

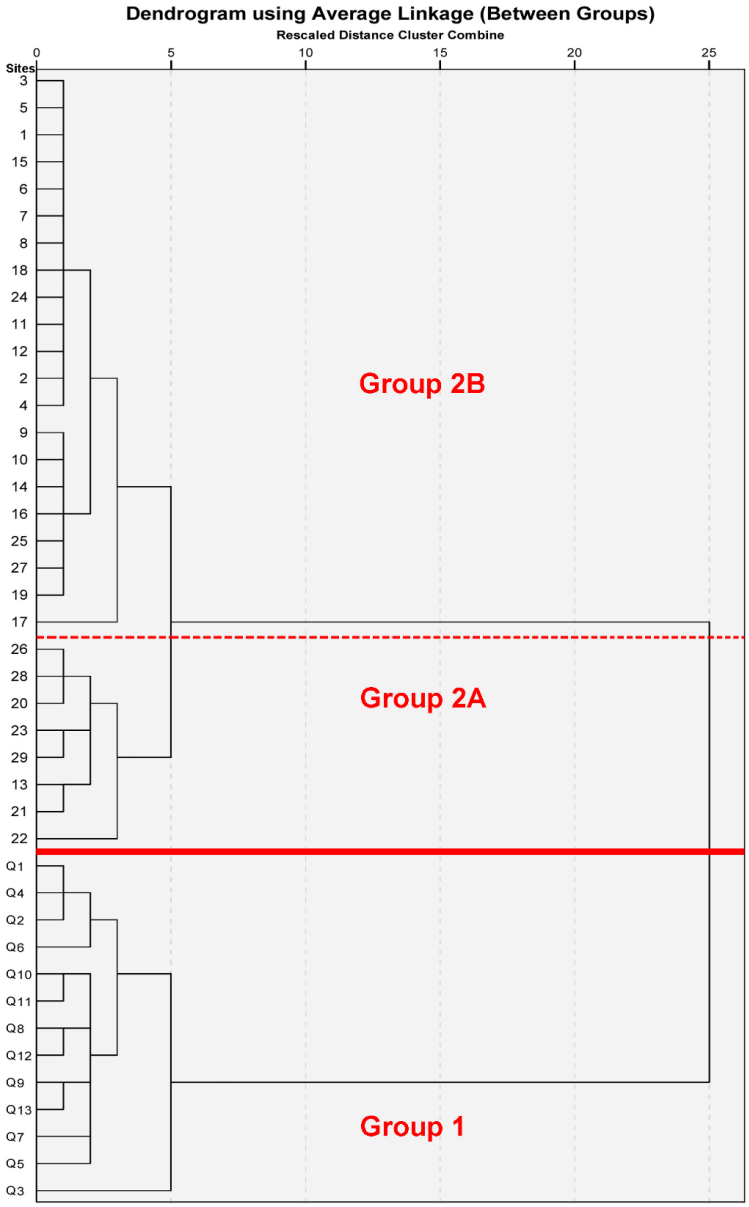

Figure 23. Cluster analysis dendrogram of the sampled waters. Group 1 consists of Lake Qarun water and Group 2 of irrigation and drainage waters (Paper **III**).

This is also confirmed by the significant differences in mean values of the relevant parameters between irrigation waters, drainage waters and Lake Qarun waters demonstrated by means plot (Figs. 4 and 21). The location of site 13 in Sub-Group 2A indicates that this site has chemical characteristics similar to drainage waters. In fact the highest concentrations of Al, Cr, Co, Cu, Fe and Ni in irrigation waters were recorded at that site and these concentrations are similar to those of drainage waters. This is an indication that location 13 is affected by pollution from the Sinnuris wastewater treatment plant or from another source. In contrast, the drainage waters (sites 18, 19, 24, 25 and 27) plotting in irrigation waters Sub-Group 2B is probably due to: (1) Locations of some sites such as 18, 19 and 24 at the head of a drainage system (Fig. 1) having comparably lower concentrations of Al, Fe, Cr, Co, and Ba. (2) At some regions in Fayoum (e.g. sites 25 and 27), a mixture of brackish drainage water and fresh irrigation water is used for irrigation due to the water scarcity in the catchment. This can cause dilution of the dissolved trace metals and consequently give the samples a similar chemical fingerprint.

In Group 1, sample Q3 differs from the other lake samples, which might be due to the position of this site close to the El-Bats drain mouth outlet and consequently a drainage water influence (Fig. 1). In Sub-Group 2A, site 22 is different from the others, which is due to a substantial enrichment of Al, Cr, Co, Fe and Ni at site 22 (Appendix I). In Sub-Group 2B, site 17 is distinct from other sites in the same group because this site has the highest TDS and EC of all the irrigation and drainage waters.

4.7.2. Microbiological criteria

Results of bacterial analysis are an indicator of water quality in many ways. Total Coliform bacteria (TC) in drinking water can cause severe human illness, but their existence in large quantities is mainly used to assess potential for the occurrence of other more infectious pathogens associated with sewage. The presence of TC bacteria can be used as indicator for the potential presence of fecal and disease-causing bacteria [83]. FC and FS are bacteria whose presence indicates contamination of waters with human or animal waste [84]. For ideal protection of human health, drinking water should not have any pathogenic microorganisms or any bacteria indicative of fecal pollution [85]. Yet all irrigation waters in the investigated area, which are used as drinking water in rural regions without treatment, contain TC, FC and FS

(Appendix I). Effluents from sewage and wastewater treatment plants and agricultural fields result in elevated levels of bacteria in drainage waters. Drainage water sampling site 25 contains the highest levels of TC and FC in this water type, which is most likely due to its location near a sewage treatment plant and receiving agriculture returns from nearby meadows. Yet irrigation waters also contain higher levels of pathogens (Appendix I) because some households discharge their sewage directly into the irrigation canals. Moreover, improper disposal of sewage or on-site sanitation tank overflows into these canals is common in the investigation area. Irrigation water sampling site 11, for example, has the highest level of FS and was sampled very close to household pipe outlets. Most households discard their garbage and dead animals in the drains and irrigation canals, which consequently increases the contamination levels of all bacterial species. This has very serious health implications especially when untreated water from these canals is used as drinking water. The IOB [86] stated that most of the prevalent diseases in the Fayoum watershed are water borne and result from people being exposed to contaminants by standing in the water during irrigation or by swimming, which was quite often observed in the course of the field work, where even children were swimming in these polluted canals. Furthermore, indirect infection due to transferring disease-causing organisms (pathogens) into the crops and vegetables can also cause diseases.

The lowest levels of TC, FC and FS were recorded in Lake Qarun waters. This is probably due to the higher salinity and alkalinity of the lake water, which is unfavorable for the organisms.

4.7.3. Evaluation of water quality for drinking and irrigation

Both irrigation and drainage waters are discussed in this section. Lake Qarun water, because of its salinity, is used neither for irrigation nor for drinking and therefore it is not further considered here.

Due to water scarcity, the reuse of drainage waters for irrigation is quite common in the Fayoum Governorate. In addition, water in irrigation canals is used for both irrigation and drinking as not all households are connected to tap water networks. Moreover, low water pressure is the most common problem throughout the water network and distribution system in Fayoum [86]. As a result, some people alternatively use water from irrigation canals, carts with

water tanks and groundwater wells for domestic purposes [86]. This results in many people using untreated water from irrigation canals as drinking water. Accordingly, irrigation canal water quality monitoring and evaluation against the world drinking water standards are vital tasks in the Fayoum Governorate.

4.7.3.1. Drinking water quality

Irrigation water used for drinking should be evaluated against drinking water quality standards. Based on the World Health Organization (WHO) [87] guidelines (Appendix I), the studied irrigation waters (samples1–17) were found to have acceptable concentrations of Ba, Cr, Cu, Mn, Ni and Mo. In the case of NO_3^-, most waters, except at sampling sites 11, 12, 13 and 16, were below the guideline concentrations. The higher concentrations of NO_3^- in the irrigation canals are mostly from anthropogenic sources.

Nearly all irrigation canal samples have higher concentrations of Al than the WHO recommends (Appendix I). Elevated concentrations of Al in drinking water can be harmful and a study in the USA showed that mean Al concentrations in treated water of facilities using an Al sulfate coagulant reached up to 1300 µg/L [88]. Some epidemiological studies even suggest a possible association between Al in drinking water and Alzheimer's disease [88]. The Nile water at site 1, which represents the source water to the Fayoum watershed, has an Al concentration of 1980 µg/L. This concentration increases as the water runs through the watershed due to the fact that Al sulfate salts are used as coagulants in drinking water treatment plants, causing increased Al concentrations in public water supplies. This also increases the Al concentrations in household sewage. Moreover, the sludges from the coagulation process are disposed of along the banks of the irrigation canals, which are then eroded and further increase the Al concentrations in the water. The high Al concentration at sampling site 13 (8350 µg/L) is probably due to its proximity to the effluents from a sewage water treatment plant.

Regarding bacterial contamination, the water in in the irrigation canals contains substantially elevated levels of TC, FC and FS bacteria which are presented in the current study for the first time. Consequently, these waters are harmful and present serious health risks. IOB [86] monitored the prevalence of water-borne diseases such as enteritis or intestinal protozoans and of vectors such as bilharzia, malaria, viral encephalitis and other viral diseases. This link to the

causes of diseases is confirmed by the present research. IOB [86] also reports that in comparison to national means, the prevalence of infections and vector-borne diseases in Fayoum shows the following characteristics:

- Prevalence of viral encephalitis is higher,
- Prevalence of infectious hepatitis and of polio are equal to the national means, but cause concern,
- Diphtheria, tuberculosis, rabies, bronchopneumonia and tetanus are all present, and require vigilance to keep outbreaks under control if village environmental conditions continue to deteriorate.

Accordingly, we recommend that local and national health organizations further investigate water quality and health status in the Fayoum watershed, as our findings clearly indicate that there is a direct relationship between these two issues. Installing a working sanitation network needs to include all villages in the watershed and is an essential task. Raising public awareness through media or campaigns can help reduce the discharge of untreated sewage into waters.

4.7.3.2. Irrigation water quality

Due to the reuse of drainage waters for irrigation, both irrigation and drainage waters were evaluated for their suitability in agriculture. The assessed parameters are salinity, trace metals and microbiological criteria.

In Figure 24 [89], all irrigation and drainage waters were plotted on a graph in which the EC is taken as a salinity hazard and the sodium adsorption ration (SAR) as an alkalinity. As shown in this figure, all drainage waters and some irrigation waters (samples 12, 13, 15 and 16) have a high EC and low SAR. As can be seen, irrigation canal sample 17 has very high EC and high SAR indicators, restricting its irrigation use. Because highly saline water cannot be used on soils with poor drainage, plants with a good salt tolerance should be selected for agriculture [90, 91].

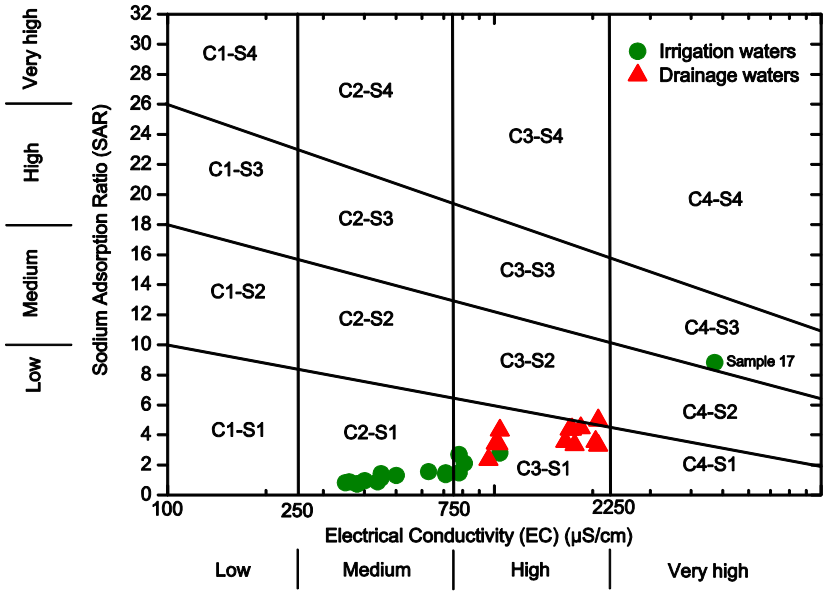

Figure 24. Salinity and alkalinity hazard applied to evaluate the studied irrigation and drainage waters and their suitability for agricultural purposes. Sample 17 (irrigation water) has the highest salinity and alkalinity hazards (Paper **III**).

Most of the soils in the Fayoum watershed are characterized by poor drainage [92-94] and consequently, using high salinity waters for irrigation can cause soil salinization under the prevailing hot and arid conditions. In fact the degradation of soil productivity is a commonly observed feature in the watershed [51, 92-94].

The recommended limits of trace elements in irrigation water are shown in Appendix I [90, 91]. Accordingly, both irrigation and drainage waters are suitable for agricultural purposes except samples 13, 20, 21, 22, 23, 26, 28 and 29, which contain Al and Fe concentrations higher than 5000 µg/L. Irrigation with water containing Al concentrations above 5000 µg/L can cause non-productivity in acid soils with pH < 5.5 [91]. Though irrigation with water having Fe concentrations above 5000 µg/L is not toxic to plants in aerated soils, it can contribute to soil acidification and reduce the bioavailability of essential phosphorus and Mo [91].

The WHO [95] and the Food and Agricultural Organization (FAO) [90, 91] recommend that irrigation water for crops that are likely to be eaten uncooked should not exceed 1000 CFU/100 mL fecal coliforms (FC). Thus, as all irrigation and drainage waters in the Fayoum watershed have FC > 1000 CFU/100 mL (Appendix I), they are not suitable for crops that are eaten uncooked. Coliform contamination is a health risk not only in drinking waters but also in surface waters, a vital issue which should be of serious concern to national and local health organizations.

4.8. Spatial distribution of grain sizes in Lake Qarun sediments

The spatial distribution of grain sizes in the Lake Qarun sediments (Fig. 25) is mainly influenced by the proximity of sites close to drain outlets. Clay and silt, which are carried by the major drains, are deposited in the lake's south-eastern side close to the El-Bats and El-Wadi drain mouths (Figs. 1 and 25). The relatively high clay and silt content at the eastern side and the middle of the lake reflects the input of the El-Bats and El-Wadi drains, while the high content of clay at the western side of the lake is probably due to the low energy of waves in this area resulting in the calm conditions required for clay deposition. In contrast, the highest sand content is found on the northern and northern-western side and is most likely due to the sand grains derived from sand and rock exposures on the northern side of the lake and the fact that the western side is only affected by minor drains.

4.9. (Semi-)Metal contents of Lake Qarun sediments

There is a clear relationship between the spatial distribution of (semi-)metals and the sediment grain sizes at Lake Qarun (Fig. 25). All (semi-)metals except Mn follow the same distribution of clay and silt in the lake sediments (Table 3, Fig. 25). The enrichment of (semi-)metals in the fine silt and clay fraction (< 63 µm) is due to the large specific surface area of this fraction and also to the strong adsorptive properties of clay minerals [96]. The similar spatial distribution of Fe, Al, Cr, Co, Cu, Ni, Pb, Zn, Sb, and V (Fig. 25) indicates either similar sources or similar mechanisms of precipitation. The dissimilarity of the Mn distribution possibly indicates a different mechanism of Mn precipitation in the lake.

Table 3

(Semi-)metal concentrations (in mg/kg dry wt.) and percentages of sand, silt and clay in Lake Qarun sediments (sites Q1–Q13).

Site	Mn	Fe	Co	Cr	Cu	Ni	Pb	Zn	Sb	Al	V	Clay%	Silt%	Sand%
Q1	1000	17000	11.2	24	10	14	2.5	27	0.83	11000	45	9	48	43
Q2	700	9400	6.07	14	7	10	<2	20	<0.5	6330	26	10	8	82
Q3	400	40000	17.7	60	41	36	4.5	91	2.07	35100	96	62	38	0
Q4	300	18000	8.29	25	20	19	4.2	40	0.67	16400	68	30	38	32
Q5	300	23000	10.5	36	25	25	5.5	50	0.98	21700	82	18	60	22
Q6	400	27000	13.7	37	20	24	3.9	44	1.3	20300	52	30	25	45
Q7	900	12000	9.32	18	6.9	9.3	2.6	21	<0.5	7210	23	10	7	83
Q8	600	17000	9.41	24	11	16	2.9	30	1	13300	36	18	26	56
Q9	600	38000	16.3	52	26	33	4.6	62	1.73	32200	74	49	50	1
Q10	0.1	1100	0.4	<3	<1.5	<3	<2	<5	<0.5	492	3.1	2	2	96
Q11	0.1	2700	0.93	3.3	<1.5	<3	<2	5.6	<0.5	1880	8	4	0	96
Q12	200	17000	4.24	32	8	9.9	3	36	0.72	13800	39	2	7	91
Q13	100	19000	4.56	33	5.9	9.5	3.2	39	0.84	14900	39	30	60	10
Average shale[a]	850	47200	19	90	45	68	20	95	1.5	80000	130	NA	NA	NA

[a] Turekian and Wedepohl [97]
NA: Not Applicable

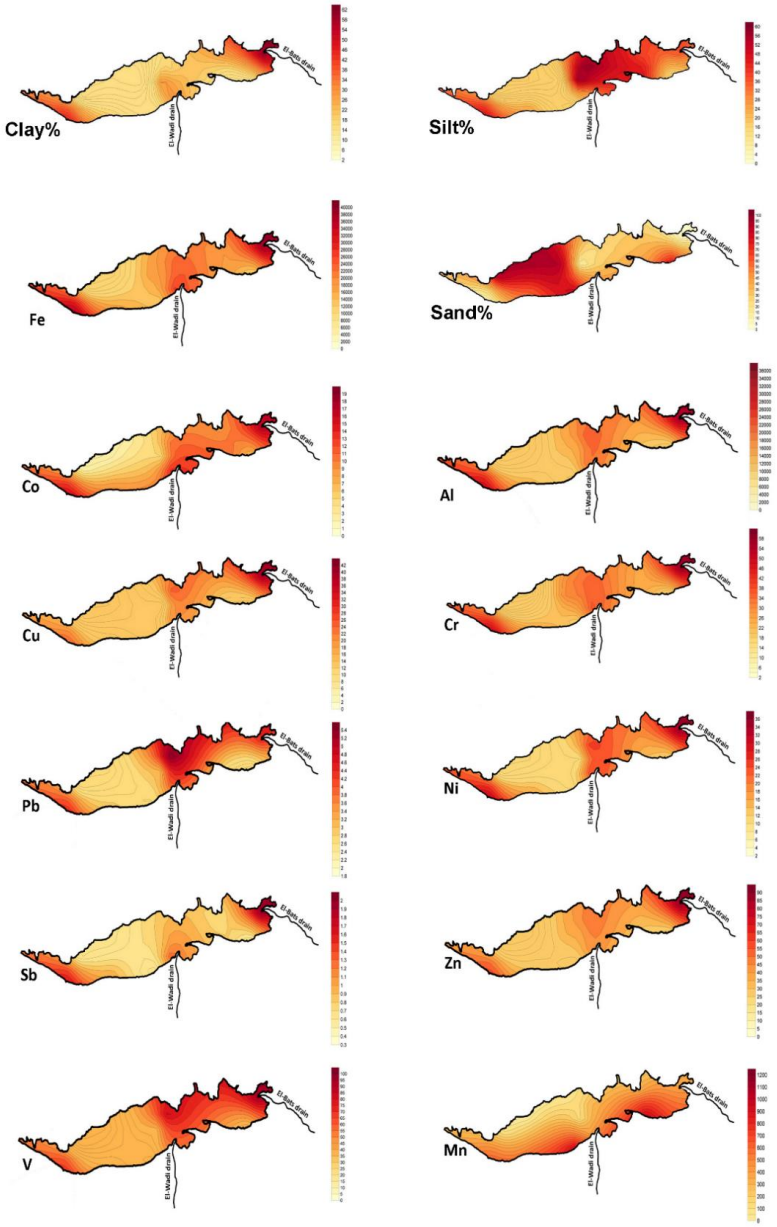

Figure 25. Spatial distribution of selected (semi-)metals (in mg/kg dry wt.) and grain size fractions (in %) in Lake Qarun sediments (Paper **III**).

Spatial distributions of Cr, Co, Cu, Ni, Pb, Zn, Sb, and V follow the distribution of Fe and Al (Fig. 25), which may reflect the adsorption property of Fe and Al oxides to other (semi-)metals.

There also appears to be a relationship between the concentration of metals in the source water (El-Wadi and El-Bats drains) and the metal content of the lake sediments. Cd and As were recorded below detection limits in both the lake sediments and the source waters, while Pb was recorded below the detection limit in the source waters and was found in very low concentrations in the lake sediments (Table 3). In contrast, metals such as Fe, Al, Cr, Co, Cu, Ni and Mn were detected in both the lake sediments and the source waters. For example, Fe and Al were recorded in the first order of metal concentrations in both the source waters and the lake sediments (Appendix I and Table 3). This indicates that the El-Wadi and El-Bats drains are the main sources of metals in the lake. The location of sediment sites with higher metal contents close to the drain mouths indicates that these metals are transported by these drains into the lake either as dissolved constituents or as particulate metals associated with suspended matter.

5. CONCLUSIONS AND PROSPECTIVES

This research investigated the water quality and geochemistry of the surface waters in the Fayoum catchment and Lake Qarun. It introduced an integrative approach to the geochemical evolution of Nile water through its course within the Fayoum Depression until it reaches Lake Qarun. The chemistry of the water developed from Ca-Mg-HCO_3 type at the head waters to Ca-Mg-Cl-SO_4 and eventually to Na-Cl downstream at Lake Qarun. The relative increase in SO_4 and Cl compared to HCO_3 and in Na compared to Ca and Mg towards Lake Qarun was attributed to the dissolution of soluble salts (evaporites) and to evapoconcentration. Evaporation-crystallization is the main mechanism controlling the evolution of Lake Qarun brine. This was confirmed both by Gibb's plot and the $\delta^{18}O$ results. Geochemical modeling of lake evolution was first conducted using Hardie and Eugster's evolutionary model and then with a simulated evaporation model by PHREEQC. Both models demonstrated that the lake brine evolved from drainage waters via an evaporation-crystallization process and that after the precipitation of calcite and gypsum it should reach the final composition "Na–Mg–SO_4–Cl". As simulated by PHREEQC, further evaporation of lake brine can drive halite to precipitate at the latest stages of evaporation.

The real crystallization sequence during evaporation of lake brine at the EMISAL concentration ponds showed fractional crystallization of calcite, gypsum and halite, which supported the modeling data. After crystallization of halite, the crystallization sequence during evaporation of the residual brine (bittern) was investigated using a Jänecke phase diagram at 35 °C. This diagram was more useful than PHREEQC for predicting the evaporation path especially in the case of this highly concentrated bittern. This is because PHREEQC has limitations for working on brines with high ionic strength. The predicted crystallization path using a Jänecke phase diagram at 35 °C showed that halite, hexahydrite, kainite and kieserite should appear during evaporation of the bittern. Yet the real crystallized mineral salts were only halite and hexahydrite. The absence of kainite was due to its metastability while the absence of kieserite was due to opposed relative humidity. The presence of a specific $MgSO_4.nH_2O$ phase in ancient evaporite deposits can be used as a paleoclimatic indicator. Closed basin lake systems are sensitive to climate which consequently makes them important indicators of climate changes. These changes can be recorded in sedimentary archives of past climates. Over time,

hydrochemical variations due to changes in the seasonality and amount of precipitation can be reflected in the mineralogy of evaporites of closed basin lakes, and also can provide important indications of past climate.

Evaluation of surface water quality for agricultural purposes shows that some irrigation waters and all drainage waters had high salinities and therefore cannot be used for irrigation. Especially in the light of the poor drainage conditions of the soils, reusing saline drainage waters causes soil salinization and consequently soil degradation which finally negatively affects the soil productivity.

Regarding water quality in the Fyaoum Governorate, all drainage waters and agricultural returns are conveyed to Lake Qarun. Compared to the other waters, the lake water has relatively low concentrations of (semi)metals due to their adsorption on the lake sediments. Waters from irrigation canals which are used as a drinking water supply showed higher concentrations of Al. All other (semi-)metals investigated have low concentrations in all waters and are below the permissible concentration limits. In contrast, irrigation and drainage waters suffer from high levels of TC, FC and FS. The high levels of these bacteria indicate human and animal fecal sources. This is due to the fact that some households have sewage pipes directly connected to the irrigation canals. Moreover, improper disposal of sewage or on-site sanitation tank overflowing into these canals is commonly observed. Consequently, these waters cannot be used for drinking or agricultural purposes without treatment, because of the high risk to human health. Yet many people in the Fayoum watershed, especially in rural regions, use these untreated waters, resulting in the prevalence of water-borne diseases. Egypt is suffering from water scarcity and therefore needs every drop of clean water. Therefore, it is recommended that environmental protection laws are enforced in Egypt to protect the water resources. Furthermore, public awareness-raising by environmental protection agencies and the media, especially in rural areas, is crucial from a health perspective. Finally, the sanitation network needs to be extended to all regions in the Fayoum watershed to minimize the pollution caused by unconfined septic tanks and their negative impact on both groundwater and surface water quality.

The spatial distribution of (semi-)metal contents and grain size analysis of the sediments showed that high concentrations of (semi-)metals are observed at sites with higher clay contents. There is a direct relationship between the concentration of (semi-)metals in the source water (El-Wadi and El-Bats drains) and the metal content of the lake sediments.

This thesis presents the framework for a broad regional study, most needed, for future regional groundwater projections. Study of the importance of the composition of contributing subsurface aquifer(s) to the solute and water budget of Lake Qarun and/or the seepages from the lake to these aquifer (s) could be the subject for further research investigations.

REFERENCES

[1] S.C. Fritz, Twentieth-century salinity and water level fluctuations in Devil's Lake, N. Dakota: a test of diatom based transfer function, Limnol. Oceanogr. 35 (1990) 1771-1781.

[2] IPCC, Climate Change 2001: Impacts, Adaptation and Vulnerability, Cambridge University Press, UK, 2001.

[3] R. Khaydarov, R. Khaydarov, Environmental Change in the Aral Sea Region, in: Liotta PH, Mouat DA, Kepner WG, Lancaster JM (Eds.), Environmental Change and Human Security: Recognizing and Acting on Hazard Impacts, NATO Science for Peace and Security Series C: Environmental Security, Springer Science+Business Media B.V., Netherlands, 2008, pp. 433-447.

[4] EC-IFAS (Executive Committee of the International Fund for saving the Aral Sea), The Aral Sea and its Challenges, United Nations Economic and Social Commission for Asia and the Pacific, Expert Group Meeting on Improving Access to Water, Sanitation and Energy Services in Asia and the Pacific by addressing the Water-Food Energy Nexus, 20-22 March 2013. Bangkok, Thailand. (2013).

[5] H.P. Eugster, Geochemistry of Evaporitic Lacustrine Deposits, Annu.Rev.Earth Planet.Sci. 8 (1980) 35-63.

[6] L.A. Hardie, H.P. Eugster, The evolution of closed-basin brines, Mineral Soc. Am. Spec. Pap. 3 (1970) 273-290.

[7] H.P. Eugster, LA Hardie, Saline Lakes, in: A. Lerman (Eds.), Lakes: Chemistry, Geology, Physics. Springer, New York, 1978, pp. 237-293.

[8] W.B. Langbein, Salinity and hydrology of closed lakes, US Geol. Surv. Prof. Pap. 412. 412 (1961) 1-20.

[9] B.F. Jones, Geochemical evolution of closed basin water in the western Great Basin, Proceedings of the Second Symposium on Salt. Northern Ohio Geological Society, Cleveland, Ohio. (1966) 181-200.

[10] B.F. Jones, A.S. van Denburgh, Geochemical influences on the chemical character of closed lakes, Symposium of Garda, Hydrology of Lakes and Reservoirs, Proceedings of the International Association for Scientific Hydrology. 70 (1966) 438-446.

[11] R.M. Garrels, F.T. Mackenzie, Origin of the Chemical Compositions of Some Springs and Lakes, American Chemical Society, 1967, pp. 222-242.

[12] J.I. Drever, The Geochemistry of Natural Waters, Prentice- Hall, Englewood Cliffs 1982.

[13] F. Fayazi, R. Lak, M. Nakhaei, Hydrogeochemistry and brine evolution of Maharlou Saline Lake, southwest of Iran, Carbonates and Evaporites. 22 (2007) 33-42.

[14] D.T. Long, W.B. Lyons, M.E. Hines, Influence of hydrogeology, microbiology and landscape history on the geochemistry of acid hypersaline waters, N.W. Victoria, Appl.Geochem. 24 (2009) 285-296.

[15] L.C. Radke, K.W.F. Howard, P.A. Gell, Chemical diversity in south-eastern Australian saline lakes. I: geochemical causes, Mar.Freshwater Res. 53 (2002) 941-959.

[16] L.C. Radke, K.W.F. Howard, Influence of groundwater on the evaporative evolution of saline lakes in the Wimmera of south-eastern Australia, Hydrobiologia. 591 (2007) 185-205.

[17] B.N. Ryzhenko, E.V. Cherkasova, Chemical composition of natural waters and brines as a result of hydrogeochemical processes in water-rock-gas systems, Geochem.Int. 50 (2012) 1101-1150.

[18] A. Fathi, R. Flower, Water quality and phytoplankton communities in Lake Qarun (Egypt), Aquat.Sci. 67 (2005) 350-362.

[19] F.A. Hassan, Holocene lakes and prehistoric settlements of the Western Faiyum, Egypt, Journal of Archaeological Science. 13 (1986) 483-501.

[20] A.H. Meshal, The problem of the salinity increase in Lake Qarun (Egypt) and a proposed solution, Journal du Conseil. 37 (1977) 137-143.

[21] W. Wolters, N.S. Ghobrial, H.M. Van Leeuwen, M.G. Bos, Managing the water balance of The Fayoum Depression, Egypt, Irrigation and Drainage Systems. 3 (1989) 103-123.

[22] M.M. Ishak, S. Abdel-Malek, Some ecological aspects of Lake Qarun, Fayoum, Egypt. Part I. Physico-chemical environment, Hydrobiologia. 74 (1980) 173-178.

[23] A.A. Mageed, Distribution and salinity ranges of zooplankton organisms at El Fayoum Depression (El-Fayoum-Egypt), Egypt J. Aquat Biol. & Fish. 2 (1998) 51-71.

[24] J. Ball, A Contribution to the Geography of Egypt, Survey and Mines Department, Cairo, Egypt., 1939.

[25] E. El Sayed, K.A. Guindy, Hydrochemical investigation of El Fayium locality with special reference to the sulphate enrichment phenomenon in Lake Qarun, Mansoura Sci. Bull. 26 (1999) 1-21.

[26] M. Naguib, Studies on the ecology of Lake Qarun (Fayoum, Egypt). Part I, Kieler Meeresforschungen. 14 (1958) 187-222.

[27] G.F. Soliman, The Hydrology of Lake Qarun, Fayyum Provience, Egypt. Part II: The successive increase of salinity in the Lake Qarun, Bull. Inst. Oceanogr. & Fisheries. ARE. 15 (1989) 93-105.

[28] M. Rasmy, S.F. Estefan, Geochemistry of saline minerals separated from Lake Qarun brine, Chem.Geol. 40 (1983) 269-277.

[29] A.M. El-Maghraby, N.M. Dowidar, The occurrence of marine plankton organisms in Lake Qarun, Egypt, P.-v. Reun. Commn int Explor. Scient. Mer Mediterr. 19 (1969) 849-851.

[30] R. Abu-Zied, K.W. Keatings, R.J. Flower, Environmental controls on foraminifera in Lake Qarun, Egypt, The Journal of Foraminiferal Research. 37 (2007) 136-149.

[31] R.J. Flower, C. Stickley, N.L. Rose, S. Peglar, A.A. Fathi, P.G. Appleby, Environmental Changes at the Desert Margin: An Assessment of Recent Paleolimnological Records in Lake Qarun, Middle Egypt, J.Paleolimnol. 35 (2006) 1-24.

[32] A.A. Zalat, Calcareous nannoplankton and diatoms from the Eocene/Pliocene sediments, Fayoum depression, Egypt, J.Afr.Earth Sci. 20 (1995) 227-244.

[33] G. Gupta, Z. Abd El–Hamid, Water quality of lake Qarun, Egypt, Int.J.Environ.Stud. 60 (2003) 651-657.

[34] S.A. Mansour, M.M. Sidky, Ecotoxicological Studies. 6. The first comparative study between Lake Qarun and Wadi El-Rayan wetland (Egypt), with respect to contamination of their major components, Food Chem. 82 (2003) 181-189.

[35] S.A. Mansour, M.M. Sidky, Ecotoxicological Studies. 3. Heavy metals contaminating water and fish from Fayoum Governorate, Egypt, Food Chem. 78 (2002) 15-22.

[36] H. Hussein, R. Amer, A. Gaballah, Y. Refaat, A. Abdel-Wahab, Pollution Monitoring for Lake Qarun, Advances in Environmental Biology. 2 (2008) 70-80.

[37] R. Abd Ellah, Outlook on past, present and future status of water salinity in Lake Qarun, Egypt, World Journal of Fish and Marine Sciences. 1 (2009) 51-55.

[38] A.M. Abdel-Satar, M.E. Goher, M.F. Sayed, Recent environemntal changes in water and sediment quality of Lake Qarun, Egypt, Journal of Fisheries and Aquatic Science. 5 (2010) 56-69.

[39] K.W. Keatings, I. Hawkes, J.A. Holmes, R.J. Flower, M.J. Leng, R. Abu-Zied, et al., Evaluation of ostracod-based palaeoenvironmental reconstruction with instrumental data from the arid Faiyum Depression, Egypt, J.Paleolimnol. 38 (2007) 261-283.

[40] K. Keatings, J. Holmes, R. Flower, D. Horne, J. Whittaker, R. Abu-Zied, Ostracods and the Holocene palaeolimnology of Lake Qarun, with special reference to past humanâ€“environment interactions in the Faiyum (Egypt), Hydrobiologia. 654 (2010) 155-176.

[41] H.M. Baioumy, H. Kayanne, R. Tada, Reconstruction of lake-level and climate changes in Lake Qarun, Egypt, during the last 7000 years, J.Great Lakes Res. 36 (2010) 318-327.

[42] H. Baioumy, H. Kayanne, R. Tada, Record of Holocene aridification (6000–7000 BP) in Egypt (NE Africa): Authigenic carbonate minerals from laminated sediments in Lake Qarun, Quaternary International. 245 (2011) 170-177.

[43] S.Z. Sabae, Bacteriological and chemical studies on benthic layers of Lake Qarun El-Fayoum, Egypt, Ph.D. Thesis Fac. Sci. Tanta Univ. (1996) 1-192.

[44] S.Z. Sabae, Studies on aquatic bacteria of Lake Qarun, El-Fayoum, Egypt. M. Sc. Thesis. Fac. Sci. Tanta Univ. (1993) 1-168.

[45] S.Z. Sabae, S.A. Rabeh, Bacterial indices of sewage pollution in Lake Qarun, El-Fayoum, Egypt, Egypt. J. Aquat. Biol. Fish. 4 (2000) 103-116.

[46] S. Abdel-Malek, M.M. Ishak, Some ecological aspects of Lake Qarun, Fayoum, Egypt. Part II. Production of plankton and benthic organisms, Hydrobiologia. 75 (1980) 201-208.

[47] A.M. Abdel-Moniem, Biodiversity of phytoplankton structure in Lake Qarun (El-Fayoum) and its use as indicators for environmental pollution, Egyptian J. of Phycology. 2 (2001) 17-31.

[48] A.A. Mageed, Effect of some environmental factors on the biodiversity of holozooplankton community in Lake Qarun, Egypt, Egyptian Journal of Aquatic Research. 31 (2005) 230-249.

[49] F.K. Ali, S.A. El-Shafai, F.A. Samhan, W.K.B. Khalil, Effect of water pollution on expression of immune response genes of Solea aegyptiaca in Lake Qarun, African Journal of Biotechnology. 7 (2008) 1418-1425.

[50] T. Saif, A. Kamil, A. Fayed, Ecophysiological studies on Seagrass (Ruppia cirrohsa) Petagna Grande, in Lake Qarun, Egypt with emphasis on remote sensing and rough set approach, Academic Journal of Plant Sciences. 1 (2008) 62-71.

[51] R.R. Ali, W.A.M. Abdel Kawy, Land degradation risk assessment of El Fayoum depression, Egypt, Arabian Journal of Geosciences. 6 (2013) 2767-2776.

[52] G.M. El-Shabrawy, H.J. Dumont, The Fayum Depression and Its Lakes, in: H.J. Dumont (Eds.), The Nile: Origin, Environments, Limnology and Human Use, Springer, Netherlands, 2009, pp. 95-124.

[53] A.S. Elsheikh, E.M. Elmiligi, S.M. Ibraheem, Hydrology of Qarun Lake, El Fayoum Depression, Egypt, Bull. N.R.C., Egypt. 33 (2008) 1-26.

[54] W. Abdel Kawy, A. Belal, Spatial analysis techniques to survey the heavy metals content of the cultivated land in El-Fayoum depression, Egypt, Arabian Journal of Geosciences. 5 (2012) 1247-1258.

[55] M.A. Hammad, S.M. Abo-El-Ennan, F. Abed, Pedological studies on the Fayoum area, Egypt, landscapes and soil morphology, Egypt J. Soil Sci. 23 (1983) 99-114.

[56] R. Said, The Nile River: Geology, Hydrology and Utilisation, Pergamon Press, Tarrytown, New York, 1993.

[57] A.M. Tamer, Subsurface geology of the Fayoum region, M. Sc. Thesis. Alexandria University. (1968).

[58] M. Metwaly, G. El-Qady, U. Massoud, A. El-Kenawy, J. Matsushima, N. Al-Arifi, Integrated geoelectrical survey for groundwater and shallow subsurface evaluation: case study at Siliyin spring, El-Fayoum, Egypt, Int.J.Earth Sci. 99 (2010) 1427-1436.

[59] APHA, Standard Methods for the Examination of Water and Wastewater, American Public Health Association, Washington, DC, USA, 1998.

[60] C.D. Klein Gebbinck, S. Kim, M. Knyf, J. Wyman, A new online technique for the simultaneous measurement of the $\delta^{13}C$ value of dissolved inorganic carbon and the $\delta^{18}O$ value of water from a single solution sample using continuous-flow isotope ratio mass spectrometry, Rapid Communications in Mass Spectrometry. 28 (2014) 553-562.

[61] D. Kroetsch, C. Wang, Particle size distribution, in: Carter MR, Gregorich EG (Eds.), Soil sampling and methods of analysis, Taylor & Francis, Boca Raton, 2008, pp. 713-725.

[62] D.L. Parkhurst, C.A.J. Appelo, Description of input and examples for PHREEQC version 3—A computer program for speciation, batch-reaction, one-dimensional transport, and inverse geochemical calculations, U.S. Geological Survey Techniques and Methods, book 6, chap. A43, 2013, 497p.

[63] D.L. Parkhurst, C.A.J. Appelo, User's Guide to PHREEQC (version 2) – A computer Program for speciation, batch-reaction, one-dimensional transport, and inverse geochemical calculations, U.S. Geological Survey, Denver, Colorado. 1999, 312p.

[64] D. Banks, V.P. Parnachev, B. Frengstad, W. Holden, O.V. Karnachuk, A.A. Vedernikov, The evolution of alkaline, saline ground- and surface waters in the southern Siberian steppes, Appl.Geochem. 19 (2004) 1905-1926.

[65] M. Smith, J.S. Compton, Origin and evolution of major salts in the Darling pans, Western Cape, South Africa, Appl.Geochem. 19 (2004) 645-664.

[66] B. Merkel, B. Planer-Friedrich, Hydrogeochemical Modeling Programs, in: D. Nordstrom (Eds.), Groundwater Geochemistry–A Practical Guide to Modeling of Natural and Contaminated Aquatic Systems, 1st ed., Springer Verlag, 2005, pp. 67-110.

[67] J. Gat, Oxygen and hydrogen isotopes in the hydrologic cycle, Annu.Rev.Earth Planet.Sci. 24 (1996) 225-262.

[68] X. Huang, M. Sillanpää, E.T. Gjessing, R.D. Vogt, Water quality in the Tibetan Plateau: Major ions and trace elements in the headwaters of four major Asian rivers, Sci.Total Environ. 407 (2009) 6242-6254.

[69] R.T. Kimblin, The chemistry and origin of groundwater in Triassic sandstone and Quaternary deposits, northwest England and some UK comparisons, Journal of Hydrology. 172 (1995) 293-311.

[70] W.J. Deutsch, Groundwater Geochemistry: Fundamentals and Applications to Contamination, Boca Raton: Lewis Publishers, Florida 1997.

[71] R.M. Dargam, P.J. Depetris, Geochemistry of waters and brines from the Salinas Grandes basin, Córdoba, Argentina. II. Gypsum dissolution-calcite precipitation, and brine evolution, Int.J.Salt Lake Res. 5 (1996) 81-101.

[72] R.J. Gibbs, Mechanisms Controlling World Water Chemistry, Science. 170 (1970) 1088-1090.

[73] M. Bąbel, B.C. Schreiber, 9.17 - Geochemistry of Evaporites and Evolution of Seawater, in: H.D. Holland, K.K. Turekian (Eds.), Treatise on Geochemistry, 2nd ed., Elsevier, Oxford, 2014, pp. 483-560.

[74] M.A. McCaffrey, B. Lazar, H.D. Holland, The evaporation path of seawater and the coprecipitation of Br^- and K^+ with halite, Journal of Sedimentary Research. 57 (1987) 928-937.

[75] E. Usdowski, M. Dietzel, Atlas and data of solid-solution equilibria of marine evaporites, Springer-Verlag, Berlin, 1998.

[76] H.P. Eugster, C.E. Harvie, J.H. Weare, Mineral equilibria in a six-component seawater system, Na-K-Mg-Ca-SO_4-Cl- H_2O, at 25 °C, Geochim.Cosmochim.Acta. 44 (1980) 1335-1347.

[77] A. M'nif, R. Rokbani, Minerals successions crystallisation related to tunisian natural brines, Crystal Research and Technology. 39 (2004) 40-49.

[78] M. Steiger, K. Linnow, H. Juling, G. Gülker, A. El Jarad, S. Brüggerhoff, et al., Hydration of $MgSO_4 \cdot H_2O$ and Generation of Stress in Porous Materials, Crystal Growth & Design. 8 (2008) 336-343.

[79] D.T. Vaniman, D.L. Bish, S.J. Chipera, C.I. Fialips, J. William Carey, W.C. Feldman, Magnesium sulphate salts and the history of water on Mars, Nature. 431 (2004) 663-665.

[80] C. Balarew, Solubilities in seawater-type systems: Some technical and environmental friendly applications, Pure & Appl. Chem. 65 (1993) 213-218.

[81] W. Stumm, J.J. Morgan, Aquatic Chemistry, Chemical Equilibria and Rates in Natural Waters, John Wiley & Sons, Inc., New York, 1996.

[82] H.P. Eugster, B.F. Jones, Behavior of major solutes during closed-basin brine evolution, American Journal of Science. 279 (1979) 609-631.

[83] USEPA, Total Colifrom Rule, U.S. Environmental Protection Agency, Washington, DC., 1995, EPA 570/9-91-200.

[84] USEPA, National Primary Drinking Water Regulations, U.S. Environmental Protection Agency, Washington, DC., 2009, EPA 816-F-09-004.

[85] WHO, Volume 3, Surveillance and control of community supplies, in: WHO (Eds.), Guidelines for drinking-water quality, 2nd ed., World Health Organization, Geneva, 1997.

[86] IOB, Drinking water supply and sanitation programme supported by the Netherlands in Fayoum Governorate, Arab Republic of Egypt, 1990-2009, Policy and Operations Evaluation Department, IOB Impact Evaluations. 327, Ministry of Foreign Affairs of the Netherlands (2010) 1-204.

[87] WHO, Volume 1, Recommendations, in: WHO (Eds.), Guidelines for Drinking-water Quality, 3rd ed., World Health Organization, Geneva, 2008.

[88] WHO, Aluminium in drinking-water, World Health Organization, Geneva, 2010, WHO/HSE/WSH/10.01/13.

[89] U.S. Salinity Laboratory, Diagnosis and improvement of saline and alkali soils. Agriculture Hand Book No. 60, USDA, 1954, 160p.

[90] FAO, Users manual for irrigation with treated wastewater, FAO, 2003, TC/D/Y5009F/1/10.03/100.

[91] FAO, FAO irrigation and drainage paper47, FAO, Rome, 1992.

[92] T. Abdel Aal, A.M. Ibrahim, Studies on the Micromorphology of Salt-Affected Soils from El-Fayoum Depression, Egypt, in: S.A. Shahid, F.K. Taha, M.A. Abdelfattah (Eds.) Developments in Soil Classification, Land Use Planning and Policy Implications. Springer, Netherlands, 2013, pp. 373-392.

[93] M. Abd-Elgawad, M. Shendi, D. Sofi, H.A. Abdurrahman, A. Ahmed, Geographical Distribution of Soil Salinity, Alkalinity, and Calcicity Within Fayoum and Tamia Districts, Fayoum Governorate, Egypt, in: S.A. Shahid, F.K. Taha, M.A. Abdelfattah (Eds.) Developments in Soil Classification, Land Use Planning and Policy Implications. Springer, Netherlands, 2013, pp. 219-236.

[94] M. Shendi, M. Abdelfattah, A. Harbi, Spatial Monitoring of Soil Salinity and Prospective Conservation Study for Sinnuris District Soils, Fayoum, Egypt, in: S.A. Shahid, F.K. Taha, M.A. Abdelfattah (Eds.) Developments in Soil Classification, Land Use Planning and Policy Implications. Springer, Netherlands, 2013, pp. 199-217.

[95] WHO, Health Guidelines for the Use of Wastewater in Agriculture and Aquaculture, World Health Organization. Technical Report Series No. 778, 1989, 76p.

[96] M.N. Bodur, M. Ergin, Geochemical characteristics of the recent sediments from the Sea of Marmara, Chem.Geol. 115 (1994) 73-101.

[97] K.K. Turekian, K.H. Wedepohl, Distribution of the Elements in Some Major Units of the Earth's Crust, Geological Society of America Bulletin. 72 (1961) 175-192.

APPENDICES

Appendix I: Physiochemical and microbiological parameters measured in surface waters in the Fayoum Catchment, Egypt.

Water system	Site	pH	EC mS/cm	Ca^{2+} mg/L	Mg^{2+} mg/L	Na^{+} mg/L	K^{+} mg/L	HCO_3^{-} mg/L	SO_4^{2-} mg/L	Cl^{-} mg/L	SiO_2 mg/L	TDS mg/L	$\delta^{18}O^{b}$ ‰
Irrigation waters	1	7.70	0.38	36.16	9.43	19.78	3.21	120.0	38.20	23.18	5.11	255.07	+3.09
	2	7.70	0.45	36.10	10.60	30.20	3.90	132.8	52.32	37.68	5.06	308.66	+3.12
	3	7.70	0.39	36.20	9.89	19.58	3.04	122.8	39.90	25.75	4.73	261.89	+3.21
	4	7.60	0.44	31.90	9.30	22.00	3.90	128.8	51.90	33.79	4.53	286.12	+3.19
	5	7.80	0.42	38.10	10.30	22.40	3.31	122.4	47.80	28.72	6.23	279.26	+3.22
	6	7.60	0.40	34.00	9.90	24.70	3.80	136.8	39.43	25.38	5.07	279.08	+3.22
	7	7.53	0.45	37.10	10.80	38.40	4.30	135.6	48.50	33.72	5.98	314.40	+3.13
	8	7.50	0.50	37.70	11.60	35.80	4.50	144.8	56.90	39.32	5.71	336.33	+3.26
	9	7.60	0.36	32.10	9.60	21.90	3.80	130.8	28.90	16.68	4.74	248.52	+3.19
	10	7.60	0.65	43.30	16.16	47.20	8.22	165.2	72.70	56.06	10.60	419.44	+3.33
	11	7.50	0.68	46.32	15.22	45.20	4.72	174.0	75.90	61.60	9.87	432.83	+3.24
	12	7.50	0.76	47.91	15.96	46.10	5.17	182.4	73.34	57.10	10.73	438.71	+3.27
	13	7.77	0.87	54.20	19.79	71.40	5.53	184.8	118.00	82.20	11.82	547.74	+3.30
	14	7.50	0.60	46.32	15.22	45.20	4.72	174.0	75.90	61.60	9.87	432.83	+3.24
	15	7.50	0.91	47.91	15.96	46.10	5.17	182.4	73.34	57.10	10.73	438.71	+3.27
	16	7.90	1.11	62.00	20.49	100.10	6.13	173.2	154.90	151.10	8.62	676.54	+3.37
	17	7.70	3.76	144.40	37.73	506.20	39.10	212.4	593.60	807.80	9.14	2350.37	+4.22
Mean		7.61	0.77	47.75	14.59	67.19	6.62	154.31	96.56	94.05	7.56	488.62	+3.29
SD		0.12	0.80	26.23	7.01	115.02	8.46	28.21	131.83	186.62	2.66	493.66	+0.25
Drainage waters	18	7.50	1.01	49.20	19.30	112.60	7.00	198.8	147.80	116.96	8.87	660.53	+3.39
	19	7.60	0.97	73.27	15.73	85.50	6.13	154.0	154.10	119.28	8.53	616.54	+3.49
	20	7.60	1.38	77.90	23.49	139.60	7.78	183.2	207.90	190.30	12.47	842.64	+3.56
	21	7.60	1.60	93.09	26.55	142.40	8.67	192.8	276.80	241.50	14.15	995.96	+3.57
	22	7.80	1.73	100.20	28.60	156.50	6.95	204.4	292.30	260.50	14.69	1064.14	+3.62
	23	7.70	1.84	188.00	65.89	481.60	17.10	277.5	510.30	730.30	12.61	2283.30	+3.62
	24	7.50	1.10	53.33	22.20	117.20	8.63	224.4	141.60	116.47	10.84	694.67	+3.24
	25	7.70	1.91	82.30	32.51	182.40	15.10	295.2	291.10	303.90	15.14	1217.65	+3.34
	26	7.60	1.98	120.00	27.58	204.90	10.25	190.8	380.80	308.60	13.26	1256.19	+3.61
	27	7.50	1.94	106.30	26.56	193.80	10.49	196.0	361.60	308.60	13.52	1216.87	+3.49
	28	7.50	2.10	106.00	30.52	203.30	11.90	186.4	393.30	332.14	11.72	1275.28	+3.48
	29	7.50	2.40	166.80	63.60	425.00	23.30	220.1	502.00	758.30	13.14	2172.24	+3.50
Mean		7.58	1.66	101.37	31.88	203.73	11.11	210.30	304.97	315.57	12.41	1191.33	+3.49
SD		0.10	0.46	41.54	16.05	123.07	5.08	39.95	128.79	215.40	2.10	539.52	0.12
Lake Qarun waters	Q1	8.20	34.10	419	970	9361	285	180	11808	11526	9	34557	+7.54
	Q2	8.20	32.30	431	1045	9602	305	201	11580	11823	8	34994	+7.29
	Q3	8.20	32.50	358	847	7941	250	176	8705	10544	10	28830	+7.14
	Q4	8.30	34.10	514	1027	9458	326	181	11417	11695	8	34627	+7.60
	Q5	8.40	36.70	524	1148	9919	480	184	10695	12340	7	35297	+7.86
	Q6	7.80	34.80	394	1131	9550	289	192	10453	12306	19	34333	+7.62
	Q7	8.20	34.40	453	1239	10166	283	160	12392	12092	8	36792	+7.67
	Q8	8.30	35.40	329	1177	12125	387	157	12387	12278	6	38846	+7.81
	Q9	8.30	36.70	484	1267	9949	300	156	12376	12317	6	36855	+7.95
	Q10	8.30	36.80	497	1238	10163	297	166	13461	12415	6	38243	+7.93
	Q11	8.30	37.00	463	1217	10888	290	157	13630	12472	7	39124	+7.93
	Q12	8.40	36.90	453	1203	12271	362	157	12207	12384	6	39042	+7.89
	Q13	8.30	36.60	450	1100	10159	296	171	12283	12509	10	36977	+7.79
Mean[a]		8.22	35.25	444	1124	10119	319	172	11800	12054	8	36040	+7.69
SD		0.15	1.69	58	123	1143	60	15	1302	550	3	2800	0.25

Water system	Site	Al µg/L	Ba µg/L	Cr µg/L	Co µg/L	Cu µg/L	Fe µg/L	Li µg/L	Mn µg/L	Ni µg/L	Mo µg/L	PO_4^{3-} mg/L	NO_3^- mg/L
Irrigation waters	1	1980	38.3	3.11	1.165	<5	1840	1.97	63.97	1.91	<2.1	0.02	11.98
	2	340	32.23	2.31	<1	7.42	420	1.09	38.12	2.58	<2.1	0.06	18.08
	3	1990	38.5	3.28	1.48	<5	2310	1.81	67.4	2.07	<2.1	0.03	11.01
	4	200	42.11	<1.9	<1	6.43	200	1.02	68.4	1.59	<2.1	0.09	21.83
	5	2050	39.43	4.41	1.33	<5	2410	2.05	69.5	2.72	<2.1	0.06	10.87
	6	2500	39.01	3.47	<1	5.83	2700	1.99	66.74	3.96	<2.1	0.12	14.72
	7	1200	36.72	<1.9	<1	6.32	1400	1.39	45.04	4.52	<2.1	0.14	16.88
	8	800	39.04	1.94	<1	7	1100	1	101.2	1.96	<2.1	0.15	17.72
	9	3210	44.07	<1.9	<1	8.03	3740	<1	80.2	2.96	<2.1	0.13	18.08
	10	3060	48.76	4.6	2.22	<5	3440	2.1	127.1	3.09	<2.1	0.12	35.67
	11	1800	44.71	2.56	1.164	<5	1840	1.95	132.1	1.57	<2.1	0.39	55.96
	12	1410	48.74	3.71	<1	6.76	1820	2.03	149.5	2.37	<2.1	0.33	81.15
	13	8350	69.73	11.88	4.72	6.73	9340	4.45	233.6	7.31	<2.1	0.15	55.21
	14	3800	45.71	5.89	2.14	6.07	3970	2.95	104.9	3.95	<2.1	0.06	39.03
	15	1770	49.23	5.57	1.12	14.79	2470	2.33	188.1	3.79	<2.1	0.52	45.04
	16	3590	46.38	6.88	1.57	9.45	3770	2.41	241.04	5.37	<2.1	0.24	52.95
	17	4500	65.7	<1.9	<1	11.15	530	25.5	213.8	3.42	<2.1	0.55	46.54
Mean		2502.9	45.2	4.6	1.9	8.0	2547.1	3.5	117.1	3.2	NA	0.19	32.5
SD		1926.7	9.7	2.6	1.1	2.6	2107.0	5.9	66.3	1.5	NA	0.16	20.8
WHO (2008)[c]		200	–	50	–	2000	–	–	400	70	70	–	–
FAO (1992, 2003)[d]		5000	–	100	50	200	5000	2500	200	200	10	–	–
Drainage waters	18	1400	39.7	<1.913	<1	6.83	1700	1.54	102.8	2.63	<2.1	0.27	26.17
	19	4960	44.19	7.89	2.36	<5	4650	6.52	68.7	3.84	<2.1	0.09	11.40
	20	7030	59.98	11.24	2.76	10.22	6560	5.17	146.1	7.22	<2.1	0.31	69.31
	21	9310	62.12	14.09	3.33	11.23	8320	6.008	172.8	8.84	<2.1	0.33	49.02
	22	12500	65.77	17.79	3.8	13.4	10410	8.36	175.3	10.51	5	0.33	56.93
	23	9720	59.4	14.05	2.83	39.5	7850	7.52	156.2	13.6	5.37	0.36	52.91
	24	1150	52.9	4.09	1	14.3	1720	2.09	181.8	2.8	5.18	0.82	47.96
	25	4460	64.6	6.9	1.6	38.8	4510	3.63	270.3	5.6	6.08	2.85	47.78
	26	7290	51.6	10.85	3.13	6.38	6270	11.21	111.5	5.51	<2.1	0.18	24.18
	27	4240	46.8	6.73	2.09	4.08	3890	8.62	983	3.54	<2.1	0.39	22.76
	28	6850	53.2	12.04	2.56	13.6	5890	11.06	294	7.32	5.82	0.52	53.48
	29	10600	68.4	12.36	2.68	29.4	7190	11.09	238.1	7.17	5.33	0.67	50.74
Mean		6625.8	55.7	10.7	2.6	17.1	5746.7	6.9	241.7	6.5	5.5	0.59	42.7
SD		3544.3	9.1	4.0	0.8	12.8	2604.2	3.4	242.8	3.3	0.4	0.74	17.3
FAO (1992, 2003)[d]		5000	–	100	50	200	5000	2500	200	200	10	–	–
Lake Qarun waters	Q1	490	8.36	3.85	<1	<5	120	7.5	4.84	<1	2.77	0.03	19.20
	Q2	180	7.65	4.55	<1	<5	90	8.83	6.79	<1	2.34	0.12	15.61
	Q3	470	10.7	3.64	<1	<5	240	8.42	10.4	<1	2.56	0.18	19.43
	Q4	70	8.1	3.17	<1	<5	<79	8.46	4.29	<1	2.37	0.12	20.39
	Q5	50	7.46	2.87	<1	<5	<79	9.03	2.32	<1	2.23	0.12	20.61
	Q6	1210	9.07	3.82	<1	<5	550	8.74	5.45	<1	2.48	0.39	23.90
	Q7	190	7.42	2.74	<1	<5	83	7.7	4.23	<1	<2.1	0.03	19.28
	Q8	400	5.6	4.45	<1	<5	<79	9.14	1.77	<1	<2.1	0.03	19.04
	Q9	60	7.48	2.23	<1	<5	<79	7.97	4.13	<1	<2.1	0.03	19.27
	Q10	60	7.33	<1.913	<1	<5	<79	7.48	3.34	<1	2.22	0.03	18.96
	Q11	770	8.17	2.73	<1	<5	410	7.59	4.61	<1	<2.1	0.03	18.22
	Q12	240	7.98	2.07	<1	<5	<79	7.56	2.14	<1	2.22	0.09	19.09
	Q13	90	10.1	3.64	<1	<5	<79	9.82	3.34	<1	2.16	0.03	20.30
Mean		329.2	8.1	3.3	NA	NA	248.8	8.3	4.4	NA	2.4	0.09	19.50
SD		343.7	1.3	0.8	NA	NA	192.9	0.8	2.3	NA	0.2	0.10	1.8

Water system	Sites	Total Coliform CFU/100 mL	Fecal Coliform CFU/100 mL	*Fecal Streptococcus* CFU/100 mL
Irrigation waters	1	2.2×10^5	1.00×10^4	1.00×10^3
	2	1.0×10^4	1.00×10^4	2.00×10^3
	3	1.43×10^4	4.00×10^3	2.33×10^4
	4	1.80×10^5	1.00×10^4	1.00×10^4
	5	1.60×10^4	5.50×10^3	2.23×10^3
	6	3.00×10^5	2.00×10^4	2.50×10^4
	7	1.00×10^5	6.00×10^4	1.80×10^4
	8	5.00×10^5	5.00×10^4	8.00×10^3
	9	3.80×10^5	3.00×10^4	1.40×10^4
	10	4.00×10^5	9.00×10^4	3.00×10^4
	11	9.25×10^6	1.29×10^6	9.00×10^5
	12	4.45×10^6	4.90×10^5	3.00×10^5
	13	8.30×10^4	4.00×10^4	5.00×10^3
	14	5.00×10^4	3.45×10^3	7.00×10^3
	15	7.50×10^4	1.70×10^4	4.00×10^4
	16	3.80×10^4	1.20×10^4	2.20×10^4
	17	2.00×10^4	9.00×10^3	1.20×10^3
WHO (2008)[c]		absent	absent	absent
FAO (1992, 2003)[d]		–	≤1000	–
Drainage waters	18	1.20×10^6	2.00×10^5	3.30×10^4
	19	2.05×10^5	7.10×10^4	6.40×10^3
	20	3.20×10^5	2.30×10^4	1.00×10^4
	21	5.30×10^6	8.20×10^5	5.60×10^4
	22	6.50×10^4	1.20×10^4	1.00×10^4
	23	7.80×10^4	1.90×10^4	5.00×10^4
	24	2.95×10^6	7.80×10^5	3.00×10^5
	25	1.85×10^7	2.60×10^6	1.00×10^5
	26	4.40×10^5	1.25×10^4	1.40×10^4
	27	2.60×10^5	7.80×10^4	5.80×10^3
	28	5.00×10^5	7.90×10^4	1.50×10^4
	29	1.16×10^4	2.60×10^5	2.30×10^4
FAO (1992, 2003)[d]		–	≤1000	–
Lake Qarun waters	Q1	80	4	1
	Q2	290	20	20
	Q3	88	80	1
	Q4	20	1	62
	Q5	10	1	6
	Q6	330	112	34
	Q7	140	56	40
	Q8	200	186	2
	Q9	2	1	8
	Q10	10	1	1
	Q11	10	1	1
	Q12	2	1	2
	Q13	2	1	54

[a] Mean values of the parameters measured in water samples collected during June 2010, 2011 and 2012 from Lake Qarun.
[b] $\delta^{18}O$ was only measured in June 2012.
[c] World Health Organization Guidelines for Drinking Water Quality (WHO, 2008). The evaluation was applied only to waters from irrigation canals which are used as drinking water supply in the Fayoum Governorate.
[d] Food and Agricultural Organization recommended maximum concentrations for waters used in irrigation (FAO 1992, 2003). This evaluation was applied to irrigation and drainage waters. Note that drainage waters are reused for irrigation in the Fayoum Governorate.
NA: Not Applicable.
–: No available data.
SD: Standard Deviation

Paper I

Hydrogeochemical processes controlling the water chemistry of a closed saline lake located in Sahara Desert: Lake Qarun, Egypt

Mahmoud S.M. Abdel Wahed, Essam A. Mohamed, Mohamed I. El-Sayed, Adel M'nif, Mika Sillanpää

Aquatic Geochemistry 21(2015)31-57

Aquat Geochem (2015) 21:31–57
DOI 10.1007/s10498-015-9253-3

ORIGINAL PAPER

Hydrogeochemical Processes Controlling the Water Chemistry of a Closed Saline Lake Located in Sahara Desert: Lake Qarun, Egypt

Mahmoud S. M. Abdel Wahed · Essam A. Mohamed · Mohamed I. El-Sayed · Adel M'nif · Mika Sillanpää

Received: 27 October 2014 / Accepted: 29 January 2015 / Published online: 6 February 2015

Abstract We present here the first detailed hydrogeochemical study about Lake Qarun. It is a closed, saline, and alkaline lake located in the North African Sahara Desert. It has no outflow except by evaporation. This lake is the deepest area in the Fayoum Depression with elevation 43 m below sea level. In this area, Nile River is the main source of water and Lake Qarun acts as the main reservoir of all drainage waters. Along the flow path of water, the salinity of water increases with increasing proximity to Lake Qarun and the water chemistry has developed from Ca–Mg–HCO_3 at head waters to Na–Cl–SO_4 in low lands and in Lake Qarun. The main processes that control the water chemistry in the studied area are dissolution of soluble salts along with continuous evapoconcentration. The progressive evaporation of drainage water inflow has increased the concentrations of Na, Mg, Cl, and SO_4 in Lake Qarun water, while Ca and HCO_3 have been depleted through $CaCO_3$ precipitation. This is confirmed by the application of Hardie and Eugster's model parallel with a PHREEQC simulated evaporation model. Both models demonstrated that the evolution of lake water during evaporation should reach the final composition of "Na–Mg–SO_4–Cl." Oxygen isotope ($\delta^{18}O$) values of the studied water samples showed a strong positive correlation with electrical conductivity values supporting the effect of evapoconcentration process on the evolution of the lake brine. This study presented an integrated geochemical approach that can help in understanding similar cases studies in arid environments.

Keywords Geochemical evolution · Lake Qarun · Fayoum Depression · Evapoconcentration · Geochemical modeling · Sahara Desert

M. S. M. Abdel Wahed (✉) · M. Sillanpää
Laboratory of Green Chemistry, LUT Chemistry Department, Lappeenranta University of Technology, Sammonkatu 12, 50130 Mikkeli, Finland
e-mail: m.abdelwahed80@yahoo.com; mahmoud.abdel-wahed@lut.fi

M. S. M. Abdel Wahed · E. A. Mohamed · M. I. El-Sayed
Geology Department, Faculty of Science, Beni-Suef University, Beni Suef, Egypt

A. M'nif
Centre National de Recherche en Sciences des Matériaux, Technopole Borj Cedria, B.P. 73, 8027 Soliman, Tunisia

1 Introduction

In a closed hydrological system, the composition of concentrated lake brines largely depends on labile lithologies that are leached and altered by inflow waters in the drainage basin surrounding a salt lake (Eugster 1980; Hardie and Eugster 1970). Closed lakes are exclusive features of the arid and semiarid zones where they are salty with variable degrees of salinity.

Lake Qarun, the object of the present investigation, is one of the largest inland lakes in the North African Sahara Desert. The lake water is alkaline with pH values between 8.0 and 8.7, and saline with average total dissolved salts (TDS) of 36 g/L. The lake level is at $\approx$43 m below sea level, which makes it the deepest area in the Nile River flood plain and in the Fayoum Depression (Figs. 1, 2). It is one of oldest lakes in Egypt. A full historical background and a summary of past environmental changes for the lake may be found in the scientific literatures (e.g., Ball 1939; Flower et al. 2006; Meshal 1977). The lake is surrounded by cultivated lands on its southern and south eastern sides which slope sharply toward the lake. This provides a natural aid forming a drainage water disposal site from the cultivated lands of the whole Depression of Fayoum. The agriculture drainage water annually carries 470 $\times$ 10^6 kg of dissolved salts into Lake Qarun (Rasmy and Estefan 1983). The evolution of the lake water chemistry is mainly based on the chemical composition of the inflow drainage waters. Because the lake has no outlet and the climatic

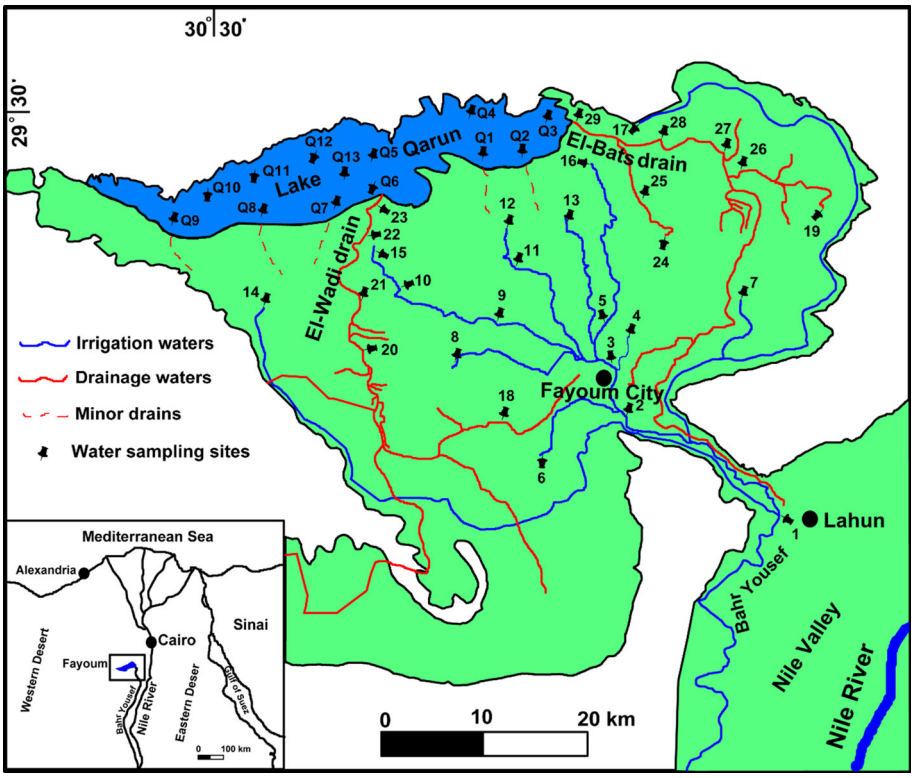

Fig. 1 Location map of the Fayoum area, showing the sampling sites of the studied water samples

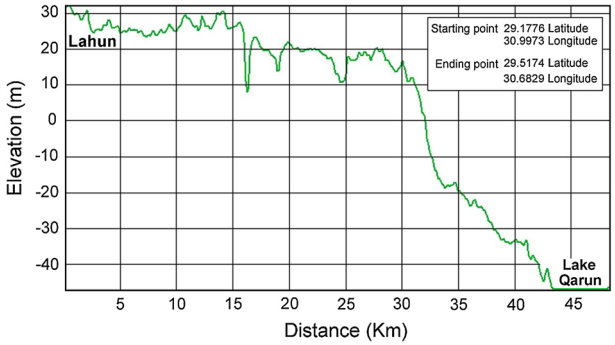

Fig. 2 Cross section illustrates the land slope from Lahun to Lake Qarun

conditions are warm and dry almost all the year, the lake brine gradually evaporates and its salinity increases. As a result, the lake has undergone marked salinization with accompanying changes in aquatic biota (Flower et al. 2006).

The objectives of the present work are mainly focused on the following:

1. Study in details the geochemical evolution of the surface water in the Fayoum Depression through its flow path from Nile at Lahun toward Lake Qarun (Fig. 1).
2. Identification the geochemical processes controlling the surface water chemistry in the Fayoum Depression.
3. Deduce a detailed geochemical model that demonstrates the evolution of Lake Qarun water.
4. Carry out a simulated evaporation model of Lake Qarun water to study the geochemical changes expected by further evaporation of lake water, assuming that the lake has no outflow except by evaporation.

2 Study Area and Methods

2.1 Site Description

Lake Qarun is located between the longitudes of 30°24′ & 30°49′E and latitudes of 29°24′ & 29°33′N, about 95 km south west of Cairo (Fig. 1). The lake has an irregular elongated shape of about 45 km length and 5.7 km mean width with an average area of about 240 km^2. The average depth of the lake is approximately 4.2 m. The deepest region ($\approx$8 m) is located in the middle of the lake while shallowest region lies in the eastern portion of the lake. Nearly 67 % of the lake area is between the 2 and 5 m depth contours, while only 18 % of the lake area is deeper than 5 m (Baioumy et al. 2010).

Nile River, the main source of fresh water, is reaching the Fayoum region via the Bahr Yousef channel (Fig. 1). Agricultural returns have been collected as drainage water and passed into Lake Qarun through two main drains, El-Wadi and El-Bats, with other minor drains between them (Fig. 1). To the north, the area is completely covered by sand and rock with several exposures of diatomite. This landscape is not irrigated and is virtually devoid of vegetation.

2.2 Climate

The studied catchment lies in Egypt's arid belt with a hot, long dry summer and a mild short winter, and consequently, the climate is generally warm and dry (Baioumy et al. 2010). In addition, it is characterized by low seasonal rainfall and a high evaporation rate. Rainfall is extremely low at <10 mm annually (Flower et al. 2006). The lowest evaporation rate (1.9 mm/day) is recorded in January while the highest value (7.3 mm/day) is recorded in June and the annual mean relative humidity varies between 50 and 62 % (Ali and Abdel Kawy 2013).

2.3 Hydrology

The irrigation and agricultural system in the Fayoum region depends mainly on Nile water. Fayoum City (Fig. 1), the principal town in the area, is a water distribution center for the Fayoum (domestic demands), and a network of canals and small pumping stations deliver water to the agricultural regions. Lake Qarun is a natural sink for drainage water from this area as it is surrounded from the south and southeast by cultivated land which slopes steeply toward the lake (Figs. 1, 2). Drainage waters are passed to Lake Qarun through two principal drains named El-Wadi and El-Bats drains (Fig. 1). The lake receives drainage water with a volume of about 338×10^6 m^3/year from El-Bats and El-Wadi drains in addition to about 67.8×10^6 m^3/year from groundwater while it losses about 415×10^6 m^3/year by evaporation (El-Shabrawy and Dumont 2009; Meshal 1977). The lake itself has no outflow except by evaporation (Meshal 1977; Wolters et al. 1989).

2.4 Geology and Geomorphology

Fayoum is a natural depression in the Western Desert of Egypt, extending over 6,068 km^2. Tableland areas surround the Fayoum Depression from the east, west, and south separating it from neighboring depressions, the Nile valley, and Wadi El Rayan. Most of the cultivated soils in the Fayoum Depression are deep alluvial loam or clayey, derived mainly from the Nile flood alluvium. The Fayoum Depression has a dense net of irrigation canals and drains. The Fayoum Depression area includes three main landscapes, i.e., lacustrine plain, alluvial–lacustrine plain, and alluvial plain (Abdel Kawy and Belal 2013; Ali and Abdel Kawy 2013). The southern shore of Lake Qarun is mostly surrounded by lacustrine deposits. These deposits cover an area of 198 km^2 and are classified as highly saline and poor productivity soils (Abdel Kawy and Belal 2013). The current status of soil salinity, sodicity, and water table indicate that most lacustrine and alluvial–lacustrine soils in the Fayoum Depression are actually being degraded by salinization, sodification, and waterlogging (Ali and Abdel Kawy 2013).

Geologically, the stratigraphic sequence in the area ranges in age from Quaternary to Tertiary (Fig. 3). The Fayoum Depression itself is excavated in Middle Eocene rocks, which composed essentially of gyps-ferrous shale, white marls, limestone, and sand (Hammad et al. 1983; Said 1993). The Quaternary deposits are widely distributed over the Fayoum area in the form of eolian, Nilotic (alluvial sediments), and lacustrine deposits. The alluvial sediments are composed of sands and gravels of variable sizes intercalated with calcareous silt and clay contents (Tamer 1968). The lacustrine deposits include claystone, gypsum, and calcareous materials intercalated with ferruginous sandy silt (Metwaly et al. 2010). The lacustrine deposits have prevailed in the area and extend to the south of Lake Qarun. In the whole area, Quaternary sediments directly overlay the limestone deposits of the Eocene age.

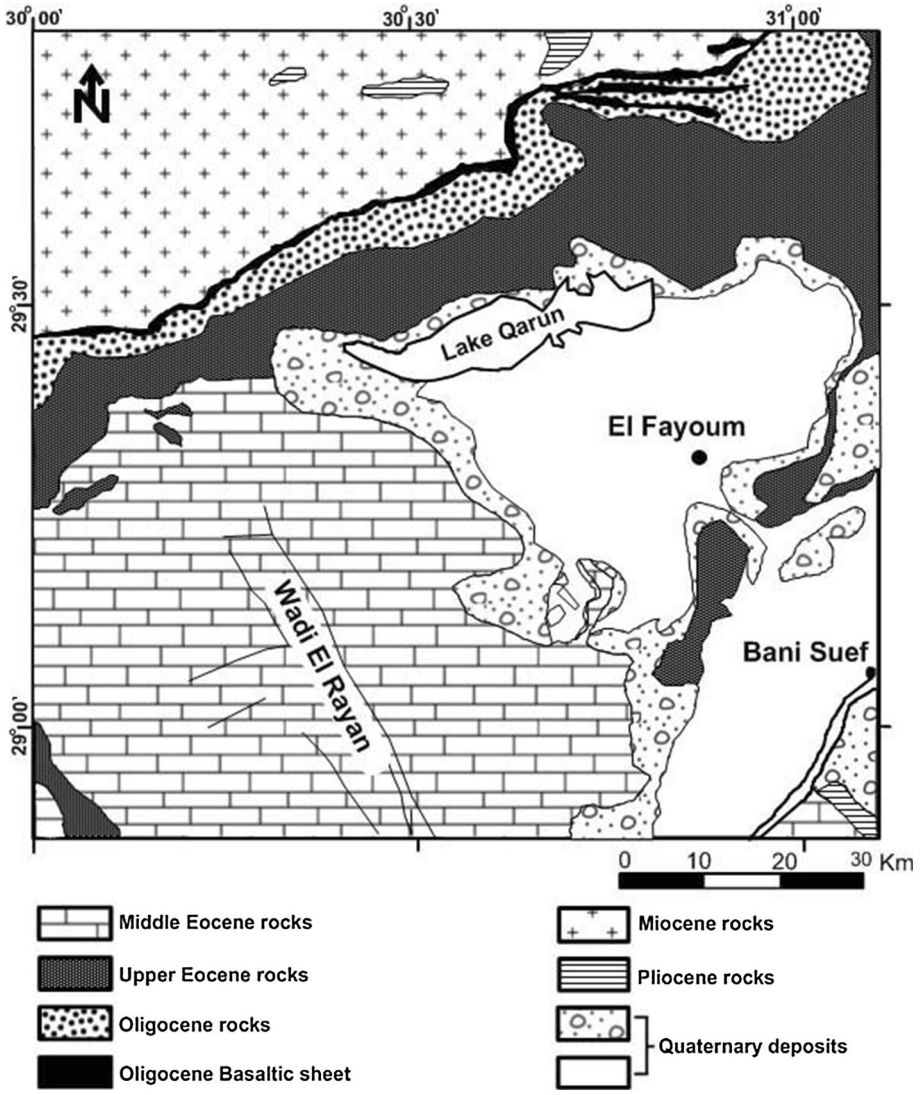

Fig. 3 Geological map of Fayoum area

2.5 Sampling and Sample Analysis

In June 2010, 2011, and 2012, surface water samples at Lake Qarun were collected regularly from 13 sites (Q1–Q13). In June 2012, additional surface water samples from irrigation canals and the drainage network were collected from 29 sites (samples 1–29) (Fig. 1). All samples were analyzed for sodium (Na^+), calcium (Ca^{2+}), magnesium (Mg^{2+}), potassium (K^+), sulfate (SO_4^{2-}), chloride (Cl^-), bicarbonate (HCO_3^-), silica (SiO_2) and oxygen isotopes ($\delta^{18}O$). At all sampling locations, GPS coordinates were recorded. Measurements of electrical conductivity (EC), pH, and temperature were carried out in the field using a SG78-SevenGo Duo pro (pH/Ion/Conductivity) portable meter with

an accuracy ±0.002 pH units, ±0.5 % of full-scale EC, and ±0.1 °C for temperature. After in situ measurements, the water samples for major ions analysis were filtered through a 0.45-μm disposable cellulose acetate syringe membrane filter (33 mm diameter, white rim, Whatman GmbH, Germany). The filtered samples were transferred into preacid-washed polyethylene (PE) containers which divided into three portions: (1) water samples acidified to pH <2 for main cations analysis; (2) water samples for main anion analysis; and (3) water samples for oxygen isotopes analysis. All sampling containers were left to dry for 2 days after acid or deionized washing. The PE bottles were filled without air bubbles and tightly capped immediately with PE screw caps. Then, the water samples were stored in double PE plastic bags, kept at 4 °C, and transported to the laboratory as soon as possible after sampling. Analysis of HCO_3^- was conducted immediately after samples reached the laboratory and the remaining analyses within the next 24 h. Total dissolved solids (TDS) were calculated using the sum of the major ions (Na^+, K^+, Ca^{2+}, Mg^{2+}, HCO_3^-, SO_4^{2-}, Cl^-, and SiO_2), assuming that the fraction below 0.45 μm can be considered "dissolved." All analyses, except $\delta^{18}O$, were carried out at the Water Quality Central Laboratory, Fayoum Drinking Water and Sanitation Company, Fayoum, Egypt. The analyses were done in accordance with approved analytic methods (APHA 1998) as summarized in Table 1. All analytical procedures are accredited according to ISO/IEC 17025.

Water samples were analyzed for oxygen isotope composition ($\delta^{18}O$) using a Gas Bench II system (Thermo Finnigan, Bremen, Germany) coupled with a Thermo Finnigan Delta plus XP isotope ratio mass spectrometer in the stable isotopologues laboratory at McMaster University, Canada. The details of the analytical procedures are described in Klein Gebbinck et al. (2014).

All oxygen isotope results were obtained by calculating the mean of the last 10 measurements and normalized by using two inter-laboratory water standards (i.e., MRSI-1 and MRSI-2). The δ18O values of the samples were reported normalized to V-SMOW, and the precision for replicate sample analyses is ≤0.08 ‰.

Saturation indices (SI) of the dissolved minerals in water samples were calculated using the PHREEQC version 3 software (PHREEQC-3) (Parkhurst and Appelo 2013). In addition, a simulated evaporation model of Lake Qarun water was carried out also using PHREEQC-3 software. This software was compiled on March 13, 2014. It is a computer program that is designed to perform a wide variety of aqueous geochemical calculations. One of the new features of the PHREEQC version 3 is the Pitzer aqueous model (Pitzer database), which can be used for high-salinity waters that are beyond the range of application for the Debye-Hückel theory (Parkhurst and Appelo 2013).

Table 1 Analytical methods of the studied water samples, after APHA (1998)

Analytical parameters	Method (APHA 1998)	Uncertainty (%)
SO_4^{2-}	4500-SO_4^{2-} E	12.9
Cl^-	4500-Cl^- B	4.1
HCO_3^-	2320-B Titration method	1.8
Na^+	3120 B, ICP method by ICP-OES	3.6
K^+	3120 B, ICP method by ICP-OES	5
Mg^{2+}	3120 B, ICP method by ICP-OES	11.6
Ca^{2+}	3120 B, ICP method by ICP-OES	9
SiO_2	4500-SiO_2 C	8.7

Table 2 General parameters and major ion chemistry of the surface waters in Fayoum Depression, Egypt

Water system	Sampling sites	pH	EC	Ca^{2+}	Mg^{2+}	Na^{+}	K^{+}	HCO_3^{-}	SO_4^{2-}	Cl^{-}	SiO_2	TDS	$\delta^{18}O^{b}$
Irrigation waters	1	7.70	0.38	36.16	9.43	19.78	3.21	120.00	38.20	23.18	5.11	255.07	+3.09
	2	7.70	0.45	36.10	10.60	30.20	3.90	132.80	52.32	37.68	5.06	308.66	+3.12
	3	7.70	0.39	36.20	9.89	19.58	3.04	122.80	39.90	25.75	4.73	261.89	+3.21
	4	7.60	0.44	31.90	9.30	22.00	3.90	128.80	51.90	33.79	4.53	286.12	+3.19
	5	7.80	0.42	38.10	10.30	22.40	3.31	122.40	47.80	28.72	6.23	279.26	+3.22
	6	7.60	0.40	34.00	9.90	24.70	3.80	136.80	39.43	25.38	5.07	279.08	+3.22
	7	7.53	0.45	37.10	10.80	38.40	4.30	135.60	48.50	33.72	5.98	314.40	+3.13
	8	7.50	0.50	37.70	11.60	35.80	4.50	144.80	56.90	39.32	5.71	336.33	+3.26
	9	7.60	0.36	32.10	9.60	21.90	3.80	130.80	28.90	16.68	4.74	248.52	+3.19
	10	7.60	0.65	43.30	16.16	47.20	8.22	165.20	72.70	56.06	10.60	419.44	+3.33
	11	7.50	0.68	46.32	15.22	45.20	4.72	174.00	75.90	61.60	9.87	432.83	+3.24
	12	7.50	0.76	47.91	15.96	46.10	5.17	182.40	73.34	57.10	10.73	438.71	+3.27
	13	7.77	0.87	54.20	19.79	71.40	5.53	184.80	118.00	82.20	11.82	547.74	+3.30
	14	7.50	0.60	46.32	15.22	45.20	4.72	174.00	75.90	61.60	9.87	432.83	+3.24
	15	7.50	0.91	47.91	15.96	46.10	5.17	182.40	73.34	57.10	10.73	438.71	+3.27
	16	7.90	1.11	62.00	20.49	100.10	6.13	173.20	154.90	151.10	8.62	676.54	+3.37
	17	7.70	3.76	144.40	37.73	506.20	39.10	212.40	593.60	807.80	9.14	2,350.37	+4.22
Drainage waters	18	7.50	1.01	49.20	19.30	112.60	7.00	198.80	147.80	116.96	8.87	660.53	+3.39
	19	7.60	0.97	73.27	15.73	85.50	6.13	154.00	154.10	119.28	8.53	616.54	+3.49
	20	7.60	1.38	77.90	23.49	139.60	7.78	183.20	207.90	190.30	12.47	842.64	+3.56
	21	7.60	1.60	93.09	26.55	142.40	8.67	192.80	276.80	241.50	14.15	995.96	+3.57
	22	7.80	1.73	100.20	28.60	156.50	6.95	204.40	292.30	260.50	14.69	1,064.14	+3.62
	23[a]	7.70	1.84	188.00	65.89	481.60	17.10	277.50	510.30	730.30	12.61	2,283.30	+3.62
	24	7.50	1.10	53.33	22.20	117.20	8.63	224.40	141.60	116.47	10.84	694.67	+3.24
	25	7.70	1.91	82.30	32.51	182.40	15.10	295.20	291.10	303.90	15.14	1,217.65	+3.34

Table 2 continued

Water system	Sampling sites	pH	EC	Ca^{2+}	Mg^{2+}	Na^{+}	K^{+}	HCO_3^{-}	SO_4^{2-}	Cl^{-}	SiO_2	TDS	$\delta^{18}O^{b}$
	26	7.60	1.98	120.00	27.58	204.90	10.25	190.80	380.80	308.60	13.26	1,256.19	+3.61
	27	7.50	1.94	106.30	26.56	193.80	10.49	196.00	361.60	308.60	13.52	1,216.87	+3.49
	28	7.50	2.10	106.00	30.52	203.30	11.90	186.40	393.30	332.14	11.72	1,275.28	+3.48
	29[a]	7.50	2.40	166.80	63.60	425.00	23.30	220.10	502.00	758.30	13.14	2,172.24	+3.50
Lake Qarun waters[a]	Q1	8.20	34.10	418.80	969.87	9,360.60	285.33	179.53	11,808.00	11,525.50	8.90	34,556.53	+7.54
	Q2	8.20	32.30	430.97	1,045.23	9,601.67	304.67	201.00	11,580.00	11,822.67	8.30	34,994.51	+7.29
	Q3	8.20	32.50	357.90	846.60	7,940.66	250.33	175.73	8,704.80	10,544.30	9.90	28,830.22	+7.14
	Q4	8.30	34.10	514.47	1,027.03	9,458.33	325.50	181.07	11,417.43	11,695.00	8.10	34,626.93	+7.60
	Q5	8.40	36.70	523.53	1,147.67	9,919.33	480.00	184.37	10,695.30	12,339.77	6.50	35,296.47	+7.86
	Q6	7.80	34.80	394.00	1,131.33	9,549.65	289.00	192.13	10,453.00	12,305.67	18.50	34,333.28	+7.62
	Q7	8.20	34.40	453.33	1,238.73	10,165.68	282.67	159.90	12,392.00	12,092.00	7.50	36,791.81	+7.67
	Q8	8.30	35.40	329.40	1,177.33	12,124.70	386.67	156.45	12,387.00	12,278.33	6.01	38,845.89	+7.81
	Q9	8.30	36.70	483.83	1,267.17	9,949.00	300.00	156.33	12,376.00	12,317.10	5.90	36,855.33	+7.95
	Q10	8.30	36.80	496.97	1,237.50	10,162.60	296.67	166.10	13,461.33	12,415.10	6.40	38,242.67	+7.93
	Q11	8.30	37.00	463.43	1,217.33	10,887.67	289.83	157.20	13,630.00	12,472.37	6.50	39,124.33	+7.93
	Q12	8.40	36.90	453.20	1,203.00	12,271.00	362.00	157.13	12,207.00	12,383.67	5.50	39,042.50	+7.89
	Q13	8.30	36.60	449.53	1,100.17	10,158.50	296.00	170.73	12,283.33	12,509.37	9.70	36,977.33	+7.79

Water system	Sampling sites	SI Calcite	SI Gypsum	SI Halite
Irrigation waters	1	−0.05	−2.21	−7.91
	2	−0.08	−2.09	−7.50
	3	−0.06	−2.19	−7.87
	4	−0.22	−2.13	−7.69
	5	0.04	−2.10	−7.76
	6	−0.20	−2.22	−7.76

Table 2 continued

Water system	Sampling sites	SI Calcite	SI Gypsum	SI Halite
	7	−0.25	−2.12	−7.45
	8	−0.26	−2.05	−7.41
	9	−0.20	−2.37	−7.99
	10	0.01	−1.93	−7.16
	11	−0.06	−1.88	−7.13
	12	0.04	−1.89	−7.17
	13	0.26	−1.68	−6.82
	14	−0.08	−1.93	−7.18
	15	0.00	−1.70	−6.64
	16	0.43	−1.55	−6.42
	17	0.48	−0.90	−5.06
Drainage waters	18	−0.11	−1.64	−6.46
	19	0.14	−1.47	−6.59
	20	0.21	−1.37	−6.19
	21	0.28	−1.22	−6.08
	22	0.49	−1.17	−6.01
	23	0.72	−0.87	−5.12
	24	0.04	−1.64	−6.46
	25	0.46	−1.27	−5.88
	26	0.28	−1.03	−5.83
	27	0.20	−1.09	−5.85
	28	0.17	−1.07	−5.80
	29	0.36	−0.91	−5.15
Lake Qarun waters	Q1	0.81	−0.07	−2.83
	Q2	0.89	−0.07	−2.80

Table 2 continued

Water system	Sampling sites	SI Calcite	SI Gypsum	SI Halite
	Q3	0.79	−0.20	−2.93
	Q4	0.98	0.01	−2.81
	Q5	1.05	−0.01	−2.76
	Q6	0.49	−0.14	−2.78
	Q7	0.80	−0.04	−2.77
	Q8	0.71	−0.19	−2.69
	Q9	0.90	−0.01	−2.77
	Q10	0.92	0.02	−2.76
	Q11	0.90	−0.02	−2.74
	Q12	0.90	−0.06	−2.68
	Q13	0.88	−0.05	−2.76

Units are in mg/L, except EC (mS/cm), pH, $\delta^{18}O$, and saturation index (SI)

[a] Average values of water samples collected during June 2010, 2011, and 2012 from Lake Qarun (Q1–Q13) and from El-Wadi and El-Bats drains outlets (samples 23 and 29, respectively)

[b] $\delta^{18}O$ was measured only during June 2012

3 Results and Discussion

The physiochemical results of the investigated water samples are presented in Table 2. The data showed that the TDS trend increases from the head of Fayoum irrigation system at sampling site 1 toward Lake Qarun (Fig. 4). In general, the concentrations of most ions and TDS are in the order; lake water $\ggg$ drainage water > irrigation water (Table 2). Only one sample (sampling site 17) from irrigation canals was found to have a TDS value of 2,350.37 mg/L, which is more than the TDS of drainage waters (Table 2). This is because the water depth was very shallow when this sample was taken during sampling and also the water flowed for a long distance from sampling site 1 to sampling site 17. Therefore, water salinity increased by evaporation. Sample 17 has the highest value of $\delta^{18}O$ (+4.22) among all irrigation waters and drainage waters (Table 2). The $\delta^{18}O$ is concentrated in water as a result of evaporative concentration (Gat 1996).

According to the spatial distribution of TDS values of Fayoum surface waters, it was found that water salinity increases with increasing proximity to Lake Qarun (Fig. 4). In Lake Qarun, it is noted that the TDS of the lake water is low at the eastern part and gradually increases north-westward. This could be due to the dilution effect of drainage water discharging into the lake from the southeastern side rather than the northwestern. The effect of dilution is observed near the outlet mouths of El-Bats and El-Wadi drains which have lower TDS than the other sites in the lake (Fig. 4).

3.1 Hydrochemical Water Types

Chadha (1999) developed a new diagram for geochemical classification of natural waters and interpretation of chemical data. In this diagram, the difference in milliequivalent percentage between alkaline earth (Ca + Mg) and alkali metals (Na + K) is plotted on the *X* axis, and the difference in milliequivalent percentage between weak acidic anions

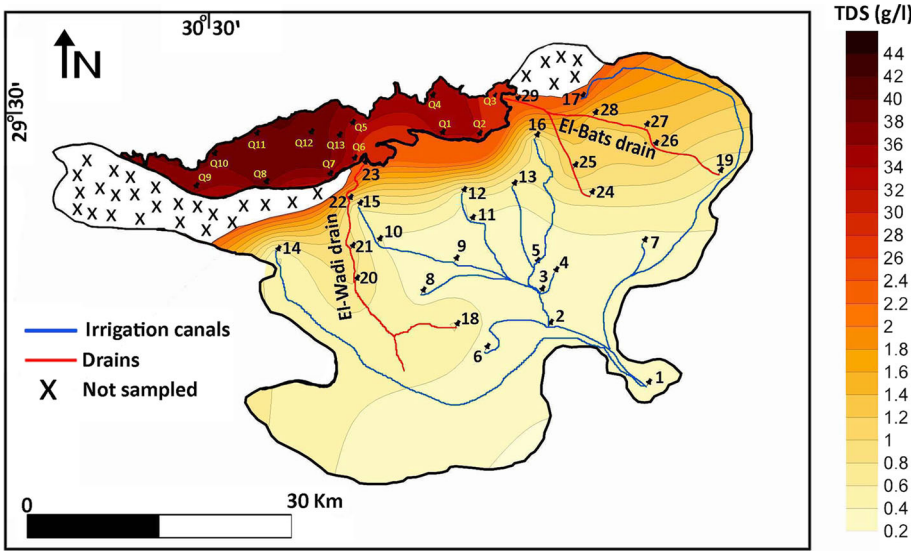

Fig. 4 Spatial distribution of TDS on the studied area showing that salinity increases with increasing proximity to Lake Qarun

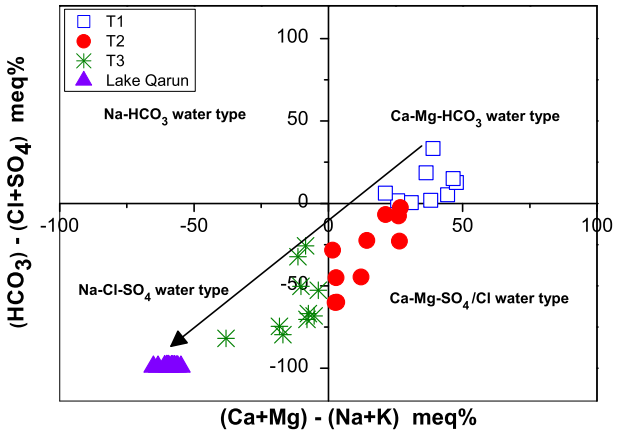

Fig. 5 Chadha diagram showing the hydrochemical water types of the studied water samples (Chadha 1999)

(CO_3 + HCO_3) and strong acidic anions (Cl + SO_4) plotted on the *Y* axis. Plotting of the studied water samples on the diagram revealed the presence of three hydrochemical water facies: water type 1 (T1), water type 2 (T2) and water type 3 (T3) (Fig. 5).

3.1.1 Water Type 1 (T1): (Ca–Mg–HCO_3)

This type is mainly irrigation water, collected from sites 1–9 close to the head of Fayoum irrigation system (Fig. 1). These waters are almost always fresh with minimum TDS (248.52 mg/L) at sampling site 9 and maximum TDS (336.33 mg/L) at sampling site 8. The waters of T1 type are slightly alkaline (pH 7.50–7.77, Table 2). This water type is characterized by higher concentrations of weak acidic anions mainly HCO_3 than strong acidic anions (Cl + SO_4) (Fig. 5). It also has higher concentrations of alkali earth elements (Ca + Mg) than alkali metals (Na + K). All waters of T1 type are undersaturated with respect to calcite except only one sample (sample 5) is just at saturation (Table 2; Fig. 6). All T1 waters are undersaturated with respect to gypsum and halite (Fig. 6).

3.1.2 Water Type 2 (T2): (Ca–Mg–SO_4/Cl)

This water type includes samples 10, 11, 12, 13, 14, 15, 16, 19, 21, and 22. These water samples are characterized by higher concentrations of strong acidic anions (Cl + SO_4) than weak acidic anions mainly HCO_3 and higher concentrations of alkali earth elements (Ca + Mg) than alkali metals (K + Na) (Fig. 5). Water type (T2) includes both irrigation waters (sampling sites 10–16) and drainage waters (sampling sites 19, 21 and 22) (Fig. 1). The T2 waters are much closer to Lake Qarun than those of T1 (Fig. 1). The TDS of T2 waters collected from irrigation canals ranges from 419.44 mg/L (sample 10) to 676.54 mg/L (sample 16) while it ranges from 616.54 mg/L (sample 19) to 1,064.14 mg/L (sample 22) for samples collected from drainage waters (Table 2). The waters of type T2 have pH ranges 7.50–7.90 (Table 2). Most of T2 waters are supersaturated with respect to calcite except two samples; samples 11 and 14 are still undersaturated (Table 2; Fig. 6). All T2 waters still undersaturated with respect to gypsum and halite (Fig. 6).

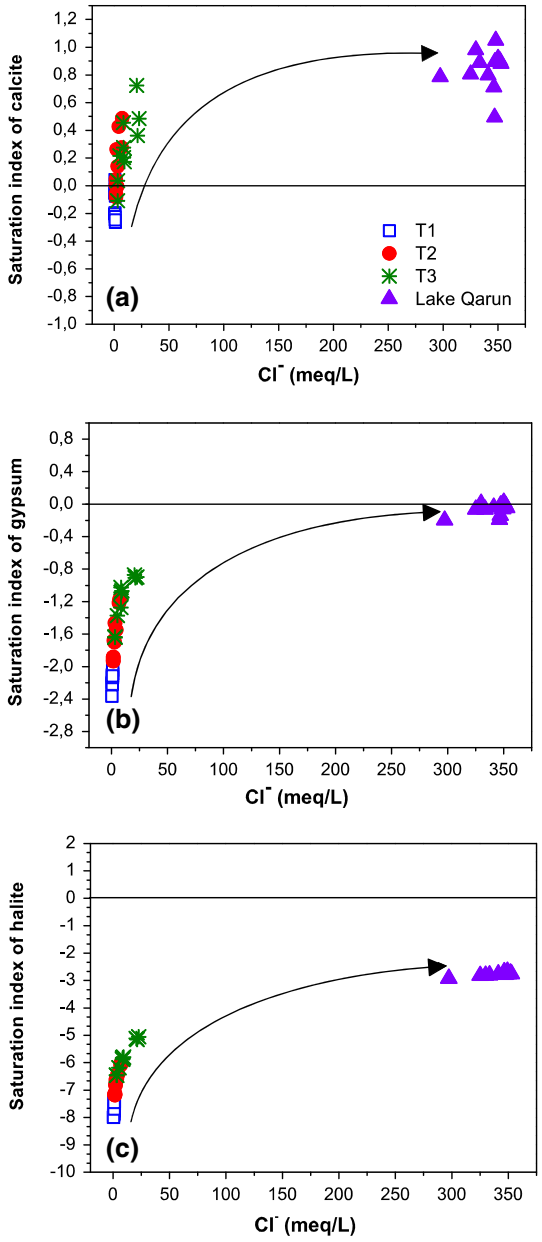

Fig. 6 Calculated saturation indices of **a** calcite, **b** gypsum, and **c** halite of the studied water samples. All saturation indices increase toward Lake Qarun due to the effect of the evapoconcentration process

3.1.3 Water Type 3 (T3): (Na–Cl–SO_4)

This water type includes water samples collecting from sites 17, 18, 20, 23, 24, 25, 26, 27, 28, and 29. All of these water samples were taken from drains except sample 17 which was taken from an irrigation canal. All drainage waters are conveyed into the two main drains, El-Wadi and El-Bats. Water samples 23 and 29 were collected from the outlet mouths of

El-Wadi and El-Bats drains, respectively, which represent the main inputs of drainage water to Lake Qarun (Fig. 1). Samples 23 and 29 have the highest salinities among all drainage waters (2,283.30 and 2,172.24 mg/L, respectively). On the other hand, sample 17 has the highest salinity (2,350.37 mg/L) between all irrigation and drainage waters that were collected from Fayoum (Table 2; see also Sect. 3). All waters of T3 type are characterized by higher concentrations of strong acidic anions (Cl + SO_4) than weak acidic anions mainly HCO_3 and higher concentrations of alkali metals (K + Na) than alkali earth elements (Ca + Mg) (Fig. 5). The pH of T3 water type ranges from 7.50 to 7.70. All T3 waters are supersaturated with respect to calcite except only one sample (sample 18) is still undersaturated (Table 2; Fig. 6). On the other hand, all T3 waters are undersaturated with respect to gypsum and halite (Fig. 6).

3.1.4 Lake Qarun Water; (Na–Cl–SO_4)

Lake Qarun water samples lie in the field of T3 water type. They are characterized by very high TDS values and high pH values as compared to the irrigation and drainage waters (Table 2). The highest TDS recorded at site Q11 with value 39,124.33 mg/L and the highest pH recorded at sites Q5 and Q12 with value 8.40 for both samples. The lake water is supersaturated with respect to calcite at all locations (Fig. 6). On the other hand, only two locations in Lake Qarun (Q4 and Q10) just reached the saturation state with respect to gypsum while the other locations still undersaturation (Table 2; Fig. 6). The lake water still undersaturation with respect to halite at all locations (Fig. 6).

3.2 Geochemical Evolution of Irrigation and Drainage Waters in the Fayoum Depression

The geochemical alteration of the Nile water (main source of fresh water) through its course along Fayoum Depression is the main concern of this section. As shown in Chadha diagram (Fig. 5), the surface water in Fayoum Depression have evolved from Ca–Mg–HCO_3 water type (T1) at the head of Fayoum irrigation system to the Na–Cl–SO_4 water type (T3) close to and at Lake Qarun passing through a transitional Ca–Mg–SO_4/Cl water type (T2). The HCO_3^- decreases proportionally relative to Cl^- and SO_4^{2-}, and also Ca^{2+} and Mg^{2+} decrease proportionally relative to Na^+ with increasing proximity to Lake Qarun (Fig. 5).

Yan et al. (2002) concluded that weathering of carbonate rocks leads to freshwaters low in dissolved silica (<20 mg/L) with a SiO_2/HCO_3 molar ratio 0.02. Also, ternary plots of cations (Na + K − Mg − Ca) as well as anions (Cl + SO_4 − HCO_3 − Si) could explore the relative importance of different weathering regimes (Stallard and Edmond 1981). Accordingly, the T1 waters have SiO_2 ranges 4.53–6.23 mg/L (Table 2) with an average SiO_2/HCO_3 molar ratio equal to 0.04 (calculated from Table 2), and they fall in the cluster toward HCO_3 and Ca apexes (Fig. 7). This suggests that weathering of carbonates is the dominant process contributing to this water type. All T1 waters are undersaturated with respect to calcite (Fig. 6a). Limestone which is composed mainly of calcite is abundant at the studied area. Consequently, congruent dissolution of calcite should give Ca/HCO_3 molar ratio equals to 0.5 as shown in the following reaction:

$$\underset{\text{Calcite}}{CaCO_3} + H_2O + CO_2 \rightarrow Ca^{2+} + 2HCO_3^- \quad (1)$$

The plotting of Ca^{2+} versus HCO_3^- showed that all samples fall close to the 1:2 line with some points having little excess of HCO_3^- (Fig. 8). The influx of CO_2 that might be

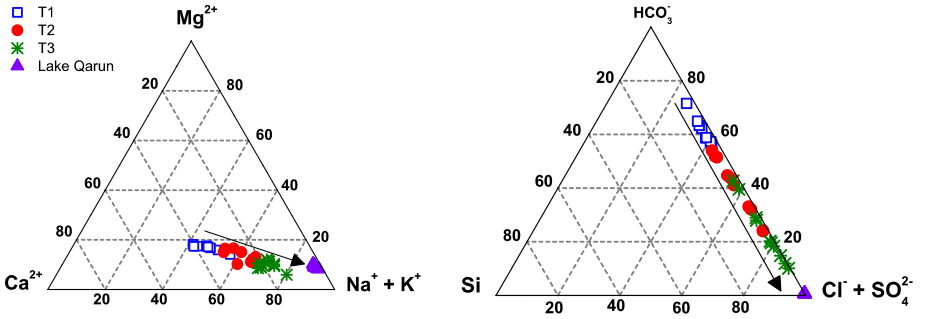

Fig. 7 Ternary diagram showing the chemical trends of the studied water samples (in mmol%). The points have evolved from HCO_3^- apex to Cl^- and SO_4^{2-} apexes and from Ca^{2+} and Mg^{2+} apexes to $Na^+ + K^+$ apex as water flows toward Lake Qarun

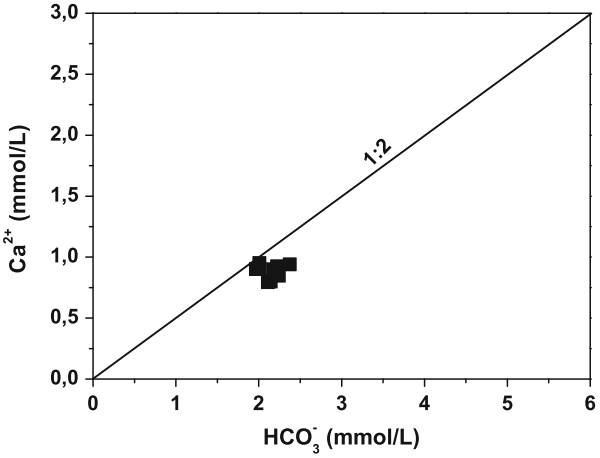

Fig. 8 Binary plot of Ca^{2+} versus HCO_3^- of T1 waters. Most of T1 waters lie close to the 1:2 line

released by the decay of organic materials can be mobilized and takes part in chemical reactions (Hem 1986). If it is assumed that each CO_2 molecule could react with solid CO_3 to give two HCO_3^- ions (Eq. 1), reactions with noncarbonate minerals would yield one HCO_3^- ion for each participating CO_2 molecule which could contribute to the little excess HCO_3^- over Ca^{2+} in T1 waters (Hem 1986).

As the surface water flows toward Lake Qarun, waters of T2 and T3 types have evolved from T1 type with an increase of Cl^- and SO_4^{2-} relative to HCO_3^- along with an increase of Na^+ relative to Ca^{2+} and Mg^{2+} (Figs. 5, 7). The colocation of Na^+, Cl^-, and SO_4^{2-} can be explained by the fact that various evaporites are present in the studied area (Huang et al. 2009). Gypsum is abundant in the current studied area (Fayoum Depression). Also, gypsum is added to improve Fayoum soil productivity especially to the lands close to the southern shore of Lake Qarun. These lands cover an area of 198 km^2 and are classified as highly saline and poor productivity soils (Abdel Kawy and Belal 2013). In addition, most lacustrine and alluvial–lacustrine soils in the Fayoum Depression are actually degraded by salinization. Salts crusts on the soil surfaces are observed during hot and dry conditions in summer. Most of the drainage and irrigation waters samples of T2 and T3 lie in the regions

of lacustrine and alluvial–lacustrine soils which are rich in gypsum and soil salts. As a result, congruent dissolution of soluble minerals such as gypsum ($CaSO_4{\cdot}2H_2O$) or halite (NaCl) from these types of soils can lead to very high Na^+, SO_4^{2-}, and Cl^- concentrations in T2 and T3 waters (Eugster 1980). Also, the subsequent leaching of readily soluble salts (e.g., NaCl) from the soil surface progressively increases the salinity of the surface water and raises the level of Na^+ and Cl^- in the agricultural returns.

Mineral equilibrium and saturation indices calculations could predict the reactive mineralogy (Deutsch 1997). The SI of calcite, gypsum, and halite for all the studied water samples is given in Fig. 6. The results showed that waters of T1 are undersaturated with respect to calcite, gypsum, and halite. Close to Lake Qarun, most waters of T2 and T3 types became supersaturated with respect to calcite and still undersaturated with respect to gypsum and halite (Fig. 6). Therefore, the dissolution of gypsum and halite is expected to contribute to the solute budget of T2 and T3 waters. As the saturation state indicates the direction of the process, precipitations of carbonate minerals accompanied by the dissolution of evaporites such as gypsum and halite possibly have influenced the chemical evolution of water from Ca–Mg–HCO_3 at locations of T1 type to Na–SO_4–Cl at locations of T3 passing through a transitional Ca–Mg–SO_4/Cl at locations of T2 (Figs. 5, 6, 7).

To verify the contribution of gypsum and halite dissolution to T2 and T3 waters, binary plotting of $[(Ca^{2+} + Mg^{2+}) - 0.5\ HCO_3^-]$ against SO_4^{2-} and also Na^+ against Cl^- were studied. The contribution of gypsum to the concentration of Ca^{2+} can be estimated by studying the relationship between the noncarbonate mineral-derived Ca and Mg using the formula $[(Ca^{2+} + Mg^{2+}) - 0.5\ HCO_3^-]$ plotted against SO_4^{2-} (Kimblin 1995). The binary plotting of $[(Ca^{2+} + Mg^{2+}) - 0.5\ HCO_3^-]$ against SO_4^{2-} for all irrigation and drainage waters showed strong positive correlations $R^2 = 0.969$ and $R^2 = 0.785$ for T2 and T3, respectively, while in the case of T1 showed a weak correlation $R^2 = 0.039$ (Fig. 9). As a result, the dissolution of gypsum probably influences the chemistry of T2 and T3 waters and not influences T1 waters. In the presence of HCO_3^-, the Ca^{2+} ion supplied by gypsum dissolution increases the ion activity product ($a_{Ca}^{2+} + a_{CO3}^{2-}$) and subsequently

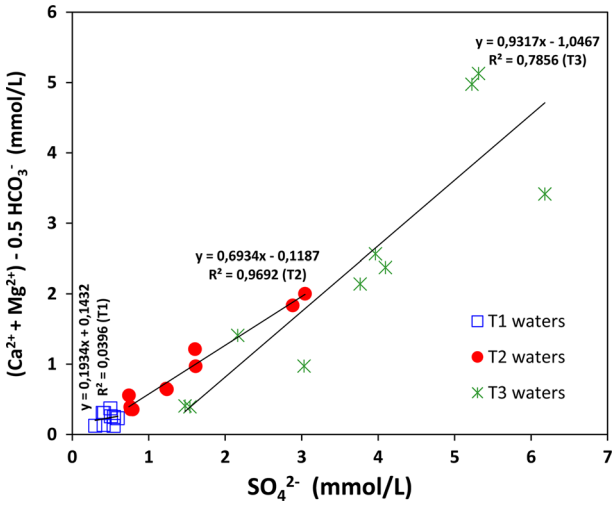

Fig. 9 Binary Plot of $(Ca^{2+} + Mg^{2+}) - 0.5\ HCO_3^-$ against SO_4^{2-} of irrigation and drainage waters in Fayoum Depression shows the contribution of gypsum dissolution to T2 and T3 waters

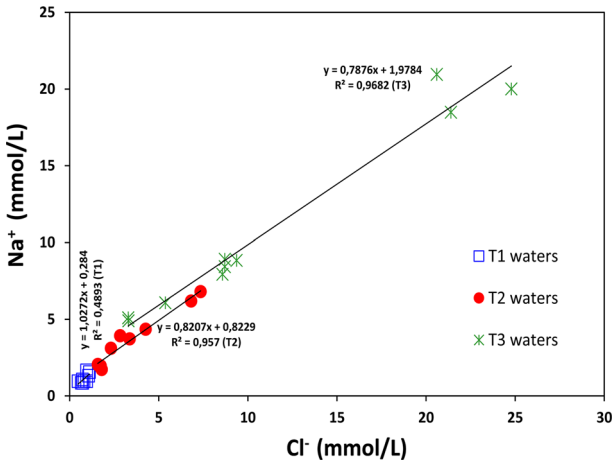

Fig. 10 Binary plot of Na^+ versus Cl^- of irrigation and drainage waters showing the significant dissolution effect of NaCl salt on T2 and T3 waters

increases the saturation index of calcite (Dargam and Depetris 1996). This process may explain why the saturation state with respect to calcite changed from undersaturation in the case of T1 to supersaturation for T2 and T3 waters (Fig. 6).

The binary plotting of Na^+ against Cl^- for all irrigation and drainage waters showed strong positive correlations in the case of T2 waters ($R^2 = 0.957$) and T3 waters ($R^2 = 0.968$) while in the case of T1 showed a weak correlation ($R^2 = 0.480$) (Fig. 10). This indicates that halite dissolution has significantly impacted the chemical composition of T2 and T3 waters.

The contribution of evaporite dissolution to T2 and T3 waters is also evidenced in the ternary plot where the irrigation and drainage waters of T2 and T3 fall in the cluster toward Na + K apex and Cl + SO_4 apex (Fig. 7).

3.3 Hydrogeochemical Evolution of Lake Qarun

Lake Qarun water has a Na–SO_4–Cl water type (Fig. 5). T3 waters specially samples 23 and 29, which represent the outlet mouths of El-Wadi and El-Bats drains, respectively, have the same Na–SO_4–Cl water type like Lake Qarun (Fig. 5). As mentioned previously, El-Bats and El-Wadi drains represent the main sources of drainage water recharge to Lake Qarun (Fig. 1). Thus, Lake Qarun as a closed system seems to be evolved geochemically from drainage water inflow as a result of progressive evaporation. Gibbs (1970) suggested a simple plot of TDS versus the weight ratio of $Na^+/(Na^+ + Ca^{2+})$ could provide information on the relative importance of the major natural mechanisms controlling surface water chemistry (Fig. 11). In the present study, a Gibbs plot of data indicates that T1 and T2 water chemistry are mainly controlled by rock weathering. Some of T3 waters lie in the rock weathering domain while others are controlled by evaporation-crystallization process. This supports the earlier suggestions that weathering of carbonates controls the chemistry of T1 waters while T2 and T3 waters are controlled by weathering of evaporites. Some waters of T3 lie on the field of evaporation crystallization perhaps due to the fact that much of the evaporation can be ascribed to the use of water for irrigation, where a greater surface

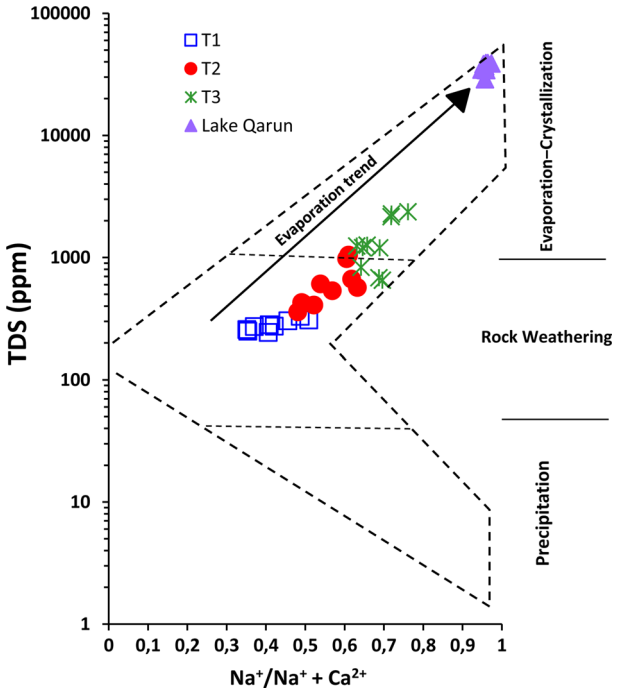

Fig. 11 Gibbs plot showing the mechanisms controlling the major ion composition of the surface water in Fayoum Depression. Lake Qarun water is mainly controlled by evaporation-crystallization process

area of water is made available for evaporation before the remaining water is returned to drains as drainage waters (agriculture returns). Also, intensive agriculture practicing can increase the weathering and erosion of soil salts resulting in a higher TDS of the agriculture returns. Lake Qarun water is characterized by a high Na/(Na + Ca) ratio and a high TDS concentration, suggesting that it is mainly controlled by an evaporation-crystallization process (Fig. 11). The chemical composition of surface water in Fayoum Depression evolves (in a sequence of water samples taken in a Lake Qarun direction) from rock-weathering-type waters found in headwaters to more concentrated sodic waters found in Lake Qarun as a result of evaporation and concentration of salts accompanied by the crystallization of $CaCO_3$. This is most likely because the saturation index of calcite evolves from undersaturation state in headwaters (T1) to supersaturation state in Lake Qarun (Fig. 6). The hot and dry climatic conditions prevailed throughout the area strengthen the evaporation trend from head waters to Lake Qarun that clearly obvious on Gibbs's model (Fig. 11). Thus, under arid conditions, the continuous evaporation under a very long span of time leads to a dramatic effect in the water chemistry of Lake Qarun, resulting in the higher levels of Na^+ and Cl^- than those found in the transition and upstream areas as well as a drastic increase in the TDS of the lake water (Fig. 11). In the ternary plot (Fig. 7), Lake Qarun waters plotted very close to the Na + K and Cl + SO_4 apexes. In Lake Qarun, HCO_3^- decreases proportionally relative to Cl^- and SO_4^{2-} while Ca^{2+} and Mg^{2+} decrease proportionally relative to Na^+ (Figs. 5, 7). The increase of Na^+, Cl^-, and SO_4^{2-} in Lake Qarun is mainly due to solute accumulation by evaporation while the depletion of Ca^{2+} and HCO_3^- could be due to carbonate mineral precipitation.

All saturation indices of calcite, gypsum, and halite increase with increasing proximity to Lake Qarun and the highest values recorded in the lake itself (Fig. 6). This indicates that continuous water loss by evaporation in Lake Qarun causes the increase in concentration of these minerals.

3.4 Application of Hardie and Eugster's Model

Hardie and Eugster (1970) suggested a model that interprets the chemistry of waters undergoing evaporation in terms of a succession of chemical divides. A chemical divide is a point in the evolution sequence of brine in which precipitation of a mineral depletes the water in certain cations or anions with further evaporation moves the solution along a distinct pathway. This was called "fractionation by mineral precipitation" (Eugster 1980) or principle of chemical divide as described by Drever (1982) and is now popularized under the name of "chemical divide" (Bąbel and Schreiber 2014). The main idea of the principal of chemical divide is that the molar ratio of the component ions of precipitated salt must change, unless it is exactly equal to one in the initial solution at the beginning of evaporation process (Bąbel and Schreiber 2014; Drever 1982). Therefore, the ion with the lower concentration at the onset of evaporitic precipitation will progressively decrease in concentration, whereas the other ion showing initially higher concentration will build up in solution. The Hardie and Eugster's model has been simply modified by Drever (1982) (Fig. 12). This modified model is obviously very simple, and it is generalized to cover a wide range of starting compositions of the water to be evaporated. With almost of natural waters, the first mineral to precipitate, and hence to cause the first chemical divide, is calcite (Drever 1982). Further evaporation moves the solution along path I or path II depends on whether the calcium concentration (in equivalents) is greater or less than the carbonate alkalinity (in equivalents) (Fig. 12). In almost of natural waters, the alkalinity is mainly expressed as HCO_3^- (Eugster 1980; Eugster and Hardie 1978). In the present case, close to the head of the Fayoum irrigation system, the waters of type T1 (samples 1–9) have $2mCa^{2+} < mHCO_3^-$ on average. The total average of $mHCO_3^-$ of T1 waters is

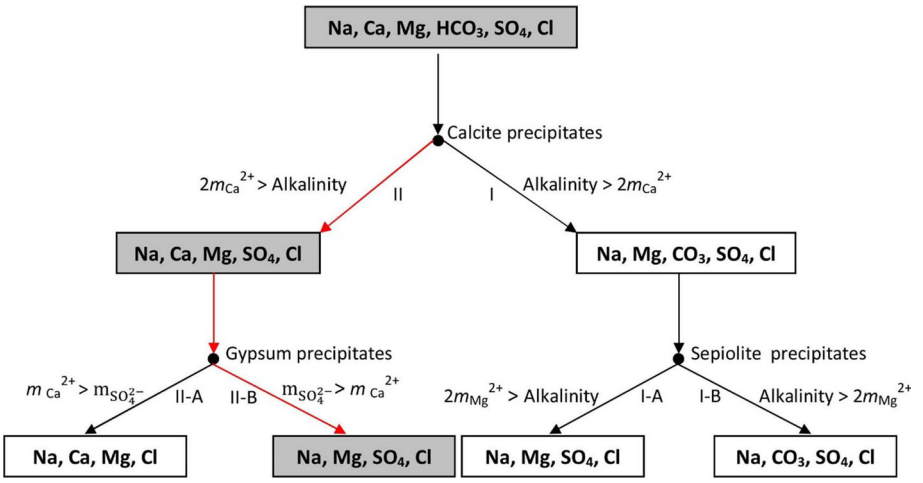

Fig. 12 Some possible paths during evaporation of natural water (a model modified from Hardie and Eugster 1970 by Drever 1982). Lake Qarun water should evolve along the path II–IIB

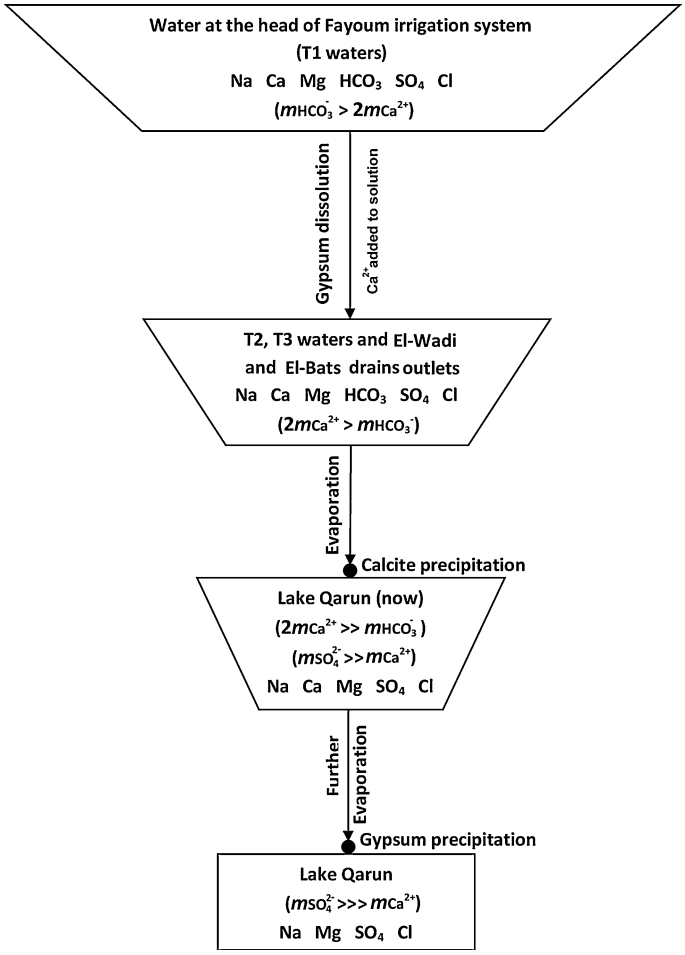

Fig. 13 Suggested flow chart shows the possible path for the geochemical evolution of surface water in Fayoum Depression

2.14 mmol/L while the total average of $2m\mathrm{Ca}^{2+}$ is 1.77 mmol/L (calculated from data in Table 2). This initial composition, during evaporation, should force the solution to follow path I (Fig. 12). But, along the flow path of surface water toward Lake Qarun, the Ca^{2+} supplied by gypsum dissolution produced a significant increasing of the $2m\mathrm{Ca}^{2+}/m\mathrm{HCO_3}^-$ ratio (Fig. 13). As a result, the average composition of water turned from $2m\mathrm{Ca}^{2+} < m\mathrm{HCO_3}^-$ at the head of the Fayoum irrigation system (T1 waters) to $2m\mathrm{Ca}^{2+} > m\mathrm{HCO_3}^-$ in low lands at T2 and T3 waters (Fig. 13). The calculated average of $2m\mathrm{Ca}^{2+}$ for all T2 and T3 waters became 4 mmol/L while $m\mathrm{HCO_3}^-$ became 3.1 mmol/L (calculated from data in Table 2).

Furthermore, the drainage waters at El-Wadi and El-Bats drains outlets (samples 23 and 29, respectively), which represent the main sources of surface water to Lake Qarun, have also an average $2m\mathrm{Ca}^{2+} > m\mathrm{HCO_3}^-$ with an average $2m\mathrm{Ca}^{2+}$ equal to 5.6 mmol/L and an average $m\mathrm{HCO_3}^-$ of 3.3 mmol/L (calculated from data in Table 2).

As discussed above, the drainage waters at El-Wadi and El-Bats drains outlets, as the main inflow to Lake Qarun, have a $2m\mathrm{Ca}^{2+} > m\mathrm{HCO_3}^-$. During evaporation, this solution

should follow path II (Fig. 12). In Lake Qarun, calcite precipitation (the first chemical divide) causes Ca^{2+} to build up in solution while HCO_3^- diminishes and the lake water progressively evolved to $2mCa^{2+} \gg mHCO_3^-$ (Fig. 13; Table 2). On path II, the next mineral that is most likely to precipitate is gypsum, which causes the second chemical divide (Fig. 12). Further evaporation will force the solution to move along path IIA or path IIB depends on whether the Ca^{2+} concentration is greater or lesser than the concentration of SO_4^{2-} (Fig. 12). The current status of Lake Qarun water is $mSO_4^{2-} \gg mCa^{2+}$ with an average mSO_4^{2-}/mCa^{2+} ratio of lake water is ≈ 11 (calculated from data in Table 2). This means the solution will follow path IIB (Fig. 12). The precipitation of gypsum will produce $mSO_4^{2-} \ggg mCa^{2+}$ because of the initial excess of SO_4^{2-} over Ca in lake water (Fig. 13). Continuous precipitation of gypsum will remove Ca^{2+} while SO_4^{2-} will build up in solution until lake water reaches the final composition "Na–Mg–SO_4–Cl" (Figs. 12, 13). At some locations of Lake Qarun, the water reached saturation state with respect to gypsum (Fig. 6). This suggests that gypsum divide is coming next to calcite divide in Lake Qarun water which supported that the lake water will be evolved along the path II–IIB. Gypsum never appears along path I (Eugster 1980). This also supports our hypothesis that the lake water during its evolution should follow path II rather than path I. Gypsum precipitation will not greatly affect the SO_4^{2-} concentration due to the huge initial excess of SO_4^{2-} over Ca^{2+} in Lake Qarun.

3.5 Behavior of Major Ions During Evaporation of Lake Qarun Water

Water in endorheic lakes in arid and semiarid areas often becomes saline or hypersaline as a result of evaporative enrichment (Fritz 1990). To study the behavior of major solutes during lake water evolution, the concentrations of the major ions (in meq/L) are plotted against chloride (Fig. 14). In most cases, species concentrations are plotted against Cl because chloride once dissolved is assumed to act conservatively until halite precipitation and also to indicate the degree of up-concentration of solutes in the waters, either due to evaporite dissolution or to evapotranspiration (Banks et al. 2004; Smith and Compton 2004). It appears that concentrations of major ions such as Na^+, Mg^{2+}, and Ca^{2+} and SO_4^{2-} as a function of Cl^- are building up in solution by evapoconcentration (Fig. 14). Only HCO_3^- shows depletion against Cl^- during evaporation (Fig. 14a). The HCO_3^- might be removed from Lake Qarun due to precipitation of calcite. The Ca^{2+} concentration in lake water does not show depletion against Cl^- throughout calcite precipitation (Fig. 14b). This is due to the relative initial excess of Ca^{2+} over HCO_3^- in the lake water. Thus, calcite precipitation in Lake Qarun is limited by HCO_3^-. Additionally, removal of Ca^{2+} through gypsum precipitation is possibly not observably achieved. This is due to the fact that only few locations in Lake Qarun just reached saturation with respect to gypsum (Fig. 6). This means gypsum is currently not precipitating in Lake Qarun with huge amounts because it did not reach the supersatuartion state yet. Also, waters do not start to precipitate gypsum until they are nearly free of HCO_3^- (Hardie and Eugster 1970).

3.6 Simulation Model of Evaporation Trend of Lake Qarun Water

The concept of this model is to predict the changes in lake water chemistry by any further evaporation. If the rate of evaporation at the area of Lake Qarun will be constant like the present time, the predicted decreasing of water flow from Nile River to Lake Qarun after construction of the Ethiopian Dam can cause a negative value in the lake water storage. However, the predicted climatic changes via global warming can led to higher rates of

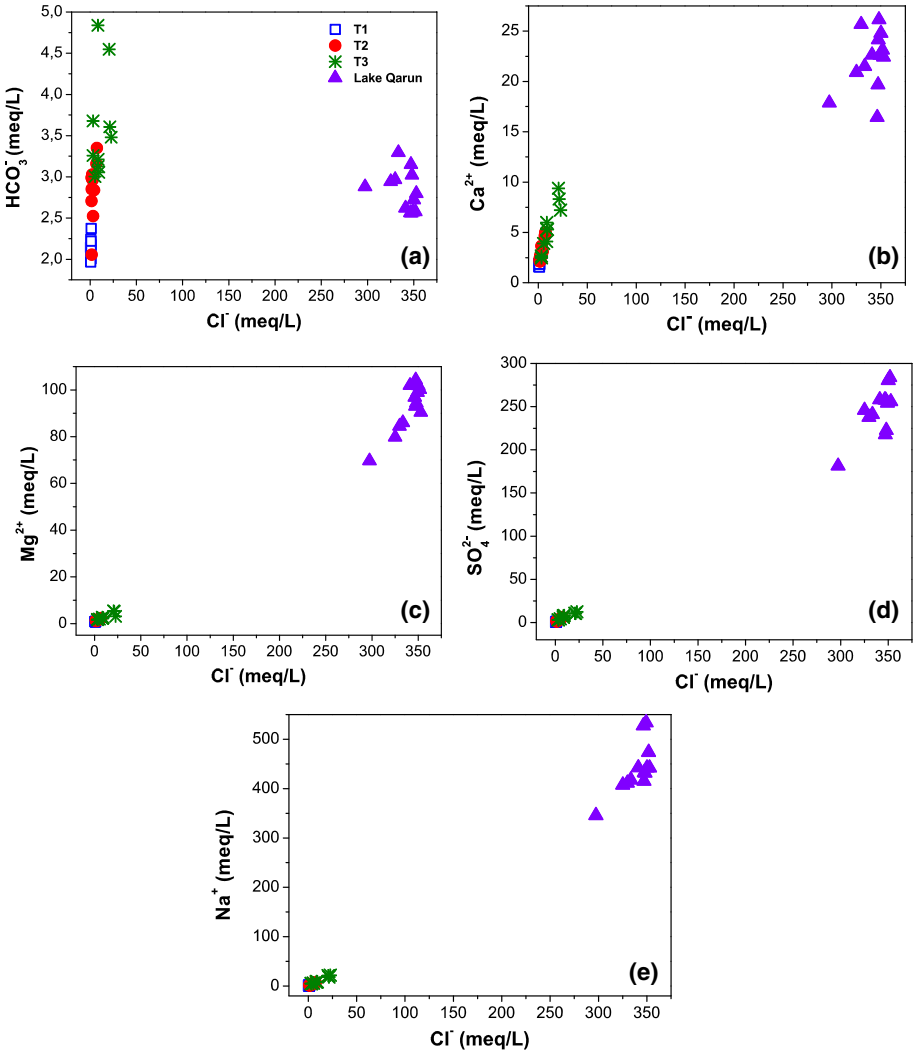

Fig. 14 Concentrations of **a** HCO_3, **b** Ca, **c** Mg, **d** SO_4, and **e** Na plotted against Cl for sampled waters. All ions in Lake Qarun increase with increasing Cl except HCO_3 which removed as a result of $CaCO_3$ precipitation

evaporation than the current situation. So, in future, a further evaporation of lake water is expected, and this will modify the geochemical behavior of lake water. Abdel Wahed et al. (2014) studied a simulated evaporation model of drainage water inflow toward Lake Qarun. They stated that the lake water has been evolved from the surface drainage water mainly by evapoconcentration process through which HCO_3^- removed by calcite precipitation and lake water just reached saturation state with respect to gypsum and still undersaturated with respect to halite. These findings by were correlated very well with the real composition of Lake Qarun water (Abdel Wahed et al. 2014).

Currently, Lake Qarun water is supersaturated with respect to calcite, saturated with respect to gypsum at some locations, and undersaturated with respect to halite at all

locations (Fig. 6). Also, HCO_3^- depleted during calcite precipitation (Fig. 14). What is the expected evolution of Lake Qarun water under further evaporation? To answer this question, a simulated evaporation model was carried out. In the present study, the simulated evaporation model was carried out at a constant partial CO_2 pressure of $10^{-3.5}$ and temperature of 25 °C. Also, whenever the water became saturated with respect to calcite, gypsum, or halite, these solid phases will precipitate and the solution will remain in equilibrium with them. The model was simulated using PHREEQC-3 software program with Pitzer database (Parkhurst and Appelo 2013). The simulated model was designed to simulate the evaporative concentration of the 1 L of water by the removal of 52.5 mol of water in 20 steps (i.e., 94.6 % of water removed). The output results of the simulated model will be compared with the Hardie and Eugster's model that was described earlier. As it is mentioned earlier, Lake Qarun water during evaporation should follow the path II–IIB (Figs. 12, 13) along which calcite and gypsum should precipitate and the water reaches the final composition "Na–Mg–SO_4–Cl" (neutral brine). Along the path II–IIB, calcite precipitation is limited by HCO_3^- while gypsum precipitation is limited by Ca^{2+}. Calcite precipitation is already observed in Lake Qarun. On the other hand, the lake water did not show depletion of Ca^{2+} as a result of gypsum precipitation. This is because only few locations in the lake are just reached the saturation state with respect to gypsum. However, because the lake water reached the saturation state with respect to gypsum, this means that any further evaporation of lake water should force gypsum to precipitate. Thus, during further evaporation through the simulated evaporation model, removal of Ca^{2+} from solution is expected due to precipitation of gypsum.

The simulated evolution of major ions species (in mol/kg_{water}) and also saturation indices of calcite, gypsum, and halite plotted against Cl^- are shown in Fig. 15. During further evaporation of Lake Qarun water, major species such as Mg^{2+}, Na^+, SO_4^{2-}, and Cl^- should build up in solution, while Ca^{2+} should be removed due to gypsum precipitation (Fig. 15a). Also, the simulated saturation indices results showed that calcite and gypsum are precipitated and became in equilibrium with the solution during the further evaporation of lake water (Fig. 15b). Calcite precipitation is limited by HCO_3^- while gypsum precipitation is limited by Ca^{2+}. On the other hand, the solution reached supersaturation with respect to halite only at the last step of evaporation (Fig. 15b). So, removal of Ca^{2+} and accumulation of SO_4 during the simulated evaporation as a result of gypsum precipitation is achieved. These findings agreed well with the Hardie and Eugster's model (Figs. 12, 13), in which gypsum divide coming next to calcite divide during evolution of Lake Qarun water by evaporation. Accordingly, by using this simulated model, it is possible to expect the evolution of Lake Qarun water through time. This can be done by monitoring of climate changes and also the changes in the ionic composition of the lake with time and input these data to the PHREEQC software and carry out the simulated model.

3.7 Stable Oxygen Isotope

Variation in the oxygen isotope composition of water is expected to be a function of evaporative enrichment. Increasing evaporative concentration is reflected by increasing $\delta^{18}O$ (Gat 1996). In the present study, the lowest $\delta^{18}O$ of value +3.09 ‰ was recorded for water sample from sampling location 1, which was taken at Lahun at the head of Fayoum irrigation system (see Fig. 1), and the highest surface water value ($\delta^{18}O = +7.95$ ‰) was recorded from the open water of Lake Qarun (Table 2). Water samples collected from the irrigation canals and drains and from the lake close to El-Bats and El-Wadi drains inflows

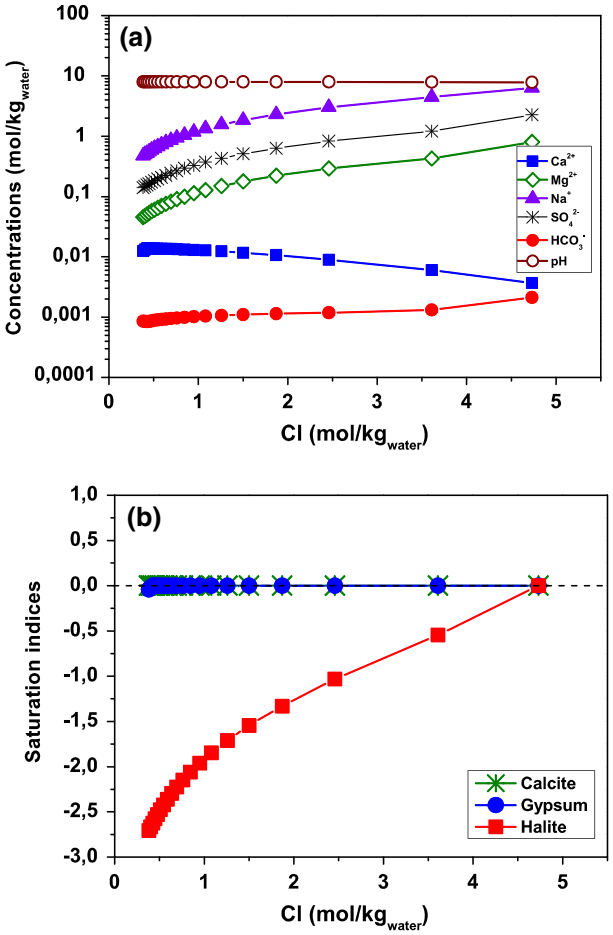

Fig. 15 **a** Modeled evaporative concentration of Lake Qarun water in equilibrium with a partial CO_2 pressure of $10^{-3.5}$ atm., using PHREEQC-3. Calcite, gypsum, and halite precipitations are permitted. **b** Evolution of mineral saturation indices of calcite, gypsum, and halite during a simulated evaporation of Lake Qarun water modeled by PHREEQC-3

had intermediate values. This suggests that the water is subjected to evaporative concentration as it flows from Lahun to Lake Qarun as evidenced by the resulting $\delta^{18}O$ values. Jusserand et al. (1988) determined the values of $\delta^{18}O$ in the waters of Lake Qarun (sampled in March and August 1984) and discussed their significance and origin. The obtained isotopic values coincide and support the results of the present study.

Given that $\delta^{18}O$ and TDS are largely expected to reflect the degree of evaporation, the rise in the electrical conductivity values of water, from Lahun to the lake, along with the increasing of $\delta^{18}O$, suggests that the water in the Fayoum has been subjected to evaporative concentration. There is a strong positive correlation ($R^2 = 0.99$) between $\delta^{18}O$ and conductivity (Fig. 16), indicating that the rise in $\delta^{18}O$ can be attributed to evaporative concentration. These findings are in good agreement with those of Gibbs's model (Fig. 11), which suggests that the water in Fayoum Depression have been geochemically evolved as a result of evaporative concentration through its course from Lahun toward Lake Qarun. However, the dissolution of preexisting evaporites can contribute to the high TDS concentrations of drainage waters, particularly those collected close to the Lake Qarun. This indicates that the high TDS of drainage waters in Fayoum Depression is possibly due to

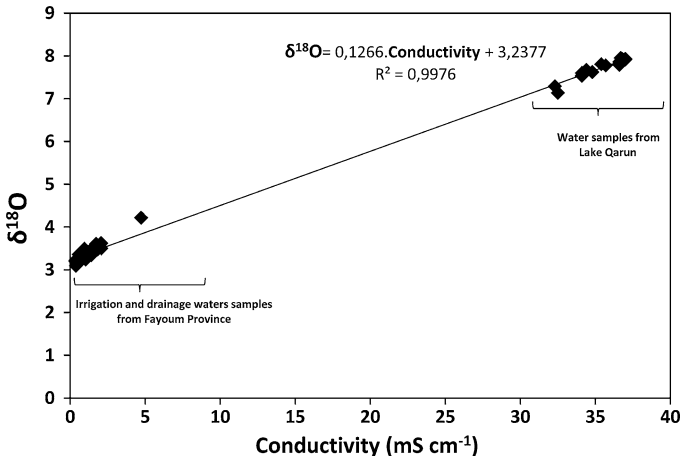

Fig. 16 Relation between $\delta^{18}O$ and conductivity of surface water samples collected from Fayoum Depression. The positive strong correlation reflects the evaporation effect on both TDS and $\delta^{18}O$ values of the surface water in Fayoum Depression

evaporites weathering as well as evapoconcentration process. In some cases of surface runoff with high TDS, it is difficult to distinguish between dissolution of evaporites and evaporation effect on Gibbs's model (Baca and Threlkeld 2000). This is because Gibbs's model (Gibbs 1970) always suggested that the high TDS of surface runoff is controlled only by evaporation. However, both results of $\delta^{18}O$ and Gibbs's model indicate that the Lake Qarun water is mainly controlled by the evaporation-crystallization process (Figs. 11, 16).

4 Conclusion

The geochemical evolution of Lake Qarun water was studied using a number of samples collected from the lake and its surroundings. The sampling plan covered the area's main source of Nile water (water from the Bahr Yousef channel), irrigation waters, drainage water, and lake water. The water evolved along its flow path from Ca–Mg–HCO_3 fresh water at the main source, Bahr Yousef, to higher salinity Na–Cl–SO_4 drainage waters reaching Lake Qarun. The more saline drainage waters evolve from the initial Bahr Yousef water through processes dominated by the dissolution of evaporite minerals such as gypsum and halite from the Fayoum area and also by evapoconcentration. The dissolution of gypsum leads to increased SO_4^{2-} and Ca^{2+} levels but the high activity of Ca^{2+} in the presence of HCO_3^- forces calcite precipitation, while SO_4^{2-} continues to increase. In contrast, the dissolution of halite increases the Na^+ and Cl^- content of the drainage surface water. Drainage surface waters conveyed by El-Wadi and E-Bats drains represent the main inflow into Lake Qarun. The lake water composition indicates that water in the lake evolved from surface drainage water through progressive evapoconcentration. The application of Hardie and Eugster's model as well as the simulated evaporation model showed that lake water should follow the path on which $2mCa^{2+} > mHCO_3^-$ and then $mSO_4^{2-} > mCa^{2+}$. Along this path, HCO_3^- is removed through calcite precipitation followed by removing of Ca^{2+} through gypsum precipitation and the solution should reach

the final composition "Na–Mg–SO_4–Cl." Oxygen isotopes ($\delta^{18}O$) results and Gibbs's model (Gibbs 1970) demonstrated that evaporation crystallization is the main process controlling the evolution of Lake Qarun water chemistry. A simulated evaporation model was carried out to predict the impact of any further evaporation for Lake Qarun water. The model showed that by further evaporation of lake water due to the decrease in water flow to the lake as well as increasing of the rate of evaporation, calcite and gypsum will precipitate within the lake and keep in equilibrium with solution. In addition, lake water reaches supersaturation with respect halite at the latest stages of evaporation. The output results of the simulated model agreed well with the Hardie and Eugster's model and also with the observed ionic composition observed in the water of Lake Qarun.

Acknowledgments We thank all staff members working at Qarun Protected Area in Fayoum Depression for their invaluable help during the field work and samples collection. The authors are very grateful to the Lappeenranta University of Technology (Finland) for providing financial support to this study. Also, the first author would like to thank the Egyptian Ministry of Higher Education and Scientific Research for the granted scholarship. We thank our reviewers for their helpful input to improve this paper.

References

Abdel Kawy W, Belal A (2013) Use of satellite data and GIS for soil mapping and monitoring soil productivity of the cultivated land in El-Fayoum depression, Egypt. Arab J Geosci 6:723–732

Abdel Wahed MSM, Mohamed EA, El-Sayed MI, M'nif A, Sillanpää M (2014) Geochemical modeling of evaporation process in Lake Qarun, Egypt. J Afr Earth Sci 97:322–330

Ali RR, Abdel Kawy WAM (2013) Land degradation risk assessment of El Fayoum depression, Egypt. Arab J Geosci 6:2767–2776

APHA (1998) Standard methods for the examination of water and wastewater. American Public Health Association, Washington

Bąbel M, Schreiber BC (2014) 9.17—Geochemistry of evaporites and evolution of seawater. In: Holland HD, Turekian KK (eds) Treatise on geochemistry, 2nd edn. Elsevier, Oxford, pp 483–560

Baca RM, Threlkeld ST (2000) Inland dissolved salt chemistry: statistical evaluation of bivariate and ternary diagram models for surface and subsurface waters. J Limnol 59:156–166

Baioumy HM, Kayanne H, Tada R (2010) Reconstruction of lake-level and climate changes in Lake Qarun, Egypt, during the last 7000 years. J Great Lakes Res 36:318–327

Ball J (1939) A contribution to the geography of Egypt. Survey and Mines Department, Cairo

Banks D, Parnachev VP, Frengstad B, Holden W, Karnachuk OV, Vedernikov AA (2004) The evolution of alkaline, saline ground- and surface waters in the southern Siberian steppes. Appl Geochem 19:1905–1926

Chadha DK (1999) A proposed new diagram for geochemical classification of natural waters and interpretation of chemical data. Hydrogeol J 7:431–439

Dargam RM, Depetris PJ (1996) Geochemistry of waters and brines from the Salinas Grandes basin, Córdoba, Argentina. II. Gypsum dissolution-calcite precipitation, and brine evolution. Int J Salt Lake Res 5:81–101

Deutsch WJ (1997) Groundwater geochemistry: fundamentals and applications to contamination. Lewis Publishers, Florida, Boca Raton

Drever JI (1982) The geochemistry of natural waters. Prentice-Hall, Englewood Cliffs

El-Shabrawy GM, Dumont HJ (2009) The Fayoum depression and its lakes. In: Dumont HJ (ed) The Nile: origin, environments, limnology and human use. Springer, Netherlands, pp 95–124

Eugster HP (1980) Geochemistry of evaporitic lacustrine deposits. Annu Rev Earth Planet Sci 8:35–63

Eugster HP, Hardie LA (1978) Saline lakes. In: Lerman A (ed) Lakes: chemistry, geology, physics. Springer, New York, pp 237–293

Flower RJ, Stickley C, Rose NL, Peglar S, Fathi AA, Appleby PG (2006) Environmental changes at the desert margin: an assessment of recent paleolimnological records in Lake Qarun, Middle Egypt. J Paleolimnol 35:1–24

Fritz SC (1990) Twentieth-century salinity and water level fluctuations in Devil's Lake, N. Dakota: a test of diatom based transfer function. Limnol Oceanogr 35:1771–1781

Gat J (1996) Oxygen and hydrogen isotopes in the hydrologic cycle. Annu Rev Earth Planet Sci 24:225–262

Gibbs RJ (1970) Mechanisms controlling world water chemistry. Science 170:1088–1090
Hammad MA, Abo-El-Ennan SM, Abed F (1983) Pedological studies on the Fayoum area, Egypt, landscapes and soil morphology. Egypt J Soil Sci 23:99–114
Hardie LA, Eugster HP (1970) The evolution of closed-basin brines. Mineral Soc Am Spec Pap 3:273–290
Hem JD (1986) Study and interpretation of the chemical characteristics of natural water. U.S. Geological Survey Water-Supply Paper 2254
Huang X, Sillanpää M, Gjessing ET, Vogt RD (2009) Water quality in the Tibetan Plateau: major ions and trace elements in the headwaters of four major Asian rivers. Sci Total Environ 407:6242–6254
Jusserand C, Ibrahim AWES, Guelorget O, Perthuisot JP (1988) O^{18} content and salt concentration of lagoonal and continental Egyptian waters. [Teneurs en 18O et concentration saline d'eaux paraliques et continentales égyptiennes]. Rev Sci Water 1(3):277–301
Kimblin RT (1995) The chemistry and origin of groundwater in Triassic sandstone and Quaternary deposits, northwest England and some UK comparisons. J Hydrol 172:293–311
Klein Gebbinck CD, Kim S, Knyf M, Wyman J (2014) A new online technique for the simultaneous measurement of the $\delta^{13}C$ value of dissolved inorganic carbon and the $\delta^{18}O$ value of water from a single solution sample using continuous-flow isotope ratio mass spectrometry. Rapid Commun Mass Spectrom 28:553–562
Meshal AH (1977) The problem of the salinity increase in Lake Qarun (Egypt) and a proposed solution. J Conseil 37:137–143
Metwaly M, El-Qady G, Massoud U, El-Kenawy A, Matsushima J, Al-Arifi N (2010) Integrated geoelectrical survey for groundwater and shallow subsurface evaluation: case study at Siliyin spring, El-Fayoum, Egypt. Int J Earth Sci 99:1427–1436
Parkhurst DL, Appelo CAJ (2013) Description of input and examples for PHREEQC version 3—A computer program for speciation, batch-reaction, one-dimensional transport, and inverse geochemical calculations. US Geological Survey Techniques and Methods, book 6, chap. A43, vol 3, pp 1–504
Rasmy M, Estefan SF (1983) Geochemistry of saline minerals separated from Lake Qarun brine. Chem Geol 40:269–277
Said R (1993) The Nile river: geology, hydrology and utilisation. Pergamon Press, Tarrytown
Smith M, Compton JS (2004) Origin and evolution of major salts in the Darling pans, Western Cape, South Africa. Appl Geochem 19:645–664
Stallard RF, Edmond JM (1981) Geochemistry of the Amazon: 1. Precipitation chemistry and the marine contribution to the dissolved load at the time of peak discharge. J Geophys Res Oceans 86:9844–9858
Tamer AM (1968) Subsurface geology of the Fayoum region. M.Sc. Thesis, Alexandria University
Wolters W, Ghobrial NS, Van Leeuwen HM, Bos MG (1989) Managing the water balance of the Fayoum Depression, Egypt. Irrigat Drain Syst 3:103–123
Yan JP, Hinderer M, Einsele G (2002) Geochemical evolution of closed-basin lakes: general model and application to Lakes Qinghai and Turkana. Sediment Geol 148:105–122

Paper II

Geochemical modeling of evaporation process in Lake Qarun, Egypt

Mahmoud S.M. Abdel Wahed, Essam A. Mohamed, Mohamed I. El-Sayed,
Adel M'nif, Mika Sillanpää

Journal of African Earth Sciences 97(2014)322-330

Journal of African Earth Sciences 97 (2014) 322–330

Contents lists available at ScienceDirect

Journal of African Earth Sciences

journal homepage: www.elsevier.com/locate/jafrearsci

Geochemical modeling of evaporation process in Lake Qarun, Egypt

Mahmoud S.M. Abdel Wahed [a,b,*], Essam A. Mohamed [b], Mohamed I. El-Sayed [b], Adel M'nif [c], Mika Sillanpää [a]

[a] Lappeenranta University of Technology, LUT Chemistry Department, Laboratory of Green Chemistry, Sammonkatu 12, FI-50130 Mikkeli, Finland
[b] Beni-Suef University, Faculty of Science, Geology Department, Egypt
[c] Centre National de Recherche en Sciences des Matériaux, Technopole Borj Cedria, B.P.73, 8027 Soliman, Tunisia

ARTICLE INFO

Article history:
Received 11 July 2013
Received in revised form 14 May 2014
Accepted 17 May 2014
Available online 9 June 2014

Keywords:
Geochemical modeling
Evapoconcentration
Lake Qarun
Progressive evaporation
Simulated evaporation model

ABSTRACT

Lake Qarun is an inland closed saline lake. It lies within the Fayoum Depression in the Western Desert of Egypt. Evaporation modeling has been carried out using PHREEQC to simulate the geochemical evolution of surface drainage waters inflow towards lake water. In the case of Lake Qarun, it is the first attempt to carry out such kind of modeling. Performance of this model helped to address the different sources of dissolved major ions to Lake Qarun and to identify the mechanisms control the lake's water chemistry. The model demonstrated that evaporation–crystallization process is the main mechanism controlling the evolution of lake water chemistry where major ions Na^+, Mg^{2+}, Cl^- and SO_4^{2-} have been built up in the lake by evaporation while Ca^{2+} and HCO_3^- are depleted by calcite precipitation. Moreover, the simulated model reproduced the real data observed in Lake Qarun except in the case of SO_4^{2-} which is in real more enriched in the lake than the model output. The additional source of SO_4^{2-} is reported to be from groundwater. The models result agreed well with the modified evolutionary Hardie and Eugster's scheme (1970) in which the final major composition of Lake Qarun water is Na–Mg–SO_4–Cl type. In future, the monitoring of Lake Qarun chemistry with detection of any other sources of elements and/or local reactions inside the lake can be detected by performing the simulated evaporation model reported by the present study.

1. Introduction

Closed lakes are exclusive features of the arid and semiarid zones where annual evaporation exceeds rainfall. Closed lakes are salty with varying degrees. This is caused by evaporation exceeding inflow, by the inflow being saline or both (Eugster and Hardie, 1978). Based on major ions such as Na^+, K^+, Mg^{2+}, Ca^{2+}, SO_4^{2-}, Cl^-, and HCO_3^-, Hardie and Eugster (1970) generalized an evolutionary model that interprets the chemistry of waters undergoing evaporation in terms of a succession of chemical divides. A chemical divide is a point in the evolution sequence of brine at which precipitation of a mineral depletes the water in certain cations or anions and further evaporation moves the solution along a distinct pathway. The main concept of chemical divide is that whenever a binary salt is precipitated during evaporation, and the effective ratio of the two ions in the salt is different from the ratio of the concentrations of these ions in solution, further evaporation will result in an increase in the concentration of the ion present in greater relative concentration in solution, and a decrease in the concentration of the ion present in lower relative concentration (Drever, 1982). Although there are many modifications of the basic Hardie-Eugster evolutionary model, this study will only be based on the modification proposed by Drever (1982).

Simulated evaporation of natural waters by PHREEQC is widely used because of its capability of removing moles of water from the solution (Parkhurst and Appelo, 1999; Smith and Compton, 2004). PHREEQC is publicly available, expandable, and well documented geochemical modeling code with an extensive thermodynamic database. Also, the capabilities of PHREEQC include simulating the chemical behavior of aqueous solutions composed of all major solutes.

Lake Qarun, the object of the present study, is one of the largest inland saline closed lakes in the North African Great Sahara. This lake is the deepest area in the River Nile flood plain, making it the final destination of both natural (subsurface flow) and artificial (agricultural) drainage in the Fayoum Depression (Fig. 1). Since the lake has no natural outlet (Wolters et al., 1989), the drainage water impounded is subject to concentration by evaporation. An average of about 385×10^6 kg of salts are washed out annually from

* Corresponding author at: Lappeenranta University of Technology, LUT Chemistry Department, Laboratory of Green Chemistry, Sammonkatu 12, FI-50130 Mikkeli, Finland. Tel.: +358 503484584.
E-mail addresses: mahmoud.abdel-wahed@lut.fi, m.abdelwahed80@yahoo.com (M.S.M. Abdel Wahed).

http://dx.doi.org/10.1016/j.jafrearsci.2014.05.008
1464-343X/

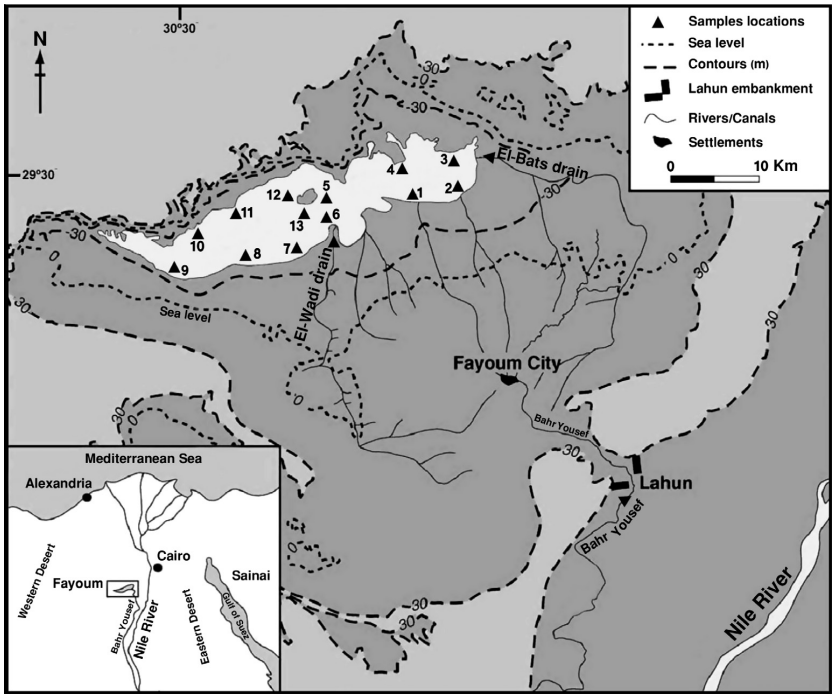

Fig. 1. Location map of Fayoum with sampling sites (triangles) and sampling codes (numbers inside the lake).

cultivated land and conveyed to the lake (Meshal, 1977). A volume of fresh water nearly equal to that of the inflowing water is lost annually from the lake through evaporation while the dissolved salts are left in the lake (Meshal, 1977). The lake brine is subjected to gradual evaporation resulting in an increase in its salinity (Gorgy, 1959). The current salinity of Lake Qarun is ≈35 g/kg on average. The increase in salinity has been attributed mainly to the evaporative concentration of drainage water within the lake (Ball, 1939; Meshal, 1977; Rasmy and Estefan, 1983).

The aim of the present work is to simulate an evaporation model using PHREEQC software along with the Hardie-Eugster evolutionary model to assess the geochemical evolution of Lake Qarun water. To test the validity of the simulated PHREEQC model, its output results will be compared with the real and experimental data of the lake water. The studying of this simulated model will be useful in different ways such as (1) to identify the geochemical processes controlling Lake Qarun chemistry, (2) to define the different sources of elements to the lake, and (3) to anticipate future evolution of the lake water composition with any change in the chemistry and inflow rate of drainage water to the lake, as well as changes in the evaporation rate.

2. Study area and methods

2.1. Site description

Lake Qarun is a closed saline basin located between the longitudes of 30° 24′ & 30° 49′ E and latitudes of 29° 24′ & 29° 33′ N in the lowest northern part of the Fayoum Depression, about 95 km south west of Cairo (Fig. 1). The lake is at 43 m below sea level. It has an irregular elongated shape of about 45 km length and 6 km mean width with an average area of about 240 km^2. The water depth ranges from 5 to 8 m, decreasing toward the lake shores. The River Nile is the main source of fresh water, reaching the Fayoum region via Bahr Yousef (Fig. 1). Agricultural returns are collected as drainage water and passed into Lake Qarun from the south and southeast through two main drains, El-Wadi and El-Bats, with other minor drains between them (Fig. 1). To the north, the area is completely covered by sand and rock with several exposures of diatomite (Aleem, 1958).

Lake Qarun water is currently alkaline, saline and turbid. The lake comprises two main basins. The western basin has a maximum depth of 8.4 m whereas the eastern basin is shallower with a maximum depth of less than 5 m (Flower et al., 2006). The water temperature ranges seasonally between about 15 and 33 °C (Ball, 1939; El Sayed and Guindy, 1999).

2.2. Climate

The studied area lies in Egypt's arid belt characterized by hot long dry summer and mild short winter, in addition to low seasonal rainfall and a high evaporation rate. Fayoum district climactic data shows that the mean annual rainfall is 7.2 mm/year (Ali and Abdel Kawy, 2012). Currently, the mean minimum and maximum annual temperatures are 14.5 °C and 31 °C, respectively. The lowest evaporation rate (1.9 mm/day) is recorded in January while the highest value (7.3 mm/day) is recorded in June and the annual mean relative humidity varies between 50% and 62% (Ali and Abdel Kawy, 2012). The climate in the Lake Qarun region is generally dry (Baioumy et al., 2010).

2.3. Hydrology

The irrigation and agricultural system in the Fayoum region depends mainly on Nile water. Fayoum City, the principal town

in the area, is a water distribution center for the Fayoum (domestic demands) and a network of canals and small pumping stations deliver water to the agricultural regions. The lake is surrounded to the south and southeast by cultivated land which slopes steeply towards the lake, forming a sink for drainage water (Fig. 1). The lake is used now as a general reservoir for agricultural drainage wastewater as well as sewage waters. It is known that agriculture returns and excess water are passed to Lake Qarun by two principal drains named El-Wadi and El-Bats drains (El-Shabrawy and Dumont, 2009). El-Bats drain receives agricultural drainage water as well as crude sewage water from the eastern and northeastern part of the Fayoum Depression while El-Wadi drain receives drainage water from the middle region of the Fayoum Depression, which is discharged into the middle part of the lake (Fig. 1). The lake gains drainage water about 338×10^6 m^3/year from El-Bats and El-Wadi drains and about 67.8×10^6 m^3/year from groundwater while it losses about 415×10^6 m^3/year by evaporation (Meshal, 1977; Abd Ellah, 1999; Keatings et al., 2007; El-Shabrawy and Dumont, 2009). So, the net water budget is negative by 9.2×10^6 m^3/year. A volume of fresh water nearly equal to that of the inflowing water is lost annually from the lake through evaporation (Meshal, 1977).

2.4. Sampling and sample analysis

In summers (June 2010, June 2011 and June 2012), surface water samples were collected from Lake Qarun, the main recharge sources (El-Bats and El-Wadi drains) and the Nile water (Bahr Yousef) (Fig. 1). Samples locations were recorded with a handheld Garmin-GPS device. Measurements of electrical conductivity (EC), pH, and temperature were carried out in the field using a SG78-SevenGo Duo pro (pH/Ion/Conductivity) portable meter. TDS (Total dissolved salts) was measured by the total summation of dissolved major ions. Polythene bottles were cleaned by acid steam stripping and left for 2 days followed by thorough rinsing with distilled water. In situ, the polythene bottles were rinsed by the collected water at each station and then filled with water, tightly sealed without any air bubbles and labeled. The samples were transported to the laboratory for analyses within 1 h of sample collection and some analyses were conducted immediately (e.g. HCO_3^-). Samples were filtered through a 0.45 μm cellulose acetate membrane filter for major ion analysis and kept in a refrigerator at 4 °C. All water samples were analyzed for major ions (Na^+, K^+, Mg^{2+}, Ca^{2+}, SO_4^{2-}, Cl^-, and HCO_3^-) in accordance with approved analytic methods, as summarized in Table 1 (APHA, 1998). All analyses were carried out in the Water Quality Central Laboratory, Fayoum Drinking Water and Sanitation Company, Fayoum, Egypt. This laboratory was awarded the ISO/IEC 17025/2005. Saturation indices (SI) of the studied water samples were calculated using the PHREEQC–2 (Parkhurst and Appelo, 1999).

3. Simulated evaporation model

Simulated geochemical modeling of evaporation process was done using PHREEQC-2 (Parkhurst and Appelo, 1999; Smith and Compton, 2004; Banks et al., 2004). Simulated evaporation of natural waters by PHREEQC is widely used because of its capability of removing moles of water from the solution (Parkhurst and Appelo, 1999; Smith and Compton, 2004). Merkel and Planer-Friedrich (2005) offered a practical guide for modeling natural and contaminated aquatic systems. They reported some guide instructions regarding PHREEQC software, which were useful in the present study. The modeling hypothesis is that the Lake Qarun evolved geochemically through the progressive evaporation of drainage water inflow coupled with progressive removal of mineral phases as saturation ceilings are reached. As mentioned earlier, the 20th century's increase in salinity was mainly attributed to evaporative concentration of drainage water within the lake (Ball, 1939; Meshal, 1977; Rasmy and Estefan, 1983). As a starting point of the simulated hydrogeochemical model, water samples from the two drains (El Bats and El Wadi) were selected that could potentially be representative of inflow feeding Lake Qarun system. Taking the major ions composition in Table 2 of El-Wadi and E-Bats drains as two starting points, PHREEQC-2 Interactive version 2.18 was used for modeling. The models were designed to simulate the evaporative concentration of 1 L of water by the removal of 52.73 mol of water in 40 steps for both samples (i.e., 95% of water removed). This concentration factor is regarded as plausible for relatively closed systems (such as lakes), given that annual potential evapotranspiration exceeds inflow (Parkhurst and Appelo, 1999; Banks et al. 2004). At every step of the 40 steps, the solution was equilibrated with a partial CO_2 pressure of $10^{-3.5}$ atmospheres (i.e., approximately atmospheric). The following mineral phases were allowed to precipitate out when (and if) they became oversaturated: calcite, gypsum and halite.

Table 1
Analytical methods of water samples, after APHA (1998).

Analytic parameter	Method (APHA, 1998)
SO_4^{2-}	4500-$SO4^{2-}$ E
Cl^-	4500-Cl^- B
HCO_3^-	2320-B Titration method
Na^+, K^+, Mg^{2+} and Ca^{2+}	3120 B, ICP method by ICP-OES

4. Results and discussion

The mean values of major ions concentrations of the investigated water samples collected from the three environmental matrices during the period June 2010, 2011 and 2012 are given in Table 2. The data showed that the concentrations of most ions and TDS are in the following order: lake water > drainage water > Bahr Yousef water (Nile water). Bahr Yousef has an order of cations abundance (as meq%) as $Ca^{2+} > Na^+ > Mg^{2+} > K^+$ while the abundance of anions is in the order $HCO_3^- > SO_4^{2-} \geqslant Cl^-$. Drainage water inflow showed that the order of cations dominance is $Na^+ \gg Ca^{2+} \geqslant Mg^{2+} > K^+$ and the order of anions is $Cl^- \gg SO_4^{2-} > HCO_3^-$. At the last station (Lake Qarun), the order of cations dominance is $Na^+ \gg Mg^{2+} > Ca^{2+} > K^+$ and the anions is $Cl^- \gg SO_4^{2-} \gg HCO_3^-$.

4.1. Brine type and geochemical evolution of Lake Qarun water during evaporation

Eugster and Hardie (1978) suggested a classification scheme for lake brines based on the chemical composition of saline lakes (in mol%) in terms of the major cations ($Na^+ + K^+$), Ca^{2+} and Mg^{2+}; and anions Cl^-, SO_4^{2-} and ($HCO_3^- + CO_3^{2-}$). The same authors gave a numerical expression for lake brines, namely the "brine type", according to the field in which the ionic composition of the lake brine fits into the representative diagrams for cations and anions respectively (Fig. 2). Based on the data given in Table 2, Lake Qarun water has the brine type 4–5, the drainage water has 3–3 type, and seawater has the type 4–1 (Fig. 2). Bahr Yousef water is not classified here in this diagram because it is a freshwater type (Risacher and Fritz, 1991). The cation field being listed before the anion field and the ions of higher concentrations before lower ones. Consequently, Lake Qarun brine can be specified by the chemical label Na–(Mg)–Cl–SO_4, drainage water is labeled as Na–(Ca)–(Mg)–Cl–(SO_4)–(HCO_3), and seawater is Na–(Mg)–Cl. Parentheses indicate that the mole ratio of the included ion is less than 25 mol%. Ions with mole ratios less than 5 are not included in such chemical

Table 2
Mean values of major ions concentrations (in mg/l) of surface water samples collected from Bahr Yousef (Nile water), from El-Wadi and El-Bats drains (drainage water inflow) and from Lake Qarun during the periods June 2010, June 2011 and June 2012.

Sample code	K^+	Na^+	Mg^{2+}	Ca^{2+}	Cl^-	SO_4^{2-}	HCO_3^-	pH	TDS
Bahr Yousef (Nile water)									
	3.89	23.45	9.63	33.36	24.44	37.10	126.93	7.77	258.8
Drainage water inflow									
El-Wadi drain	17	481.67	65.89	188.03	730.33	510.31	277.47	7.6	2270.7
El-Bats drain	23.3	425	63.6	166.8	758.33	502	220.07	7.73	2158.77
Lake Qarun water samples									
1	285.33	9360.6	969.87	418.8	11525.5	11808	179.53	8.19	34547.7
2	304.67	9601.67	1045.23	430.97	11822.67	11580	201	8.23	34986.2
3	250.33	7940.66	846.6	357.9	10544.3	8704.8	175.73	8.2	28820.33
4	325.5	9458.33	1027.03	514.47	11695	11417.43	181.07	8.29	34618.83
5	480	9919.33	1147.67	523.53	12339.77	10695.33	184.37	8.38	35290
6	289	9549.65	1131.33	394	12305.67	10453	192.13	7.82	34314.8
7	282.67	10165.68	1238.73	453.33	12092	12392	159.9	8.23	36784.3
8	386.67	12124.7	1177.33	329.4	12278.33	12387	156.45	8.29	38839.85
9	300	9949	1267.17	483.83	12317.1	12376	156.33	8.33	36849.43
10	296.67	10162.6	1237.5	496.97	12415.1	13461.33	166.1	8.32	38236.33
11	289.83	10887.67	1217.33	463.43	12472.37	13630	157.2	8.34	39117.83
12	362	12271	1203	453.2	12383.67	12207	157.13	8.37	39037
13	296	10158.5	1100.17	449.53	12509.37	12283.33	170.73	8.27	36967.63
Seawater (Rasmy and Estefan, 1983)									
	387	10760	1294	413	19353	2712	142	-	35136

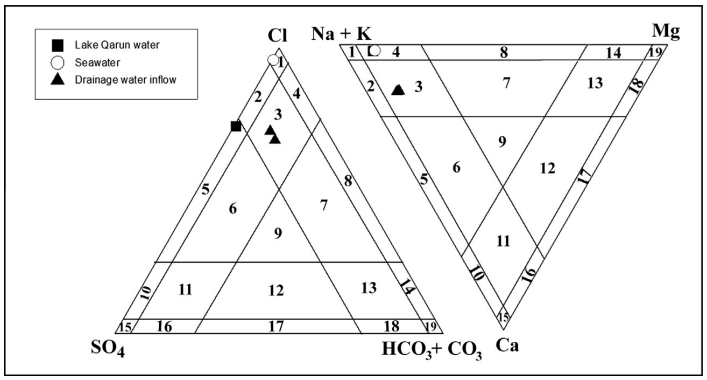

Fig. 2. Plot of the studied water samples on the brine classification scheme in mol%, after Eugster and Hardie (1978).

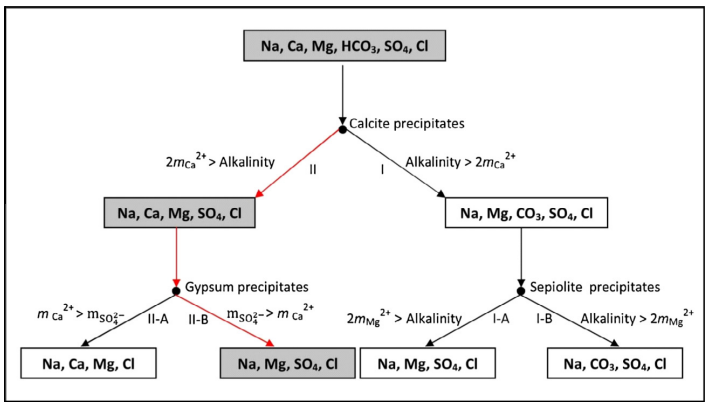

Fig. 3. Some possible paths for the evaporation model of natural waters made by Hardie and Eugster (1970) and modified by Drever (1982). Noting that, during evaporation, Lake Qarun evolves along the path II → IIB.

labels (Eugster and Hardie, 1978). It seems that the Lake Qarun water evolved from the drainage water inflow by progressive evaporation and removal of Ca and HCO_3. Moreover, the lake water composition is higher in SO_4^{2-} and lower in Cl^- than seawater.

Herczeg and Lyons (1991) showed that the main initial conditions required for the formation of the Na^+–Mg^{2+}–Cl^-–SO_4^{2-} brines are (1) $2mCa^{2+}/HCO_3^-$ mole ratio > 1, allowing Ca^{2+} to build up in solution during calcite precipitation whilst HCO_3^- diminishes, and (2) SO_4^{2-}/Ca^{2+} mole ratio $\gg$ 1, allowing SO_4^{2-} to build up in solution during gypsum precipitation whilst Ca^{2+} diminishes. Similarly, Drever (1982) modified the evolutionary scheme made by Hardie and Eugster (1970) as shown in Fig. 3. In this scheme, alkalinity is represented by HCO_3^- (Eugster and Hardie, 1978; Eugster, 1980). Based on this scheme, after calcite precipitation, the solution will follow path I when $mHCO_3^- > 2mCa^{2+}$ or follow path II when the opposite is true (Fig. 3). In Qarun Lake, the initial drainage water inflow has $2mCa^{2+}/HCO_3^- > 1$ (see Table 2). During evaporation, calcite precipitation causes Ca^{2+} to build up in solution whilst HCO_3^- diminishes. This is due to the effects of chemical divide principle (Drever, 1982). The result of this principle is that the small differences in ionic ratios in the dilute starting composition can produce brines of different and diverse composition as the water chemistry evolves during evaporation. Calcite precipitation in Lake Qarun was reported by Baioumy et al. (2010) and also confirmed in the present study (Fig. 4). As a result, after calcite precipitation, Lake Qarun water has $2mCa^{2+} \gg HCO_3^-$ (see Table 2). Thus, the solution should follow path II (Fig. 3). In the next step, Lake Qarun has $mSO_4^{2-} \gg mCa^{2+}$. So, during consequent evaporation, gypsum should precipitate and then the solution will follow path II-B. At some locations of Lake Qarun, the lake water reached saturation state with respect to gypsum (Fig. 4 and Table 2). In fact, gypsum precipitation in Lake Qarun will not greatly affect the SO_4^{2-} concentration due to the initial excess of SO_4^{2-} over Ca^{2+} where the average mSO_4^{2-}/mCa^{2+} is ≈11. Therefore, the solution should evolve until reaching the final composition "Na–Mg–SO_4–Cl" (Fig. 3).

4.2. Behavior of major ions during evaporation of Lake Qarun water (real data)

Water in endorheic lakes in arid and semi-arid areas often becomes saline or hypersaline as a result of evaporative enrichment (Fritz, 1990). To study the behavior of major solutes during lake water evolution, the concentrations of the major ions and saturation indices (SI) are plotted against chloride. In most cases, species concentrations or saturation indices are plotted against Cl^- because chloride once dissolved is assumed to act conservatively until halite precipitation and also to indicate the degree of up-concentration of solutes in the waters, either due to evaporite dissolution or to evapotranspiration (Eugster and Jones, 1979; Banks et al., 2004; Smith and Compton, 2004).

The Saturation Indices of calcite, gypsum and halite versus Cl^- for Bahr Yousef, drainage water inflow and Lake Qarun water samples are given in Fig. 4. All waters appear to be supersaturated with respect to calcite and undersaturated with respect to halite. On the other hand, Bahr Yousef water and drainage water inflow are undersaturated with respect to gypsum while some locations in Lake Qarun reached saturation state with respect to gypsum (Fig. 4 and Table 2). It seems that the saturation indices of gypsum and halite increase toward Lake Qarun due to the evaporite dissolution and/or evapoconcentration process (Fig. 4).

Using the mean concentrations of the major ions of all water samples given in Table 2, all species (in meq/l) are plotted against Cl^- (Fig. 5). The plotting of HCO_3^- versus Cl^- of the studied water samples showed HCO_3^- depletion in Lake Qarun during progressive evaporation (Fig. 5a). It seems that the HCO_3^- is removed from Lake Qarun due to precipitation of carbonate species. Calcite is the first mineral to precipitate at earlier stage of brine evaporation. The precipitation of $CaCO_3$ is evidenced by the supersaturation of lake water with respect to calcite (Fig. 4). During evaporation of the saline lakes, the total carbonate ($HCO_3^- + CO_3^{2-}$) decreases for both CO_2 degassing and mineral precipitation (Eugster and Jones, 1979).

Calcium concentration in lake water increases with Cl^- relative to HCO_3^- during evaporation because calcite precipitation is limited by HCO_3^- (Fig. 5b). However, the concentration of Ca^{2+} against Cl^- is much lower than other cations such as Na^+ and Mg. The average maximum concentration of Ca^{2+} recorded in Lake Qarun is 22.1 (meq/l) while Na^+ and Mg^{2+} recorded 440.15 and 92.45 (meq/l), respectively. The Ca^{2+} trend does not show depletion against Cl^- because gypsum may not heavily precipitate from Lake Qarun water. This is due to the saturation index of gypsum showed that gypsum has just closed to saturation state at some locations in

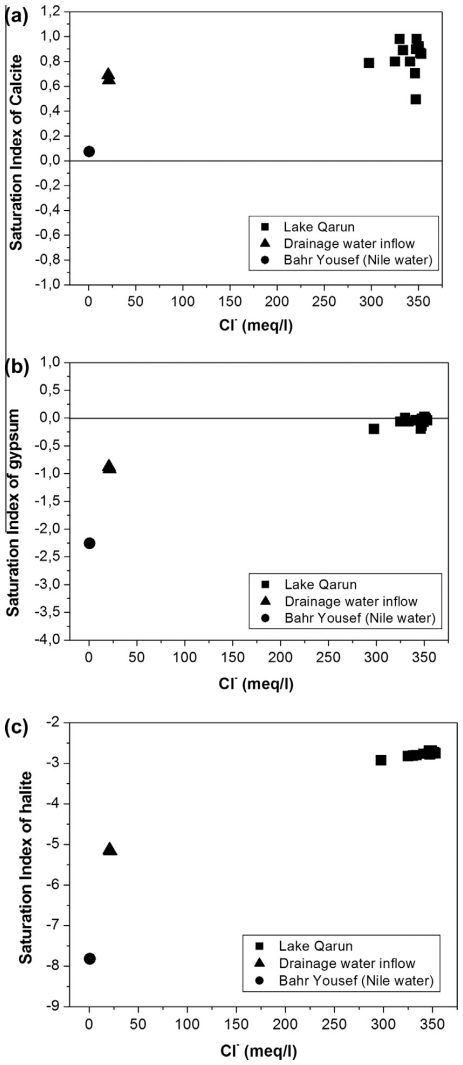

Fig. 4. Saturation indices of (a) calcite, (b) gypsum and (d) halite of the studied water samples.

Qarun Lake (Fig. 4). In addition, the waters do not start to precipitate gypsum until they are nearly free of HCO_3^- (Hardie and Eugster, 1970).

Magnesium behaves conservatively during lake water evolution (Fig. 5c). The removal of Ca^{2+} from the brine during calcite precipitation results in an increasing Mg:Ca ratio and, as a result, calcite precipitating from brines evolves from low to high-Mg calcite (Eugster, 1980). Because of the relatively low concentrations of Ca^{2+} and alkalinity in the lake water compared to Mg^{2+}, uptake of Mg^{2+} into calcite does not noticeably affect the concentration of Mg in the lake.

Potassium increases continuously throughout lake water evolution during evaporation. The plotting of K^+ against Cl^- shows no depletion of K^+ throughout brine evolution and K^+ tend to accumulate at late stages of evaporation (Fig. 5d). It seems that K^+ is not significantly adsorbed by clay sediments in Lake Qarun. But, K^+ concentration in Lake Qarun is too much low compared to Na and Mg^{2+}. The maximum K recorded 8.16 (meq/l) while Na^+ and Mg^{2+} recorded 440.15 and 92.45 (meq/l), respectively. K^+ concentration is the least dissolved cation in the drainage water inflow. Consequently, during evaporation all cations should build up proportionally in Qarun Lake based on their initial concentrations in the inflowing drainage waters. Only one exception is that Ca^{2+} concentration is much more than K^+ in the drainage water inflow, however, there is no big difference between these two ions concentrations in Qarun Lake (see Table 2). This is due to the depletion in Ca^{2+} ion through precipitation of calcite in the lake.

Sulfate steady increases versus Cl^- during lake water evolution and shows no depletion during the different stages of evaporation (Fig. 5e). As mentioned earlier, gypsum precipitation in the Lake Qarun will not significantly affect the concentration of SO_4 due to its initial great excess over Ca^{2+}. Moreover, according to the principle of the chemical divide discussed above, by gypsum precipitation SO_4^{2-} will accumulate during evaporation while Ca^{2+} will be removed.

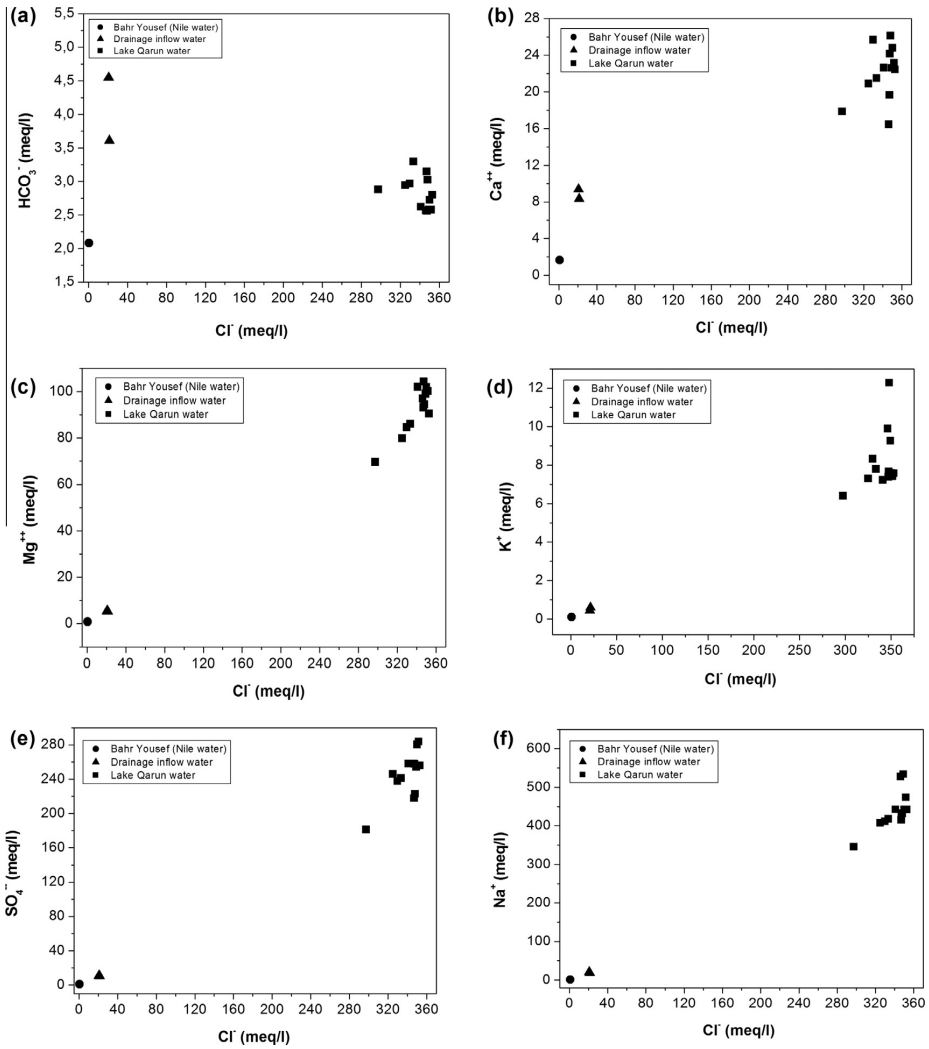

Fig. 5. Concentrations of (a) HCO_3, (b) Ca, (c) Mg, (d) K, (e) SO_4 and (f) Na plotted against Cl for sampled waters.

Sodium behaves conservatively versus Cl^- during the lake water evolution (Fig. 5f). Na^+ and Cl^- are the most dominant ions in the drainage water inflow and also in Lake Qarun water. The two ions act conservatively during evaporation until halite starts to precipitate. Lake Qarun did not reach yet supersaturation with respect to halite (Fig. 4).

4.3. Modeling evolution of Lake Qarun water from the surface drainage water inflow (simulated data)

In this section, the validity of the simulated model has been tested by comparing its output results with the real and experimental data of Lake Qarun.

Selected modeling results for initial water compositions of the two selected samples (El-Wadi and El-Bats drains) are shown in Fig. 6. In both models, during the first step, there is an initial abrupt increase in pH of the model run. This is because of equilibration of the selected water samples with the partial pressure of atmospheric CO_2 gas by CO_2 degassing. This process affects pH but not alkalinity, as pointed out by Appelo and Postma (1996) and Banks et al. (2004);

$$HCO_3^- = CO_2 + OH^-$$

After that, in both models, pH shows a steady rise due to the relative excess of OH^-. During next steps, slightly lower pH values were observed during precipitation of calcite. This is due to the buffering effect of this reaction:

$$Ca^{2+} + HCO_3^- = CaCO_3 + H^+$$

At the latest steps of evaporation, after calcite precipitation and starting of gypsum precipitation, the pH starts gradually increase again.

Both water samples gave similar results during the modeling runs. Indeed, Na, Mg and SO_4^{2-} increase in proportion to Cl^- (Fig. 6a and b) and both samples have an initial Ca^{2+} (as meq/l) exceeding HCO_3^- concentration. During calcite precipitation, HCO_3^- decreases because calcite precipitation is limited by HCO_3. Then, according to the chemical divide rule, Ca^{2+} concentration increases until waters become in equilibrium with gypsum, at which Ca^{2+} concentration stabilizes and then decreases at the last step. Sulfate seems not significantly affected by gypsum precipitation due to its initial excess over Ca^{2+}. So, when solution starts to precipitate gypsum, the SO_4^{2-} continues to build up in solution. The final solutions in both models show steady increasing in Na, Mg and SO_4 against Cl. The high level of Na^+, Cl^- and SO_4^{2-} is strongly controlled by increased concentration due to evaporation (Huang et al., 2009). According to the classification made by Eugster and Hardie (1978) for lake brines (as mol%), in both models, the resultant simulated waters at step 40 (final step) are of Na–(Mg)–Cl–(SO_4) type. This result is much similar to the real brine classification of Lake Qarun water, which is Na–(Mg)–Cl–SO_4 (see Fig. 2 and Section 4.1). Parentheses indicate that the mole ratio of the included ion is less than 25 mol%. So, the only difference is that the real lake water is enriched in SO_4^{2-} than the final step of the simulated model. This means that there is other additional source of SO_4 rather than the surface drainage water. The main source of SO_4^{2-} ion in lake water is probably groundwater (El Sayed and Guindy, 1999; Fathi and Flower, 2005; Keatings et al., 2007).

It is noticed that, the modeling data (Fig. 6) reproduced the trends seen in real hydrochemical data (see Fig. 5). Results indicated that, calcite precipitation causes Na^+, Mg^{2+}, SO_4^{2-} and Cl^- to accumulate in the water preferentially over HCO_3^- and Ca^{2+}. Additionally, the calculated saturation indices of calcite, gypsum and halite evolved similarly in the modeled data (Fig. 7) and the real data (Fig. 4). Indeed, both data showed (1) calcite precipitation,

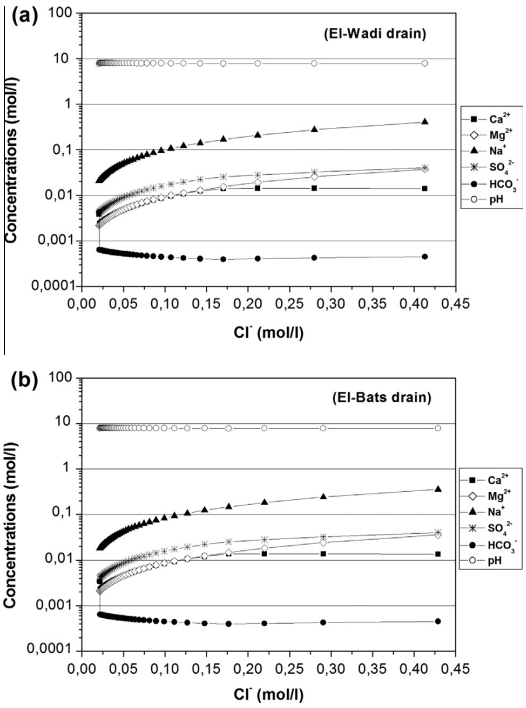

Fig. 6. Modeled evaporative concentration of selected water samples, (a) El-Wadi drain and (b) El-Bats drain, in equilibrium with a partial CO_2 pressure of $10^{-3.5}$ atm., using PHREEQC-2 Interactive, in 40 steps. Calcite, gypsum and halite precipitation are permitted.

but the saturation limit (SI = 0) used in the model to control calcite precipitation, as opposed to the observed fact that real calcite SIs exceed zero, presumably due to kinetic factors (Banks et al., 2004), (2) Gypsum remains undersaturated at most salinities, but at latest stages it reaches saturation state in Lake Qarun, and (3) halite remains undersaturated in all waters.

The modeling runs demonstrate the Hardie and Eugster (1970) concept of saline surface water evolution that invokes the common ion effect to explain how initial water compositions during each evapoconcentration step controlling the next one and the solution is eventually gravitating towards a limited number of final compositions. It appears that the results of the modeling runs agree with the hydrochemical evolution path of Lake Qarun as shown in Fig. 3. Both results showed that Lake Qarun water has Na, Mg, SO_4, and Cl as final major constituents.

Table 3 demonstrated that modeling not only reproduces the trends seen in real hydrochemical data, but also yields final concentrations of major ions which are consistent with those observed in Lake Qarun. Only minor differences are noted. For example, SO_4^{2-} concentration was higher in Lake Qarun than the simulated results, which means that there is another additional source of SO_4 rather than the surface drainage water. The main source of SO_4^{2-} ion in lake water is probably groundwater (El Sayed and Guindy, 1999; Fathi and Flower, 2005). Another observation revealed that maximum alkalinities in Lake Qarun are higher than those predicted by the models. This observation reflects the effect of continuous drainage water inflow with higher HCO_3^- to the lake and/or because calcite precipitates more slowly in Lake Qarun than the increase in concentration of Ca^{2+} and HCO_3 as evaporation proceeds (Smith and Compton, 2004).

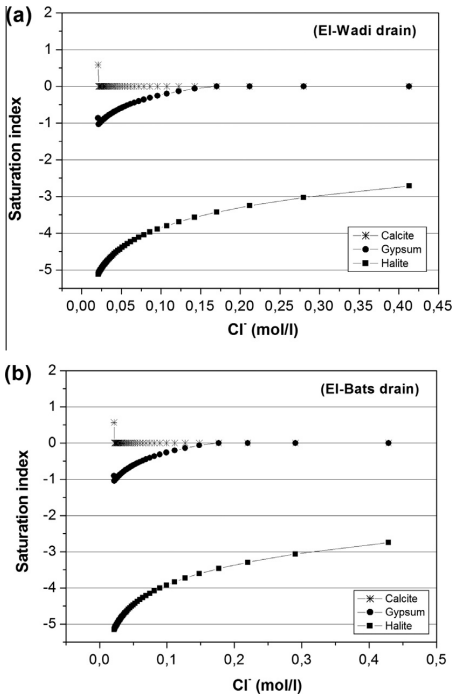

Fig. 7. Evolution of mineral saturation indices during evaporation model by PHREEQC-2 Interactive, in 40 steps. (a) El-Wadi drain and (b) El-Bats drain.

Table 3
The evaporated end-product (at Step 40) of PHREEQC-2 modeling of evaporative concentration of initial surface drainage water inflow from El-Wadi and El-Bats drains, with calcite, gypsum and halite precipitation allowed, compared with the real composition of Lake Qarun water.

Ion (mg/l)	Modeled El-Wadi drain at step 40	Modeled El-Bats drain at step 40	Real Lake Qarun water data MIN–MAX (see Table 1)
Ca	564.02	547.39	329.4–523.53
Na	9313.71	8211.34	7940.67–12271
Mg	909.91	869.97	846.6–1267.17
HCO_3	27.33	27.63	156.33–201
SO_4	3828.58	3876.58	8704.8–13630
Cl	14637.31	15198.83	10544.3–12509.37
pH	7.81	7.81	7.82–8.38

5. Conclusion

El-Wadi and El-Bats drains conveying most of the drainage surface waters to Lake Qarun, representing therefore the main inflow. Simple evaporation modeling has been carried out using PHREEQC to simulate the evolution of surface drainage waters inflow towards Lake Qarun. The modeling data showed good agreements with the real hydrochemical trends and major ion concentrations seen in Lake Qarun. The most important findings established by the simulated evaporation model during this study can be listed as follows:

- Currently, the model demonstrated that evaporation–crystallization process is the main mechanism controlling the geochemical evolution of Qarun Lake. Evaporation makes ions such as Na^+, Mg^{2+}, SO_4^{2-}, and Cl^- to build up in solution while crystallization of $CaCO_3$ causes depletion of HCO_3^- and Ca^{2+} relatively to the other dissolved ions.
- The model also showed that the lake composition depends largely on the composition of the inflowing drainage waters.
- As well, the model managed to differentiate between the different sources of elements to Qarun Lake. This is illustrated in the case of SO_4 where its concentration by the evaporation model was lower than the real concentration in the lake. This means that there is an additional source of SO_4 originating from groundwater source.
- In the future, after verification of the simulated model in predicting the real concentrations of elements in Qarun Lake made by evaporation during this study, it will be easier to monitor any change in the chemistry of Qarun Lake with time. This monitoring can be performed by following up the changes in the composition and rate of inflow of the surface drainage water as well as the rate of evaporation in the area of the lake.
- Now, it is known that Egypt will suffer from decreasing of water inflows from upstream after the construction of Ethiopian Dam. Consequently, this will affect negatively the amount of inflowing water to Qarun Lake. So, the rate of evaporation in Qarun Lake is expected to increase specially with the predicted climate change via global warming. Therefore, the good agreement between the experimental results and the theoretical data predicted by the model validate its applicability to predict future development of the lake through high rates of evaporation. These changes can be simulated and expected by applying the simulated evaporation model described by this study.

Acknowledgments

The authors wish to thank all staff members working at Qarun Protected Area in Fayoum Province for their invaluable help during the field work and samples collection. The authors are very grateful to the Lappeenranta University of Technology (Finland) for providing financial support to this study. Also, the first author would like to thank the Egyptian Ministry of Higher Education and Scientific Research for the granted scholarship.

References

Abd Ellah, G.R., 1999. Physical Limnology of Fayoum Depression and Their Budget. Ph. D. Thesis. Faculty of Sciences, South Valley University, Aswan, p. 140.
Aleem, A., 1958. A taxonomic and palaeoecological investigation of the diatom flora of the extinct Fayoum Lake (Upper Egypt). Univ. Alexandria Bull. 2, 17–44.
Ali, R.R., Abdel Kawy, W.A.M., 2012. Land degradation risk assessment of El Fayoum Depression, Egypt. Arab J. Geosci. In press, doi: http://dx.doi.org/10.1007/s12517-012-0524-7.
American Public Health Association (APHA), 1998. Standard Methods for the Examination of Water and Wastewater, 20th ed. American Public Health Association, Washington, DC, USA.
Appelo, C.A.J., Postma, D., 1996. Geochemistry, Groundwater and Pollution. Balkema, Rotterdam.
Baioumy, H.M., Kayanne, H., Tada, R., 2010. Reconstruction of lake-level and climate changes in Lake Qarun, Egypt, during the last 7000 years. J. Great Lakes Res. 36, 318–327.
Ball, J., 1939. A Contribution to the Geography of Egypt. Survey and Mines Department, Cairo.
Banks, D., Parnachev, V.P., Frengstad, B., Holden, W., Karnachuk, O.V., Vedernikov, A.A., 2004. The evolution of alkaline, saline ground- and surface waters in the southern Siberian steppes. Appl. Geochem. 19, 1905–1926.
Drever, J.I., 1982. The Geochemistry of Natural Waters. Prentice- Hall, Englewood Cliffs, p. 388.
El Sayed, E., Guindy, K.A., 1999. Hydrochemical investigation of El Fayium locality with special reference to the sulphate enrichment phenomenon in Lake Qarun. Mansoura Sci Bull. 26 (1), 1–21.
El-Shabrawy, G.M., Dumont, H.J., 2009. The Fayum Depression and Its Lakes. In: Dumont, H.J. (Ed.), The Nile: Origin, Environments. Limnology and Human Use. Springer Sciences and Business Media B.V, Netherlands, pp. 95–124.
Eugster, H.P., 1980. Geochemistry of evaporitic lacustrine deposits. Ann. Rev. Earth Planet. Sci. 8, 35–63.

Eugster, H.P., Hardie, L.A., 1978. Saline Lakes. In: Lerman, A. (Ed.), Lakes: Chemistry, Geology, Physics. Springer, New York, NY, pp. 237–293.
Eugster, H.P., Jones, B.F., 1979. Behaviour of major solutes during closed-basin brine evolution. Am. J. Sci. 279, 609–631.
Fathi, A.A., Flower, R.J., 2005. Water quality and phytoplankton communities in Lake Qarun (Egypt). Aquat. Sci. 67, 350–362.
Flower, R.J., Stickley, C., Rose, N.L., Peglar, S., Fathi, A.A., Appleby, P.G., 2006. Environmental change at the desert margin: an assessment of recent paleolimnological records in Lake Qarun, Middle Egypt. J. Paleolimnol. 35, 1–24.
Fritz, S.C., 1990. Twentieth-century salinity and water level fluctuations in Devil's Lake, N. Dakota: a test of diatom based transfer function. Limnol. Oceanogr. 35, 1771–1781.
Gorgy, S., 1959. The use of energy equations in the calculation of the rate of evaporation from Lake Qarun. Alexandria Inst. Hydrobiol. Alexandria, Notes Mem. 42, 1–26.
Hardie, L.A., Eugster, H.P., 1970. The evolution of closed-basin brines. Miner. Soc. Am. Spec. Pap. 3, 273–290.
Herczeg, A.L., Lyons, W.B., 1991. A chemical model for the evolution of Australian sodium chloride lake brines. Palaeogeogr. Palaeoclimatol. Palaeoecol. 84, 43–53.
Huang, X., Sillanpää, M., Gjessing, E.T., Vogt, D.R., 2009. Water quality in the Tibetan Plateau: major ions and trace elements in the headwaters of four major Asian rivers. Sci. Tot. Environ. 407, 6242–6254.
Keatings, K.W., Hawkes, I., Holmes, J.A., Flower, R.J., Leng, M.J., Abu-Zied, R.H., Lord, A.R., 2007. Evaluation of ostracod-based palaeoenvironmental reconstruction with instrumental data from the arid Faiyum Depression, Egypt. J. Paleolimnol. 38, 261–283.
Merkel, B., Planer-Friedrich, B., 2005. Hydrogeochemical Modeling Programs. In: D. Nordstrom (Ed.), Groundwater Geochemistry – A Practical Guide to Modeling of Natural and Contaminated Aquatic Systems. Springer Verlag, p. 200.
Meshal, A.H., 1977. The problem of salinity increase in Lake Qarun (Egypt) and a proposed solution. J. Cons. Int. Explor. Mer. 37, 137–143.
Parkhurst, D.L., Appelo, C.A.J., 1999. User's Guide to PHREEQC (version 2) – A Computer Program for Speciation, Batch-Reaction, One-Dimensional Transport, and Inverse Geochemical Calculations: Geological Survey, Denver, Colorado, p. 312.
Rasmy, M., Estefan, S.F., 1983. Geochemistry of saline minerals separated from Lake Qarun brine. Chem. Geol. 40, 269–277.
Risacher, F., Fritz, B., 1991. Geochemistry of Bolivian salars, Lipez, southern Altiplano: origin of solutes and brine evolution. Geochim. Cosmochim. Acta 55, 687–705.
Smith, M., Compton, J.S., 2004. Origin and evolution of major salts in the Darling pans, Western Cape, South Africa. Appl. Geochem. 19, 645–664.
Wolters, W., Ghobrial, N.S., Van Leeuwen, H.M., Bos, M.G., 1989. Managing the water balance of the Fayoum Depression. Egypt. Irrig. Drain. Syst. 3, 103–123.

Paper III

Assessment of water quality in surface waters of the Fayoum watershed, Egypt

Mahmoud S.M. Abdel Wahed, Essam A. Mohamed, Christian Wolkersdorfer,
Mohamed I. El-Sayed, Adel M'nif, Mika Sillanpää

Environmental Earth Sciences (2015) DOI: 10.1007/s12665-015-4186-0

Assessment of water quality in surface waters of the Fayoum watershed, Egypt

Mahmoud S. M. Abdel Wahed, Essam A. Mohamed, Christian Wolkersdorfer, Mohamed I. El-Sayed, Adel M'nif & Mika Sillanpää

Environmental Earth Sciences

ISSN 1866-6280

Environ Earth Sci
DOI 10.1007/s12665-015-4186-0

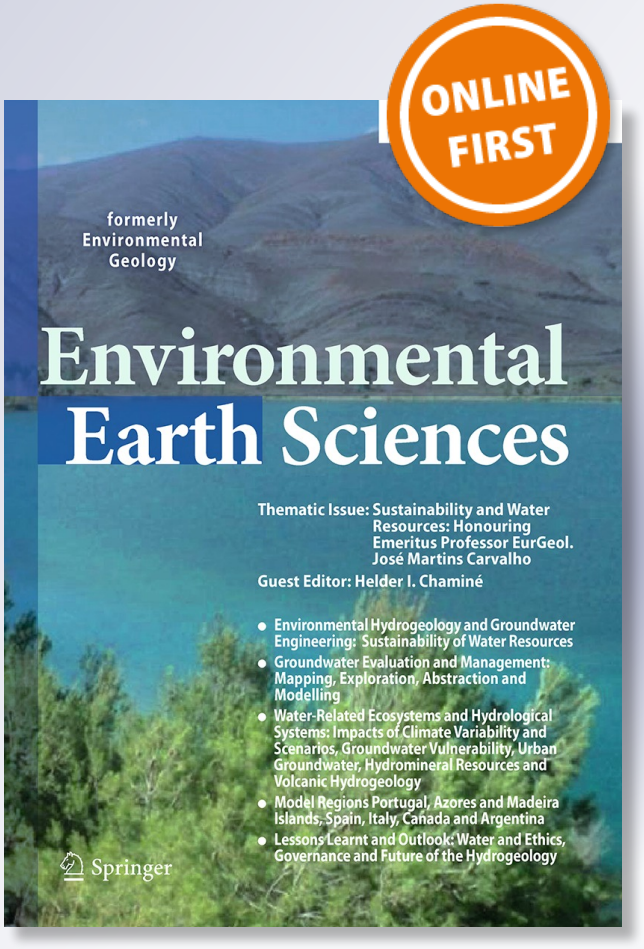

Springer

Environ Earth Sci
DOI 10.1007/s12665-015-4186-0

ORIGINAL ARTICLE

Assessment of water quality in surface waters of the Fayoum watershed, Egypt

Mahmoud S. M. Abdel Wahed · Essam A. Mohamed · Christian Wolkersdorfer · Mohamed I. El-Sayed · Adel M'nif · Mika Sillanpää

Received: 28 October 2014 / Accepted: 11 February 2015

Abstract This paper presents the first assessment study of the surface water quality in the Egyptian Fayoum Governorate (Province). A total of 42 water samples from irrigation and drainage canals as well as Lake Qarun were collected. Major ions, (semi-)metals, nutrients, salinity and microbiological parameters were examined. The results showed that the highest salinities and highest concentrations of Na^+, K^+, Ca^{2+}, Mg^{2+}, SO_4^{2-}, Cl^- and $\delta^{18}O$ were recorded in Lake Qarun due to up-concentration by evaporation. The highest concentrations of Al, Ba, Cr, Co, Cu, Ni, Fe and Mn were recorded in drainage waters. Tracking the fate of contaminants through sources–sink pathways helped to determine the potential sources of pollution. The highly impacted sites were located close to point sources of pollution such as sewage water treatment plants. Water used as drinking water supply has higher levels of Al and it can be harmful. High levels of microbiological contamination were recorded in irrigation and drainage waters, which therefore might cause water-borne diseases. Improper disposal of sewage or on-site sanitation tank overflowing into these waters is the main cause of microbiological contamination. Drainage and irrigation waters generally have high salinities resulting in soil salinization and degradation. Lake Qarun, a closed saline and alkaline lake, acts as the reservoir for left-over drainage waters. The results show that the lake has a self-cleaning system where most of the (semi-)metals carried by drainage waters are totally adsorbed on the lake sediments. Therefore, Lake Qarun is playing an important role in the environmental balancing in the Fayoum Governorate.

Keywords Water quality · Surface waters · Fayoum watershed · Lake Qarun · Drinking water · Microbiological contamination

Electronic supplementary material The online version of this article (doi:10.1007/s12665-015-4186-0) contains supplementary material, which is available to authorized users.

M. S. M. Abdel Wahed · C. Wolkersdorfer · M. Sillanpää
Laboratory of Green Chemistry, LUT Chemistry Department, Lappeenranta University of Technology, Sammonkatu 12, 50130 Mikkeli, Finland

M. S. M. Abdel Wahed (✉) · E. A. Mohamed · M. I. El-Sayed
Geology Department, Faculty of Science, Beni-Suef University, Beni-Suef, Egypt
e-mail: m.abdelwahed80@yahoo.com

C. Wolkersdorfer
Tshwane University of Technology (TUT), Private Bag X680, Pretoria 0001, South Africa

A. M'nif
Centre National de Recherche en Sciences des Matériaux, Technopole Borj Cedria, B.P.73, 8027 Soliman, Tunisia

Introduction

Egypt has been suffering from severe water scarcity in recent years. The per capita share of water has dropped substantially to less than 1000 m^3/year, which is classified as the "Water poverty limit" and it is projected that the value decreases to 500 m^3/capita in the year 2025 (Abdel Wahaab 2003). The current water budget in Egypt shows that the annual water demand exceeds the available fresh water by 6 Gm^3/year. Meanwhile, the water demand is continually increasing due to population growth, industrial development and the rise in living standards.

Water quality deterioration is one of the major factors playing havoc with water security and public health in Egypt. The declining water quality has become a global

Published online: 25 February 2015

issue of concern as human population grows, industrial and agricultural activities expand and potential changes in climate might threaten the hydrological cycle (WWAP 2009). Poor water quality has a direct impact on the water quantity in a number of ways: polluted water that cannot be used for drinking, bathing, industry or agriculture effectively reduces the amount of useable water within a given area. Generally, the water crisis tends to be regarded as a water quantity problem; however, water quality is documented in many countries as a major factor (Ongley 1999). In recent years, the contribution of degraded water to the water crisis is also measured in loss of beneficial use: that is, water lost for beneficial human, agricultural, and ecological uses through excessive pollution by pathogens, nutrients, (semi-)metals, organic matter, salinity and other toxic wastes. Poor water quality has been mainly linked with public health concerns through transmission of water-borne diseases. This problem is well known in Africa and in many other developing countries (Ongley 1999).

The River Nile is the lifeline of Egypt as it services the country's industrial and agricultural demand and is the primary source of drinking water for the population. Because of the critical situation of water insufficiency in Egypt, water quality monitoring of the River Nile is essential to maximize the utilization of every drop of water.

Fayoum, which means "The Lake" (Piacentini 1997), and its catchment have a unique character: although it is considered as oasis, it is mainly fed by Nile water that enters the Fayoum depression via a waterway called Bahr Yousef (Fig. 1). Fayoum is a closed basin in an arid region with an internal drainage resulting in no water outflow except by evaporation (Abdel Wahed et al. 2014). This means that all dissolved constituents will stay and concentrate in the depression either in the water or in the sediments. The irrigation and agricultural system in the Fayoum region depend on this water. However, due to water scarcity, the secondary source of irrigation water in Fayoum is the reuse of drainage water. Reusing of drainage waters in agriculture has some general limitations because of the potentially high (semi-)metal and pathogen content (FAO 2003). Consequently, water-borne diseases are a particular concern in the Fayoum Governorate due to this extensive irrigation by low quality water as well as inadequate sanitation arrangements. This is an indication that the water quality not only has a direct impact on the water quantity but also on the human health.

Lake Qarun, a closed saline lake, is acting as a natural sink for agricultural drainage water in the Fayoum Depression. It is playing an important role in the environmental balancing because it is collecting all excess waters from the Fayoum region. Additionally, it is a wetland of international importance for waterbirds and it is the main source of fish in Fayoum (Fathi and Flower 2005). Some copepod species are endemic to Lake Qarun (*Paracartia latisetosa, Apocyclops panamensis* and *Mesochra holdeti*) (Mageed 1998). Because of the biological diversity and archaeological and geological importance of the lake ecosystem, it was declared as a nature reserve in 1989.

Previous studies in the Fayoum watershed mainly focused on Lake Qarun. Mansour and Sidky (2002, 2003) and Gupta and Abd El-Hamid (2003) for example investigated the influence of those waters on the lake water quality while Abdel Kawy and Belal (2012) studied the concentrations of selected (semi-)metals in the irrigation and drainage waters in the watershed [the term (semi-)metals is used as a substitute for the longer term "metals and semi-metals"]. Yet, those investigations focused only on single aspects of the watershed and did not conduct a holistic approach for all of the watershed's water types and lake sediments. In addition, the data in these publications show a lack of detailed information about the applied methodology as well as inconsistencies in their interpretation of the results.

The evaluation of surface water quality in the Fayoum Governorate was tackled throughout the current work. Water from irrigation canals is used as a water supply for drinking and irrigation. In rural areas of developing countries, surface water is susceptible to pollution due to the lack of awareness and education of people living in these regions. Consequently, this study aims to present an integrated monitoring and evaluation of the water quality in the Fayoum Governorate against the criteria of the World Health Organization (WHO) guidelines for drinking water quality and the Food and Agriculture Organization of the United Nations (FAO) guidelines for irrigation water quality. Moreover, determination of the potential sources of pollution and tracking the fate of contaminants through sources–sink pathways are considered. Concentrations of metals in both water and sediments of Lake Qarun are also investigated.

Materials and methods

Site and Lake Qarun catchment description

The Fayoum Governorate with a population of 2.48 million (January 2005 census) and Fayoum City as the principal town is occupying a natural closed depression in the Western Desert of Egypt between 29°02′ and 29°35′N and 30°23′ and 31°05′E. It extends over 6068 km^2 and is situated about 95 km southwest of Cairo (Fig. 1). The Nile River, on which the irrigation and agricultural system mainly depend, is the main source of water and the province has an internal drainage with Lake Qarun as the general receiver for agricultural wastewater. The studied

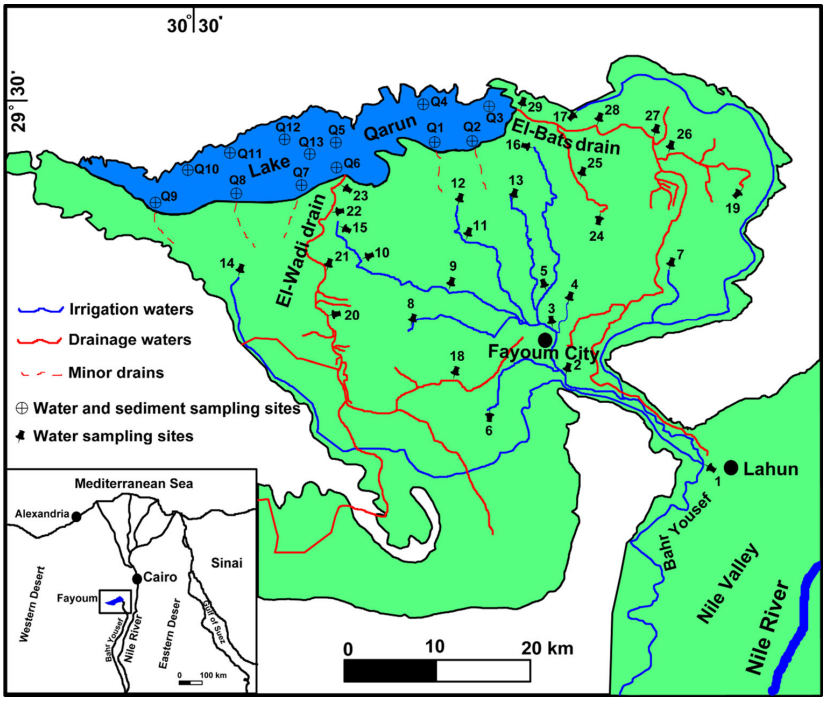

Fig. 1 Location map showing the study area and sampling sites

catchment lies in Egypt's arid belt with a hot long dry summer and a mild short winter and consequently, the climate is generally warm and dry (Baioumy et al. 2010). In addition, it is characterized by low seasonal rainfall and a high evaporation rate. Fayoum City is a water distribution center for domestic demands in the province and a network of canals and small pumping stations delivers water also to the agricultural regions. While all other Egyptian Governorates are conveyed to the Nile River, the Fayoum Governorate is unique in such as all its drainage water flows to Lake Qarun.

Lake Qarun is the deepest part in the Fayoum Depression with an elevation of ≈43 m below sea level (Figs. 1, 2). It is a closed, saline and alkaline lake with no outflow except evaporation. About 67 % of the lake has a water depth between 2 and 5 m, while 18 % of the lake is deeper than 5 m. The deepest region (≈8 m) is located in the middle while the shallowest region lies in the eastern portion of the lake (Baioumy et al. 2010). To the north, the area is completely covered by sand and rock exposures without any vegetation while in the south and southeast, cultivated land slopes steeply towards the lake "a natural sink for agricultural drainage water".

To track the concentration of (semi-)metals and ions in the studied catchment, it is important to follow the course of the Nile water once it enters the catchment area for irrigation and domestic uses. Within the catchment, all studied water samples can be categorized into irrigation waters, drainage waters and Lake Qarun waters (Fig. 1). Agricultural returns and all excess waters including treated and untreated domestic sewage are usually collected in the drains. However, in some parts, the effluents from sewage treatment plants discharge directly into the irrigation canals. Subsequently, most waters flow into two major drains: El-Wadi and El-Bats, which, together with minor drains, finally drain into Lake Qarun (Fig. 1).

Sampling and analysis

Water

In June 2010, 2011 and 2012, surface water samples at Lake Qarun were collected regularly from 13 sites (Q1–Q13). In June 2012, additional surface water samples from irrigation canals and the drainage network were collected from 29 sites (samples 1–29) (Fig. 1). All samples were analyzed for Na^+, Ca^{2+}, Mg^{2+}, K^+, SO_4^{2-}, Cl^- and HCO_3^-. In June 2012, the water from these sites was also analyzed for Cu, Pb, Zn, Mo, Cd, Co, Cr, Ni, Li, Mn, Al, Fe, Se, Be, As, Ba, PO_4^{3-}, NO_3^- and oxygen isotopes ($\delta^{18}O$). In April 2013, water samples from all previous sites were collected

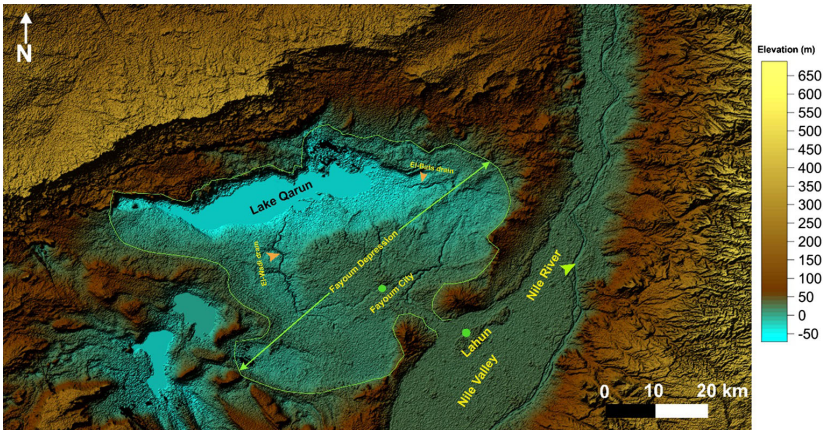

Fig. 2 Digital elevation map showing the land slopes from Lahun to Lake Qarun. The lake occupies the deepest part in the Fayoum Depression

for microbiological analysis of total coliform (TC), fecal (thermotolerant) coliform (FC) and *Fecal streptococcus* (FS).

At all sampling locations, measurements of electrical conductivity (EC), pH and temperature were carried out in the field using a SG78-SevenGo Duo pro (pH/ion/conductivity) portable meter. After in situ measurements, the water samples for major ions and (semi-)metals analyses were filtered through a 0.45 µm disposable cellulose acetate syringe membrane filter (white rim, Whatman GmbH, Germany). The filtered samples were transferred into pre-acid-washed polyethylene containers which divided into three portions: (1) acidified to pH < 2 for all (semi-)metals analysis; (2) for main anion analysis and (3) for oxygen isotopes analysis. Water samples for microbiological analysis were collected using sterilized dark glass bottles. Then, the water samples were kept at 4 °C and transported to the laboratory very soon after sampling. Microbiological, HCO_3^- and NO_3^- analyses were conducted immediately after samples reached the laboratory and the remaining analyses within the next 24 h. Total dissolved solids (TDS) were calculated using the sum of the major ions (Na^+, K^+, Ca^{2+}, Mg^{2+}, HCO_3^-, SO_4^{2-}, Cl^-, SiO_2 and NO_3^-), assuming that the fraction below 0.45 µm can be considered "dissolved", which is not exactly true, as constituents commonly attach to (nano-)particles. Major ions, (semi-)metals and microbiological analyses were carried out at the Water Quality Central Laboratory, Fayoum Drinking Water and Sanitation Company, Fayoum, Egypt which accredited according to ISO/IEC 17025. The analyses were done in accordance with approved analytic methods (APHA 1998, see the electronic supplementary appendix 1 for more details).

Water samples were analyzed for oxygen isotope composition ($\delta^{18}O$) using a Gas Bench II system (Thermo Finnigan, Bremen, Germany) coupled with a Thermo Finnigan Delta plus XP isotope ratio mass spectrometer in the stable isotopologues laboratory at McMaster University, Canada. The details of the analytical procedures are described in Klein Gebbinck et al. (2014). All oxygen isotope results were obtained by calculating the mean of the last 10 measurements and normalized by using two inter-laboratory water standards (i.e. MRSI-1 and MRSI-2). The $\delta^{18}O$ values of the samples were reported normalized to V-SMOW and the precision for replicate sample analyses is $\leq$0.08 %.

Sediments

As Lake Qarun is a sink for the drainage waters in the Fayoum Governorate, the (semi-)metal contents in the Lake sediments were also investigated. For this purpose, surficial lake sediment samples were collected in June 2010 from the 13 sites Q1–Q13 (Fig. 1). The upper 15 cm of the sediments was taken with a grab sampler, collected in acid-rinsed polyethylene plastic bags and kept at 4 °C. These samples were air dried at room temperature and sieved through a 2 mm nylon sieve to remove coarse debris and fragments of shells. Afterwards, the samples were squashed and mildly ground to pass a 63 µm nylon mesh using a set of agate mortar and pestle. Subsequent analysis of (semi-)metal contents was conducted for the <63 µm grain size fraction. For analysis, the sediment samples were digested using aqua regia and the extractions were analyzed for Cu, Pb, Zn, Mo, Cd, Co, Cr, Ni, Mn, Al, Fe, As, Hg and Sb. The (semi-)metal analysis were conducted at Viljavuuspalvelu Oy (Soil Analysis Service Ltd), Mikkeli, Finland. Cu, Mn, Al, Fe, Co, V, Mo and Zn were detected with a Thermo Scientific ICAP 6000, while As, Ni, Pb, Sb, Cr and Cd were detected with a PerkinElmer SIMAA6100 GAAS. Hg was measured with a PerkinElmer AAnalyst 100 and FIMS 100

instrument. All analytical procedures are accredited by FINAS according to ISO/IEC 17025.

In addition to chemical analyses, grain size analyses were conducted. After the sediments were air dried at room temperature, 50 g of the sample was taken and treated with 35 % H_2O_2 and 1 N HCl to remove organic matter and carbonate, respectively. After treatment, sediment samples were wet sieved through a 63 μm nylon mesh and the sand fraction (>63 μm) dried and weighted. The remaining fraction of silt and clay (<63 μm) was determined by the pipette method based on the method described in Kroetsch and Wang (2008) at Viljavuuspalvelu Oy (Soil Analysis Service Ltd), Mikkeli, Finland.

Results

Electrical conductivity (EC) and total dissolved solids (TDS)

Water salinity, expressed by the electrical conductivity (EC) and total dissolved solids (TDS), is an important parameter to evaluate the suitability of irrigation and drainage waters for agriculture because they are an alternative source for irrigation water in the Fayoum Governorate. The EC and TDS results show that the salinity of water increases in the order: irrigation waters < drainage waters <<< lake waters (Fig. 3). In general, electrical conductivities of drainage waters are higher than those of irrigation waters. One exception is sample 17 from an irrigation canal (3.76 mS/cm), which has the maximum of all irrigation and drainage waters (Table 1).

Major ions and nutrients

The results for the major ions show that the mean concentrations of Na^+, K^+, Ca^{2+}, Mg^{2+}, SO_4^{2-} and Cl^- increase in the order irrigation waters < drainage waters <<< lake waters (Fig. 3) and follows the trend of the EC. On the other hand, the mean concentration of HCO_3^- decreased in in the order drainage waters > lake water > irrigation water while the mean concentration of SiO_2 decreased from drainage waters > lake water ≥ irrigation water (Fig. 4). As can be seen from the Piper plot (Fig. 5), during the course of the water from its source at Lahun towards Lake Qarun, the relative equivalents of Na^+ increase compared to $Ca^{2+} + Mg^{2+}$, while the relative equivalents of SO_4^{2-} and Cl^- proportionally increase compared to HCO_3^-. This means that the surface water during its SE–NW course through the Fayoum watershed changes from a Ca–Mg–HCO_3 type to a transitional Ca–Mg–Cl–SO_4 type and ends up as a Na–Cl type (Fig. 5). The mean concentrations of NO_3^- and PO_4^{3-} of the studied different waters showed that they are increasing in the order drainage waters > irrigation waters > lake water (Fig. 4).

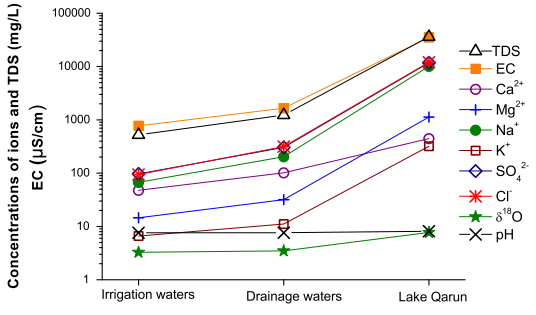

Fig. 3 Means plot showing increasing concentrations of Na^+, K^+, Ca^{2+}, Mg^{2+}, Cl^- and SO_4^{2-}, EC, TDS, $\delta^{18}O$ and pH as waters flow towards Lake Qarun

"Dissolved" (semi-)metals

As shown in Table 1, the metals Al, Ba, Cr, Co, Cu, Ni, Fe, Li and Mn were detected with different concentrations in all waters with the highest mean concentrations in drainage waters and lowest in Lake Qarun. One exception is Li, which has the highest mean concentration in Lake Qarun (Table 1; Fig. 4). Mo was measured below the detection limit in the irrigation waters, detected in some drainage waters and detected in lower concentrations in the lake water. All the other (semi-)metals (As, Be, Cd, Pb, Zn, Se) are below their respective detection limits. In general, the mean concentrations of the metals Al, Ba, Cr, Co, Cu, Ni, Fe and Mn are in the order drainage waters > irrigation waters > lake water (Fig. 4). In the irrigation water samples, the highest concentrations of Al, Ba, Cr, Co, Fe and Ni were observed at sampling site 13. Yet, drainage water sampling site 22 has the highest concentrations of Al, Cr, Co and Fe.

Microbiological results

Out of all waters, the highest levels of total coliforms (TC) and fecal coliforms (FC) were observed in water sample 25 (1.85×10^7 CFU/100 mL and 2.6×10^6 CFU/100 mL, respectively; Table 1) and the highest concentration of *F. streptococcus* (FS) in irrigation water sample 11 (9×10^5 CFU/100 mL). The highest levels of TC and FC in irrigation waters were also recorded in sample 11 (9.25×10^6 CFU/100 mL and 1.29×10^6 CFU/100 mL, respectively). In all waters, the lowest levels of TC, FC and FS were generally recorded in Lake Qarun.

Table 1 Physiochemical and microbiological parameters measured in surface waters in the Fayoum Catchment, Egypt

Water system	Site	PH	EC mS/cm	Ca^{2+} mg/L	Mg^{2+} mg/L	Na^{+} mg/L	K^{+} mg/L	HCO_3^{-} mg/L	SO_4^{2-} mg/L	Cl^{-} mg/L	SiO_2 mg/L	TDS mg/L	$\delta^{18}O^{b}$ ‰
Irrigation waters	1	7.70	0.38	36.16	9.43	19.78	3.21	120.0	38.20	23.18	5.11	255.07	+3.09
	2	7.70	0.45	36.10	10.60	30.20	3.90	132.8	52.32	37.68	5.06	308.66	+3.12
	3	7.70	0.39	36.20	9.89	19.58	3.04	122.8	39.90	25.75	4.73	261.89	+3.21
	4	7.60	0.44	31.90	9.30	22.00	3.90	128.8	51.90	33.79	4.53	286.12	+3.19
	5	7.80	0.42	38.10	10.30	22.40	3.31	122.4	47.80	28.72	6.23	279.26	+3.22
	6	7.60	0.40	34.00	9.90	24.70	3.80	136.8	39.43	25.38	5.07	279.08	+3.22
	7	7.53	0.45	37.10	10.80	38.40	4.30	135.6	48.50	33.72	5.98	314.40	+3.13
	8	7.50	0.50	37.70	11.60	35.80	4.50	144.8	56.90	39.32	5.71	336.33	+3.26
	9	7.60	0.36	32.10	9.60	21.90	3.80	130.8	28.90	16.68	4.74	248.52	+3.19
	10	7.60	0.65	43.30	16.16	47.20	8.22	165.2	72.70	56.06	10.60	419.44	+3.33
	11	7.50	0.68	46.32	15.22	45.20	4.72	174.0	75.90	61.60	9.87	432.83	+3.24
	12	7.50	0.76	47.91	15.96	46.10	5.17	182.4	73.34	57.10	10.73	438.71	+3.27
	13	7.77	0.87	54.20	19.79	71.40	5.53	184.8	118.00	82.20	11.82	547.74	+3.30
	14	7.50	0.60	46.32	15.22	45.20	4.72	174.0	75.90	61.60	9.87	432.83	+3.24
	15	7.50	0.91	47.91	15.96	46.10	5.17	182.4	73.34	57.10	10.73	438.71	+3.27
	16	7.90	1.11	62.00	20.49	100.10	6.13	173.2	154.90	151.10	8.62	676.54	+3.37
	17	7.70	3.76	144.40	37.73	506.20	39.10	212.4	593.60	807.80	9.14	2350.37	+4.22
Mean		7.61	0.77	47.75	14.59	67.19	6.62	154.31	96.56	94.05	7.56	488.62	+3.29
SD		0.12	0.80	26.23	7.01	115.02	8.46	28.21	131.83	186.62	2.66	493.66	+0.25
Drainage water	18	7.50	1.01	49.20	19.30	112.60	7.00	198.8	147.80	116.96	8.87	660.53	+3.39
	19	7.60	0.97	73.27	15.73	85.50	6.13	154.0	154.10	119.28	8.53	616.54	+3.49
	20	7.60	1.38	77.90	23.49	139.60	7.78	183.2	207.90	190.30	12.47	842.64	+3.56
	21	7.60	1.60	93.09	26.55	142.40	8.67	192.8	276.80	241.50	14.15	995.96	+3.57
	22	7.80	1.73	100.20	28.60	156.50	6.95	204.4	292.30	260.50	14.69	1064.14	+3.62
	23	7.70	1.84	188.00	65.89	481.60	17.10	277.5	510.30	730.30	12.61	2283.30	+3.62
	24	7.50	1.10	53.33	22.20	117.20	8.63	224.4	141.60	116.47	10.84	694.67	+3.24
	25	7.70	1.91	82.30	32.51	182.40	15.10	295.2	291.10	303.90	15.14	1217.65	+3.34
	26	7.60	1.98	120.00	27.58	204.90	10.25	190.8	380.80	308.60	13.26	1256.19	+3.61
	27	7.50	1.94	106.30	26.56	193.80	10.49	196.0	361.60	308.60	13.52	1216.87	+3.49
	28	7.50	2.10	106.00	30.52	203.30	11.90	186.4	393.30	332.14	11.72	1275.28	+3.48
	29	7.50	2.40	166.80	63.60	425.00	23.30	220.1	502.00	758.30	13.14	2172.24	+3.50
Mean		7.58	1.66	101.37	31.88	203.73	11.11	210.30	304.97	315.57	12.41	1191.33	+3.49
SD		0.10	0.46	41.54	16.05	123.07	5.08	39.95	128.79	215.40	2.10	539.52	0.12
Lake Qarun waters	Q1	8.20	34.10	419	970	9361	285	180	11808	11526	9	34557	+7.54
	Q2	8.20	32.30	431	1045	9602	305	201	11580	11823	8	34994	+7.29
	Q3	8.20	32.50	358	847	7941	250	176	8705	10544	10	28830	+7.14
	Q4	8.30	34.10	514	1027	9458	326	181	11417	11695	8	34627	+7.60
	Q5	8.40	36.70	524	1148	9919	480	184	10695	12340	7	35297	+7.86
	Q6	7.80	34.80	394	1131	9550	289	192	10453	12306	19	34333	+7.62
	Q7	8.20	34.40	453	1239	10166	283	160	12392	12092	8	36792	+7.67
	Q8	8.30	35.40	329	1177	12125	387	157	12387	12278	6	38846	+7.81
	Q9	8.30	36.70	484	1267	9949	300	156	12376	12317	6	36855	+7.95
	Q10	8.30	36.80	497	1238	10163	297	166	13461	12415	6	38243	+7.93
	Q11	8.30	37.00	463	1217	10888	290	157	13630	12472	7	39124	+7.93
	Q12	8.40	36.90	453	1203	12271	362	157	12207	12384	6	39042	+7.89
	Q13	8.30	36.60	450	1100	10159	296	171	12283	12509	10	36977	+7.79
Mean		8.22	35.25	444	1124	10119	319	172	11800	12054	8	36040	+7.69
SD		0.15	1.69	58	123	1143	60	15	1302	550	3	2800	0.25

Table 1 continued

Water system	Site	Al µg/L	Ba µg/L	Cr µg/L	Co µg/L	Cu µg/L	Fe µg/L	Li µg/L	Mn µg/L	Ni µg/L	Mo µg/L	PO_4^{3-} mg/L	NO_3^- mg/L
Irrigation waters	1	1980	38.3	3.11	1.165	>5	1840	1.97	63.97	1.91	<2.1	0.02	11.98
	2	340	32.23	2.31	<1	7.42	420	1.09	38.12	2.58	<2.1	0.06	18.08
	3	1990	38.5	3.28	1.48	<5	2310	1.81	67.4	2.07	<2.1	0.03	11.01
	4	200	42.11	<1.9	<1	6.43	200	1.02	68.4	1.59	<2.1	0.09	21.83
	5	2050	39.43	4.41	1.33	<5	2410	2.05	69.5	2.72	<2.1	0.06	10.87
	6	2500	39.01	3.47	<1	5.83	2700	1.99	66.74	3.96	<2.1	0.12	14.72
	7	1200	36.72	<1.9	<1	6.32	1400	1.39	45.04	4.52	<2.1	0.14	16.88
	8	800	39.04	1.94	<1	7	1100	1	101.2	1.96	<2.1	0.15	17.72
	9	3210	44.07	<1.9	<1	8.03	3740	<1	80.2	2.96	<2.1	0.13	18.08
	10	3060	48.76	4.6	2.22	<5	3440	2.1	127.1	3.09	<2.1	0.12	35.67
	11	1800	44.71	2.56	1.164	<5	1840	1.95	132.1	1.57	<2.1	0.39	55.96
	12	1410	48.74	3.71	<1	6.76	1820	2.03	149.5	2.37	<2.1	0.33	81.15
	13	8350	69.73	11.88	4.72	6.73	9340	4.45	233.6	7.31	<2.1	0.15	55.21
	14	3800	45.71	5.89	2.14	6.07	3970	2.95	104.9	3.95	<2.1	0.06	39.03
	15	1770	49.23	5.57	1.12	14.79	2470	2.33	188.1	3.79	<2.1	0.52	45.04
	16	3590	46.38	6.88	1.57	9.45	3770	2.41	241.04	5.37	<2.1	0.24	52.95
	17	4500	65.7	<1.9	<1	11.15	530	25.5	213.8	3.42	<2.1	0.55	46.54
Mean		2502.9	45.2	4.6	1.9	8.0	2547.1	3.5	117.1	3.2	NA	0.19	32.5
SD		1926.7	9.7	2.6	1.1	2.6	2107.0	5.9	66.3	1.5	NA	0.16	20.8
WHO (2008)[c]		200	–	50	–	2000	–	–	400	70	70	–	–
FAO (1992, 2003)[d]		5000	–	100	50	200	5000	2500	200	200	10	–	–
Drainage water	18	1400	39.7	<1.913	<1	6.83	1700	1.54	102.8	2.63	<2.1	0.27	26.17
	19	4960	44.19	7.89	2.36	<5	4650	6.52	68.7	3.84	<2.1	0.09	11.40
	20	7030	59.98	11.24	2.76	10.22	6560	5.17	146.1	7.22	<2.1	0.31	69.31
	21	9310	62.12	14.09	3.33	11.23	8320	6.008	172.8	8.84	<2.1	0.33	49.02
	22	12500	65.77	17.79	3.8	13.4	10410	8.36	175.3	10.51	5	0.33	56.93
	23	9720	59.4	14.05	2.83	39.5	7850	7.52	156.2	13.6	5.37	0.36	52.91
	24	1150	52.9	4.09	1	14.3	1720	2.09	181.8	2.8	5.18	0.82	47.96
	25	4460	64.6	6.9	1.6	38.8	4510	3.63	270.3	5.6	6.08	2.85	47.78
	26	7290	51.6	10.85	3.13	6.38	6270	11.21	111.5	5.51	<2.1	0.18	24.18
	27	4240	46.8	6.73	2.09	4.08	3890	8.62	983	3.54	<2.1	0.39	22.76
	28	6850	53.2	12.04	2.56	13.6	5890	11.06	294	7.32	5.82	0.52	53.48
	29	10600	68.4	12.36	2.68	29.4	7190	11.09	238.1	7.17	5.33	0.67	50.74
Mean		6625.8	55.7	10.7	2.6	17.1	5746.7	6.9	241.7	6.5	5.5	0.59	42.7
SD		3544.3	9.1	4.0	0.8	12.8	2604.2	3.4	242.8	3.3	0.4	0.74	17.3
FAO (1992, 2003)[d]		5000	–	100	50	200	5000	2500	200	200	10	–	–
Lake Qarun waters	Q1	490	8.36	3.85	<1	<5	120	7.5	4.84	<1	2.77	0.03	19.20
	Q2	180	7.65	4.55	<1	<5	90	8.83	6.79	<1	2.34	0.12	15.61
	Q3	470	10.7	3.64	<1	<5	240	8.42	10.4	<1	2.56	0.18	19.43
	Q4	70	8.1	3.17	<1	<5	<79	8.46	4.29	<1	2.37	0.12	20.39
	Q5	50	7.46	2.87	<1	<5	<79	9.03	2.32	<1	2.23	0.12	20.61
	Q6	1210	9.07	3.82	<1	<5	550	8.74	5.45	<1	2.48	0.39	23.90
	Q7	190	7.42	2.74	<1	<5	83	7.7	4.23	<1	<2.1	0.03	19.28
	Q8	400	5.6	4.45	<1	<5	<79	9.14	1.77	<1	<2.1	0.03	19.04
	Q9	60	7.48	2.23	<1	<5	<79	7.97	4.13	<1	<2.1	0.03	19.27
	Q10	60	7.33	<1.913	<1	<5	<79	7.48	3.34	<1	2.22	0.03	18.96
	Q11	770	8.17	2.73	<1	<5	410	7.59	4.61	<1	<2.1	0.03	18.22
	Q12	240	7.98	2.07	<1	<5	<79	7.56	2.14	<1	2.22	0.09	19.09
	Q13	90	10.1	3.64	<1	<5	<79	9.82	3.34	<1	2.16	0.03	20.30

Table 1 continued

Water system	Site	Al µg/L	Ba µg/L	Cr µg/L	Co µg/L	Cu µg/L	Fe µg/L	Li µg/L	Mn µg/L	Ni µg/L	Mo µg/L	PO_4^{3-} mg/L	NO_3^- mg/L
Mean		329.2	8.1	3.3	NA	NA	248.8	8.3	4.4	NA	2.4	0.09	19.50
SD		343.7	1.3	0.8	NA	NA	192.9	0.8	2.3	NA	0.2	0.10	1.8

Water system	Sites	Total Coliform CFU/100 mL	Fecal Coliform CFU/100 mL	*Fecal Streptococcus* CFU/100 mL
Irrigation waters	1	2.2×10^5	1.00×10^4	1.00×10^3
	2	1.0×10^4	1.00×10^4	2.00×10^3
	3	1.43×10^4	4.00×10^3	2.33×10^4
	4	1.80×10^5	1.00×10^4	1.00×10^4
	5	1.60×10^4	5.50×10^3	2.23×10^3
	6	3.00×10^5	2.00×10^4	2.50×10^4
	7	1.00×10^5	6.00×10^4	1.80×10^4
	8	5.00×10^5	5.00×10^4	8.00×10^3
	9	3.80×10^5	3.00×10^4	1.40×10^4
	10	4.00×10^5	9.00×10^4	3.00×10^4
	11	9.25×10^6	1.29×10^6	9.00×10^5
	12	4.45×10^6	4.90×10^5	3.00×10^5
	13	8.30×10^4	4.00×10^4	5.00×10^3
	14	5.00×10^4	3.45×10^3	7.00×10^3
	15	7.50×10^4	1.70×10^4	4.00×10^4
	16	3.80×10^4	1.20×10^4	2.20×10^4
	17	2.00×10^4	9.00×10^3	1.20×10^3
WHO (2008)[c]		Absent	Absent	Absent
FAO (1992, 2003)[d]		–	≤1000	–
Drainage water	18	1.20×10^6	2.00×10^5	3.30×10^4
	19	2.05×10^5	7.10×10^4	6.40×10^3
	20	3.20×10^5	2.30×10^4	1.00×10^4
	21	5.30×10^6	8.20×10^5	5.60×10^4
	22	6.50×10^4	1.20×10^4	1.00×10^4
	23	7.80×10^4	1.90×10^4	5.00×10^4
	24	2.95×10^6	7.80×10^5	3.00×10^5
	25	1.85×10^7	2.60×10^6	1.00×10^5
	26	4.40×10^5	1.25×10^4	1.40×10^4
	27	2.60×10^5	7.80×10^4	5.80×10^3
	28	5.00×10^5	7.90×10^4	1.50×10^4
	29	1.16×10^4	2.60×10^5	2.30×10^4
FAO (1992, 2003)[d]		–	≤1000	–
Lake Qarun waters	Q1	80	4	1
	Q2	290	20	20
	Q3	88	80	1
	Q4	20	1	62
	Q5	10	1	6
	Q6	330	112	34
	Q7	140	56	40
	Q8	200	186	2
	Q9	2	1	8
	Q10	10	1	1
	Q11	10	1	1

Table 1 continued

Water system	Sites	Total Coliform CFU/100 mL	Fecal Coliform CFU/100 mL	*Fecal Streptococcus* CFU/100 mL
	Q12	2	1	2
	Q13	2	1	54

NA not applicable, – no available data, *SD* standard deviation

[a] Mean values of the parameters measured in water samples collected during June 2010, 2011 and 2012 from Lake Qarun

[b] $\delta^{18}O$ was only measured in June 2012

[c] Guidelines for drinking water quality according to World Health Organization (WHO 2008). The evaluation was applied only for waters from irrigation canals which are used as drinking water supply in the Fayoum Governorate

[d] Recommended maximum concentrations for waters used in irrigation according to FAO (1992, 2003). This evaluation was applied for irrigation and drainage waters. Note that drainage waters are reused for irrigation in the Fayoum Governorate

Grain size analysis

The results of grain size analyses from sediments in Lake Qarun (Table 2; Fig. 6) show that the highest clay content was recorded close to the El-Bats drain mouth outlet at sampling site Q3 (62 % clay) and at sampling site Q9 (49 % clay). In the middle of the lake, the highest silt content was recorded at sampling sites Q5 and Q13 (60 % silt at both sites) and the highest sand content at the north-western part of the lake at sampling sites Q10 and Q11 (96 % sand at both sites). In summary, the clay and silt fractions are concentrated in the eastern and middle parts of the lake while sand is concentrated at the northern and western parts. In the western part, high fractions of clay prevail only at sampling site Q9.

(Semi-)metals in Lake Qarun sediments

In the lake sediments, the highest concentrations of Al, Fe, Co, Cr, Cu, Ni, Zn, Sb and V were recorded at site Q3 while their lowest concentrations are at sampling sites Q10 and Q11 (Table 2; Fig. 6). In regards to Mn, the highest concentration was found at sampling site Q1 and the lowest, as for the other (semi-)metals, at sampling sites Q10 and Q11. The (semi-)metals As, Cd and Hg are below the detection limits at all lake sediment sampling sites. The spatial distribution of all (semi-)metals in Lake Qarun correlates with the spatial distribution of the clay fraction (Fig. 6). Hence, it is obvious that the sites with higher clay and silt fractions have the higher concentrations of (semi-)metals while the lowest concentrations of metals were recorded at sites with higher sand fractions.

Discussion

Hydrochemical water types

Based on the Piper plot (Fig. 5), the studied waters can be classified into three water types; Ca–Mg–HCO_3, Ca–Mg–Cl–SO_4 and Na–Cl. As described earlier, the waters evolve from the Ca–Mg–HCO_3 type to the Ca–Mg–Cl–SO_4 type and eventually to the Na–Cl type downstream and at Lake Qarun. This relative increase of SO_4 and Cl compared to HCO_3 as well as the relative increase of Na compared to Ca and Mg towards Lake Qarun indicates the presence of evaporites in the studied area. Since the climate of the Fayoum catchment is always dry and hot, dissolved Na, Mg, Cl and SO_4 concentrations continue to build up in the Lake with the dominance of Na and Cl, while Ca and HCO_3 precipitate as carbonates (Abdel Wahed et al. 2014).

Behavior and sources of major ions and (semi-)metals in the studied waters

Mechanisms governing the chemical composition and behavior of the studied waters were assessed by finding interrelationships and identifying co-variations of parameters, using a Principal Component Analysis (PCA) with SPSS 21. PCA can provide a clarifying view of the parameter interrelationships. Therefore, this analysis was carried out with the complete set of the measured parameters of all samples (Table 1). Despite considerable parameter variations among individual samples, the first two principal components (PC1 and PC2) of the PCA represent 77.9 % of the total variances in the irrigation, drainage and lake waters (Fig. 7). Two intercorrelated groups can be identified by the PCA. The first one consists of the major ions Na^+, K^+, Ca^{2+}, Mg^{2+}, Cl^- and SO_4^{2-} as well as EC, TDS, $\delta^{18}O$ and pH. The co-location of these major ions with EC, TDS and $\delta^{18}O$ indicates that they have a similarly hydrogeochemical controlled which can be seen by the evaporative concentration process. However, dissolution of evaporites can also contribute to the concentrations of these ions in the drainage waters.

The initial pH of the solution at equilibrium can be calculated by the following equations (Stumm and Morgan 1996):

$$CO_{2(g)} + H_2O \rightleftharpoons HCO_3^- + H^+ \; K_H K_1$$

$$\{H^+\} = \frac{K_H K_1 p_{CO_2}}{\{HCO_3^-\}}$$

where K_1 is the dissociation constant of H_2CO_3, K_H is the equilibrium constant of the CO_2 solubility in water.

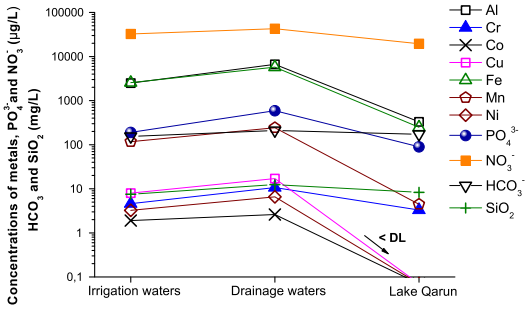

Fig. 4 Means plot showing the behavior of Al, Fe, Co, Ni, Cu, Mn, NO_3^-, PO_4^{3-}, HCO_3^- and SiO_2 with highest values in drainage waters and lower in Lake Qarun. "*<DL*" means that Cu, Ni and Co are below detection limits in Lake Qarun

Yet, during evaporation evolution, the co-existence of pH with Na^+, K^+, Ca^{2+}, Mg^{2+}, Cl^-, SO_4^{2-}, EC, TDS and $\delta^{18}O$ while HCO_3^- is located on the opposite side of the PC plot can be explained by the following equation (Eugster and Jones 1979):

$$2HCO_3^- \rightarrow CO_3^{2-} + CO_{2(g)} \uparrow + H_2O$$

This mechanism, where CO_2 is degassing from the lake, explains the pH increase associated with the concentration of evaporatives in alkaline lakes whereas the carbonate alkalinity ($HCO_3^- + 2CO_3^{2-}$) stays unaltered (Eugster and Jones 1979; Abdel Wahed et al. 2014; Banks et al. 2004). Total carbonate ($HCO_3^- + CO_3^{2-}$) decreases in closed saline lakes due to degassing and carbonate minerals precipitation (Eugster and Jones 1979). The presence of Ca^{2+} independent from HCO_3^- is possibly due to the initial excess of Ca^{2+} relative to HCO_3^- in the inflowing drainage waters to Lake Qarun. In addition, through $CaCO_3$ precipitation, the HCO_3^- is depleted while unreacted Ca^{2+} builds up in solution (Abdel Wahed et al. 2014). The plotting of the mean concentrations of Na^+, K^+, Ca^{2+}, Mg^{2+}, Cl^- and SO_4^{2-} as well as EC, TDS, $\delta^{18}O$ and pH for the different water types (irrigation waters, drainage waters and Lake Qarun waters) showed similar

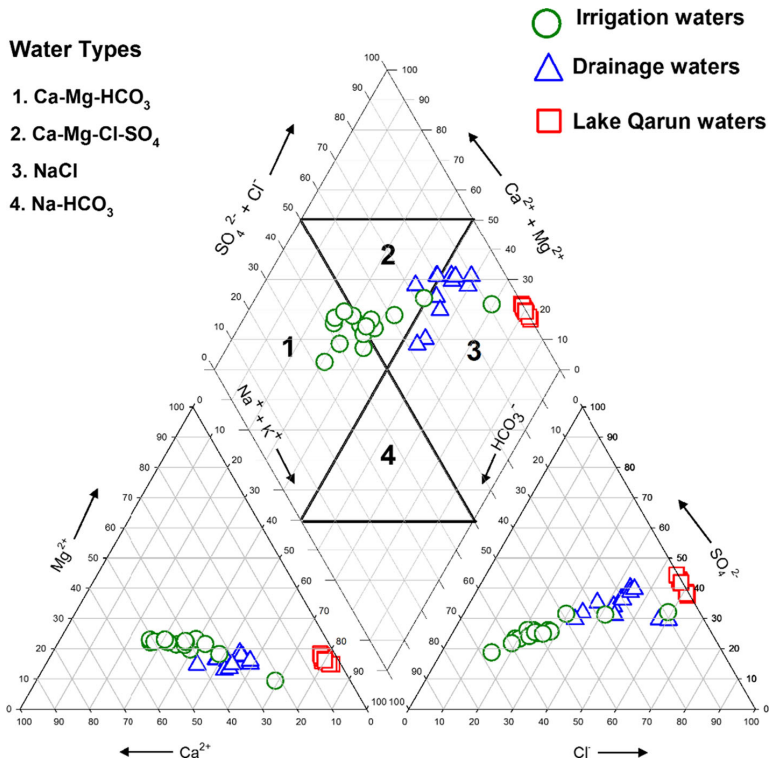

Fig. 5 Piper plot of the different water types. The water evolves from a Ca–Mg–HCO_3 type at the head waters to Na–Cl downstream and at Lake Qarun passing through the Ca–Mg–Cl–SO_4 type

Table 2 (Semi-)metal concentrations (in mg/kg dry wt.) and percentages of sand, silt and clay in Lake Qarun sediments (sites Q1–Q13)

Site	Mn	Fe	Co	Cr	Cu	Ni	Pb	Zn	Sb	Al	V	Clay %	Silt %	Sand %
Q1	1000	17000	11.2	24	10	14	2.5	27	0.83	11000	45	9	48	43
Q2	700	9400	6.07	14	7	10	<2	20	<0.5	6330	26	10	8	82
Q3	400	40000	17.7	60	41	36	4.5	91	2.07	35100	96	62	38	0
Q4	300	18000	8.29	25	20	19	4.2	40	0.67	16400	68	30	38	32
Q5	300	23000	10.5	36	25	25	5.5	50	0.98	21700	82	18	60	22
Q6	400	27000	13.7	37	20	24	3.9	44	1.3	20300	52	30	25	45
Q7	900	12000	9.32	18	6.9	9.3	2.6	21	<0.5	7210	23	10	7	83
Q8	600	17000	9.41	24	11	16	2.9	30	1	13300	36	18	26	56
Q9	600	38000	16.3	52	26	33	4.6	62	1.73	32200	74	49	50	1
Q10	0.1	1100	0.4	<3	<1.5	<3	<2	<5	<0.5	492	3.1	2	2	96
Q11	0.1	2700	0.93	3.3	<1.5	<3	<2	5.6	<0.5	1880	8	4	0	96
Q12	200	17000	4.24	32	8	9.9	3	36	0.72	13800	39	2	7	91
Q13	100	19000	4.56	33	5.9	9.5	3.2	39	0.84	14900	39	30	60	10
Average shale[a]	850	47200	19	90	45	68	20	95	1.5	80000	130	NA	NA	NA

NA not applicable

[a] Turekian and Wedepohl (1961)

trends where all these parameters increase on the way to Lake Qarun (Fig. 3). This demonstrates why these parameters plot together on the PC plot.

In the second assemblage, parameters that plot in the same area of the PC plot are Al, Fe, Co, Ni, Cu, Mn, NO_3^-, PO_4^{3-}, HCO_3^- and SiO_2 (Fig. 7), which gives indication to a similar geochemical development, processes or sources. They increase from irrigation waters to drainage waters and decrease in Lake Qarun (Fig. 4). The presence of NO_3^- and PO_4^{3-} in this group indicates the contribution of fertilizers to the water chemistry whilst SiO_2 and HCO_3^- most likely indicate the weathering of clay and silicate minerals from the soils. Lake Qarun is the main sink of all constituents carried by the drainage water inlets. Adsorption of metals on the surface of lake sediments under alkaline conditions is possibly the main mechanism behind the depletion of these metals in the lake water. In addition, the presence of pH on the opposite side of metals on the PC plot reflects the negative relationship between the mobility of these metals and pH in Lake Qarun (Fig. 7).

Interrelations between the studied parameters can provide useful information on potential contamination sources. For this purpose, correlation matrices (CM) with the different variables Na^+, K^+, Ca^{2+}, Mg^{2+}, Cl^-, SO_4^{2-}, HCO_3^-, SiO_2, Al, Fe, Co, Cr, Ni, Cu, Mn, Mo, Li, Ba, NO_3^-, PO_4^{3-}, EC, TDS and $\delta^{18}O$ were calculated with SPSS (Table 3). As can be seen, Al, Fe, Cr, Co, Ni, Cu and Ba are statistically significantly correlated. This association of Al and Fe with the other metals indicates their common origin, mainly from natural sources such as weathering processes and is supported by the positive correlation between these metals, SiO_2 and HCO_3^-. The statistically significant correlation between PO_4^{3-} and NO_3^- as well as PO_4^{3-}, Cu and Mo indicates the fertilizer inputs to the surface runoff. On the other hand, NO_3^- is also correlated with Al, Fe, Cr, Co, Ni, and Cu indicating additional sources of NO_3^-. The pH is negatively correlated with Al, Fe, Cr, Co, Ni, Cu, Mn and Ba, which reflects the decreasing solubility of these metals with increasing pH. This is supported by the depletion of these metals in Lake Qarun, which has the highest pH value among all studied waters. Major ions including Na^+, K^+, Ca^{2+}, Mg^{2+}, Cl^- and SO_4^{2-} are significantly positively correlated with EC, TDS and $\delta^{18}O$. This indicates that evaporative concentration is the main process behind the concentration increase of these ions. Li was also positively correlated with EC, TDS and $\delta^{18}O$, indicating an increasing Li concentration due to evapoconcentration. Consequently, the CM results support the results obtained by PCA. Both statistical analyses identified two distinctive variable groups: Group A, which includes Na^+, K^+, Ca^{2+}, Mg^{2+}, Cl^-, SO_4^{2-}, EC, TDS, $\delta^{18}O$ and pH. These variables are statistically significantly correlated with each other and were found in higher concentrations in Lake Qarun compared to irrigation and drainage waters (Figs. 3, 7). Group B, which includes Al, Fe, Cr, Co, Ni, Cu, Mn, SiO_2, HCO_3^-, PO_4^{3-} and NO_3^-, is statistically significantly associated and shows lower concentrations in Lake Qarun as compared to irrigation and drainage waters (Figs. 4 and 7).

Cluster analysis (CA) was applied to group the similar water sampling sites (spatial variability) based on the measured physiochemical parameters. Hierarchical agglomerative CA was performed by SPSS® using between-

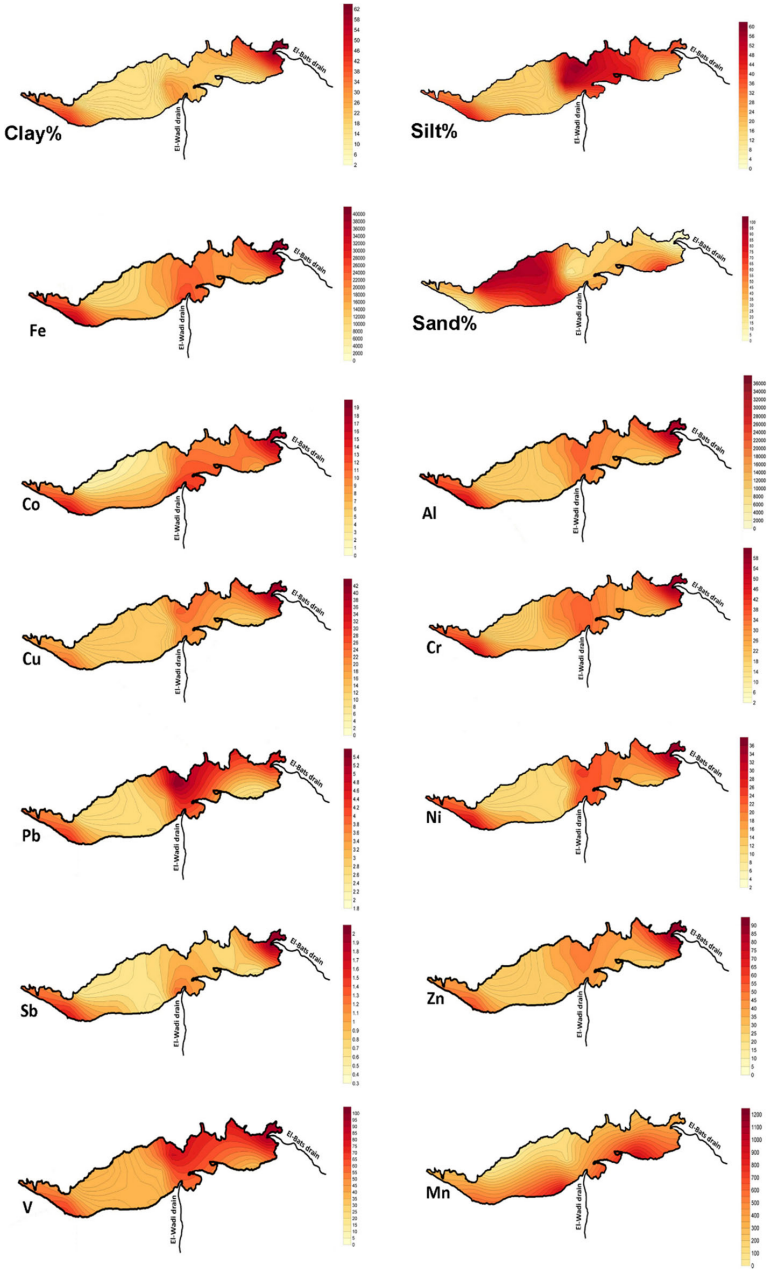

Fig. 6 Spatial distribution of selected (semi-)metals (in mg/kg dry wt.) and grain size fractions (in %) in the Lake Qarun sediments

groups linkage with Euclidean distances as a measure of similarity. The dendrogram of the sampling sites (Fig. 8) shows that there are two distinct groups. Group 1 consists of the Lake Qarun sampling sites (Q1–Q13). These are sampling sites that have lower concentrations of Al, Fe, Cr, Co, Ni, Cu, Mn, SiO_2, HCO_3^-, PO_4^{3-} and NO_3^- and higher concentrations of Na^+, K^+, Ca^{2+}, Mg^{2+}, Cl^-, SO_4^{2-}, EC, TDS, $\delta^{18}O$ and pH. Group 2 consists of irrigation water sites as well as drainage water sites which have higher concentrations of Al, Fe, Cr, Co, Ni, Cu, Mn, SiO_2, HCO_3^-,

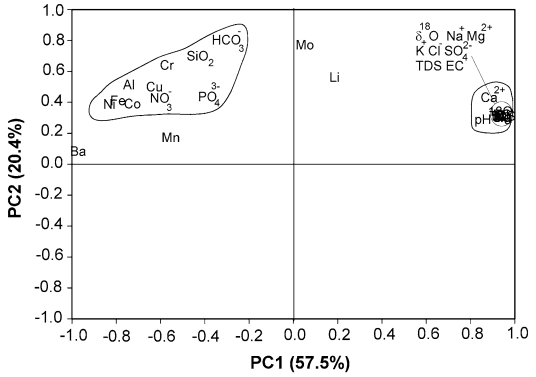

Fig. 7 Principal component analysis (PC2 vs. PC1) of the studied parameters in all studied waters. The first component (PC1) represents 57.5 % of total variations, the second component (PC2) another 20.4 % of the total variation in all data. Two distinct parameters assemblages can be identified and are discussed in the text

PO_4^{3-} and NO_3^- and lower concentrations of Na^+, K^+, Ca^{2+}, Mg^{2+}, Cl^-, SO_4^{2-}, EC, TDS, $\delta^{18}O$ and pH as compared to sites of Group 1.

Group 2 can be further subdivided into the drainage (Group 2A, except irrigation water site 13) and the irrigation waters sites (Group 2B, except drainage water sites 18, 19, 24, 25 and 27). The cluster classifications varied with significance levels between Group 1, Sub-Group 2A and Sub-Group 2B. This is also confirmed by the significant differences in the mean values of the relevant parameters among irrigation waters, drainage waters and Lake Qarun waters as shown by means plot (Figs. 3, 4).

The location of site 13 in Sub-Group 2A indicates that this site has chemical characteristics similar to drainage waters. In fact, the highest concentrations of Al, Cr, Co, Cu, Fe and Ni out of all irrigation waters were recorded at that site and those concentrations are similar to those of drainage waters. This is an indication for location 13 being impacted by pollution from the Sinnuris wastewater treatment plant or from any other point sources. On the other hand, the drainage waters (sites 18, 19, 24, 25 and 27) plotting in the irrigation waters Sub-Group 2B are probably due to: (1) locations of some sites such as 18, 19 and 24 at the head of a drainage system (Fig. 1) having comparably lower concentrations of Al, Fe, Cr, Co, and Ba. (2) At some regions in Fayoum (e.g. sites 25 and 27), mixing of brackish drainage waters with fresh irrigation waters is used as irrigation water due to the water scarcity in the catchment. This can cause dilution of the dissolved trace metals and consequently a similar chemical fingerprint of the samples.

In Group 1, sample Q3 differs from the other lake samples, which might be due to the position of this site close to the El-Bats drain mouth outlet and consequently a drainage water influence (Fig. 1). In Sub-Group 2A, site 22 is different from the others, which is due to a substantial enrichment of Al, Cr, Co, Fe and Ni (Table 1). In Sub-Group 2B, site 17 is distinct from other sits in the same group because this site has the highest TDS and EC among all irrigation waters and drainage waters.

Microbiological criteria

Results of bacterial analysis are an indicator of water quality in many aspects. Coliform bacteria (TC) in drinking water can produce serious human illness, but their abundance is primarily used to assess the potential for the presence of other more virulent pathogens associated with sewage. The presence of TC bacteria indicates the possible presence of fecal and disease-causing bacteria (USEPA 1995). FC and FS are bacteria whose presence indicates that the water may be contaminated with human or animal wastes (USEPA 2009). Ideally, drinking water should not contain any microorganisms known to be pathogenic or any bacteria indicative of fecal pollution (WHO 1997). However, all irrigation waters in the investigated area, which are used as drinking water in rural regions without treatment, contain total TC, FC and FS (Table 1). Effluents from sewage and wastewater treatment plants as well as agriculture fields result in elevated levels of bacteria in the drainage waters. Drainage water sampling site 25 contains the highest levels of TC and FC in this water type, which is most likely due to its location near a sewage treatment plant and receiving agriculture returns from nearby meadows. However, also irrigation waters contain higher levels of pathogens (Table 1) because some households discharge their sewage directly into the irrigation canals. Moreover, improper disposal of sewage or on-site sanitation tank overflows into these canals is common in the investigation area. Irrigation water sampling site 11, for example, has the highest level of FS and was sampled very close to household pipe outlets. Most of the households discard their garbage and dead animals in the drains and irrigation canals, which consequently increase the contamination levels of all bacterial species. This situation is very serious regarding the health issues especially when untreated water from these canals is used as drinking water. IOB (2010) stated that most of the prevalent diseases in the Fayoum watershed are water-borne diseases resulting from people being exposed to contaminants by standing in the water during irrigation or by swimming, which was quite often observed in the course of the field work where even children were swimming in these polluted canals. Furthermore, indirect infection due to transferring disease-causing organisms (pathogens) into the crops and vegetables can cause diseases.

Table 3 Correlation matrix of the analyzed parameters in the studied water samples

	Al	Ba	Cr	Co	Cu	Fe	Li	Mn	Ni	Mo	PH	PO_4^{3-}	NO_3^-
Al	1												
Ba	0.775**	1											
Cr	0.896**	0.566**	1										
Co	0.882**	0.729**	0.881**	1									
Cu	0.611**	0.654**	0.513**	0.420**	1								
Fe	0.960**	0.791**	0.896**	0.935**	0.566**	1							
Li	0.240	−0.042	0.182	0.051	0.065	0.021	1						
Mn	0.419**	0.535**	0.351*	0.452**	0.338*	0.427**	0.118	1					
Ni	0.914**	0.822**	0.819**	0.807**	0.741**	0.916**	0.044	0.408**	1				
Mo	0.264	−0.014	0.381*	0.120	0.540**	0.178	0.280	0.016	0.235	1			
pH	−0.424**	−0.788**	−0.224	−0.425**	−0.400**	−0.485**	0.311*	−0.463**	−0.545**	0.236	1		
PO_4^{3-}	0.253	0.431**	0.212	0.190	0.711**	0.245	0.054	0.343*	0.299	0.499**	−0.257	1	
NO_3^-	0.582**	0.663**	0.557**	0.525**	0.554**	0.581**	0.083	0.349*	0.615**	0.223	−0.411**	0.406**	1
Ca^{2+}	−0.410**	−0.824**	−0.217	−0.452**	−0.350*	−0.502**	0.424**	−0.397**	−0.546**	0.352*	0.877**	−0.216	−0.360*
Mg^{2+}	−0.528**	−0.897**	−0.320*	−0.535**	−0.458**	−0.592**	0.314*	−0.466**	−0.653**	0.258	0.885**	−0.263	−0.429**
Na^+	−0.529**	−0.897**	−0.317*	−0.538**	−0.460**	−0.595**	0.315*	−0.466**	−0.655**	0.254	0.899**	−0.265	−0.432**
K^+	−0.522**	−0.880**	−0.311*	−0.532**	−0.448**	−0.590**	0.336*	−0.455**	−0.645**	0.255	0.910**	−0.249	−0.419**
HCO_3^-	0.468**	0.363*	0.488**	0.350*	0.740**	0.396**	0.359*	0.349*	0.478**	0.651**	−0.100	0.711**	0.566**
SO_4^{2-}	−0.528**	−0.896**	−0.319*	−0.535**	−0.461**	−0.593**	0.308*	−0.463**	−0.654**	0.258	0.891**	−0.269	−0.433**
Cl^-	−0.527**	−0.899**	−0.314*	−0.539**	−0.458**	−0.595**	0.324*	−0.466**	−0.656**	0.268	0.895**	−0.259	−0.430**
SiO_2	0.617**	0.444**	0.675**	0.585**	0.471**	0.587**	0.282	0.445**	0.517**	0.400**	−0.291	0.504**	0.605**
$\delta^{18}O$	−0.497**	−0.879**	−0.295	−0.520**	−0.450**	−0.575**	0.373*	−0.450**	−0.634**	0.267	0.895**	−0.257	−0.408**
TDS	−0.527**	−0.898**	−0.315*	−0.537**	−0.457**	−0.594**	0.318*	−0.464**	−0.654**	0.263	0.897**	−0.263	−0.429**
EC	−0.524**	−0.895**	−0.313*	−0.536**	−0.458**	−0.593**	0.331*	−0.459**	−0.655**	0.269	0.897**	−0.254	−0.425**

	Ca^{2+}	Mg^{2+}	Na^+	K^+	HCO_3^-	SO_4^{2-}	Cl^-	SiO_2	$\delta^{18}O$	TDS	EC
Ca^{2+}	1										
Mg^{2+}	0.970**	1									
Na^+	0.961**	0.995**	1								
K^+	0.959**	0.975**	0.980**	1							
HCO_3^-	0.0675	−0.0662	−0.0684	−0.0415	1						
SO_4^{2-}	0.970**	0.996**	0.994**	0.968**	−0.066	1					
Cl^-	0.974**	0.996**	0.995**	0.979**	−0.050	0.995**	1				
SiO_2	−0.097	−0.185	−0.195	−0.198	0.737**	−0.195	−0.165	1			
$\delta^{18}O$	0.979**	0.994**	0.992**	0.978**	−0.029	0.993**	0.997**	−0.148	1		
TDS	0.971**	0.998**	0.998**	0.978**	−0.057	0.998**	0.999**	−0.182	0.996**	1	
EC	0.975**	0.995**	0.994**	0.979**	−0.048	0.994**	0.999**	−0.164	0.998**	0.998**	1

** Correlation is significant at the 0.01 level

* Correlation is significant at the 0.05 level

The lowest levels of TC, FC and FS were recorded in Lake Qarun waters. This is probably due to the higher salinity and alkalinity of the lake water, which is unfavorable for the organisms.

Evaluation of water quality for drinking and irrigation

Introductory remark

Both irrigation and drainage waters are discussed in this section. Lake Qarun water, because of its salinity, is neither used for irrigation nor for drinking and therefore it is not further considered in this section.

Due to water scarcity, the reuse of drainage waters for irrigation is quite common in the Fayoum Governorate. In addition, water in irrigation canals is used for both irrigation and drinking as not all households are connected to tap water networks. Moreover, a limited water pressure is still a widespread problem throughout the water network and the distribution system in Fayoum (IOB 2010). As a result, some households continue to use water from canals, carts with water tanks and, in a few cases, pumped groundwater for domestic purposes. Accordingly, water quality monitoring as well as the evaluation of all waters in irrigation canals against the world drinking water standards is vital task in the Fayoum Governorate.

Drinking water quality

Irrigation water used as drinking water should be evaluated against drinking water quality standards. Based on the WHO (2008) guidelines (Table 1), the studied irrigation waters (samples 1–17) were found to have acceptable concentrations of Ba, Cr, Cu, Mn, Ni and Mo. In the case of NO_3^-, most waters, except at sampling sites 11, 12, 13 and 16, were below the guideline concentrations. The higher concentrations of NO_3^- in the irrigation canals are most likely due to anthropogenic sources.

Nearly all irrigation canal samples have higher concentrations of Al compared to the WHO's guideline (Table 1). Elevated concentrations of Al in drinking water can be harmful in treated water of facilities using an Al sulfate coagulant. Some epidemiological studies even suggest a possible association between Al in drinking water and Alzheimer disease (WHO 2010). The Nile water at site 1, which represents the source water to the Fayoum watershed, has an Al concentration of 1980 μg/L. This concentration increases as the water runs through the watershed due to the fact that Al sulfate salts are used as coagulants in drinking water treatment plants causing increased Al concentrations in public water supplies. Subsequently, this also increases the Al concentrations in household sewage. Moreover, the sludges from the coagulation process are disposed along the banks of the irrigation canals, which are then eroded and further increase the Al concentrations in the water. The high Al concentration at sampling site 13 (8350 μg/L) is probably due to its location close to the effluents from a sewage water treatment plant.

Regarding bacterial contamination, drinking water should not contain any microorganisms known to be pathogenic or any bacteria indicative of fecal pollution (WHO 1997, 2008). Yet, the water in the irrigation canals contains substantially elevated TC, FC and FS bacteria which, for the first time, is presented in the current study. Consequently, these waters are harmful and result in serious health risks. IOB (2010) monitored the prevalence of waterborne diseases such as enteritis or intestinal protozoans as well as vectors such as bilharzia, malaria, viral encephalitis and other viral diseases. This connection between diseases and their causes is confirmed by the findings of the present study. IOB (2010) also reports that in comparison to national means, the prevalence of infections and vector-borne diseases in Fayoum shows the following characteristics:

- Prevalence of viral encephalitis is higher,
- Prevalence of infectious hepatitis and of polio is equal to the national means, but cause concern,
- Diphtheria, tuberculosis, rabies, bronchopneumonia and tetanus are all present, and require vigilance to keep outbreaks under control if village environmental conditions continue to deteriorate.

Accordingly, we recommend the local and national health organizations to further investigate the water quality and health status in the Fayoum watershed, as our findings clearly indicate the direct relationship between the two issues. Installing a working sanitation network needs to include all villages in the watershed and is seen as an essential task. Raising the people's awareness through media or awareness campaigns can help to reduce the discharge of untreated sewage into running waters.

Irrigation water quality

Due to the reuse of drainage waters for irrigation, irrigation and drainage waters were evaluated for their suitability in agriculture. The assessed parameters are salinity, trace metals and microbiological criteria.

All irrigation and drainage waters were plotted on a graph in which the EC is taken as a salinity hazard and the sodium adsorption ration (SAR) as an alkalinity hazard (Fig. 9; US Salinity Laboratory 1954). All drainage waters and some irrigation waters (samples 12, 13, 15 and 16) have a high EC and low SAR. As can be seen, irrigation canal sample 17 has very high EC and high SAR indicators, restricting it for irrigation purposes. Because water of high salinity cannot be used on soils with poor drainage, plants with a good salt

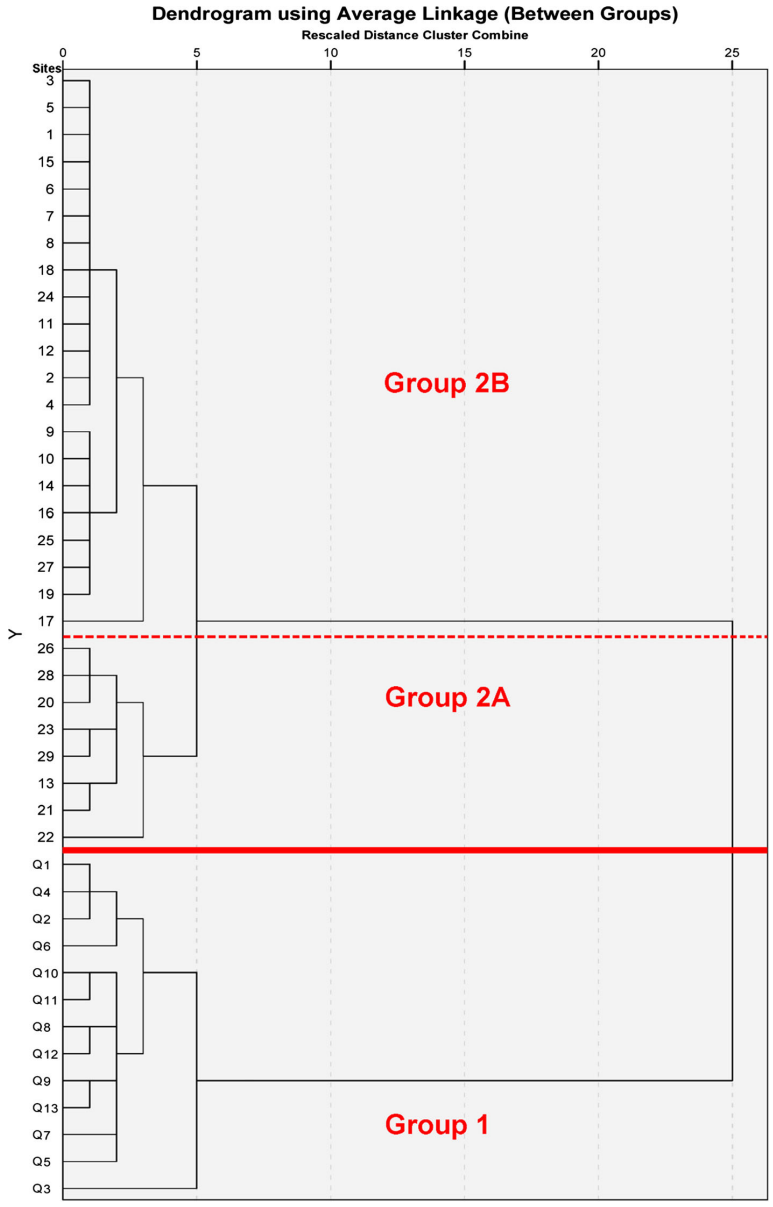

Fig. 8 Cluster analysis dendrogram of the sampled waters. Group 1 consists of Lake Qarun water and Group 2 of irrigation and drainage waters

tolerance should be selected (FAO 1992, 2003). Most of the soils in the Fayoum watershed are characterized by poor drainage and consequently, using high salinity waters for irrigation can cause soil salinization under the prevailing hot and arid conditions. In fact, the degradation of soil productivity is a commonly observed feature in the watershed (Ali and Abdel Kawy 2013; Abd-Elgawad et al. 2013; Abdel Aal and Ibrahim 2013; Shendi et al. 2013).

The recommended limits of trace elements in irrigation water are shown in Table 1. Accordingly, both irrigation and drainage waters are suitable for agricultural purposes except samples 13, 20, 21, 22, 23, 26, 28 and 29, which contain concentrations higher than 5000 µg/L for Al and Fe. Irrigation with water containing Al concentrations above 5000 µg/L can cause non-productivity in acid soils with pH $<$ 5.5. Though irrigation with water having Fe

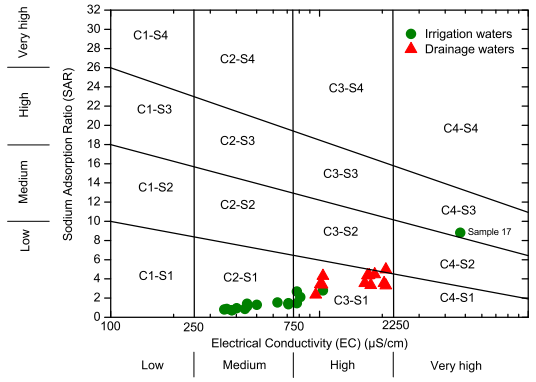

Fig. 9 Salinity and alkalinity hazard applied for evaluating the studied irrigation and drainage waters and their suitability for agricultural purposes. Sample 17 (irrigation water) has the highest salinity and alkalinity hazards

concentrations above 5000 µg/L is not toxic to plants in aerated soils, it can contribute to soil acidification and reduces the bioavailability of essential phosphorus and Mo (FAO 1992, 2003).

WHO (1989) and FAO (1992, 2003) recommend that irrigation water for crops that are likely to be eaten uncooked should not exceed 1000 CFU/100 mL fecal coliforms (FC). Thus, as all irrigation and drainage waters in the Fayoum watershed have FC > 1000 CFU/100 mL (Table 1), they are not suitable for crops that are eaten uncooked. Beside the coliform's health risk in drinking waters, this is a second health risk associated with the bacterial contamination of surface waters and raises the alert for the national and local health organizations to take action towards this vital issue.

Spatial distribution of grain sizes in Lake Qarun sediments

The spatial distribution of grain sizes in the Lake Qarun sediments (Fig. 6) is mainly influenced by the proximity of sites close to drain outlets. Clay and silt, which is carried by the major drains, is deposited in the lake's south-eastern side close to the El-Bats and El-Wadi drain mouths (Figs. 1 and 6). The high relative clay and silt contents at the eastern side and the middle of the lake reflect the input of the El-Bats and El-Wadi drain, while the high content of clay at the western side of the lake is probably due to the low energy of waves in this area resulting in calm conditions required for clay deposition. On the other hand, the highest sand content prevails in the northern and northern-western side and is most likely due to the sand grains derived from sand and rock exposures in the northern side of the lake and the fact that the western side is only affected by minor drains.

(Semi-)metal contents of Lake Qarun sediments

Lake Qarun shows a clear relationship between the spatial distribution of (semi-)metals and the sediment's grain sizes (Fig. 6). All (semi-)metals except Mn follow the same distribution of clay and silt in the lake sediments (Table 2; Fig. 6). The enrichment of (semi-)metals in the fine silt and clay fraction (<63 µm) is due to the large specific surface area of this fraction and also to the strong adsorptive properties of clay minerals and organic matters found in clay (Bodur and Ergin 1994). The similar spatial distribution of Fe, Al, Cr, Co, Cu, Ni, Pb, Zn, Sb, and V (Fig. 6) indicates either similar sources or similar mechanisms of precipitation. The dissimilarity of the Mn distribution in lake sediments possibly indicates different mechanism of Mn precipitation in the lake. Spatial distributions of Cr, Co, Cu, Ni, Pb, Zn, Sb, and V follow the distribution of Fe and Al (Fig. 6), which may reflect the adsorption property of Fe and Al oxides to other (semi-)metals.

It seems as if there is also a relationship between the concentration of metals in the source water (El-Wadi and El-Bats drains) and the metal contents of the lake sediments. As and Cd were recorded below the detection limits in the lake sediments as well as the source waters and Pb was recorded below the detection limit in the source water and was found in very low concentrations in the lake sediments (Table 2). However, Zn was not detected in the source waters but detected in the lake sediments, which is most likely due to an analytical error in the water samples, as Zn is ubiquitous due to its occurrence in galvanized steel and should have been found in those samples. On the other hand, metals such as Fe, Al, Cr, Co, Cu, Ni and Mn were detected in the lake sediments and also in the source waters. For example, Fe and Al were recorded in the first order of metal concentrations in the source waters and the same in lake sediments (Tables 1 and 2). This indicates that the El-Wadi and El-Bats drains are the main sources of metals in the lake. The location of sediment sites with higher metal contents close to the drain's mouths indicates that these metals are transported by these drains into the lake either as dissolved constituents or as particulate metals associated with suspended matter.

Conclusion

Assessment of surface water quality in the Fayoum Governorate shows that the salinity and major ions including Na^+, K^+, Ca^{2+}, Mg^{2+}, SO_4^{2-} and Cl^- increase in the order irrigation waters < drainage waters ⋘ lake waters while metals such as Al, Ba, Cr, Co, Cu, Ni, Fe and Mn increase in the order lake water < irrigation

waters < drainage waters. Evaluation of drinking water from irrigation canals against the standard guidelines of the WHO showed higher concentrations of Al which can be harmful. On the other hand, some irrigation waters and all drainage waters have high salinities and therefore cannot be used for direct irrigation. Especially in the view of the poor drainage conditions of the soils, reusing saline drainage waters causes soil salinization and consequently soil degradation which finally negatively affects the soil productivity. All drainage waters and agricultural returns are conveyed to Lake Qarun. Compared to the other waters, the lake water has relatively low (semi-)metal concentrations due to their adsorption on the lake sediments. Results of the (semi-)metal contents and grain size analysis of the sediments showed that high concentrations of elements are observed at sites with higher clay contents.

The results show that irrigation and drainage water suffer from high levels of TC, FC and FS. The highest levels of TC and FC (1.85×10^7 CFU/100 mL and 2.6×10^6 CFU/100 mL, respectively) were recorded in drainage waters while the highest level of FS (9×10^5 CFU/100 mL) was recorded in irrigation waters. These high levels of microbiological contaminations indicate human and animal fecal sources. This is due to the fact that some households have sewage pipes directly connected to the irrigation canals. Moreover, improper disposal of sewage or on-site sanitation tank overflows into these canals is commonly observed. Consequently, these waters cannot be used for drinking or agricultural purposes without treatment, because of their high risks on the people's health. Yet, many people in the Fayoum watershed, especially in rural regions, use these untreated waters, which causes the prevalence of water-borne diseases.

Recommendations

Egypt is suffering from water scarcity and thence needs every drop of clean water. Therefore, it is recommended to activate environmental protection laws in Egypt to save the water resources. In addition, raising public awareness of environmental protection by the environmental protection agencies and media, especially in rural areas, is crucial from a health perspective. Finally, the sanitation network needs to be extended to all regions in the Fayoum watershed to minimize the pollution caused by unconfined septic tanks and their negative impact on both the groundwater and surface water quality.

Acknowledgments We thank all staff members working at the Qarun Protected Area in the Fayoum Depression for their invaluable help during the field work and sample collection. The authors are very grateful to the Lappeenranta University of Technology (Finland) for providing financial support to this study. Deep gratitude to the Egyptian Ministry of Higher Education and Scientific Research for the granted scholarship. We thank our anonymous reviewers for their helpful input to improve the paper.

References

Abdel Aal T, Ibrahim AM (2013) Studies on the micromorphology of salt-affected soils from El-Fayoum depression, Egypt. In: Shahid SA, Taha FK, Abdelfattah MA (eds) Developments in soil classification, land use planning and policy implications. Springer, The Netherlands, pp 373–392

Abdel Kawy W, Belal A (2012) Spatial analysis techniques to survey the heavy metals content of the cultivated land in El-Fayoum depression. Egypt Arab J Geosci 5:1247–1258

Abdel Wahaab R (2003) Sustainable development and environmental impact assessment in Egypt: historical assessment. Environmentalist 23:49–70

Abdel Wahed MSM, Mohamed EA, El-Sayed MI, M'nif A, Sillanpää M (2014) Geochemical modeling of evaporation process in Lake Qarun. Egypt J Afr Earth Sci 97:322–330

Abd-Elgawad M, Shendi M, Sofi D, Abdurrahman HA, Ahmed A (2013) Geographical distribution of soil salinity, alkalinity, and calcicity within Fayoum and Tamia districts, Fayoum Governorate, Egypt. In: Shahid SA, Taha FK, Abdelfattah MA (eds) Developments in soil classification, land use planning and policy implications. Springer, The Netherlands, pp 219–236

Ali RR, Abdel Kawy WAM (2013) Land degradation risk assessment of El Fayoum depression. Egypt Arab J Geosci 6:2767–2776

APHA (1998) Standard methods for the examination of water and wastewater. American Public Health Association, Washington, DC

Baioumy HM, Kayanne H, Tada R (2010) Reconstruction of lake-level and climate changes in Lake Qarun, Egypt, during the last 7000 years. J Great Lakes Res 36:318–327

Banks D, Parnachev VP, Frengstad B, Holden W, Karnachuk OV, Vedernikov AA (2004) The evolution of alkaline, saline ground- and surface waters in the southern Siberian steppes. Appl Geochem 19:1905–1926

Bodur MN, Ergin M (1994) Geochemical characteristics of the recent sediments from the Sea of Marmara. Chem Geol 115:73–101

Eugster HP, Jones BF (1979) Behavior of major solutes during closed-basin brine evolution. Am J Sci 279:609–631

FAO (1992) FAO irrigation and drainage paper47. FAO, Rome

FAO (2003) Users manual for irrigation with treated wastewater. FAO, TC/D/Y5009F/1/10.03/100

Fathi AA, Flower RJ (2005) Water quality and phytoplankton communities in Lake Qarun (Egypt). Aquat Sci 67:350–362

Gupta G, Abd El-Hamid Z (2003) Water quality of lake Qarun. Egypt Int J Environ Stud 60:651–657

IOB (2010) Drinking water supply and sanitation programme supported by the Netherlands in Fayoum Governorate, Arab Republic of Egypt, 1990–2009. Policy and Operations Evaluation Department, IOB Impact Evaluations 327, Ministry of Foreign Affairs of the Netherlands, pp 1–204

Klein Gebbinck CD, Kim S, Knyf M, Wyman J (2014) A new online technique for the simultaneous measurement of the $\delta^{13}C$ value of dissolved inorganic carbon and the$\delta^{18}O$ value of water from a single solution sample using continuous-flow isotope ratio mass spectrometry. Rapid Commun Mass Spectrom 28:553–562

Kroetsch D, Wang C (2008) Particle Size Distribution. In: Carter MR, Gregorich EG (eds) Soil sampling and methods of analysis. Taylor & Francis, Boca Raton, pp 713–725

Mageed AAA (1998) Distribution and salinity ranges of zooplankton organisms at El-Fayoum depression (El-Fayoum-Egypt). Egypt J Aquat Biol Fish 2:51–71

Mansour SA, Sidky MM (2002) Ecotoxicological Studies. 3. Heavy metals contaminating water and fish from Fayoum Governorate. Egypt Food Chem 78:15–22

Mansour SA, Sidky MM (2003) Ecotoxicological Studies. 6. The first comparative study between Lake Qarun and Wadi El-Rayan wetland (Egypt), with respect to contamination of their major components. Food Chem 82:181–189

Ongley ED (1999) Water quality management: design, financing and sustainability considerations. In: In Proceedings of the African Water Resources Policy Conference, Nairobi, 26–28 May, The World Bank

Piacentini P (1997) Il Fayyum nell'Antico Regno. in Archeologia e papiri nel Fayyum, Siracusa, 23–24 May, 1996. Atti, Siracusa, pp 21–39

Shendi M, Abdelfattah M, Harbi A (2013) Spatial monitoring of soil salinity and prospective conservation study for Sinnuris District soils, Fayoum, Egypt. In: Shahid SA, Taha FK, Abdelfattah MA (eds) Developments in Soil Classification, Land Use Planning and Policy Implications. Springer, The Netherlands, pp 199–217

Stumm W, Morgan JJ (1996) Aquatic chemistry, chemical equilibria and rates in natural waters. Wiley, New York

Turekian KK, Wedepohl KH (1961) Distribution of the elements in some major units of the earth's crust. Geol Soc Am Bull 72:175–192

USEPA (1995) Total Colifrom Rule. U S Environmental Protection Agency, Washington, DC EPA 570/9-91-200

USEPA (2009) National Primary Drinking Water Regulations. US Environmental Protection Agency, Washington, DC EPA 816-F-09-004

US Salinity Laboratory (1954) Diagnosis and improvement of saline and alkali soils. Agriculture Hand Book No 60, USDA, 160 p

WHO (1989) Health Guidelines for the Use of Wastewater in Agriculture and Aquaculture. World Health Organization Technical Report Series No. 778, p 76

WHO (1997) Volume 3, Surveillance and control of community supplies. In: WHO (ed) Guidelines for drinking-water quality, 2nd edn. WHO, Geneva

WHO (2008) Volume 1, Recommendations. In: WHO (World Health Organization) (ed) Guidelines for Drinking-water Quality, 3rd edn. WHO, Geneva

WHO (2010) Aluminium in drinking-water. WHO/HSE/WSH/10 01/13. WHO, Geneva

WWAP (2009) World Water Development Report 3 "Water in a Changing World". UNESCO, Paris, France

Paper IV

Crystallization sequence during evaporation of a high concentrated brine involving the system Na–K–Mg–Cl–SO_4–H_2O

Mahmoud S.M. Abdel Wahed, Essam A. Mohamed, Mohamed I. El-Sayed, Adel M'nif, Mika Sillanpää

Desalination 355(2015)11-21

Desalination 355 (2015) 11–21

Contents lists available at ScienceDirect

Desalination

journal homepage: www.elsevier.com/locate/desal

Crystallization sequence during evaporation of a high concentrated brine involving the system Na–K–Mg–Cl–SO_4-H_2O

Mahmoud S.M. Abdel Wahed [a,b,*], Essam A. Mohamed [b], Mohamed I. El-Sayed [b], Adel M'nif [c], Mika Sillanpää [a]

[a] Lappeenranta University of Technology, LUT Chemistry Department, Laboratory of Green Chemistry, Sammonkatu 12, FI-50130 Mikkeli, Finland
[b] Beni-Suef University, Faculty of Science, Geology Department, Beni-Suef, Egypt
[c] Centre National de Recherche en Sciences des Matériaux, Technopole Borj Cedria, B.P.73, 8027 Soliman, Tunisia

HIGHLIGHTS

- Evaporation of brine involving Na–K–Mg–Cl–SO_4-H_2O system was performed.
- Using the Jänecke phase diagram at 35 °C was useful to predict the evaporation path.
- The precipitated mineral phases were mainly halite and hexahydrite.
- The experimental results were in a good agreement with the field observations.
- We proposed conditions for NaCl and $MgSO_4 \cdot 7H_2O$ production management at EMISAL.

ARTICLE INFO

Article history:
Received 11 July 2014
Received in revised form 7 October 2014
Accepted 8 October 2014
Available online xxxx

Keywords:
Mineral crystallization
Solar evaporation
Jänecke phase diagram
K–Mg salts
Fayoum

ABSTRACT

The crystallization sequence during evaporation of a high concentrated brine collected from the solar evaporation ponds of Egyptian Salts and Minerals Company (EMISAL) was studied. The study included natural solar evaporation in the field at EMISAL site and also experimental isothermal evaporation at 35 °C in the lab. A crystallization path was simulated by the Jänecke phase diagram at 35 °C involving the system Na^+, K^+, Mg^{2+}/Cl^-, and SO_4^{2-}// H_2O. The X-Ray Diffraction (XRD) and Scanning Electron Microscope (SEM) of the solid phases precipitated during the lab and filed works showed similar results where halite and hexahydrite were the real main solid phases precipitated from the brine. But, the crystallization sequence predicted by the Jänecke diagram showed that halite, hexahydrite, kainite and kieserite solid phases should appear during evaporation of the brine. The absence of kainite and kieserite from the real precipitated solid assemblage was attributed to the metastability of kainite and the critical relative humidity conditions for kieserite. The precipitation of K–Mg salts from the studied brine was very sensitive to the climatic conditions. Economically, the present study proposed the optimum conditions at which NaCl salt and magnesium sulfate salts can be produced at high quantity and quality from EMISAL concentration ponds.

1. Introduction

Lake Qarun is one of the largest inland lakes in the North African Great Sahara, about 95 km south west of Cairo (Fig. 1). It is an enclosed, saline, alkaline, inland lake located between the longitudes of 30° 24′ & 30° 49′ E and latitudes of 29° 24′ & 29° 33′ N in the deepest part of the Fayoum Depression. This provides a natural aid for using the lake as a sink for drainage water of the cultivated lands of the whole Province of Fayoum, where it is surrounded by cultivated lands from its southern and south eastern sides which steeply incline toward the lake. The agricultural activities in the Fayoum Depression depend mainly on Nile water. The agriculture drainage water annually carries 470×10^6 kg of dissolved salts to Lake Qarun [16]. Since the lake has no outlet and the climatic conditions are warm and dry almost all the year, the lake brine gradually evaporates and its salinity increases. The total dissolved salts (TDSs) of the lake have strongly increased with time in the course of the twentieth century from 10.5 g L^{-1} in 1906 to the salinity of seawater ($\geq$35 g L^{-1}) in recent days [1]. A further increase in salinity in the twenty-first century, will eventually lead to a biological "dead waterbody" [17]. Salt extraction project was proposed as an economic and environmental solution to stop the continuous increase in Lake Qarun salinity. It was planned to keep the TDS level of the lake at 35 g L^{-1} by extracting an amount of salts equal to those carried annually by drainage water to the lake at sequential stages. The feasibility study indicates the possible economic extraction of Na_2SO_4, NaCl and Mg^{2+}

* Corresponding author at: Lappeenranta University of Technology, LUT Chemistry Department, Laboratory of Green Chemistry, Sammonkatu 12, FI-50130 Mikkeli, Finland.
E-mail addresses: mahmoud.abdel-wahed@lut.fi, m.abdelwahed80@yahoo.com (M.S.M. Abdel Wahed).

http://dx.doi.org/10.1016/j.desal.2014.10.015
0011-9164/

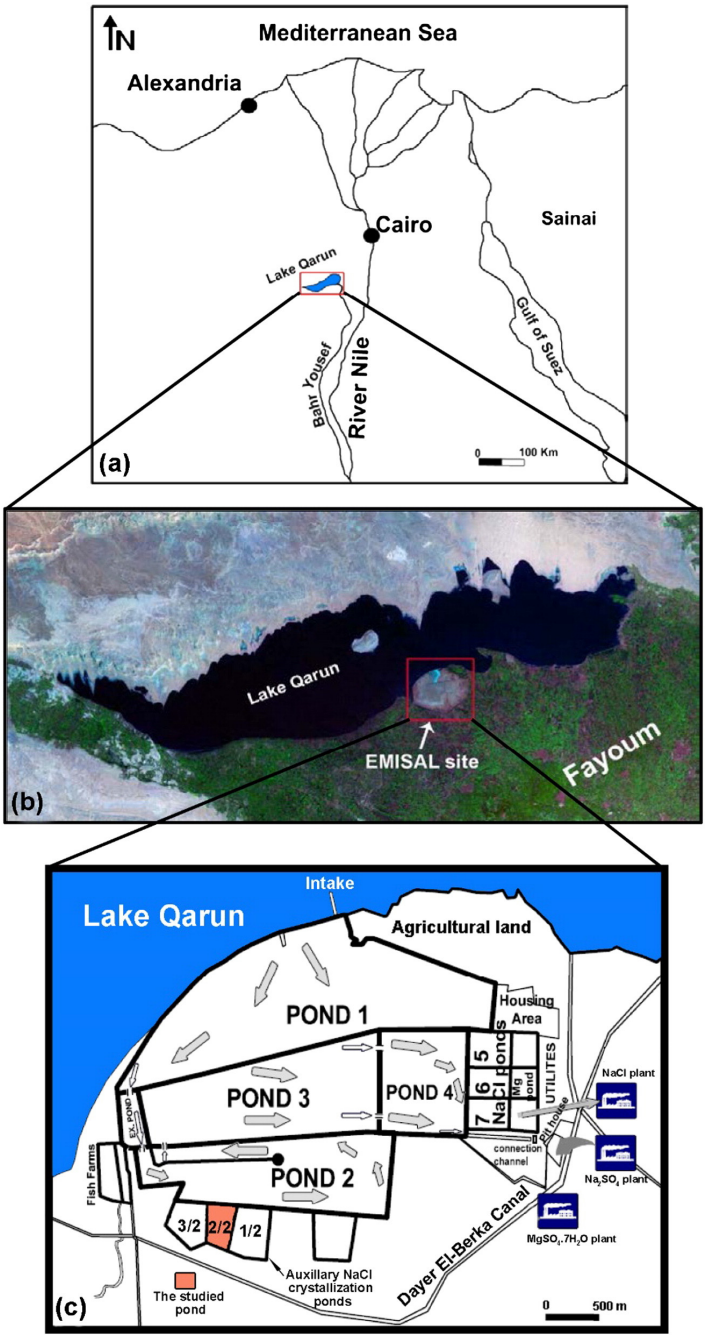

Fig. 1. Location map of the study area, (a and b) locations of Lake Qarun and EMISAL site, respectively, and (c) concentration ponds at EMISAL site.

salts from Lake Qarun water [7]. Since the execution of the approved feasibility study, the Egyptian Salts and Minerals Company (EMISAL) was the founder of this step as an industrial complex site (Fig. 1).

EMISAL was established as an environmental, ecological and economical project on Lake Qarun. There is a zone that has been cutoff from the lake and divided into a series of four successive concentration ponds for economical salt extraction (Fig. 1). The salt-extraction process is based on brine-concentration technology via evaporation–precipitation cycles under solar energy. In ponds 1 and 2, Ca and HCO_3 are removed by carbonate precipitation and the remaining Ca is subsequently removed by precipitation of gypsum ($CaSO_4 \cdot 2H_2O$) in pond 3 [2] (Fig. 1).

The brine from pond 4 is treated in the sodium sulfate plant to extract anhydrous sodium sulfate (thenardite). After the stage of anhydrous sodium sulfate production, the other dissolved salts remain in solution. The effluent from anhydrous sodium sulfate plant is pumped to storage auxiliary ponds where halite (NaCl) is crystallized (Fig. 1). The main composition of the brine in these crystallization ponds is Na–K–Mg–Cl–SO_4. This brine is highly saline ($\approx$277.470 g L^{-1}) and it is supersaturated with respect to halite [7]. After halite crystallization, the residual brine (the bittern), which is rich in potassium–magnesium salts (K–Mg salts), remains in between the halite deposits in the crystallization ponds. Then, this residual bittern is pumped out from the NaCl ponds as the raw brine feeds the third $MgSO_4 \cdot 7H_2O$ plant. The different stages during the process of salt extraction at EMISAL are given in Fig. 2.

The present study aims to find out the crystallization borders between the different dissolved mineral salts in the studied pond. As mentioned earlier, the residual bittern after crystallization of NaCl salt is used as the raw material for extracting magnesium sulfate ($MgSO_4 \cdot 7H_2O$). In modern seawater, during evaporation progress magnesium sulfate salt is predicted to precipitate after halite [4, 13]. So, determination of the crystallization limit between NaCl and the next magnesium sulfate salts will help to avoid any magnesium sulfate salts to co-precipitate as contaminants with NaCl in the auxiliary crystallization ponds. On the other hand, this will also assist to keep the magnesium sulfate salts as dissolved components at a desirable quantity in the residual bittern to produce its designed capacity. Also, this study seeks to compare between the crystallization sequence predicted by the Jänecke phase diagram and the real precipitated salts during evaporation of the studied brine. The Jänecke phase diagram is a useful diagram that shows the crystallization paths during evaporation of brines with five-component system (Mg–Na–K–Cl–SO_4-H_2O) at different temperatures [4].

2. Methodology

This study includes field and lab works. In the field, at EMISAL site, we started to follow-up the geochemical evolution of the effluent brine under solar evaporation conditions at a starting density of 1.246 in pond 2/2 (Fig. 1). In the lab, a volume of 4 L of the brine sample that has the same starting density (1.246) was selected and prepared for experimental isothermal evaporation at 35 °C. The concept was to compare between the observations in the field site and those noticed during the experimental work. Both results were correlated with the crystallization path predicted by the Jänecke phase diagram at 35 °C.

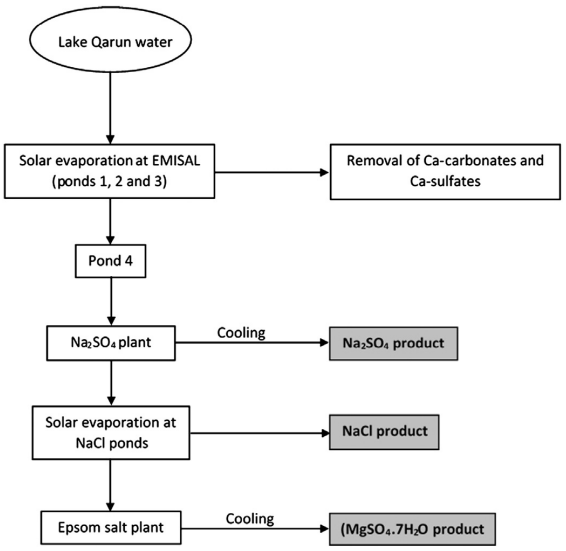

Fig. 2. Flow chart shows the different stages during the process of salt extraction at EMISAL.

2.1. Field work

Brine samples and evaporite deposits (solid samples) were collected during the period April–August 2011 from pond 2/2 at EMISAL site (Fig. 1). The climate at the studied area was always dry and hot with no rain fall during the studied period. The average highest temperatures at the site of study during April, May, June, July and August 2011 were 30, 34, 36.3, 37.1 and 36.8 °C, respectively, while the averages of the relative humidity (RH%) were 47, 44, 45, 51 and 55, respectively (data from EMISAL meteorological station). To follow-up the brine evolution, brine samples from the studied pond were collected in sequence at different densities to determine their chemical constituents. The first sample was collected at a starting density of 1.246. Brine samples with densities 1.246–1.301 were collected during April–June while others with densities 1.318–1.330 were collected during July–August. Along with brine sampling, solid samples in the closed pond 2/2 were also collected at the same density values. The brine samples were collected in clean polyethylene bottles without any air bubbles. The bottles were tightly sealed and labeled in the field. The brine samples were diluted two-fold with distilled water in order to avoid any further precipitation due to evaporation. Samples were kept in an ice box at 4 °C and transported to the laboratory for major ion analysis. Densities and temperatures were measured in situ. Densities were measured in the field by hydrometer (data were corrected for temperature) while temperatures were measured by thermometer. On the other hand, the salt (solid) samples were collected in small polyethylene plastic bags and tightly sealed and labeled in the field for examination by X-Ray Diffraction (XRD) and Scanning Electron Microscope (SEM) techniques. The salt samples were carefully kept away from any atmospheric conditions until examinations.

2.2. Experimental work

A brine sample of density 1.246 obtained from the studied pond was selected as a starting point for experimental isothermal evaporation at 35 $\pm$ 0.1 °C and RH equals to 55%. The temperature and RH conditions, at which the experimental work was done, were recorded at some periods during the field work (see Section 2.1). A volume of 4 L of the brine sample was put in a crystallizer. After that, the crystallizer was placed and fixed in a thermostatic water bath and then evaporation was started. To ensure that the temperature of the solution is 35 $\pm$ 0.1 °C, a thermometer was placed in the solution to monitor any change in the temperature. During evaporation process, brine samples were taken in sequence at different densities for chemical analysis. Measurement of densities in the lab was carried out by using a specific gravity balance. For chemical analysis, the brine samples were diluted two-fold with distilled water in order to avoid any further precipitation due to evaporation. Samples were kept at 4 °C until analysis. Simultaneously, a minute sample of the precipitated salt in the saturated liquid was slightly filtered and stocked in small plastic bags for examination by XRD and SEM techniques. The XRD and SEM examinations were carried out on the same day of solid sample collection to avoid any alteration made by atmospheric conditions. The experimental work was done at the Centre National de Recherche en Sciences des Matériaux, Technopole Borj Cedria, Soliman, Tunisia.

2.3. Analytical methods

All brine samples were analyzed for major ions (Na^+, K^+, Mg^{2+}, SO_4^{2-} and Cl^-). Sodium and K^+ were analyzed by flame atomic absorption spectrometry [3]. Magnesium ion was determined by complexometric

titration with EDTA. The SO_4^{2-} was analyzed by gravimetric method while Cl^- was determined by potentiometric method [3]. For each brine sample, the analysis for each ion was done triple and then takes the average value.

Mineral identification of the collected sediments from pond 2/2 and also those precipitated during experimental evaporation was done by XRD powder method using a PANalytical diffractometer, model X'PERT PRO MPD (PW 3040/60), with a goniometer (PW 3050/60) equipped with a copper anode (PW 3373/00) and Cu–Kα (45 kV, 40 mA). The instrument is electronically-controlled and operates with expert data collector and "X'Pert HighScore Plus" identification software that runs with the ICDD database. On the other hand, the morphology of all sediment samples was tested by "FEI Quanta 200 ESEM". The FEI Quanta 200 Environmental Scanning Electron Microscope (ESEM) is capable of running at low vacuum, thus reducing charging on insulating samples and allowing imaging without applying a conductive coating.

3. Results and discussions

The mean values and standard errors of major ion analysis of the studied brine at various densities measured during the experimental isothermal evaporation at 35 °C in the lab and also during the solar evaporation at the studied pond at EMISAL are given in Table 1.

3.1. Location of the initial studied brine on the Jänecke diagram at 35 °C and prediction of the crystallization path

Modeling of evaporation process in Lake Qarun by using PHREEQC software showed that the lake has mainly evolved from surface drainage waters by evapoconcentration process [1]. Modeling of evaporation process by using PHREEQC program has some limitations when it works on brines with high ionic strength [15]. Accordingly, the Jänecke phase diagram involving the system (Na^+, K^+, Mg^{2+}/Cl^-, SO_4^{2-}//H_2O) is suitable for the present case.

In this study, the results showed that the studied brine at density 1.246 is mainly composed of Mg^{2+}, Na^+, K^+, Cl^-, and SO_4^{2-} (Table 1). The crystallization paths and/or evaporation paths of such kind of brines can be predicted by using the Jänecke diagram at 35 °C (Fig. 3).

The graphical representation of the quinary system (Na^+, K^+, Mg^{2+}/Cl^-, SO_4^{2-}//H_2O) on the Jänecke diagram, during brine evolution, is based on the Jänecke coordinates (mole $\sum K_2 + Mg + SO_4 = 100$) [10,14]. In addition, the application of the Jänecke diagram assumed that the solution is characterized by (1) halite saturation, which means that the solution will co-precipitate halite jointly with the other salt phases separated during the evaporation progress and (2) calcium and carbonates are thought to be unimportant constituents because their concentrations in the saturated solution are low [4]. However, Ca-bearing phases such as gypsum ($CaSO_4 \cdot 2H_2O$) or anhydrite ($CaSO_4$) may be reacted back with the brines to produce glauberite ($Na_2SO_4 \cdot CaSO_4$) and polyhalite ($K_2SO_4 \cdot MgSO_4 \cdot 2CaSO_4 \cdot 2H_2O$), thus profoundly affecting the subsequent evolution of the evaporation brine [9]. In the present case, such kinds of back reactions at the studied pond 2/2 or experimentally at the lab are not expected. This is due to the fact that Ca-bearing phases (Ca-carbonates or Ca-sulfates) are removed from the solution at earlier stages of evaporation in the concentration ponds 1, 2 and 3 (Fig. 2). So, the brine under study is initially free from Ca-bearing minerals.

In Fig. 3, the crystallization path of seawater is redrawn after Usdowski and Dietzel [19] and Bąbel and Schreiber [4]. The Jänecke diagram at temperature 35 °C was chosen rather than at 25 °C because the field work was done during the summer season under hot and dry conditions. The solid phases included in the Jänecke diagram at 35 °C are summarized in Table 2.

The prediction of crystallization path during evaporation of the studied brine is mainly based on the location of the Jänecke coordinates (mole $\sum K_2 + Mg + SO_4 = 100$) of the initial brine on the Jänecke diagram at 35 °C. As shown in Fig. 2, the initial studied brine lies on the crystallization path of seawater but at more progressive evaporation stage. This is because the initial concentration of the studied brine is higher than the concentration of seawater. Along the seawater crystallization path, further evaporation should make the brine to evolve from its initial location at point "α" toward point "Z" (Fig. 3). Point "Z" is a drying-up point at which the crystallization process terminates [4]. Accordingly, if the solution will reach the drying-up point, the predicted mineral phases along the segment "α–Y–R–Z" should appear in sequences as follows:

"α": halite

"α–Y": halite + hexahydrite + kainite
"Y–R": halite + kieserite + kainite
"R–Z": halite + kieserite + carnallite
"Z": halite + kieserite + carnallite + bischofite.

It is assumed that the position of the initial brine remains unchanged during halite crystallization until the actual onset of precipitation of potash and $MgSO_4$-bearing salts [11].

Table 1
Ionic composition (in g L^{-1}) of the studied brine samples, measured at different densities. The concentrations of ions expressed as mean values ± standard errors.

Density	K^+	Na^+	Mg^{2+}	Cl^-	SO_4^{2-}	T[a] (°C)
Experimental isothermal evaporation at 35 ± 0.1 °C						
1.246	5.501 ± 0.011	74.000 ± 0.190	46.086 ± 0.139	174.873 ± 0.917	47.640 ± 0.129	35 ± 0.1
1.260	4.455 ± 0.019	38.183 ± 0.005	55.423 ± 0.572	196.090 ± 0.357	51.054 ± 0.344	35 ± 0.1
1.275	5.133 ± 0.006	32.690 ± 0.052	56.240 ± 0.230	189.865 ± 0.121	57.422 ± 0.267	35 ± 0.1
1.285	6.108 ± 0.015	29.435 ± 0.397	64.902 ± 0.229	195.420 ± 0.219	63.242 ± 0.204	35 ± 0.1
1.297	6.794 ± 0.004	23.950 ± 0.058	79.590 ± 0.367	191.094 ± 0.025	78.333 ± 0.518	35 ± 0.1
1.305	7.120 ± 0.030	20.553 ± 0.553	87.876 ± 0.215	205.370 ± 0.373	81.569 ± 0.279	35 ± 0.1
1.321	7.205 ± 0.008	10.396 ± 0.332	96.064 ± 0.281	215.270 ± 0.583	78.367 ± 0.197	35 ± 0.1
1.343	7.666 ± 0.038	7.395 ± 0.173	97.538 ± 0.149	237.311 ± 0.164	74.214 ± 0.380	35 ± 0.1
Solar evaporation at pond 2/2 at EMISAL site						
1.246	5.501 ± 0.011	74.000 ± 0.190	46.086 ± 0.139	174.873 ± 0.917	47.640 ± 0.129	23.1
1.253	4.804 ± 0.153	56.550 ± 0.554	45.680 ± 0.527	197.000 ± 0.241	48.200 ± 0.175	24.7
1.281	5.954 ± 0.275	30.311 ± 0.193	66.096 ± 0.180	234.003 ± 0.331	61.472 ± 0.347	26.8
1.290	6.135 ± 0.541	26.415 ± 0.402	80.000 ± 0.224	226.912 ± 0.086	66.000 ± 0.447	34.3
1.301	6.136 ± 0.100	25.000 ± 0.502	85.690 ± 0.291	228.000 ± 0.265	75.156 ± 0.153	34.8
1.320	6.431 ± 0.224	15.074 ± 0.169	93.555 ± 0.369	262.367 ± 1.323	61.250 ± 0.253	35.3
1.330	6.903 ± 0.487	9.650 ± 0.142	97.190 ± 0.152	287.895 ± 460	56.200 ± 0.152	35

[a] Temperature values of the solutions.

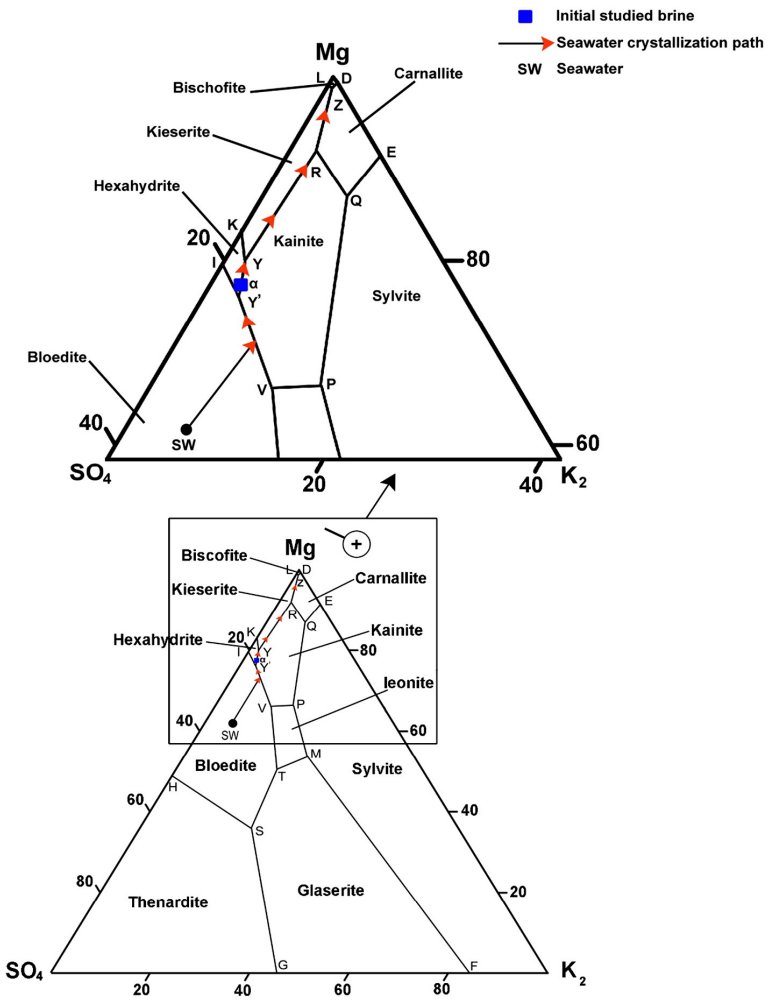

Fig. 3. Location of the studied initial brine on the Jänecke phase diagram at 35 °C involving the system Na^+, K^+, Mg^{2+}/Cl^-, and $SO_4^{2-}//H_2O$ with halite saturation throughout. The diagram and the seawater crystallization path are redrawn from Usdowski and Dietzel [19] and Bąbel and Schreiber [4].

3.2. Experimental and solar evaporation crystallization paths

The brine evolution during evaporation was represented graphically on the Jänecke diagram at 35 °C. In this diagram the Jänecke coordinates (mole $\sum K_2 + Mg + SO_4 = 100$) for a considered solution are expressed as follows:

$$K_2\% = n\,[K_2]/D * 100,\ Mg\% = n\,[Mg]/D * 100 \text{ and } SO_4\% = n\,[SO_4]/D * 100$$

where, "n" is the mole number and $D = n\,[K_2] + n\,[Mg] + n\,[SO_4]$ [14]. The Jänecke coordinates of K_2, Mg and SO_4 of the studied brine during its experimental evaporation in the lab and also during solar evaporation at the studied pond at EMISAL were calculated from the data given in Table 1 and are shown in Table 3. As shown in Fig. 4, the experimental crystallization path and also the solar crystallization path showed good agreement with the predicted crystallization path. Both paths are overlapped on the predicted crystallization path along the segment "α–Y–R–Z". But, in both cases, the evaporation process stopped at points "X" and "X*" for experimental evaporation and solar evaporation, respectively, and both of them did not reach point "Z" (Fig. 4). This is perhaps due to some extremely high-salinity conditions and above a certain concentration the brine becomes hygroscopic and adsorbs

Table 2
Solid phases appear in the Jänecke diagram at 35 °C which involves the system Na^+, K^+, Mg^{2+}/Cl^-, and $SO_4^{2-}//H_2O$ with halite saturation throughout.

Name	Chemical composition
Halite	NaCl
Sylvite	KCl
Hexahydrite	$MgSO_4 \cdot 6H_2O$
Kieserite	$MgSO_4 \cdot H_2O$
Glaserite	$K_3Na(SO_4)_2$
Thenardite	Na_2SO_4
Bloedite	$Na_2Mg(SO_4)_2 \cdot 4H_2O$
Kainite	$KMgClSO_4 \cdot 11/4H_2O$
Leonite	$K_2Mg(SO_4)_2 \cdot 4H_2O$
Bischofite	$MgCl_2 \cdot 6H_2O$
Carnallite	$KMgCl_3 \cdot 6H_2O$

Table 3
Jänecke coordinates of K_2, Mg and SO_4 during the experimental isothermal evaporation at 35 °C and also during the solar evaporation at pond 2/2 at EMISAL site.

Density	K_2%	Mg%	SO_4%	Density	K_2%	Mg%	SO_4%
Experimental isothermal evaporation at 35 °C				Solar evaporation at the studied pond at EMISAL			
1.246	2.86%	76.99%	20.15%	1.246	2.86%	76.99%	20.15%
1.260	1.99%	79.48%	18.54%	1.253	2.51%	76.93%	20.55%
1.275	2.20%	77.71%	20.09%	1.281	2.22%	79.15%	18.64%
1.285	2.29%	78.37%	19.33%	1.290	1.93%	81.12%	16.94%
1.297	2.08%	78.39%	19.53%	1.301	1.79%	80.37%	17.85%
1.305	2.00%	79.35%	18.65%	1.320	1.80%	84.24%	13.96%
1.321	1.90%	81.31%	16.79%	1.330	1.89%	85.58%	12.53%
1.343	2.01%	82.17%	15.83%				

humidity from the air rather than drying [4]. In both cases, the real mineral crystallization sequences should be precipitated according to the obtained experimental path "α–Y–X" and/or the solar evaporation path "α–Y–X*" (Fig. 4). Along both paths, the solid phases precipitated from the solution should appear as follows:

"α": halite
"α–Y": halite + hexahydrite + kainite
"Y–X" or "Y–X*": halite + kieserite + kainite.

3.3. Real crystallized sequences

The real sequences that were crystallized during the experimental isothermal evaporation of the studied brine at 35 °C and also during the solar evaporation at the studied pond at EMISAL can be investigated by following-up the variation in the concentrations of the different ions as a function of density as well as determination of the real collected salts by XRD and SEM techniques.

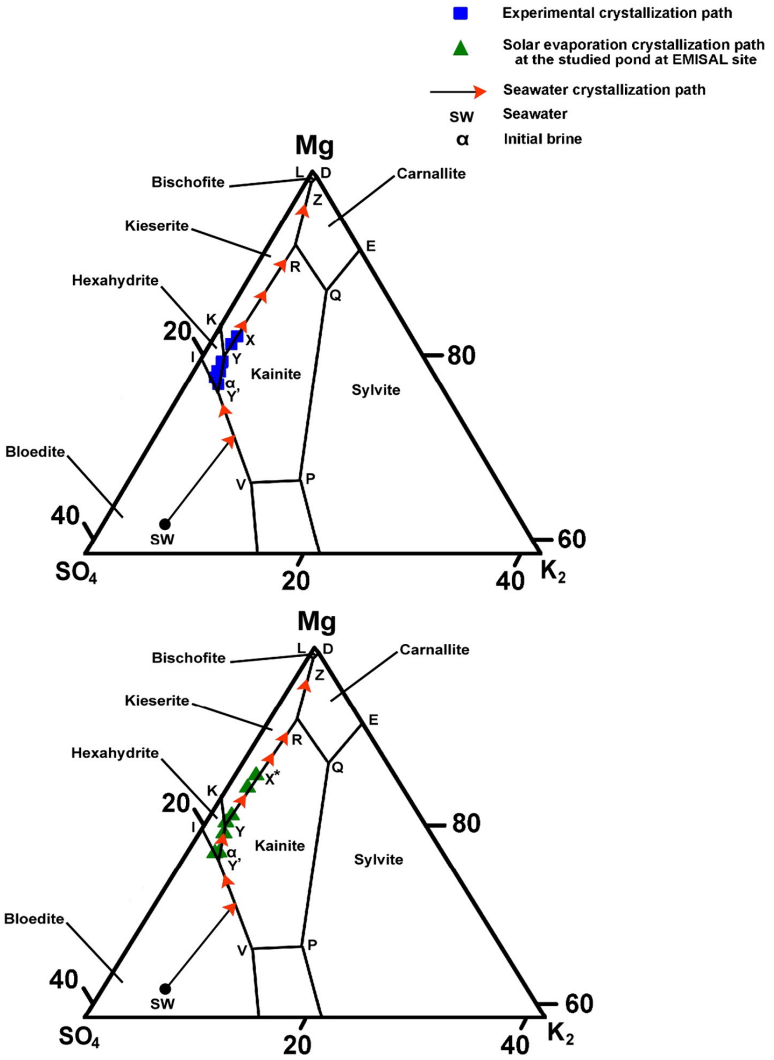

Fig. 4. Graphical representations of the Jänecke coordinates (mole $\sum K_2 + Mg + SO_4 = 100$) on the Jänecke phase diagram at 35 °C showing (i) experimental crystallization path and (ii) solar evaporation crystallization path.

3.3.1. Variation in the concentrations of the different ions as a function of density

The concentrations of Na^+, K^+, Mg^{2+}, Cl^- and SO_4^{2-}, expressed in g L^{-1}, at various densities of the brine samples collected in sequence from the studied pond and also during experimental work are given in Table 1. Major ion concentration represented as mol/1000 mol H_2O is recommended to study the brine evolution during evaporation [4,6]. Accordingly, the numbers of moles of ions per 1000 mol H_2O as a function of density can be calculated from the following equation given by Zayani et al. [21]:

$$(C_i)_j = \frac{(c_i)_j 1000}{M_i\left(n_{H_2O}\right)_j}$$

where,

$(C_i)_j$ is the concentration of the ion (i) in the sample (j), expressed in moles per 1000 mol of water,
$(c_i)_j$ is the concentration in g L^{-1} of the ion (i) in the sample (j),
M_i is the molar mass of the ion (i) and
(n_{H_2O}) is the number of moles of water in 1 L of the sample (j).

Plotting the numbers of moles of ions per 1000 mol H_2O as a function of density during evaporation is given in Fig. 5. The evolution of major ions during progressive evaporation is based on the initial concentrations of these ions at the beginning of evaporation. In other words, it is based on the principal of "chemical divide". The basic idea of the chemical divide rule is "whenever a binary salt is precipitated during evaporation, and the initial molar proportion of the two ions forming this salt is not equal in solution, further evaporation will result in an increase in the concentration of the ion present in greater relative concentration in solution, and a decrease in the concentration of the ion present in lower relative concentration" [8]. In view of that, at the beginning of evaporation at the starting density 1.246, the Cl^- ions are initially greater than the Na^+ ions and Mg^{2+} is greater than SO_4^{2-} (Fig. 5). Therefore, during the evaporation of this brine, it is expected that the precipitation of NaCl salt should cause an increase in the concentration of Cl^- and depletion in Na^+. The same effect will take place when $MgSO_4$ salts start to precipitate where Mg^{2+} should build up in the solution with decreasing SO_4^{2-} during progressive evaporation. We classified the evolution of the major ions during evaporation, and during both experimental and field works, into two main sequences as follows:

In the case of experimental work, the first sequence was observed at densities 1.246–1.305 (Fig. 5a). In this sequence, the concentration of Na^+ decreases dramatically since the beginning of evaporation. This is perhaps due to the precipitation of NaCl salt accompanied with the effect of the principal of chemical divide where the concentration of Cl^- is initially greater than Na^+. On the other hand, both Mg^{2+} and SO_4^{2-} were steadily increased with evaporation until the SO_4^{2-} ion reached its maximum concentration at density 1.305 (Fig. 5a). The second sequence of the experimental evaporation started at densities 1.305–1.343 (Fig. 5a). In this sequence, the Na^+ ions continued to decrease due to the precipitation of NaCl while Cl^- continued to increase. The SO_4^{2-} concentration after reaching its maximum value at a density of 1.305 started to decline at the next densities, while the Mg^{2+} concentration continued to build up in solution (Fig. 5a). This is possibly attributable to the precipitation of $MgSO_4$ salts. The K^+ ion showed a steady increase during the evaporation progress in the two sequences without any depletion.

In the case of solar evaporation, at the studied pond at EMISAL site, the first mineral sequence appeared at densities 1.246–1.301 while the second sequence was defined at densities 1.301–1.330 (Fig. 5b). The general evolution trends of the major ions in the two sequences observed during solar evaporation at the studied pond were similar to those of the experimental results (Fig. 5). The Na^+ ion depleted due to precipitation of NaCl salt from the beginning of evaporation. Both Mg^{2+} and SO_4^{2-} were steadily increased with evaporation until the SO_4^{2-} ions reached their maximum concentration at density 1.301 (Fig. 5b). After that, at densities 1.301–1.330, the SO_4^{2-} concentration starts to decline probably due to the precipitation of $MgSO_4$ salts. The K^+ concentration showed a steady increase during the first and second sequences without any depletion.

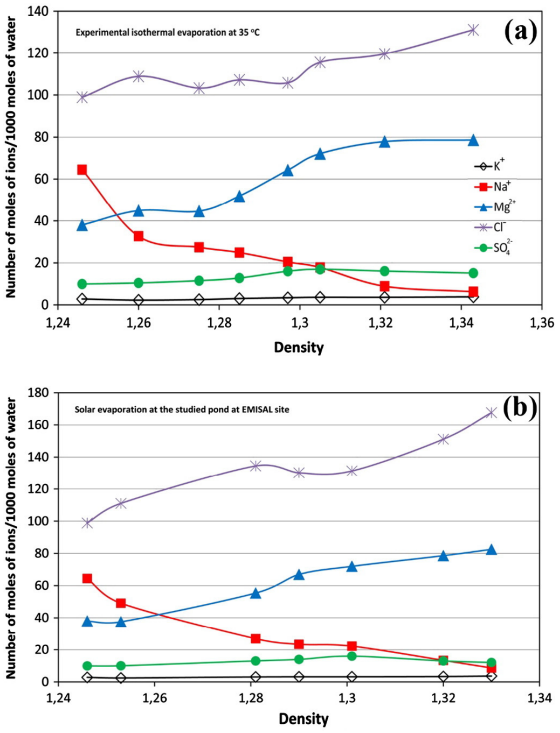

Fig. 5. Evolution of major ion concentrations during (a) experimental isothermal evaporation at 35 °C and (b) solar evaporation at the studied pond (pond 2/2) at EMISAL site.

3.3.2. XRD patterns of the real collected salts

The XRD patterns of the real solid samples of the first mineral sequence crystallized during the experimental isothermal evaporation at 35 °C (at densities 1.246–1.305) and also those crystallized during solar evaporation (at densities 1.246–1.30) showed that halite was the main dominant phase precipitated from brine (Fig. 6). The lattice spacing d (Å) values and relative intensities (I/Io) of the reflection peaks as a function of 2θ have been compared with the Joint Committee on Powder Diffraction Standards [12]. Halite was identified by its characteristic peaks at 2.82, 1.99 and 1.63 Å (JCPDS card number: 05-0628). These results agreed well with the previous results of major ion evolution during evaporation at the first sequences (see Fig. 5a and b), where the removal of Na^+ ions from the solution was attributed to NaCl precipitation.

The XRD pattern of the solid phases collected during the second sequence of mineral crystallization of both experimental evaporation and solar evaporation at densities 1.305–1.343 and 1.301–1.330, respectively, is given in Fig. 7. The XRD pattern showed that hexahydrite appeared

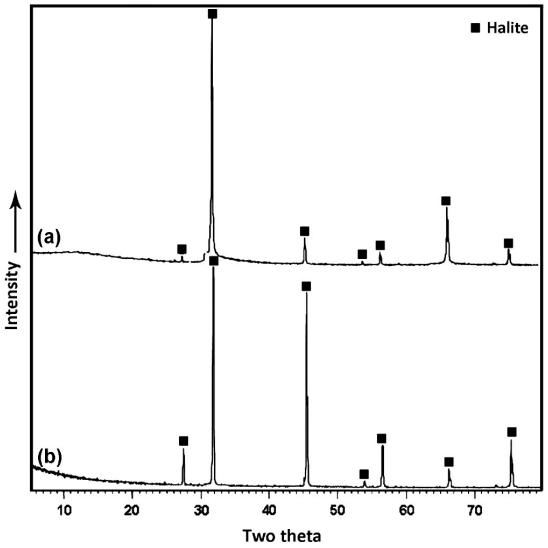

Fig. 6. XRD pattern of halite salt precipitated throughout the first sequence of crystallization (a) at densities 1.246–1.305 during experimental isothermal evaporation at 35 °C and (b) at densities 1.246–1.301 during solar evaporation at the studied pond (pond 2/2) at EMISAL site.

with halite throughout the second sequence of crystallization during the experimental evaporation (Fig. 7a) and also during the solar evaporation at EMISAL site (Fig. 7b). The presence of hexahydrite was confirmed by its characteristic diffractions at 4.39, 5.45 and 5.10 Å (JCPDS card number 24-719). The precipitation of hexahydrite is also confirmed by the depletion of SO_4^{2-} from the solutions during brine evolution (see Fig. 5). The XRD pattern of the solid sample, which was collected throughout the second sequence during solar evaporation at EMISAL site showed the standard pattern of hexahydrite mineral as the same pattern as in the JCPDS card number 24-719 (Fig. 7b).

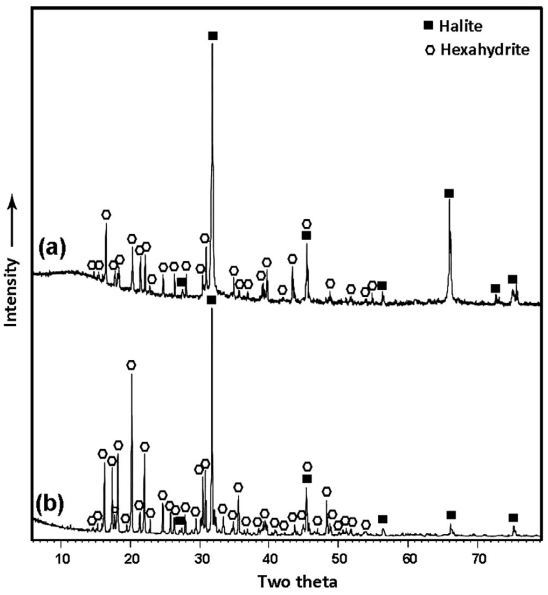

Fig. 7. XRD pattern of hexahydrite and halite salts that were precipitated throughout the second sequence of crystallization (a) at densities 1.305–1.343 during experimental isothermal evaporation at 35 °C and (b) at densities 1.301–1.330 during solar evaporation at the studied pond (pond 2/2) at EMISAL site.

3.3.3. SEM photographs of the real collected salts

The SEM photograph of the solid phases crystallized during the first sequence of experimental evaporation, at densities 1.246–1.305, illustrates the presence of halite cubic crystals (Fig. 8a). Also, well developed cubic crystals of halite were collected from the studied pond during crystallization of the first sequence by solar evaporation, at densities 1.246–1.301 (Fig. 8b). These results of SEM agreed very well with the results of XRD pattern of halite (see Fig. 6).

The experimental precipitation of hexahydrite in the lab, during the second sequence of crystallization, was confirmed by the presence of its characteristic euhedral and tabular pseudo-hexagonal crystals collected at densities 1.305–1.343 (Fig. 9a). Similar euhedral and tabular pseudo-hexagonal crystals were observed in the studied pond 2/2, during the second sequence by solar evaporation, at densities 1.301–1.330 (Fig. 9b).

The agreement between the experimental and field results revealed that the lab conditions during the experimental evaporation were quite similar to the natural conditions in the field. Furthermore, all the results of major ion evolution, XRD and SEM supported and confirmed each other.

3.4. Differences between the real crystallized salts and those predicted by the Jänecke diagram at 35 °C

The crystallization paths "α–Y–X" and "α–Y–X*" during the experimental evaporation and solar evaporation, respectively, were shown on the Jänecke diagram at 35 °C (see Fig. 4). Based on these paths, the solid phases such as halite, hexahydrite, kieserite and kainite should appear in ordered sequences (see Section 3.2). However, the real collected salt phases during evaporation of the studied brine in both cases showed the presence of halite and hexahydrite only while kainite and kieserite phases disappeared.

The absence of kainite is almost referring to its metastability [9,14]. The absence of primary kainite has often been explained by difficulties in nucleating kainite during evaporative concentration [9].

The absence of kieserite is attributed to the relative humidity (RH) in the field and in the lab was higher than the RH required to the formation of kieserite. According to the phase diagram of the $MgSO_4 + nH_2O$ system (Fig. 10), at 35 °C, hexahydrite is the only stable phase at RH ≈ 50%–65% while kieserite is only stable at RH < 50% at the same temperature [18]. In the present study, the RH in the lab was adjusted at 55% during the experimental isothermal evaporation at 35 °C. On the other hand, at EMISAL site, during July and August 2011, the RH was recorded 51% and 55% and the temperatures were recorded 37.1 and 36.8, respectively (see Section 2.1). At these periods, the crystallization of the second sequence by solar evaporation (at densities 1.301–1.330) was achieved with precipitation of hexahydrite ($MgSO_4 \cdot 6H_2O$) only rather than kieserite ($MgSO_4 \cdot H_2O$) or epsomite ($MgSO_4 \cdot 7H_2O$). Kieserite is more stable at lower RH and/or higher temperature (Fig. 10). In addition, it is easily for kieserite to convert to hexahydrite as humidity increases by hydration while hexahydrite does not easily revert to kieserite on desiccation [20]. Furthermore, the supersaturation required for crystallization of magnesium sulfate salts with water molecules lesser than six molecules for each Mg^{2+} ion (i.e. kieserite) decreases with increasing concentration of the solution [5]. Both kainite and kieserite are found to crystallize from supersaturated solutions slowly and with difficulty only when the rate of evaporation is sufficiently slow [4].

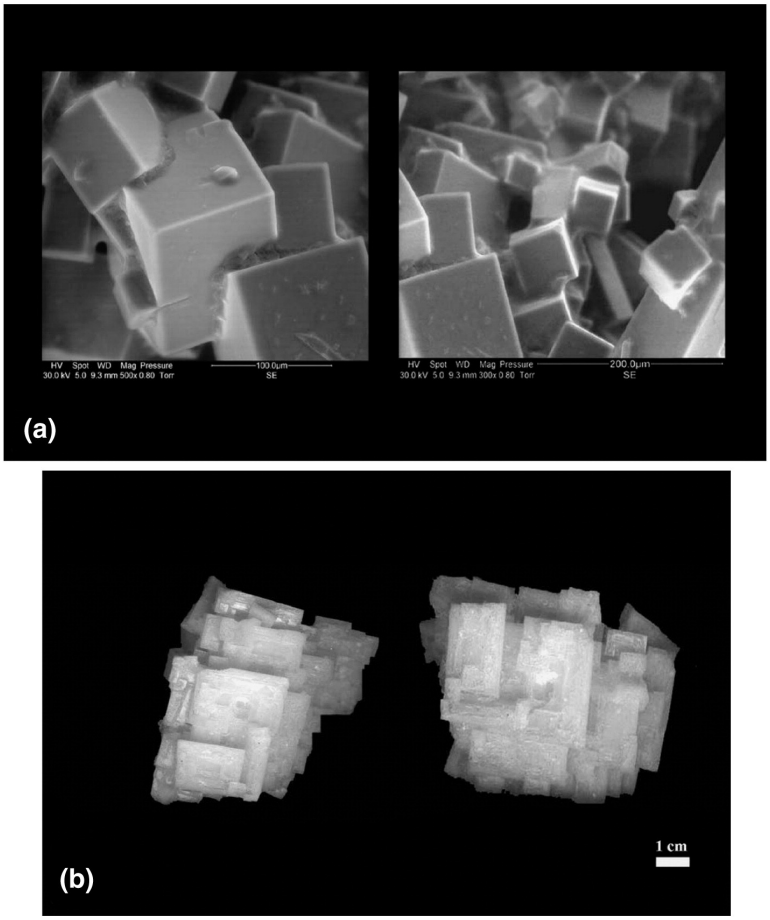

Fig. 8. (a) SEM photographs showing cubic crystals of halite salt precipitated throughout the first sequence of crystallization at densities 1.246–1.305 during experimental isothermal evaporation at 35 °C and (b) photographs showing halite cubic crystals collected from the studied pond throughout the first sequence of crystallization at densities 1.246–1.301 during solar evaporation at the studied pond (pond 2/2) at EMISAL site.

4. Conclusion

The present work dealt with studying the mineral (salt) crystallization sequences during the experimental and solar evaporation of a high concentrate brine involving the system Na^+, K^+, Mg^{2+}/Cl^-, and $SO_4^{2-}//H_2O$ collected from pond 2/2 at EMISAL site at Fayoum Province. The experimental isothermal evaporation in the lab results showed good agreement with the solar evaporation at EMISAL site. In both cases, major ion evolution, XRD and SEM results showed that the progressive evaporation of the studied brine caused the crystallization of halite and hexahydrite minerals through consequent two sequences. The first sequences involved mainly the precipitation of halite as the main solid phase at densities 1.246–1.305 and 1.246–1.301, during the experimental evaporation and solar evaporation, respectively. On the other hand, the second sequence included hexahydrite that appeared at densities 1.305–1.343 and at densities 1.301–1.330 during the experimental evaporation and solar evaporation, respectively. The crystallization path during the whole evaporation process was predicted by using the Jänecke phase diagram at 35 °C involving the system Na^+, K^+, Mg^{2+}/Cl^-, and $SO_4^{2-}//H_2O$. The predicted crystallization path of the studied brine followed the same crystallization path of seawater along which the phases such as halite, hexahydrite, kieserite, kainite, carnallite and bischofite should be appear in ordered and consequent sequences. The experimental evaporation path and also the solar evaporation path shown agreed well and overlapped on the predicted crystallization path. However, both paths did not reach the final stage at which the brine should dry-up. The mineral phases thought to appear along both paths were halite, hexahydrite, kainite and kieserite. But, the real collected salts showed only the presence of halite and hexahydrite. The absence of kainite and kieserite was referred to metastability of kainite and critical RH for kieserite precipitation. During this study, the precipitation of K–Mg salts from the studied brine pointed to the climatic conditions prevailed at the studied area.

All results revealed that, the residual brine after halite crystallization should be pumped from the halite crystallization storage pond (pond 2/2) at density $\approx$ 1.300. This is because at this density value the hexahydrite started to precipitate as contaminants with NaCl in crystallization pond (pond 2/2). Prevention of hexahydrite precipitation with halite will raise the purity of NaCl salt that will harvest from pond 2/2 and then will reduce the power needed for further washing or refining processes of the final NaCl product. Furthermore, pumping of the residual brine at this density value keeps most of the magnesium sulfate

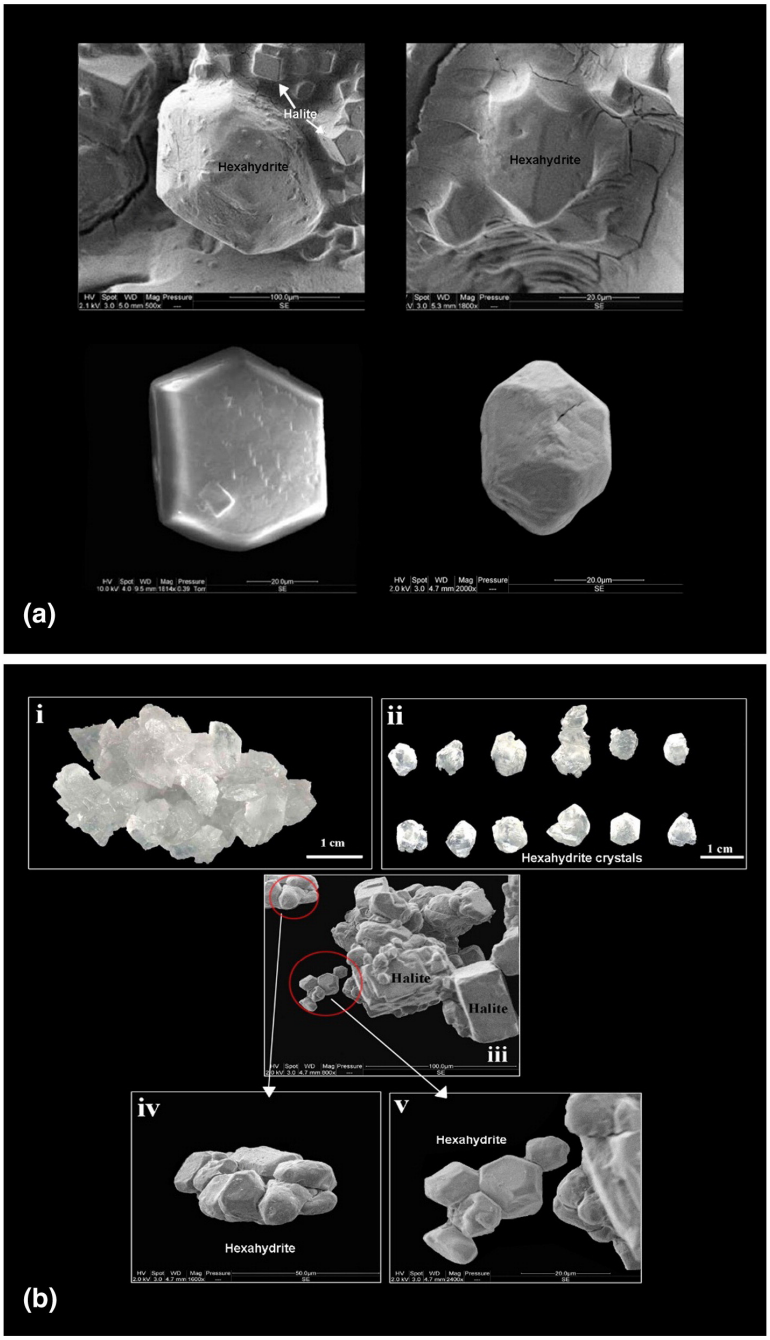

Fig. 9. (a) SEM photographs showing the start of precipitation of tabular pseudo-hexagonal crystals of hexahydrite salt with halite (white arrow) throughout the second sequence of crystallization at densities 1.305–1.343 during experimental isothermal evaporation at 35 °C and (b) photographs showing the start of the tabular pseudo-hexagonal crystals of hexahydrite salt to precipitate with halite throughout the second sequence of crystallization at densities 1.301–1.330 during solar evaporation at the studied pond (pond 2/2) at EMISAL site; (i) photograph shows a massive crystal assemblage, (ii) photograph shows some tabular pseudo-hexagonal crystals of hexahydrite separated carefully from crystal assemblage as shown in photo "i", (iii) SEM photograph of crystal assemblage as shown in photo "i", after slight grinding, shows the presence of tabular pseudo-hexagonal crystals of hexahydrite and also the presence of cubic crystals of halite, and (iv and v) close-up view on some pseudo-hexagonal crystals of hexahydrite present in photo (iii).

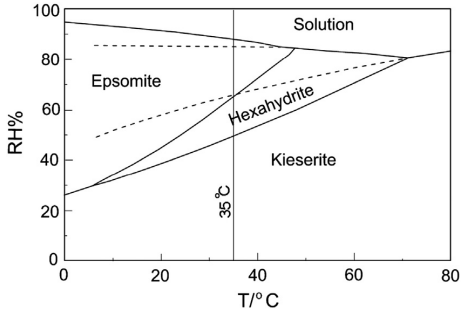

Fig. 10. RH–T phase diagram of $MgSO_4 + H_2O$ with the deliquescence-crystallization equilibria of epsomite, hexahydrite, and kieserite; dashed curves represent the metastable deliquescence humidities of kieserite and hexahydrite (modified after [18]).

salts as dissolved components in the residual brine which allows producing its designed capacity without any loss of its quantity in the NaCl pond.

Acknowledgement

The authors are thankful to EMISAL staff for their support during the sampling and field works. Also, they are deeply grateful to all staff members in the Centre National de Recherche en Sciences des Matériaux, Technopole Borj Cedria, Tunisia for their hospitality and their sincere help while performing the experimental part of this work. The authors are very grateful to the Lappeenranta University of Technology (Finland) for providing financial support to this study. Also, the first author would like to thank the Egyptian Ministry of Higher Education and Scientific Research for the scholarship grant.

References

[1] M.S.M. Abdel Wahed, E.A. Mohamed, M.I. El-Sayed, A. M'nif, M. Sillanpää, Geochemical modeling of evaporation process in Lake Qarun, Egypt, J. Afr. Earth Sci. 97 (2014) 322–330.
[2] M.W. Ali-Bik, H.I.M. Metwally, A.M.A. Wali, M.G. Kamel, Facies and geochemistry of non-marin gypsum, EMISAL, Egypt, Geol. Acta 11 (2013) 409–420.
[3] American Public Health Association (APHA), Standard Methods for the Examination of Water and Wastewater, 20th ed. American Public Health Association, Washington, DC, USA, 1998.
[4] M. Bąbel, B.C. Schreiber, Geochemistry of evaporites and evolution of seawater, in: H.D. Holland, K.K. Turekian (Eds.), Treatise on Geochemistry, Second EditionElsevier, Oxford, 2014, pp. 483–560.
[5] C. Balarew, Solubilities in seawater-type systems: some technical and environmental friendly applications, Pure Appl. Chem. 65 (1993) 213–218.
[6] O. Braitsch, Salt Deposits: Their Origin and Composition, Springer, Berlin, 1971.
[7] A.A. Dardir, A.M.A. Wali, Extraction of salts from Lake Qarun, Egypt: environmental and economic impacts, Glob. NEST J. 11 (2009) 106–113.
[8] J.I. Drever, The Geochemistry of Natural Waters, Prentice-Hall, Englewood Cliffs, 1982.
[9] H.P. Eugster, C.E. Harvie, J.H. Weare, Mineral equilibria in a six-component seawater system, Na–K–Mg–Ca–SO_4–Cl-H_2O, at 25 °C, Geochim. Cosmochim. Acta 44 (1980) 1335–1347.
[10] H. Hammi, A. M'nif, R. Rokbani, Cristallisation polytherme de l'epsomite á partir d'une saumure naturelle: application du systéme Na^+, K^+, Mg^{2+}/Cl^-, SO_4^{2-}//H_2O, J. Phys. IV France 11 (2001) 157–163.
[11] J. Horita, H. Zimmermann, H.D. Holland, Chemical evolution of seawater during the Phanerozoic: implications from the record of marine evaporites, Geochim. Cosmochim. Acta 66 (2002) 3733–3756.
[12] Joint Committee on Powder Diffraction Standards (JCPDS), Powder Diffraction File Search Manual, Inorganic Phases 1980. International Centre for Diffraction Data, Swarthmore, Pennsylvania, 1980.
[13] M.A. McCaffrey, B. Lazar, H.D. Holland, The evaporation path of seawater and the coprecipitation of Br^- and K^+ with halite, J. Sediment. Res. 57 (1987) 928–937.
[14] A. M'nif, R. Rokbani, Minerals successions crystallisation related to Tunisian natural brines, Cryst. Res. Technol. 39 (2004) 40–49.
[15] D.L. Parkhurst, C.A.J. Appelo, User's Guide to PHREEQC (Version 2) — A Computer Program for Speciation, Batch-reaction, One-dimensional Transport, and Inverse Geochemical Calculations: Geological Survey, Denver, Colorado, 1999. (312 pp.).
[16] M. Rasmy, S.F. Estefan, Geochemistry of saline minerals separated from Lake Qarun brine, Chem. Geol. 40 (1983) 269–277.
[17] G.F. Soliman, The hydrology of Lake Qarun, Fayoum Province, Egypt. Part II: the successive increase of salinity in the Lake Qarun, Bull. Inst. Oceanogr. Fish. ARE 15 (1989) 93–105.
[18] M. Steiger, K. Linnow, H. Juling, G. Gülker, A. El Jarad, S. Brüggerhoff, D. Kirchner, Hydration of $MgSO_4 \cdot H_2O$ and generation of stress in porous materials, Cryst. Growth Des. 8 (2008) 336–343.
[19] E. Usdowski, M. Dietzel, Atlas and Data of Solid-solution Equilibria of Marine Evaporites, Springer-Verlag, Berlin, 1998.
[20] D.T. Vaniman, D.L. Bish, S.J. Chipera, C.I. Fialips, J. William Carey, W.C. Feldman, Magnesium sulphate salts and the history of water on Mars, Nature 431 (2004) 663–665.
[21] L. Zayani, R. Rokbani, M. Trabelsi-Ayadi, Study of the evaporation of a brine involving the system Na^+, Mg^{2+}, K^+, Cl^-, SO_4^{2-}-H_2O crystallization of oceanic salts, J. Therm. Anal. Calorim. 57 (1999) 575–585.

ACTA UNIVERSITATIS LAPPEENRANTAENSIS

601. GUDARZI, DAVOOD. Catalytic direct synthesis of hydrogen peroxide in a novel microstructured reactor. 2014. Diss.

602. VALKEAPÄÄ, ANTTI. Development of finite elements for analysis of biomechanical structures using flexible multibody formulations. 2014. Diss.

603. SSEBUGERE, PATRICK. Persistent organic pollutants in sediments and fish from Lake Victoria, East Africa. 2014. Diss.

604. STOKLASA, JAN. Linguistic models for decision support. 2014. Diss.

605. VEPSÄLÄINEN, ARI. Heterogenous mass transfer in fluidized beds by computational fluid dynamics. 2014. Diss.

606. JUVONEN, PASI. Learning information technology business in a changing industry landscape. The case of introducing team entreneurship in renewing bachelor education in information technology in a university of applied sciences. 2014. Diss.

607. MÄKIMATTILA, MARTTI. Organizing for systemic innovations – research on knowledge, interaction and organizational interdependencies. 2014. Diss.

608. HÄMÄLÄINEN, KIMMO. Improving the usability of extruded wood-plastic composites by using modification technology. 2014. Diss.

609. PIRTTILÄ, MIIA. The cycle times of working capital: financial value chain analysis method. 2014. Diss.

610. SUIKKANEN, HEIKKI. Application and development of numerical methods for the modelling of innovative gas cooled fission reactors. 2014. Diss.

611. LI, MING. Stiffness based trajectory planning and feedforward based vibration suppression control of parallel robot machines. 2014. Diss.

612. KOKKONEN, KIRSI. From entrepreneurial opportunities to successful business networks – evidence from bioenergy. 2014. Diss.

613. MAIJANEN-KYLÄHEIKO, PÄIVI. Pursuit of change versus organizational inertia: a study on strategic renewal in the Finnish broadcasting company. 2014. Diss.

614. MBALAWATA, ISAMBI SAILON. Adaptive Markov chain Monte Carlo and Bayesian filtering for state space models. 2014. Diss.

615. UUSITALO, ANTTI. Working fluid selection and design of small-scale waste heat recovery systems based on organic rankine cycles. 2014. Diss.

616. METSO, SARI. A multimethod examination of contributors to successful on-the-job learning of vocational students. 2014. Diss.

617. SIITONEN, JANI. Advanced analysis and design methods for preparative chromatographic separation processes. 2014. Diss.

618. VIHAVAINEN, JUHANI. VVER-440 thermal hydraulics as computer code validation challenge. 2014. Diss.

619. AHONEN, PASI. Between memory and strategy: media discourse analysis of an industrial shutdown. 2014. Diss.

620. MWANGA, GASPER GODSON. Mathematical modeling and optimal control of malaria. 2014. Diss.

621. PELTOLA, PETTERI. Analysis and modelling of chemical looping combustion process with and without oxygen uncoupling. 2014. Diss.

622. NISKANEN, VILLE. Radio-frequency-based measurement methods for bearing current analysis in induction motors. 2014. Diss.

623. HYVÄRINEN, MARKO. Ultraviolet light protection and weathering properties of wood-polypropylene composites. 2014. Diss.

624. RANTANEN, NOORA. The family as a collective owner – identifying performance factors in listed companies. 2014. Diss.

625. VÄNSKÄ, MIKKO. Defining the keyhole modes – the effects on the molten pool behavior and the weld geometry in high power laser welding of stainless steels. 2014. Diss.

626. KORPELA, KARI. Value of information logistics integration in digital business ecosystem. 2014. Diss.

627. GRUDINSCHI, DANIELA. Strategic management of value networks: how to create value in cross-sector collaboration and partnerships. 2014. Diss.

628. SKLYAROVA, ANASTASIA. Hyperfine interactions in the new Fe-based superconducting structures and related magnetic phases. 2015. Diss.

629. SEMKEN, R. SCOTT. Lightweight, liquid-cooled, direct-drive generator for high–power wind turbines: motivation, concept, and performance. 2015. Diss.

630. LUOSTARINEN, LAURI. Novel virtual environment and real-time simulation based methods for improving life-cycle efficiency of non-road mobile machinery. 2015. Diss.

631. ERKKILÄ, ANNA-LEENA. Hygro-elasto-plastic behavior of planar orthotropic material. 2015. Diss.

632. KOLOSENI, DAVID. Differential evolution based classification with pool of distances and aggregation operators. 2015. Diss.

633. KARVONEN, VESA. Identification of characteristics for successful university-company partnership development. 2015. Diss.

634. KIVYIRO, PENDO. Foreign direct investment, clean development mechanism, and environmental management: a case of Sub-Saharan Africa. 2015. Diss.

635. SANKALA, ARTO. Modular double-cascade converter. 2015. Diss.

636. NIKOLAEVA, MARINA. Improving the fire retardancy of extruded/coextruded wood-plastic composites. 2015. Diss.